NOVEL HIGH ADDED VALUE MATERIALS FROM MIXED POST-CONSUMER POLYMER WASTE

CLINT BAINBRIDGE

A thesis submitted in partial fulfilment of the requirements of the Manchester Metropolitan University for the degree of Doctor of Philosophy

School of Healthcare Science
Faculty of Science & Engineering
The Manchester Metropolitan University
In collaboration with Lubrizol Ltd

March 2013

DECLARATION

The work referred to in this thesis has not been submitted in support of any application for another degree or qualification of this or any other university or institute of learning.

C. Bainbridge

April 2012

For my parents

Contents

LIST OF ABBREVIATIONS USED

Abbreviation	Meaning
ASTM	American Society for Testing and Materials
ATH	Aluminium tri-hydroxide
ATR	Attenuated total reflectance
ATR FTIR	Attenuated total reflectance Fourier-transform infra-red
BMI	Bismaleimide
BS	British standard
$CACO_3$	Calcium carbonate
CO_2	Carbon dioxide
DCP	Dicumyl peroxide
DMA	Dynamic mechanical analysis
DMTA	Dynamic mechanical thermal analysis
DSC	Differential scanning calorimetry
EVA	Ethylene vinyl acetate
FR	Flask residue
GCC	Ground calcium carbonate
HDPE	High density polyethylene
ICI	Imperial Chemical Industries
ISO	International Organisation for Standardisation
LDPE	Low density polyethylene
LLDPE	Linear low density polyethylene
MFR	Melt-flow rate
MRF	Material recovery facility
MSW	Municipal solid waste
PCC	Precipitated calcium carbonate

continued on next page

PCPW	Post-consumer polymer waste
PE	Polyethylene
PET	Poly ethylene terephthalate
PIPW	Post-industrial polymer waste
PP	Polypropylene
PS	Polystyrene
PVC	Polyvinylchloride
RDF	Refuse derived fuels
TGA	Thermo-gravimetric analysis
TMPTA	Trimethylol propane triacrylate
TR	Thimble residue
UNIS	Un-notched impact strength
VMFR	Volume melt-flow rate
WRAP	Waste Resource Action Program

ABSTRACT

Increasing awareness of the impact of today's 'disposable society' has highlighted the finite nature of mankind's resources. As such, there is increasing impetus on 'the three Rs' – Reduce, Reuse, Recycle. While many sources such as metals, glass and plastic bottles (high density polyethylene (HDPE) and poly(ethylene terephthalate) (PET)) are widely recycled, mixed polyolefins require resource-intensive separation and are rarely recycled as a comingled feedstock. Furthermore, these mixed polyolefins may be in the form of multi-material items such as food packaging which comprises of many layers of bonded materials which are impossible to segregate.

This thesis discusses a method of processing comingled mixed polyolefin waste streams by use of a compatibilising system which negates the necessity of separation. The outcome of adopting this approach resulted in the significant improvement of the mechanical properties of the materials, whilst also reducing cost by means of adding the compatibiliser system via a surface-treated filler.

Calibration curves were developed using differential scanning calorimetry (DSC) and attenuated total reflectance fourier-transform infra-red spectroscopy (ATR-FTIR) data to calculate the polyolefin ratios of unknown samples. Binary polyolefin blends of HDPE and polypropylene (PP) were also produced to investigate the associated interactions and behaviour of the systems to understand how the morphology contributes to the mechanical behaviour observed.

A commercial coupling agent know as Lubrizol Solplus C800® was used via a calcium carbonate filler as a compatibiliser in the polyolefin wastes, and in most instances significantly improved the mechanical response of the materials. Through solvent extraction and subsequent TGA analysis, it was suggested that the mechanism by which compatibilisation occurred was through the formation of an amorphous rubbery interfacial region close to the filler surface.

While it was found that Solplus C800® goes a significant way in compatibilising mixed polyolefin wastes, it was suggested that an increased functionality coupling agent would be the next logical step in this line of research. However, initial work in this area has suggested that the complexity of this topic may provide a basis for subsequent research and development.

ACKNOWLEDGEMENTS

I would like to thank my supervisors, *Dr C. M. Liauw* and *Dr G. C. Lees* for their continual support and guidance over the duration of this research. Furthermore, I would also like to thank *Dr K. A. Whitehead* for her pep talks when the going got a little tough.

I would also like to thank *Mrs E. Howarth* for the multiples of DSC runs that she performed. I am also grateful to both of my foreign exchange project students, *Martin Batiste* and *Ané Arruti Amilibia* for their assistance during their visit to the university.

Thanks also to the team at Lubrizol: *Dr D. Thetford*, *P. Sunderland*, *E. Coulbeck* and *Dr J.Schofield* for their assistance and support during the synthesis of the new compounds.

Thank you to *Rebecca* for her patience, support and continual encouragement which has motivated me during the long writing up process.

Finally, I would like to thank *my parents* for their continual support and encouragement over the years, as without it this work would not have been possible.

OBJECTIVES

The main objectives of this work are to establish a processing method by which comingled polyolefins (HDPE, LDPE, LLDPE and PP) can be blended, compatibilised and compounded to produce a material with adequate mechanical properties at an acceptable and economic cost. In doing so, many of these comingled polyolefin waste streams can be diverted from landfill and energy recovery processes into a closed loop, where they can be recycled once again at the end of their service life.

Further objectives of this work aim to establish an accurate and reliable method for the identification and classification of mixed polyolefin materials. The method needs to be simple, prompt and repeatable, using standard testing methods and apparatus.

Investigation into the effects of blending HDPE and PP is also required to understand the impact of one polymer on the other and overall properties at specific blend ratios. Furthermore, the effect of the chosen filler will need to be observed and assessed in these systems to quantify the optimum level of filler required.

In order to achieve effective compatibilisation, various established coupling agent technologies will be investigated, namely Solplus C800®. Due to the nature and original application of Solplus C800®, new coupling agents may be required which improve and extend upon the capabilities of Solplus C800®.

OVERVIEW OF THESIS

Section 1 introduces the current trends in the recycling of polymer waste and any associated issues and implications. It then goes on to provide a background on the materials used and the origins and concepts involved with coupling agent and dispersant systems. The problems associated with mixed polyolefin materials are also discussed, as are the implications of particulate filler type and loading level.

Section 2 details the experimental methods utilised during the study, including development of the calibration curves produced to classify the polymer waste streams.

Section 3 discusses the results obtained during the study.

The initial work attempted to employ Solplus C800® as a compatibilising coupling agent in mixed post-consumer polyolefin waste. While the initial results were mixed, it was soon discovered that non polyolefin materials were still present in the waste. These materials created un-melted defects in the samples which had a detrimental effect on the mechanical properties. Further separation and classification of the waste gave a more accurate indication of the levels of constituents present, and other coupling systems were initially investigated.

Due to the fact that there were some interesting trends observed with regards to the effect of Solplus C800® on the impact and rheological properties of the blends and composites, the effect of the additive was investigated at different loading levels in HDPE and PP alone. This concluded that the peroxide required to initiate the coupling reaction was affecting the bulk matrix by crosslinking the HDPE and reducing the molecular weight of the PP by chain scission. These two effects were presented as an decrease and an increase in MFR respectively.

Next, the coupling system was applied to samples of post-industrial polymer waste, which were cleaner materials, as expected. In order to better understand the results obtained, virgin blends were produced and analysed by DSC in order to create a calibration curve which allowed classification of the post industrial waste.

These blends were then reproduced with and without filler and the Solplus C800® additive system to assess the effects of the individual components across the blend composition range. This further highlighted the crosslinking and chain scission reactions taking place, yet also suggested that if the blend ratio could be controlled then the properties observed may also be controlled to a certain extent.

While the Solplus C800® has gone a significant way to providing a means of compatibilisation, it appears that a limitation of the additive is its functionality. To overcome this issue, two new additives were synthesised with increased functionality towards both the filler surface and the polymer matrix. Initial results were very promising, but work is needed to perfect the structures, functionalities and loading levels required to produce a commercial product.

Section 4 summarises the results in a series of conclusions which are detailed in the previous paragraphs.

Section 5 details the future work which is suggested by the results obtained from the application of the new compounds. As mentioned previously, this would require study of the structures and functionalities of the compounds, along with a comprehensive investigation into loading levels and any associated interactions that may occur.

1 INTRODUCTION

1.1 The polymer waste problem

The increasing tax on land-fill [1], along with mounting environmental pressure to recycle, has provided significant drive for serious attempts at the recycling of post-consumer polymer waste. Added to this is the environmental, financial and political pressure to reduce our dependency on oil [2], and a tendency to reduce the increasing volume of plastics production demanded by the packaging industry. Recycling is therefore seen as both an environmentally friendly and a politically attractive option.

A news article, on the InterPack website, states that in 2007 the worldwide consumption of plastic materials was 215 million tons and experts project it to reach around 330 million tons by 2015 [3]. At the moment the main environmental drive is the reduction of CO_2 emissions, however it may be argued that the production of polymeric materials fixes carbon into an inert form, in much the same way that nitrogen is fixed by plants. It may also be shown with suitable life cycle analysis that the amount of carbon fixed in the final polymers may go a considerable way to balance the associated amount of CO_2 produced during the processing and transportation of the materials. In addition, the reduced energy requirements to produce polymeric items when compared with the energy-intensive processes associated with the fabrication of both glass and metallic items, is also an advantage. Table 1 gives the generic composition of the post-consumer polymer waste stream in the UK for 2008 [4]. These figures show that polyolefins constitute the major proportion (60%) of this waste stream.

Table 1: Generic composition of post-consumer polymer packaging waste stream, based on WRAP 2008 figures [4].

Polymer	% wt of Waste stream	Specific Gravity (g cm^{-3})
LLDPE + LDPE	25	0.91-0.94
HDPE	13.5	0.94-0.96
PP	22.2	0.91
PS	4	1.05
PVC	3.5	1.4
PET	15.3	1.4
Other/contamination	16.5	-

LLDPE: Linear low density polyethylene; LDPE: Low density polyethylene; HDPE: High density polyethylene; PP: Polypropylene; PS: Polystyrene; PVC: Polyvinyl chloride; PET: Poly (ethylene terephthalate).

1.2 Attempts to overcome recycling issues

1.2.1 Sorting

While sorting the main recyclates (metals, glass, paper and plastic) from one-another is a fairly straight-forward process, sorting plastics into further sub-categories becomes increasingly difficult with each step. According to the waste recycling action plan (WRAP) [4], current trends in the recycling of post-consumer polymer waste involve collection, sorting, shredding, washing, and further sorting to produce reclaimed feed-stocks with varying purities up to 99%. This process commences by carefully collecting the waste items at the kerbside in specific receptacles. Herein lies the first in a series of challenges to this approach:

- Has the consumer correctly identified the items to be discarded?
- Have they sorted them correctly?
- Have they washed the items thoroughly?
- Have they discarded a non-recyclable plastic item with one which is recyclable?
- Have they bundled many different items together in a plastic bag?

The list of criteria which must be met in a situation where material is to be ‘completely’ recovered is extremely stringent and may not be constantly adhered to, causing problems for the materials recovery facility (MRF – pronounced ‘murf’).

1.2.1.1 The Materials Recovery Facility

There are two different types of MRF – 'clean' and 'dirty' [5, 6]. The former, as illustrated in Figure 1, solely processes plastic material which has been pre-sorted by the householder and, as expected, recovers the greater amount of reusable material (c.a. 80-97%) with the remainder being disposed of via landfill. The latter takes a mixed, unsorted post-consumer waste stream and attempts to sort the material into three distinct groups:

- Biologically-treated, low-grade material
- Recyclables
- Non recyclables

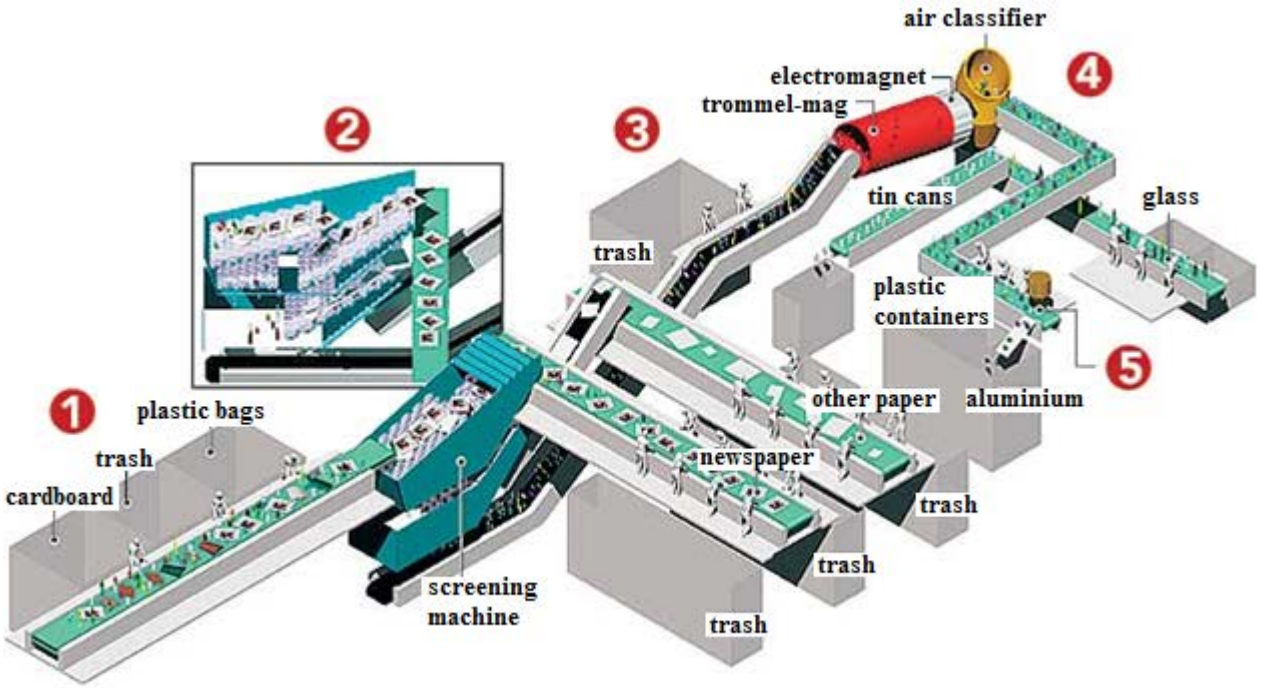

Figure 1: Illustration of a materials recovery facility [7].

1.2.1.2 Lamby Way, Cardiff – A 'Clean' MRF

The MRF plant in Cardiff sorts co-mingled recyclable materials that have been gathered via the kerbside collection scheme, and has the ability to process around 90,000 tonnes of waste per annum [8].

The process starts with bags of recyclates being loaded into a bag opening machine and mechanically opened. The contents are then fed to an incline conveyor belt which then passes to the first sorting cabin. Here, workers manually remove any undesirable materials such as textiles and wood that may be present in the waste stream. They also remove the now-opened and somewhat shredded bags that the waste was contained in, and any un-opened bags are returned to the start of the process.

Before entering the second sorting cabin, an overhead air suction system removes any plastic film or bags. Any undesirable plastic that remains is removed manually along with cardboard by workers in the cabin, and the waste is then transported to a double deck sorting machine. These machines, known as ballistic separators, house inclined rollers with over-sized square rotors and blast air from beneath to separate items according to their mass. Due to the incline of the successive rollers, this machine removes items progressively, such that heavier items like glass bottles and metal cans are removed first. Lighter items like paper and magazines are transported towards the end of the machine, where they are sent to a third sorting cabin to ensure the final stream contains only paper. This is then baled to be sold to manufacturers to recycle the material into new items.

The glass/metal stream is passed via a conveyor belt under an electromagnet which removes any ferrous metals. As non-ferrous metals such as aluminium are not magnetic, eddy currents are induced by rollers at the end of the conveyor belt to deflect the material into its own bin. This leaves the glass fraction which is directed to its respective collection area.

The final processed stream is that of plastic bottles. The stream produced is usually a mixture of poly (ethylene terephthalate) (PET) and high density polyethylene (HDPE) bottles which are sorted by means of a near infra-red sorting device. This device analyses the contents of the conveyor belt beneath it, and uses jets of air called ‘air knives’ to shoot the items into their respective collection containers. These containers are then emptied into baling machines that compact the bottles into a regular, manageable form which are then transported to a third party for reprocessing.

1.2.1.3 Closed Loop Recycling, Dagenham

A method of recycling of HDPE milk bottle waste and PET drinks bottle waste has been established [9]. Whilst this process promises to provide a sustainable route to create new milk and drinks bottles, the facility will only accept HDPE and PET bottle waste that has either been pre-sorted by a clean MRF (as detailed in Section 1.2.1.2), or collected directly from council 'bring sites'.

1.2.1.3.1 Bulk Sorting

The process commences when large 500kg bales of around 12,500 compacted plastic bottles are loaded onto a conveyor belt. At this point the bales comprise of HDPE, PET and any other contaminants that are present. Next, the bales are broken up and the sorting process begins. This step removes any undesirable metal, paper, glass and polypropylene (PP) bottle tops that would affect the purity of the final product, using methods similar to those as detailed in Section 1.2.1.1.

1.2.1.3.2 Optical Sorting

The next step is the most technically challenging, as it relies heavily on complex optical sorting machines that are programmed to recognise individual bottles that meet two specific criteria – polymer type and bottle colour. This process is repeated a second and third time and separates the bottles into five distinct types:

1. Clear PET
2. Light blue PET
3. HDPE
4. Coloured PET
5. Other plastics

From here, the coloured PET and other plastics are sent to other facilities to be recycled independently.

Subsequently, the HDPE stream is then sent through a fourth sorting machine to separate the natural HDPE milk bottles from any HDPE household cleaning product bottles, which are typically coloured. These resultant coloured bottles are sorted further by colour and sold on to manufacturers to be reprocessed into drainage pipes, wheelie bins and also garden furniture.

Next, the three individual target streams (natural HDPE, clear PET and light blue PET) are manually sorted to ensure a high purity feedstock for their respective granulating and washing cycles. Prior to washing, the flakes are sent through an apparatus that utilises an upward thrust of air to separate any flakes that are lighter than the target materials – i.e. any paper and/or labels.

1.2.1.3.3 Washing

The flakes are then washed in a solution of caustic soda to remove any ink or glue that held the labels in place. The resultant pulp then sinks, and is removed allowing the remaining flakes to progress onto the rinsing and drying step. The PET stream then undergoes a floatation process, whereby the polyolefinic flakes of any remaining lids or caps float allowing them to be skimmed off to leave the 'sunken' fraction of PET flakes. Any remaining coloured flakes from lids and caps are separated from the HDPE stream by another optical sorting step.

1.2.1.3.4 Decontamination

In order for the materials to re-enter the supply chain as a food-grade product, they must be treated in such a way that meets current legislation [10].

1.2.1.3.4.1 PET Decontamination

The PET flakes undergo a rather intense process, starting with the removal of the surface layer using a strong caustic soda solution. Next, hot air is used to evaporate all of the liquid products, before the flakes are sent through a rotating furnace for around four hours. Subsequently, the flakes are cooled, thoroughly rinsed and then dried. Finally, the stream is then optically sorted once more to

remove coloured flakes, and then laser Raman sorted to remove any remaining contaminants. From here, the flakes are bagged and sold on to manufacturers to be processed into new packaging for the cycle to start once more.

1.2.1.3.4.2 HDPE Decontamination

The process whereby HDPE is decontaminated is much less involved than that used for PET [11]. Using a Vacurema® setup [11, 12], the flakes are treated under high temperature (200°C) and low pressure conditions. The heating process creates a melt, eliminating any contamination; allowing the material to be melt-filtered and finally extruded into pellets ready for reprocessing.

1.2.1.3.5 Conclusion

It can be seen from the preceding description that the process is highly technical in nature, with numerous aspects which question the economic viability of the system. In part this includes the multitude of expensive optical and laser sorting devices, as well as the associated energy costs. While this system addresses the problem of bottle waste, it completely ignores that of mixed plastic waste.

1.2.1.4 Biffa Polymers, Redcar – A Mixed Plastics Facility

This facility is the first of its kind in the UK as of 2011 [13]. Where the Closed Loop facility is specifically designed to process plastics bottles, the Biffa facility is designed to also process pots, tubs and trays known as ‘hard/mixed plastics’. These items are identified as hard plastics as they are produced from rigid polymers such as polystyrene (PS).

The initial feedstock for the plant is usually supplied as a mixed plastics waste stream from a MRF. While in some instances this has been pre-sorted to remove the higher value plastics such as HDPE and PET, the Biffa plant can process waste streams where these plastics are present.

Much like the Closed Loop process described in Section 1.2.1.3, various machines mechanically process the incoming waste stream. As the washing and sorting stages of the Biffa plant are specifically designed for plastics, all metals, glass and paper-based residues must be removed prior to the shredding stage. This is followed by a two-step washing and centrifuge drying process, which makes this facility unique. While it can be argued that the wastewater creates a further waste stream, in this instance it is filtered and re-used (arguably still creating a small amount of residue).

The now-shredded, clean polymer flakes are then transferred to a three-tier, six-step optical sorting process to sort the flakes by polymer type and colour. This yields several end products:

- Natural-coloured LDPE, HDPE, PET and PS
- Single-coloured fractions of the above
- Multi-coloured mixtures of the individual polymers known as ‘jazz’

Due to the wide range of polymers produced by the process, a facility such as this can serve several markets. The natural-coloured HDPE and PET is forwarded on to bottle-producing facilities, the individual coloured fractions will be used where a specific colour is required, and the ‘jazz’ material will be blended together resulting in a final compound that will have a colour ranging from grey to black. This final material tends to serve lower uses such as refuse sacks, fence posts, plant pots and sometimes plastic pallets.

1.2.1.5 Bryn Posteg, Powys – A ‘Dirty’ MRF

This type of MRF [14] operates in much the same way as the ‘clean’ MRF described in Section 1.2.1.2. The fundamental difference being that this facility accepts a co-mingled municipal waste stream, which is typical of a household’s general rubbish bin. The process adopts the same basis as that of a ‘clean MRF’ and adds extra steps in order to recover recyclable materials. These extra steps include (but are not limited to) further manual sorting, use of trommels, and extensive washing. The trommels employed are large rotating cylinders with an incremental grating

size to remove stones, broken glass, bottle tops and other undesirable materials.

While a plant like this ensures that 100% of the waste stream is sorted through, the recyclates yielded will be of inferior quality to those produced by a ‘clean’ MRF. This is due in part to the contaminants present, and also the less efficient separation process that is employed. Typically [15], this type of facility will only generate around 4-20% recyclable material, and will send around 5% to landfill. A further 25-40% ‘low grade’ material is sent to be treated biologically, and the remaining 35-66% may also be sent to landfill, or more increasingly be diverted to produce refuse derived fuels (RDF).

As expected, the figures for this type of facility are significantly different to those for the clean facility due to the comingled, soiled nature of the material which is present. Furthermore the distinct problem with the ‘dirty’ facility is that of airborne debris and dust, which poses a serious health risk to the workers present.

1.2.1.6 Conclusion

Collectively, it can be argued that MRFs are resource/energy intensive processes that rely heavily on the efficiency of the machinery employed. The basic level of this machinery is the immense number of conveyor belt and vacuum systems which transport all of the materials throughout their respective facilities.

While the manufacturers [16 - 18] are somewhat reluctant to disclose the costs of their sorting machines directly, an internet search [19] reveals that sorting technology for the food industry (which is arguably the precursor to recycled polymer sorting technology) can range from £18,000 to £48,000 per unit.

Next, near infra-red devices are used to scan a moving mass of waste which is then directed to specific bins by air knife devices which deliver a jet of compressed air to the end of the conveyor belt. The materials from these bins are then further processed mechanically by industrial shredding machines, and the flaked material may then be further sorted by an expensive laser Raman device.

This illustrates the highly technical nature of the process with its many steps, where each additional sorting and characterisation step adds additional cost to the

final material. Therefore such complex separation processes may not be entirely economically viable as a long term solution.

1.2.2 Energy recovery / energy from waste

Considered a last-resort method to "recycling" of both mixed polymers and municipal solid waste (MSW) is ‘energy recovery’, which can be undertaken in many ways. The main aim of this approach is to recover as much of the invested energy from the waste stream as possible; the second is to divert waste from landfill. One would assume that this is achieved simply by incineration, but the environmental costs can far outweigh the economic benefits. This is due to the fact that combustion of the waste releases not only nitrous oxides, but also releases the extensively documented greenhouse gas, carbon dioxide (CO_2).

Much of continental Europe’s recycling agenda employs this method which goes a significant way in producing seemingly impressive figures for each country’s respective agenda [20 - 22]. With a calorific value c.a. 25 – 46 MJ kg^{-1} [23], this would equate to a potential power generating capacity of 7 – 13 kWh kg^{-1}. If this is compared to the values for coal and natural gas, 32-42 and 39 MJ kg^{-1} respectively [24], it can be seen that plastic waste can compete with traditional fuel sources used for power generation. Even though many specially designed scrubbing filters may be utilised to remove any harmful toxic or volatile organic compounds, this approach is not without its environmental caveats. As such, there are emerging technologies that are attempting to reduce the environmental impact of energy recovery [25].

Fluidised Bed Reactor System

Firstly, fluidised bed systems attempt to recover some feedstock materials, and produce some residues which are deemed suitable for energy recovery [26].

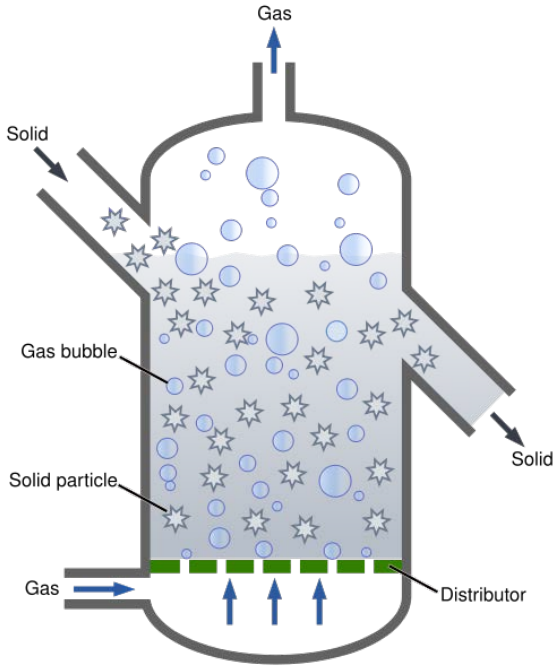

Figure 2: Schematic diagram of a fluidised bed reactor [27].

The apparatus shown in Figure 2 was originally employed in the petrochemical industry, and has also been used to produce polymers. The solid to be treated is added via an inlet port where it falls to the bottom of the heated reactor. Gas is then passed though the supporting medium (usually sand) which is suspended on a distributor plate. As the gas is introduced at a high pressure, turbulent conditions are created within the vessel which breaks down the materials introduced. Gases are then taken off from the top of the reactor, where the fluidising gas is removed to be reused and the remaining fractions are processed. Residual solids are then tapped off at the side and any remaining sand is recirculated back into the system. This process is quite effective, due to its continuous nature and the uniform temperature profile created in the reactor.

One requirement of this approach is that the material to be treated must be shredded and washed before processing. Also, while this process is advertised as one that recovers feedstock materials, much of the resultant solid residues are only suitable for combustion.

Plastic-to-Oil Processing

Another process converts a mixed plastics waste stream into oil [28] [29]. This approach is based on a thermal depolymerisation process which is similar to that of cracking crude oil into hydrocarbon fuels. Around 820kg of un-washed waste polymer feedstock is ground and shredded before being introduced into a hopper and conveyor belt feed system. The plastic flakes then proceed to the heated chamber which is the heart of the process. Here, a proprietary catalyst system is employed to crack the polymer chains into smaller molecules, and these short-chain hydrocarbons leave the reaction chamber as a gaseous mix which is held in a temporary fuel tank.

Once cooled, the petrol and diesel condenses and is treated with fuel additives before being moved to their own storage tanks. This fuel is claimed to have an ultra-low sulphur content, and has passed ASTM testing by several independent laboratories. The lighter gases such as methane, ethane, butane and propane, are then compressed into storage tanks where the butane and propane liquefy allowing them to be stored separately for sale. The two remaining light gases or "off-gas" is used to power the reaction chamber for the following stream in a continuous manner, increasing the efficiency of the system.

Currently, the operators are focusing solely on post-industrial polymer waste (PIPW) sources, as they are *"readily available…and cost effective".* It is claimed that 1kg of plastic waste produces approximately 1 litre of oil, and that 90% of the hydrocarbon content of the plastic is recovered, leaving 8% "off-gas" and 2% non-usable residues. While the "off-gas" is used to power the process, the residues are usually landfilled, but have subsequently been shown to produce a heating value c.a. 6.6 kWh kg^{-1} if incinerated. Furthermore, the operators state that the process meets the required emissions standards for the New York area where the site is located, and that it also returns oxygen to the atmosphere.

Finally, the operators state that their 30-ton capacity machines *"cost a small fraction of the £2 million to £3 million per machine of other competitors"*, yet actual costs are not disclosed [30]. It is also stated that their proprietary catalyst *"decreases conversion time and increases yield"* while being reusable and economical to produce.

As stated previously, the end goal for the energy recovery process is the generation of heat and/or electricity by incineration. However, due to emissions regulations this must be carried out in such a way as to strike a favourable balance between the economic advantages and environmental concerns.

One method which allows the industry to 'side step' any legislation is the process of co-incineration. This permits the use of any pre-treated municipal waste as a percentage of the combustible mass fed into an energy generation process.
While recovering the energy spent to initially create the material, this would be considered the most environmentally damaging method, due to the quantities of CO_2 released, as polymers are essentially long chain hydrocarbons – where short chain hydrocarbons are used as fuels. Again, it is also worth noting that a rigorous life cycle analysis has not been performed on these methods of recycling to assess their environmental impact with regards to CO_2 emissions and resource consumption.

1.2.2.1 Carbon Dioxide

If energy recovery and plastic conversion processes become more widely adopted as a means of disposing of plastic waste, then carbon dioxide levels will become increasingly compounded on top of those already created by transport and industry. Due to the hydrocarbon nature of polymers, incineration of plastics is much the same as the burning of fossil fuels. With carbon dioxide widely acknowledged as a greenhouse gas contributing to climate change, many governments are introducing strict emissions targets and controls. As many emissions limits are enforceable by law, research is greatly promoted in the area of CO_2 removal and storage. Hence there are numerous approaches to dealing with this issue, including means of removal from the atmosphere, storage and even recycling. While the following is by no means an exhaustive review of every technology currently under investigation, it provides an overview of the more traditional and novel approaches.

1.2.2.2 Carbon Sequestration

Carbon sequestration is the process of *"capturing carbon dioxide from the atmosphere and depositing it in a reservoir"* of some description [31]. This usually

involves removing the gas from the air, compressing it and then injecting it directly into the ground in such a way that it cannot escape.

This approach was initially used as a means to force any remaining oil from otherwise “dead” wells [32], but the quantities of CO_2 required for this process do not approach the emissions produced by coal-fired power stations.

1.2.2.3 Carbon Burial – Storage

Research is currently being undertaken to investigate the feasibility of simply burying the CO_2 produced by the aforementioned energy recovery processes [33 - 35]. In one method, the gas is bubbled though an amine-containing solution which absorbs the CO_2. Next, the CO_2 is removed and compressed into a supercritical fluid, and then transported to injection sites. Here it is injected 1km or more underground into porous rock that is surrounded by impermeable rock that acts as a seal. At this depth, the pressures and temperatures are such that the CO_2 remains in its pressurised supercritical state.

1.2.2.4 Recycling

A novel, approach to counter the effects of CO_2 is a process of directly recycling the gas into new fuel.

One patented form of this uses a proprietary catalyst system to convert hydrogen and carbon dioxide into a synthetic gas or “syngas” mixture in a fluidised bed reactor [36].

Another method uses sunlight and catalysts housed in a reactor apparatus to convert CO_2 into carbon monoxide [37 - 40]. The sunlight is concentrated onto the apparatus to generate the high temperatures required to break one of the C-O bonds. The resultant CO is mixed with hydrogen in the system, and using suitable catalysts hydrocarbon chains can form [41] according to the Fischer-Tropsch process (Equation 1).

$$(2n+1)\ H_2 + n\ CO \rightarrow C_nH_{(2n+2)} + n\ H_2O$$ **Equation 1**

1.2.3 Feedstock recovery

1.2.3.1 Selective dissolution

An alternative method to separation of mixed polyolefin waste is that of a selective dissolution process [42]. Here, a co-mingled polymer waste stream comprising of pre-shredded flakes is fed into an apparatus and treated with various solvents at differing temperatures to yield the original feedstock materials [43 - 44]. The flakes are first washed and then dried to remove any residues that may be present. Then the chemical processing begins, as the flakes are mixed with xylene at around 15°C to remove any polystyrene (PS) present in the waste. A filtering system holds back the un-dissolved fractions and passes the PS-rich xylene solution on to a hold tank. This process is repeated and the temperature increased to 75°C to remove the LDPE. Although specific temperatures are not disclosed, increasingly higher temperatures are employed to remove HDPE and PP respectively. After this has been completed, there are only two insoluble polymers expected to remain – PVC and PET. This remaining blend is then transferred to a smaller vessel where a cyclohexane/xylene solvent mix is added. Here, the mix is first heated to 120°C where the PVC is dissolved, and then to 180°C where the PET is finally dissolved.

Now that each of the fractions are held in their respective tanks, various additives and modifiers are introduced, and any pigments or colourants are removed. Once completed, the fractions then move on to a flash devolatilisation chamber to remove any remaining solvent and low molecular weight vapours before being processed through a devolatilising extruder to produce the final pelletised product.

Although promising, this process may be easily dismissed by the industry, due to its associated costs and numerous solvent related hazards which may be heavily criticised by today's increasingly prominent health and safety legislation. While the solvents are recycled and reused during the process, it would be naïve to assume that no vapours or toxins would escape into the surrounding environment.

In the current economic climate (2011), both the government and local authorities are in the midst of making substantial cut-backs and financial savings. As the article estimated the capital investment required in 1997 as £21 million [42], this would translate to around £30 million taking inflation into account [45]. Although this method had expected to produce polymers with a market price of around £450 per tonne, the current market value for recycled HDPE is around £900 per tonne [46], yet virgin material currently sells at £990 per tonne [47]. While the creators of the process have stated that the process creates a material that sells for a profit [42], they do not disclose the profit margin.

Furthermore, the original patents for this process were filed in 1989 & 1992, and subsequently granted in 1993 and 1994 respectively. With patents and licensing in place, one has to question the lack of widespread adoption of the technology, which may be an indication of both the feasibility and economics of the process.

1.2.4 Blending

The major benefit of this approach is the elimination of various separation steps. The major problem however is that simply mixing the different polymers gives an immiscible blend with very poor adhesion between the individual components. Such blends therefore can often have very poor mechanical properties and are not seen as desirable materials.

Melt blending of mixed post-consumer waste to form a polymer alloy is an appealing option due to its lower cost compared to mechanical sorting. As no specialised machinery is required, this approach may easily be employed permitting a recycling system to be operated in parallel with the manufacturer's current process. Furthermore, this would eliminate extensive sorting of any polymer waste streams – either post-industrial or post-consumer.

This approach has previously been investigated by Khunová et al [48]. A mixed polymer waste stream is first shredded into flakes measuring an average of 1cm in diameter and then washed. Next, the flakes are added to a tank containing water, where plastics and contaminants with a density greater than 1 g cm^{-3} sink. As shown previously (Table 1), the polyolefin fraction has a density less than unity,

allowing it to be separated from the sunken fraction. This divides the polymers into a polyolefin floating fraction, and a sunken fraction consisting of the heavy polymers – namely PVC, PET, PS. Although the incorporation of fillers into polymer blends can increase their density, packaging tends to use such small quantities that this does not prove to be an issue.

Once dried, the polyolefinic fraction is then processed using a twin-screw extruder to reactively compatibilise the otherwise immiscible blend using a magnesium hydroxide or calcium carbonate particulate mineral filler together with a 1,3-phenylene dimaleimide (BMI) interfacial modifier. This modifier serves the purpose of bonding the immiscible polymer phases together, and strongly interacting directly with the filler surface.

The results show that upon introduction of BMI, the blends show a 40% increase in tensile strength when compared to the uncompatibilised control. Furthermore, the addition of 60% w/w magnesium hydroxide with BMI improved the mechanical properties such that the tensile strength of the composite approached that of PP. It was also shown that BMI was able to enhance the properties of a composite employing ground calcium carbonate as the mineral filler.

Blend properties can be improved by adding compatibilisers. There are molecules (usually polymeric surfactants) that have affinity for the different polymers built in to their structure. In this way the “adhesion” between the different components is increased, thereby increasing mechanical properties. Compatibilisers are however expensive additives and while there are systems to compatibilise polyolefins with other polymers [49 - 52], no commercially successful polyolefin compatibilisation system has yet been developed for post-consumer polymer waste.

1.2.5 A Novel variation on blending – the objective of this PhD study

According to WRAP [4] (Table 1), post-consumer polymer packaging waste is comprised of polyethylenes, polypropylene, polystyrene, polyethylene terephthalate and polyvinyl chloride. As polyolefins constitute the majority of the waste (c.a. 60%), and generally have a density of less than unity, they can in theory be easily separated from the denser fraction by simple floatation in water. The objective of this study concerns only the polyolefin fraction of post-consumer polymer waste. Recycling routes for PET are well established [53 - 55], and routes for PVC (mainly from construction materials) are currently being explored [56 57].

Addition of a filler to an immiscible polymer blend can radically change its properties, as fillers generally have surfaces that are relatively unattractive to polymer chains [58]. If the interaction of the filler with the constituent polymers in the blend can be enhanced and controlled by chemical modification then the blend properties can be further improved. It can be envisaged that the modified filler particles act as the glue that holds the constrained immiscible components of the blend together. As the filler surface modification (the particularly expensive part) is spread over the filler particle surfaces, only a small amount is required. Further environmental / economic benefits can be gained if the filler itself is a waste material such as the dust generated from mineral processing or mining. This novel approach could potentially revolutionise the recycling of polymers. There are however major interfacial chemistry/polymer chemistry hurdles to negotiate, which this study investigates.

1.3 Polymers

1.3.1 Polyethylene

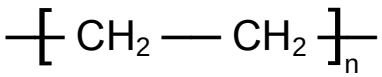

Figure 3: Repeat unit structure of polyethylene, where n represents the number of repeat units present.

Polyethylenes are widely used commodity thermoplastics with many applications. However, simply referring to the material as polyethylene is too general in some instances, as there are many sub-types named according to the type and level of polymer chain branching. Figure 4 illustrates the chain structure of the more widely used polyethylenes.

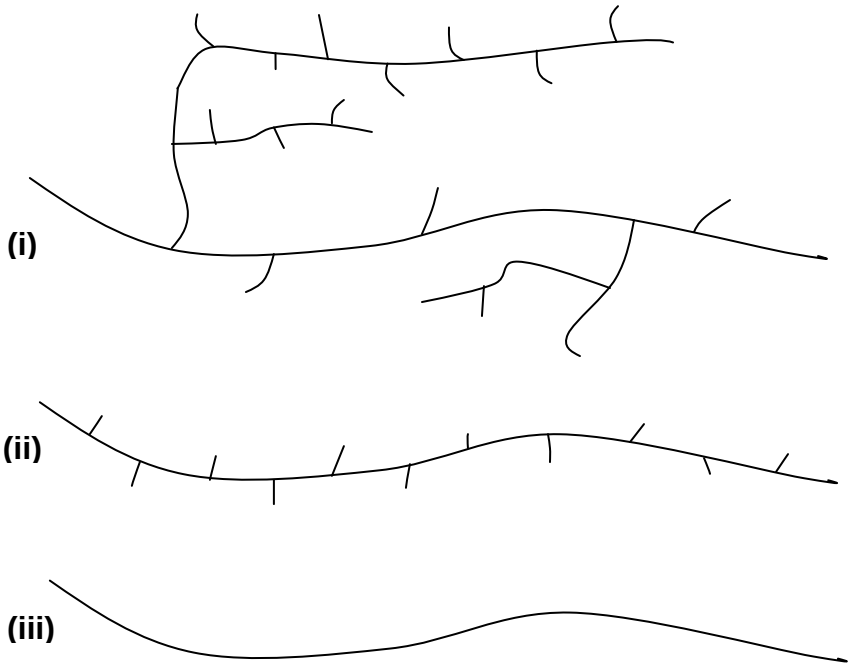

Figure 4: Schematic representation of the different forms of polyethylene;

(i) LDPE, (ii) LLDPE and (iii) HDPE. The short lines represent ethyl and n-butyl branches.

The degree of branching in polyethylenes dictates the polymer's behaviour, processability and ultimately its applications. The first polyethylenes were highly branched due to the low level of control that was achievable during the reaction process. As more sophisticated synthesis methods were developed, branching levels became more controllable and hence the density increased. This is in part due to the way in which the polyethylene chains fold to form lamellae. In low density polyethylenes, side chains prevent folding, and thus limit the level of crystallinity. However, in high density polyethylenes a lack of side chains permits levels of crystallinity up to 95% [59]. It is believed that polyethylene chains fold in such a way that a structure is formed with an orthorhombic cell. These structural differences result in the associated thermal properties as outlined in Table 2 below.

Table 2: Thermal properties of a selection of polyethylenes [60].

Polymer	T_g / °C	T_m / °C
LDPE	-95	105-120
LLDPE	-110	110-130 (dependent on branching)
HDPE	-110	120-135

1.3.1.1 Low Density Polyethylene (LDPE)

First produced by ICI in 1933, this type of polyethylene is so-called due to the extensive long and short chain branching created as a result of inter molecular and intra molecular chain transfer, occurring during the polymerisation process. The free radical polymerisation process is initiated using benzoyl peroxide, and can be operated continuously, however care must be taken in dealing with the heat generated. Due to the energy intensive high pressure (1000-3000 atm) and high temperatures (80-300°C) used, extremely turbulent conditions are created within the reaction vessel. This manifests itself as the branching mentioned previously (Figure 4 [i]), resulting in a density range of 0.91-0.94 g cm^{-3}. As the reaction is highly exothermic, sufficient cooling must be employed to prevent any reaction runaway.

The short chain branches inhibit packing of PE chains into a crystal lattice, therefore the crystalline content of LDPE is relatively low (up to 40 %). The relatively low crystalline content causes LDPE to be fairly flexible, and the long chain branches can themselves become involved in crystal structures. This gives rise to entanglements that increase the melt strength of the material, a feature which facilitates film formation.

1.3.1.2 Linear low density polyethylene (LLDPE)

Due to the harsh reaction conditions required for LDPE production together with inherently poor control over the free radical polymerisation process, polymer chemists have derived an alternative route to a branched polyethylene that makes use of the low pressure Ziegler-Natta, and more recently metallocene, polymerisation processes. In LLDPE the branches are introduced via co-monomers; but-1-ene, hex-1-ene and oct-1-ene form ethyl, butyl and hexyl branches respectively. As both Ziegler-Natta and metallocene polymerisation are living polymerisation systems, the branching can be more precisely controlled by monomer feed, which is particularly true of metallocene polymerisation. LLDPE therefore has better mechanical properties than LDPE. However, omission of the long chain branches reduces melt strength, making film formation more difficult.

1.3.1.3 High Density polyethylene (HDPE)

In contrast to the harsh conditions required to create LDPE, HDPE is formed under low pressure / low temperature conditions using a Ziegler-Natta, metal oxide (Phillips), or more recently, metallocene catalyst system. A polyethylene that has very few if any branches is created, having a regular chain structure. This regularity allows the polymer chains to adopt a planar zigzag conformation and arrange into a highly ordered crystal structure. Due to this, crystalline contents potentially up to 90% are possible. Furthermore, this is reflected in the higher stiffness and higher heat distortion temperatures when compared to those of LDPE and LLDPE. It is worth noting however that while LDPE also crystallises in a

planar zig-zag, the crystalline portions are much shorter than those for HDPE. Thus the strength of the intermolecular forces are lower, leading to a lower T_m.

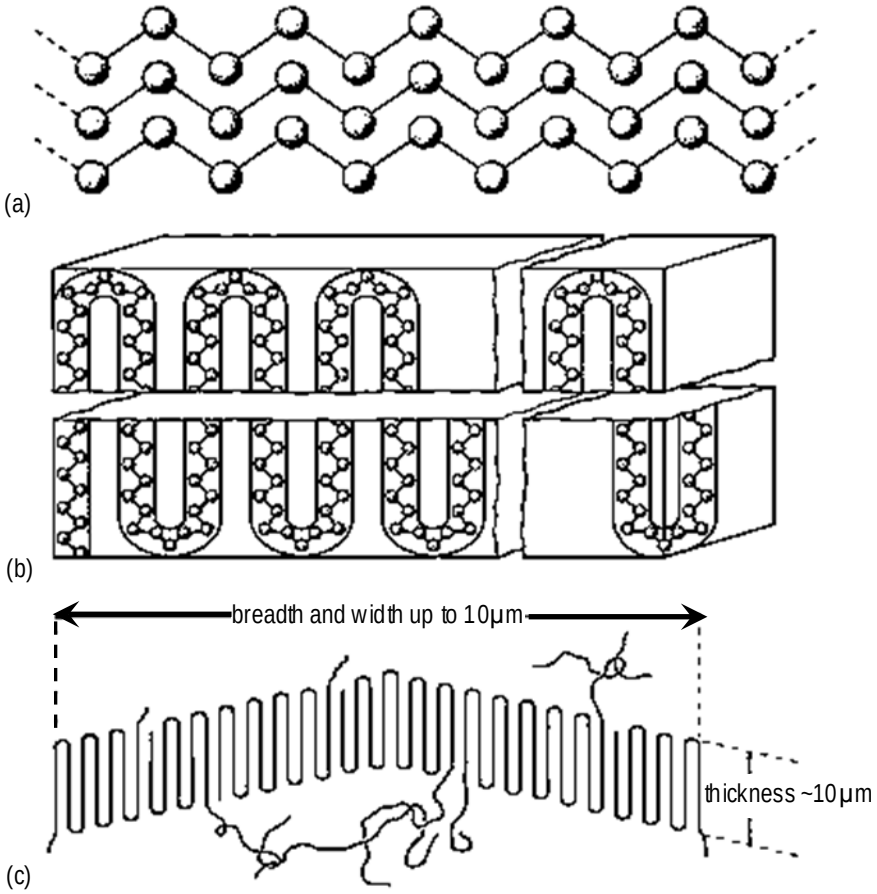

Figure 5: (a) Zig-zag conformation of PE, with stacking in crystal; (b) chain folded model for PE in lamella; (c) dimensions of PE single crystal showing non-crystalline tie molecules [61].

1.3.2 Polypropylene

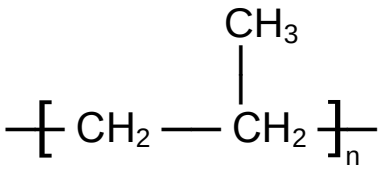

Figure 6: Repeat unit structure of polypropylene, where n represents the number of repeat units present.

In 1954, the advent of Ziegler-Natta polymerisation led to the possibility of polymerising higher olefins such that the stereochemistry of monomer addition to the active centre can be controlled. Due to the pendant methyl group present in the monomer propene, the regularity of (or in some instances lack thereof) the distribution of these pendant groups along the hydrocarbon backbone produces polymers with one of three distinct structures (Figure 7). Isotactic polypropylene is the form most widely produced, having a T_m of 160-165 ^oC and a crystalline content of around 60 %.

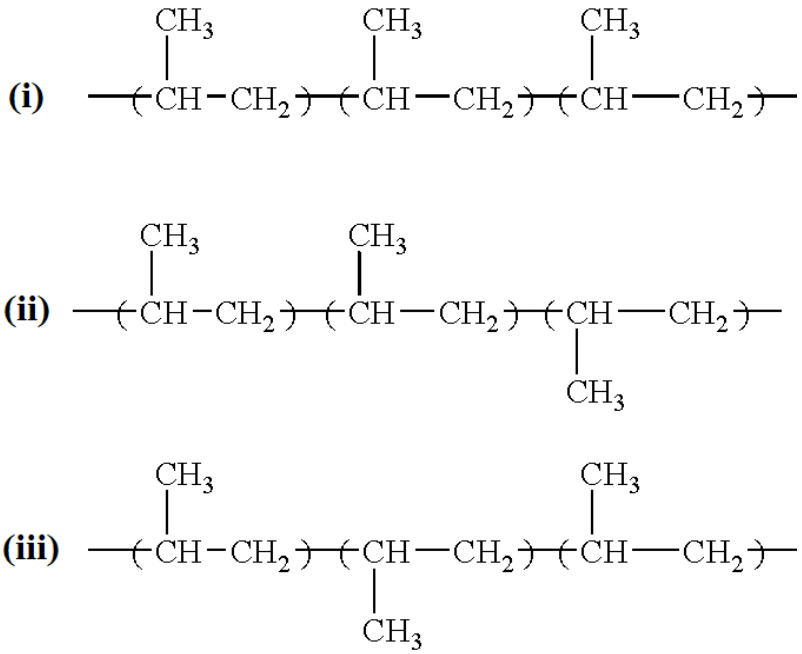

Figure 7: Tacticity in polypropylene; (i) isotactic, (ii) atactic, (iii) syndiotactic.

These pendant side groups also dictate the manner in which the polypropylene chains crystallise. Due to the steric hindrance produced by these groups, the chains can no-longer form a planar zigzag like that formed by PE chains. Instead,

a helical conformation is produced, where one turn of the helix is achieved after every three propylene repeat units.

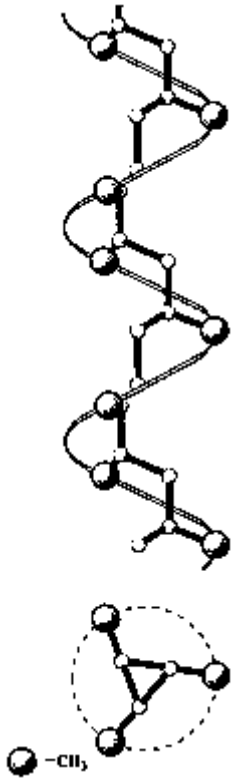

Figure 8: Helical conformation of isotactic polypropylene [62].

Isotactic polypropylene can adopt one of three crystalline forms: monoclinic (α), hexagonal (β) or trigonal (γ). The monoclinic α form is the most common, and is resultant from the majority of polypropylene melt processing. Furthermore, the most common crystal structure observed upon cooling of the polypropylene melt is the spherulite – as is usually the case with most crystalline polymers and is certainly the case with polyethylene.

1.4 Polyolefin blends

Whilst polyolefins are of a similar nature in terms of chemical composition and polarity, they will not form a miscible blend with useful mechanical properties, due to the different chain conformations that each polymer adopts in the crystal lattice. In polyethylene, a planar zigzag conformation is adopted in the crystal lattice (Figure 5), whereas polypropylene adopts a helical conformation where one rotation of the helix occurs in three repeat units (Figure 8). This makes miscibility

impossible, as co-crystallisation cannot occur - resulting in phase separation of the materials (Figure 9).

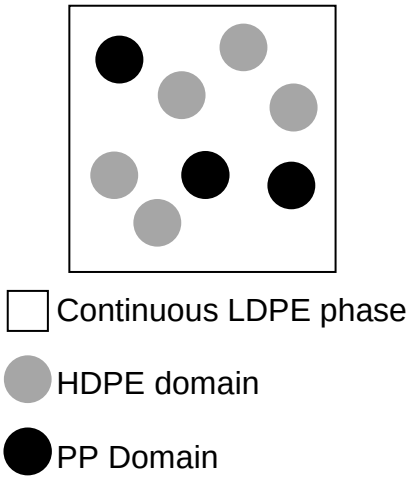

Figure 9: Schematic representation of phase separation in a ternary polymer blend.

It has been shown that miscibility is not possible as the two (or more) phases are found in the melt. Therefore, as phase separation occurs prior to cooling, the phases begin to crystallise independently of one-another. In the solid state, this results in droplets of one polymer dispersed in a continuous phase of another, which presents itself in the final blend or composite as poor mechanical properties, thus creating an essentially “weak” material. Furthermore, branching in low density polyethylene adds further complexity which needs to be considered in relation to miscibility of the polyethylenes with each other.

While HDPE and LDPE do not favour miscibility with PP, it is interesting to note that LLDPE has been shown to be at least partially miscible with PP. Various authors have shown that under the right conditions, 20 %/wt PP will begin to crystallise in molten LLDPE. As the PP crystallises, it grows into the LLDPE phase to produce diffuse spherulites with an almost fibrous appearance. This may be due to the structural and steric similarities between the methyl side groups present along the PP chains, and the short chain branches along the LLDPE chains [63].

Ideally, what is required is a system whereby the immiscible phases are joined in some way. The potentially poor mechanical properties of polyolefin blends,

particularly those based on post-consumer waste, necessitates compatibilisation in one form or another.

1.4.1 Co-polymer addition

One method of overcoming the problem of immiscibility is by adding varying amounts of co-polymers to improve mechanical properties [64 - 66] and even blending with peroxides [67]. This serves to disrupt phase separation of the immiscible phases creating a composite type material. While peroxides have been used, the literature shows that two different effects may be observed, as polyethylenes will generally undergo crosslinking and polypropylenes will undergo chain scission, creating rubbers and waxes respectively.

Another approach to overcoming this issue is the addition of a filler, which can be incorporated to improve mechanical properties and aesthetics. This discussion is developed further in the following sections.

1.5 Fillers in polyolefin blends

The incorporation of particulate fillers in polymer composites is well established, and a number of fillers are used depending on the properties required. These may include processability, formability and final application requirements of the finished part. Many fillers were used simply as a bulking agent, and served no purpose other than to reduce the cost of the final composite material [68 69]. However, more recently fillers can serve a more active role; for example, flame retardancy (e.g. magnesium and aluminium hydroxides - where thermal decomposition of the filler results in formation of their respective oxides and water, thus negating the requirement for [halogen based] flame retardant additives) [70].

Principal fillers tend to include clays, carbonates and talcs, each with their own composite enhancing properties. Due to the extent of previous work and information available in the literature [71, 72] with regards to fillers in polymers, only calcium carbonate is discussed in detail (Section 1.5.5).

1.5.1 Reinforcing fillers

While some fillers may be considered to be bulking agents with no purpose other than to reduce the final cost of a composite, there are those which are considered to be reinforcing or functional fillers. These fillers are incorporated to impart improved mechanical properties in the final article, including:

- increased stiffness and rigidity
- increased flexural modulus
- increased heat distortion temperature
- reduced creep
- reduced mould shrinkage

The properties obtained depend on many factors, including filler type, particle size, loading level and also surface treatment. These factors then dictate how the filler particles will interact with the polymer matrix, which in turn dictate the composite's final properties. Ergo, when attempting to make an assessment (either theoretically or mathematically) of a filled composite from its constituents, there are many variables to consider. This in turn makes the subject and its associated discussions inherently complex yet extremely interesting.

Firstly, the filler type can be classified by its microstructure, as illustrated in Figure 10. This microstructure can dictate the filler's effect on the final composite properties due to its aspect ratio. Fillers with a blocky, slightly irregular or spherical particle topography typically have aspect ratios from 1 to 3. While those of platy materials range from 10 to 20, and fibrous materials can have ratios well in excess of 100.

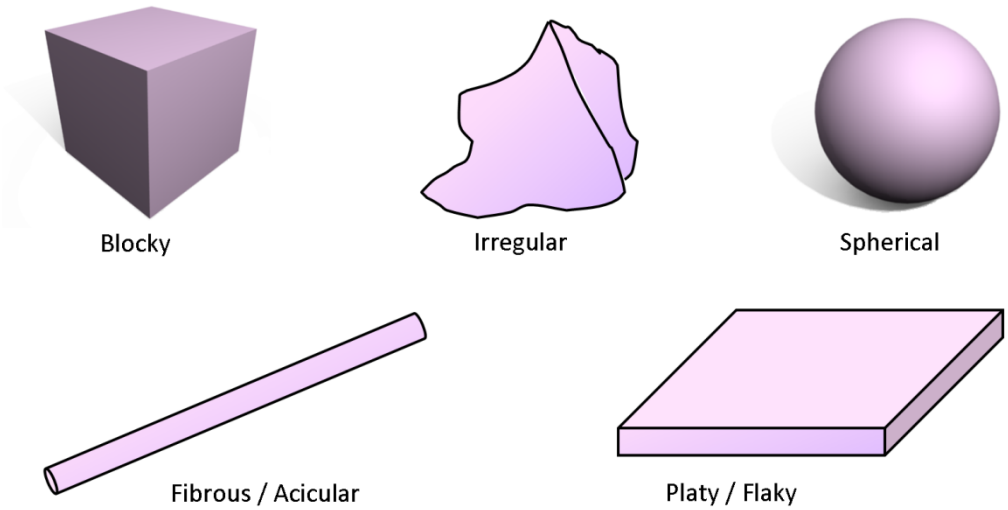

Figure 10: Schematic representation of various filler microstructures.

Higher aspect ratios are preferred due to their reinforcing capabilities, as their ability to transfer the applied forces and stresses from the bulk matrix is increased due to their highly penetrating nature.

One such example is that of glass-filled nylon. While nylon 6-6 alone has a tensile strength of 85 MPa, the presence of 30 wt % glass fibres has the effect of increasing this over two-fold to 186 MPa [73]. Furthermore, widespread use of carbon fibres mixed with epoxy resins to produce highly reinforced engineering composites can be noted. Due to the high-performance nature of these composites, their high strength-to-weight ratios make them extensively used throughout Formula 1 racing, the automotive and also the aerospace industries. Due to their high strength, rigidity and light weight, their prevalence is also becoming increasingly widespread in consumer applications such as fishing rods, laptops and even high-end loudspeaker systems [74].

1.5.2 Incorporation

1.5.2.1 Filler dispersion in polymer melts

Filler particles are often highly aggregated; if the aggregated state is retained in the polymer melt (and ultimately the solid polymer composite) the benefits of the filler will not be fully realised [75 - 77]. Hence it is imperative that these aggregates be reduced to agglomerates and be suitably dispersed throughout the polymer matrix. During dispersion of filler aggregates/agglomerates in the melt state, filler-filler interactions and filler-air interactions are replaced by polymer-filler interactions. The development of the latter interactions is dependent on the melt viscosity and how fast the polymer melt can wet the filler surface [78], which in turn depends on the filler particle's surface chemistry.

Break down of the agglomerates/aggregates is dependent on how effectively the filler-filler interactions are weakened by penetration of polymer into the aggregate and how effectively the shear stress in the melt is transferred to the aggregates. In order for this to occur, the relatively strong inter-particle Van-Der-Waals forces must first be overcome.

The ease of wetting of filler agglomerates and particles can be increased by chemical modification of the filler surface, which together with reduced filler-filler interaction, can increase the dispersion quality of fillers in polymers. This is achieved by lowering the surface energy of the filler particles to match that of the bulk polymer matrix; a process which is explored further in Section 1.6.

1.5.2.2 Filler addition

The simplest method of incorporating a mineral filler into a polymer melt is via agitated mixing. This process is utilised within the rubber industry to add carbon blacks to tyre compounds via an internal mixer. Within the mixer, paddles rotate to agitate the rubber and incorporate the particulate additives. While this is sufficient for compounding filled rubbers, the process would be unsuitable for thermoplastic composites due to the fact that the polymer's physical form is that of pellets.

Furthermore, the shear heating generated is insufficient to produce a melt; and this is also a batch process which can prove uneconomical in some instances.

Another approach is that of continuous production via extrusion, where the filler is usually fed into an extruder via a gravimetric feeder system, or in some instances via a master batch. For sufficient compounding, twin screw extruders are favoured over those with a single screw due to several advantageous factors:

- elimination of pre-blending steps
- more flexibility for downstream feeding and venting
- greater control of the mixing action

There are several configurations associated with this approach, which depends on where the filler is fed into the system. A straight forward method relies on gravity and drops the filler into the feed throat of the extruder along with the polymer. This method is acceptable for low filler levels, as there are various problems associated with the technique. Firstly, bridging may occur at higher loadings and secondly, filler agglomerates may be produced. These two situations arise due to the fact that a melt has not yet formed which is ready to accept and wet the filler particles. A more widely adopted approach is one where the filler is introduced via a side feed section which is downstream of the polymer feed section. With this arrangement, a melt has already formed, allowing better dispersion and reduced agglomeration of the particles.

Depending on the final application, typical filler levels utilised can range from 5 wt% to 40 wt% of the composite; and in some instances even up to 60 wt% in cable applications where a high proportion is required to produce the required flame retardancy.

As discussed previously, a twin screw extruder is usually required to sufficiently compound the composite materials, due to the high-shear conditions generated. These conditions facilitate the breakdown of aggregates and agglomerates, and also promote good dispersion of the filler particles throughout the polymer melt – during which the particles become wetted by the polymer matrix.

1.5.3 Effects of fillers on melt processing

The presence of hard particulate inclusions in a polymer melt with which the polymer chains can have varying degrees of interaction, can lead to a modification of polymer melt flow properties. Generally, melt viscosity increases as the level of filler increases, and as the maximum packing fraction ($V_{f\ max}$) of filler is approached the melt viscosity can increase very sharply (where maximum packing fraction is defined as the filler level at which the filler particles can touch each other). When this level is reached, the melt becomes excessively viscous resulting in unfavourable processing behaviour. The final composite can also become excessively brittle and thus unusable due to the fact that the system is now effectively a composite comprising of a majority proportion of filler with a small amount of binding polymer matrix.

In some instances low levels of a fine grade of filler can be added as a processing aid to lubricate the melt. Conversely, coarse grades with a large mean particle size can increase resistance to flow which increases the viscosity, and thus places higher torque and energy demands on the extruder. Furthermore, this increased melt viscosity drives an increase in shear heating, where the mechanical energy of the extruder screws is dissipated into thermal energy in the polymer melt. This can cause issues during processing (i.e. degradation of polymer/filler) where thermal runaway occurs if the extruder is not sufficiently cooled to offset the increased temperatures generated within the composite melt.

Another aspect to consider after the initial compounding step is the production of the final article. Although filled materials can be used to produce extruded products such as cables, window frames and decking boards, they are also used to produce parts which are injection moulded. The issues associated with the extrusion process have been discussed previously; however there can also be issues with injection moulding. For instance, if the compounded composite is too viscous, the moulding machine may not have sufficient pressure to inject the shot into the mould, resulting in a short-shot and hence an incomplete moulding. Furthermore, as mouldings become increasingly complex, mould designers are employing simulation models to predict how the mould is filled by the melt. If the

melt is more viscous than anticipated, the mould may not fill correctly resulting in weak or substandard parts [71, 72, 79].

1.5.4 Effects of fillers on mechanical properties

Addition of filler generally increases the stiffness of a composite, but can often reduce its strength and toughness. The latter effects are due to poor filler-matrix interaction often in combination with poor dispersion quality, where poorly bonded filler particles or agglomerates can be considered as defects within the matrix. Another consideration is that of particle size. If the filler particles are of a debated ideal size, then the elastic modulus can be increased due to the fact that the movement of the matrix is constrained by the immovable solid inclusions.

When considering reinforced composites, one approach to calculating the effect of the reinforcement on the matrix is to apply the rule of mixtures, which assumes that the overall modulus is equal to the sum of its parts:

$$E_c = (1 - V_f)E_p + V_f E_f \qquad \textbf{Equation 2}$$

where:

E_c = composite modulus
E_p = polymer modulus
E_f = filler modulus
V_f = volume fraction of filler

This is accurate at relatively low strain levels, where the modulus tends to increase with increasing volume percentage of filler [80].

With PP, which exhibits yield behaviour even at low strain rates, addition of mineral fillers can have a radical effect. Depending on the filler surface area, filler-matrix adhesion and the yield stress of the unfilled matrix, flexural and impact strengths can be increased. In most instances this is at the cost of a reduction in percentage elongation.

The filler dispersion quality, and filler-matrix adhesion, can be improved by chemical treatment or modification of the filler surface which is discussed in Section 1.6. One manifestation of increased filler-matrix adhesion is presented as an increase in the modulus of the final composite material.

1.5.5 Calcium carbonate

Calcium carbonate is a widely used filler in polymer composite systems, and is available in precipitated and ground forms, with the latter often being the cheaper option.

1.5.5.1 Forms of calcium carbonate

Calcium carbonate can exist in one of three polymorphs: aragonite, calcite and vaterite. Calcite is the most stable of these mineral forms and can be found as the major constituent of chalk, limestone and marble (Figure 11).

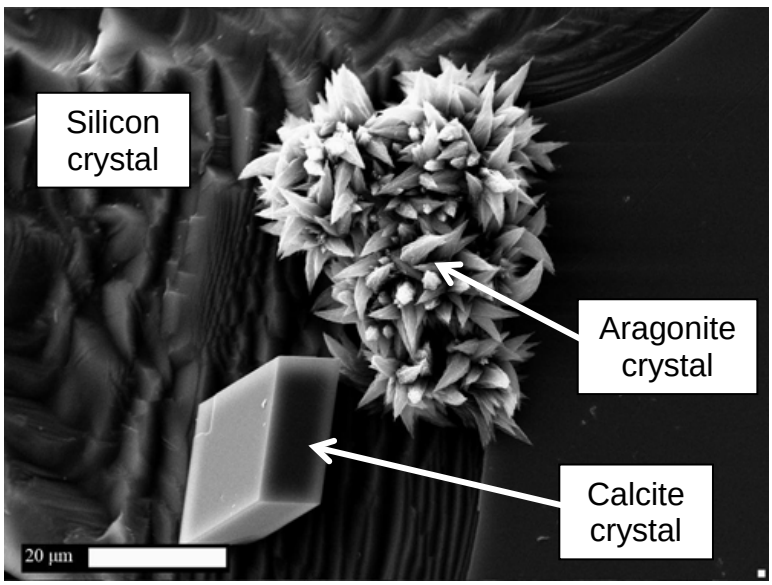

Figure 11: Polymorphs of calcium carbonate grown on the edge of a fractured silicon crystal. The rhombohedral structure is a single calcite crystal, while the polycrystalline structure is aragonite. [81]

Whilst these rock formations are sedimentary by origin, all exhibit different physical properties. For instance, chalk is a form of limestone, yet it is somewhat softer

than the latter as it is less compressed. Furthermore, marble is harder than limestone as it has undergone a high temperature, high pressure metamorphic process which forces recrystallization of the calcium carbonate to form small interlocked grains of calcite. This process also causes any impurities which are present to form grains; or in most instances forces the impurities to the grain boundaries which form the veins that are a visual characteristic of highly finished marble.

As a mineral filler, calcium carbonate is used as a white powder where various particle sizes are sorted to produce different grades of which in turn have different cost associations. While the grades comprised of the more coarse off-white particles may be cheaper, they do not favour incorporation into polymer composite systems due to their inherent yellowing of the final material. However, the finer whiter grades will incorporate much more easily, and produce better surface finishes of moulded articles – an aspect of which is reflected in their costs.

1.5.5.2 Production

The majority of calcium carbonate used in industrial processes is of the ground form (GCC), while that used in the pharmaceutical industry tends to be of the more costly precipitated variety (PCC). This is due to the fact that PCC is much more pure than GCC.

Much of the calcium carbonate used in the polymer industry is ground in one form or another, with beneficiation being the main process route. Through heavy processing and separation, powders with a mean particle size of 1-10μm are produced. As mentioned previously, finer purer grades produced from ground marble can command higher prices when compared to grades produced from chalks and limestones.

1.5.5.3 Uses

Calcium carbonate usage can be widely diverse, with applications ranging from construction to food. Furthermore, usage in the polymer industry is not exclusive to one specific polymer type.

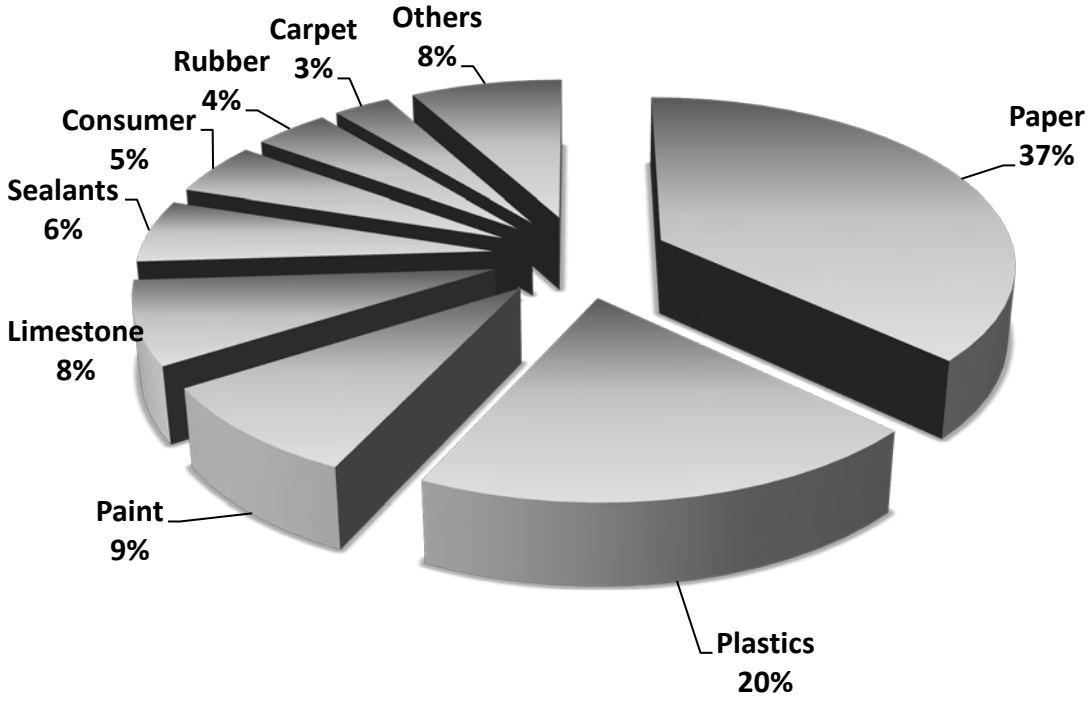

Figure 12: 2007 World estimated consumption of GCC. [82]

Figure 12 shows that after the paper industry, the polymer industry is the second major consumer of ground calcium carbonate in the world, while the rubber industry accounts for only 4%.

1.6 Filler surface modification

Agglomerated filler particles with poor dispersion and poor adhesion to the matrix tend to present themselves as defects in the final composite. As discussed previously, this is due to the particles acting as stress concentration points within the matrix. It is therefore desirable to create an increased level of interaction between these particles and the polymer matrix, in order to enable stress to be effectively transferred from matrix to filler and thus reinforce the composite. This can be achieved by means of surface treatment of the filler to modify how it interacts with the polymer chains within the continuous matrix. Filler surface modifiers can be divided broadly into two classes – dispersants and coupling agents (Table 3).

Table 3: An overview of different filler surface treatments.

<table>
<tr><th>Dispersants</th><th>Coupling Agents</th></tr>
<tr><td rowspan="3">Stearates</td><td>Silanes</td></tr>
<tr><td>Bismaleimides</td></tr>
<tr><td>Unsaturated Carboxylic Acids</td></tr>
<tr><td></td><td>Functionalised Polymers</td></tr>
<tr><td colspan="2">Titanates</td></tr>
</table>

1.6.1 Dispersants

Dispersants are able to strongly couple to the filler surface and possess chemical functionality to enable the filler surface energy and polarity to be modified such that it more closely matches that of the polymer matrix. This will enable the polymer melt to sufficiently wet the filler particles more rapidly and will also have the effect of reducing filler-filler and filler-air interactions within the aggregates. Both of these aspects can significantly increase filler dispersion quality. Whilst the wettability of the filler particles is improved in the melt state, the interaction between the “solidified” polymer and the filler particles can be greatly reduced;

relative to that where the polymer has wetted untreated filler. Due to a lack of polymer-reactive functionality, dispersants do not actively couple the matrix to the filler – at best molecular entanglement may occur. One such widely adopted dispersant is the unsaturated fatty acid: stearic acid [$CH_3(CH_2)_{16}COOH$] as illustrated in Figure 13.

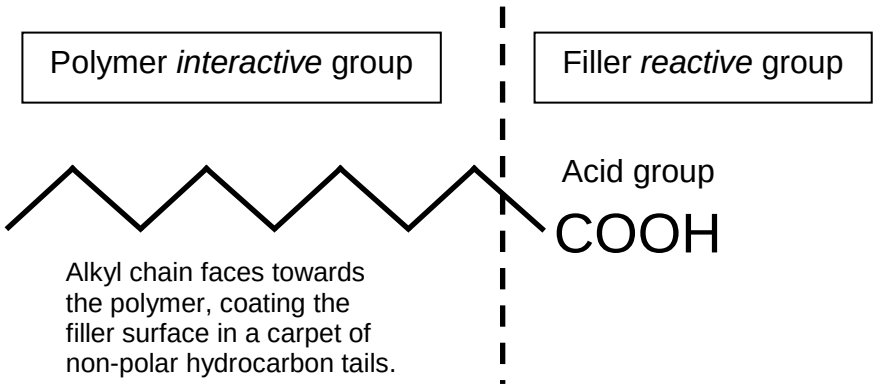

Figure 13: Representation of the stearic acid molecule.

The acid group undergoes an acid-base reaction with the filler surface and thus bonds to it, creating an organic surface coating that allows increased interaction with the bulk polymer matrix (Figure 14).

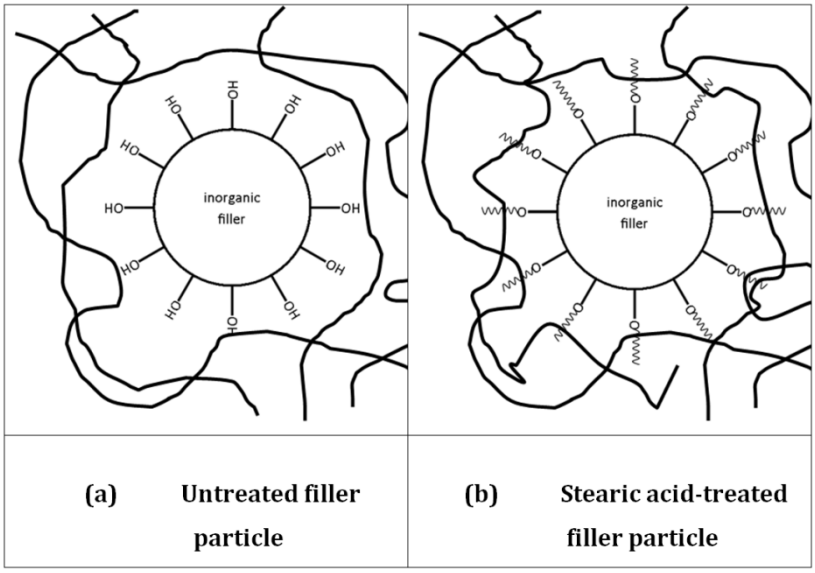

Figure 14: Schematic representation of the interactions between the polymer matrix and filler particles in (a) an untreated filler system, and (b) a stearic acid-treated filler system.

As shown in Figure 14(a), untreated filler particles exhibit little to no interaction with the bulk polymer matrix, resulting in poor dispersion and adhesion. However, the presence of a stearic acid surface treatment promotes some interaction between the hydrocarbon tails of the surface treatment molecules and the polymer chains of the bulk matrix. It is worth noting however that the hydrocarbon chain length of stearic acid is only 16-18 carbon atoms long, and thus not of sufficient length to entangle or transcrystallise with the polymer matrix. Therefore stearic acid is considered to be only weakly interacting, and the use of fatty acid coatings is characterised by low filler-polymer bond strength.

1.6.2 Silane coupling agents

In the 1940s, silane coupling agents originated from a need to treat glass fibres that were used to reinforce polyester resins. Following their commercialisation in the ‘50s, they are the most common of the coupling agents. Depending on their structure and the requisite functional groups present, silanes can range from weakly-interacting, to very strongly coupling.

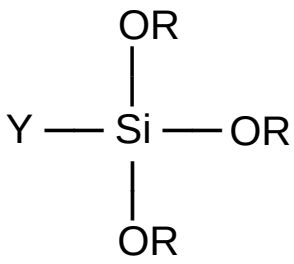

Figure 15: General formula for organosilanes, where OR is the silicon-functional group and Y is the organofunctional group.

The silicon atom at the centre brings together the polymer reactive Y group with the silicon-functional alkoxy groups which can interact with the filler surface and each other. As an adhesion promoter, the dual functionality of the molecule brings together the two weakly bonding dissimilar phases in the composite which are the organic polymer matrix and the inorganic filler particles. The organofunctional group can interact with the matrix through a variety of different mechanisms which include grafting, addition, hydrogen bonding, electrostatic attraction or simply by molecular entanglement. Often, the silicon-functional OR groups can react with OH groups on the filler surface and condense to form Si-O-Metal linkages or react with water to form a silanol group.

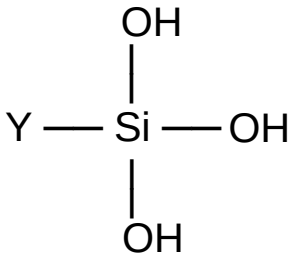

Figure 16: General formula for a silanol.

Due to the nature of the hydroxyl groups present, silanes are most effective with fillers which have high concentrations of reactive hydroxyl moieties at their surface, and as such are much less effective when used with carbonate-based mineral fillers. When treating the filler surface, the hydroxyl groups of the silane associate with the hydroxyl groups of the filler surface through hydrogen bonding (Figure 17). Once the associated water molecule is eliminated, the silane is then covalently-bonded to the filler surface.

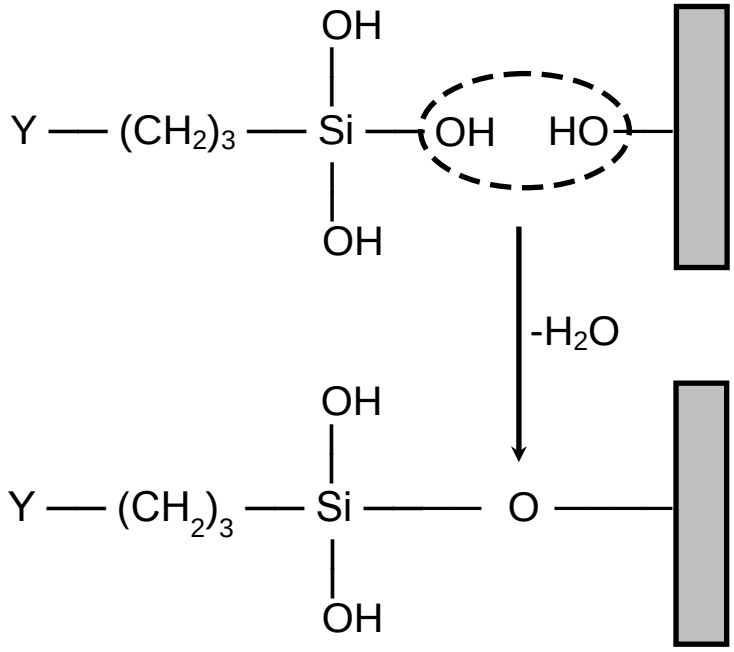

Figure 17: Schematic representation of reaction between a silane and a filler surface.

In order to sufficiently interact with the bulk polymer, the organofunctional group can be modified such that it mirrors the functionality of the host matrix. For instance, methacrylate functional silanes are utilised with acrylic polymers, while vinyl silanes are used to treat ATH in flame-retardant EVA composites. Finally, alkyl-functional silanes are used where polyolefins constitute the matrix material. In utilising this approach, the best compatibility can be realised, and the associated property enhancements can be obtained, including an increase in tensile strength and flexural modulus.

While silanes may be widely utilised in a variety of different polymeric materials across the industry, their effectiveness in PP-filled composites is somewhat disappointing when compared to other technologies [83]. Furthermore, along with

their reduced affinity for $CaCO_3$ particle surfaces, silanes have been deemed unsuitable for use in this study.

As such, the above information serves as a means of providing a historical context of the filler-matrix coupling concept and its origins.

1.6.3 Bismaleimide coupling agents

A comparative technology uses a multifunctional reactive monomer as a means of coupling an amphoteric filler to a polymer matrix by reactive compounding. 1,3-phenylene dimaleimide (BMI as shown in Figure 18) is melt blended in a similar manner to the C800 mentioned previously.

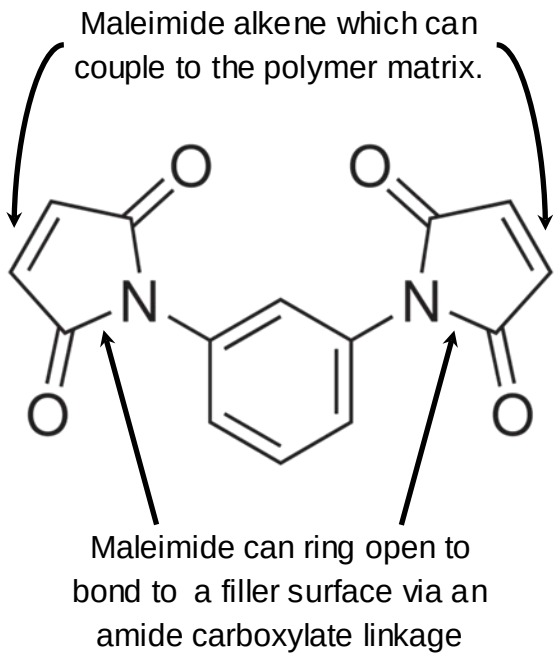

Figure 18: Chemical structure of the BMI monomer moiety and its associated functionalities.

This approach has already been implemented by Khunová et al [48], where BMI was used as a compatibilising coupling agent in composites based on post-consumer polyolefin waste and magnesium hydroxide. However, this approach results in a tendency for crosslinking of the matrix material, along with the associated toxicological risks posed with BMI. Furthermore the colour of the final composite

can be somewhat undesirable depending on the level of the treatment and the filler used as yellowing can occur.

1.6.4 Unsaturated carboxylic acid coupling agents

Coupling agents should ideally be able to do all that is described for dispersants in Section 1.6.1, but also have the ability to couple the matrix to the filler surface – i.e. be bi-functional. Figure 19 shows a representation of a coupling agent. Group Z (e.g. an acid group) should be able to react with the filler surface where hydroxyl (OH) groups are present. Group X (e.g. a vinyl group) can be included to couple to the polymer chains via macro-radical addition to an active double bond on the coupling agent molecule [83]. Alternatively, group X may be able to entangle with the polymer chains or form a polymerising network of coupling agent molecules [83]. Semi-crystalline polymers functionalised with filler reactive groups (e.g. maleanised PP) can also couple via transcrystallisation in addition to entanglement/trapping effects described above.

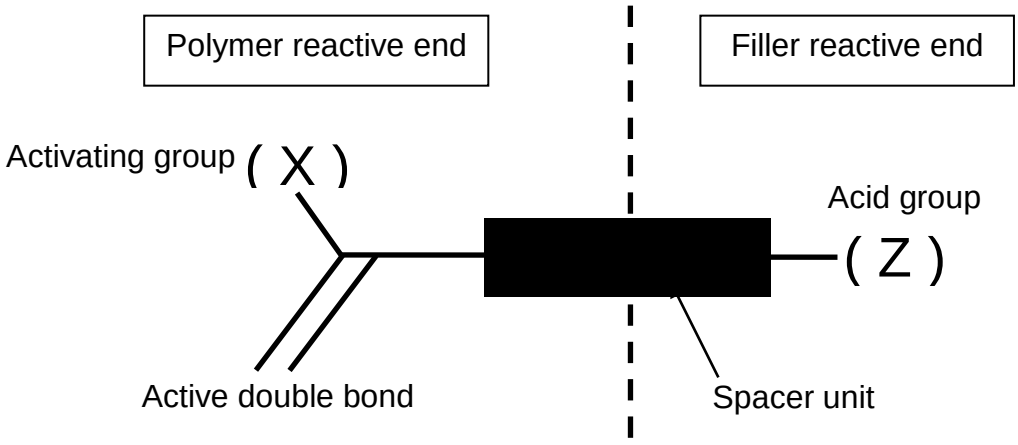

Figure 19: Representation of a coupling agent molecule.

A recently introduced coupling agent is Lubrizol Solplus C800, and it is anticipated that this molecule (and variations thereof) will have the ability to activate filler surfaces to enable compatibilisation of mixed polyolefin blends. Figure 20 illustrates the mechanism by which this process may occur.

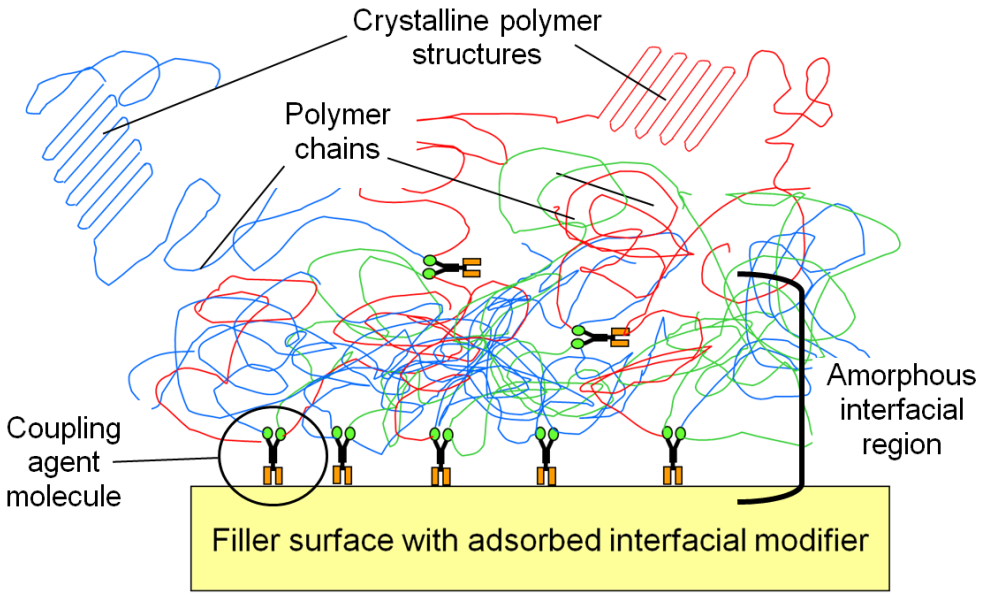

Figure 20: Schematic representation of the action of C800 at the filler surface/polymer matrix interface.

C800 attaches to basic filler surfaces via its acid group and associated acid-base reaction. Polymer macro-radicals (formed by mechanical shear or by peroxide addition) can add to the active double bond, and in turn then react with the polymer chains. In this way the immiscibility of the two polymers is overcome by using the filler ($CaCO_3$) and the coupling agent (C800) to act as the compatibilising interface, directly linking the filler surface to the polymers in the blend.

2 EXPERIMENTAL

2.1 Materials

Datasheets for the materials used in this section can be found in Appendix 2.

2.1.1 Polymers

2.1.1.1 Virgin polymers

The virgin polymers used in the study are shown in Table 4. From this point, the abbreviations in this report refer to the grades listed below, unless otherwise stated.

Table 4: Polymers used in the study.

Polymer	Manufacturer	Grade	Melt flow rate (dg min^{-1})
LDPE	LyondellBasell	Lupolen 3020EK	**0.5** (190°C / 2.16 kg)
HDPE	Borealis	MG7547S	**4** (190°C / 2.16 kg)
PP(1)	BP Solvay	HV001PF	**10** (230°C / 2.16 kg)
PP	Borealis	HD120MO	**8** (230°C / 2.16 kg)

The grades above were chosen to match as closely as possible those grades expected to be found in the post-consumer polymer packaging waste stream. These are extrusion grade LDPE used for film and carrier bag production, and injection moulding grades of both HDPE and PP used for pots, tubs and trays.

2.1.1.2 Post-industrial polymer waste (PIPW)

The PIPW was initially supplied in a washed flaked form of unknown provenance, which was then processed using a 40 mm Betol twin screw extruder at 200 °C and pelletised to form granules.

The PIPW was found to have the properties detailed in Table 5, where the % wt content of each polymer was calculated from DSC data as described in Section 3.3.1. Melt flow rate was determined according to BS1133, as described in Section 2.5.1.

Table 5: Composition data for samples of PIPW used.

PIPW Sample	PE Content (% wt)	PP Content (% wt)	Melt flow rate 230°C / 10 kg (dg min^{-1})
A	100	0	13.1
B	76	24	48.1
C	38	62	64.4

2.1.1.3 Post-consumer polyolefin waste (PCPW)

A sample of PCPW was also investigated, which was further float/sink separated according to the method followed by Khunová et al [48] in order to ensure any remaining non-polyolefin material was removed.

The PCPW was mostly polypropylene with smaller amounts of low and high density polyethylene and traces of other polymers (Table 6).

Table 6: Composition data for the PCPW sample used.

	LDPE	HDPE	PP	PS	PVC+PET
PCPW	**Composition (% wt)**				
	11.79	15.96	69.12	1.98	1.15

2.1.2 Coupling agent package and other additives

When first launched, Lubrizol Solplus® C800 was initially produced in a viscous liquid form. However, for ease of handling, a 50 % wt active powdered form was formulated, and has the trade name Solplus® C825. While Solplus® C800 was

used for the initial parts of this study, the powdered Solplus® C825 was used in the latter part of the study due to ease of handling and dosing control.

N.B. As the activity levels are taken into account when calculating the required addition levels of Solplus® (where C800 is 100% active and C825 is 50% active), the terms C800 and C825 used in subsequent sections are thus interchangeable as the coupling chemistry and technology is the same.

A small amount (see Section 2.1.3) of Akzo Nobel Perkadox® BC-40B-PD peroxide was used to initiate the coupling reaction. This is a 40 % wt active supported form of dicumyl peroxide which comes supplied as a white powder.

2.1.3 Fillers and surface modification

The filler used for the study was Imerys Carbital 110 ground marble (i.e. ground calcium carbonate - GCC), with an average particle size of 3 μm. The treated filler was produced in several batches by mixing 4 kg of untreated filler together with 1.2 % wt (on the weight of the filler) C825 (the active level of C800 was 0.6 % wt on the filler), and 5 % wt (on the C800 amount present) Perkadox® BC-40B-PD. This was then mixed by tumble blending in a large screw-top container. It should be noted that previous work has shown that in-situ treatment of filler via pre-mixing with C825 is just as effective at pre-treating the filler with the 100 % active C800 liquid [83].

2.2 Float-sink separation

In order to separate the post-consumer polymer waste, selective density separation was used. The separation media are detailed in Figure 21, where solutions of a known controlled density were produced to sequentially separate the fractions into identifiable groups via partitioning into a distinct floating and sinking fraction.

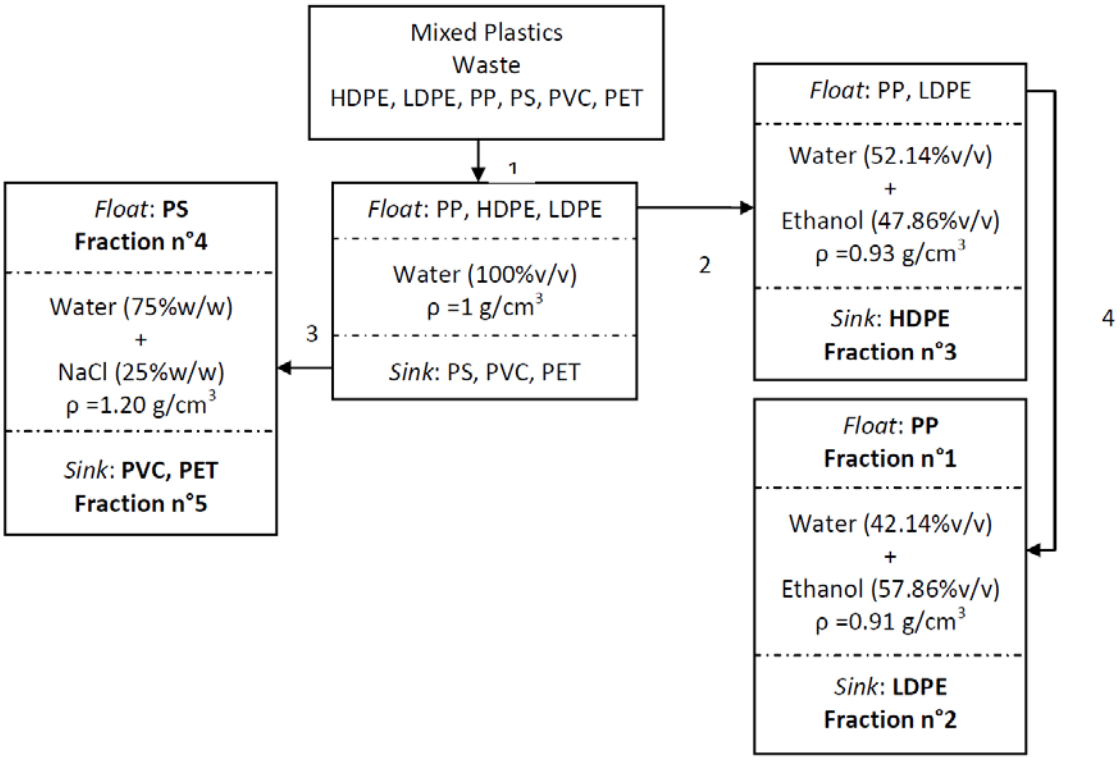

Figure 21: Schematic overview of the float-sink density separation process.

The regrind flakes were then dried in a Carbolitie oven at 80 °C for 20 minutes to remove any residual moisture.

2.3 Melt blending and test piece preparation

2.3.1 Haake Polydrive and compression moulding

For the initial classification work, a Haake Polydrive with a Rheomix 600 torque rheometer attachment was used. The mixing chamber was filled to 70% of its capacity which equated to a nominal sample size of around 50g. Samples were processed at 210 °C for 10 minutes, and then compression moulded at 200 °C for 2 minutes in a Bradley & Burton 50T electrically heated press. After this, the samples were removed and placed into a cooled Francis Shaw 50T press for a further 2 minutes to cool.

2.3.2 Twin screw extrusion and injection moulding procedures

Melt blending was carried out using a Thermo Electron HC24 twin screw extruder, with a length to diameter ratio of 28:1 and a barrel temperature of 200 °C. The output of the machine was kept to 8 kg hr^{-1} (± 0.15 kg hr^{-1}), which was passed through a water bath and subsequently pelletised. To remove any remaining moisture, the pellets were placed in a Carbolite oven at 80 °C for 20 minutes.

Once dry, the compounded material was injection moulded into tensile and impact test pieces according to BS 2782-9 (10 mm x 4 mm nominal cross section dimensions with a 50 mm gauge length) on a Battenfeld BA 230 CD Plus injection moulding machine, set at 50 °C mould temperature with a 200 °C barrel temperature and injection pressure nominally 40-50 bar.

2.4 Composite/blend preparation

2.4.1 Virgin blends

A series of virgin blends were produced in a Haake Polydrive (as per Section 2.3.1) with varying ratios of polyethylene (Borealis MG7547S) to polypropylene (BP Solvay HV001PF), and are set out in Table 7.

Table 7: Virgin blends produced using Haake Rheomix 600.

Identifier	PE content (% wt)	PP content (% wt)
H100	100	0
H95P5	95	5
H90P10	90	10
H85P15	85	15
H80P20	80	20
H75P25	75	25
H70P30	70	30
H65P35	65	35
H60P40	60	40
H55P45	55	45
H50P50	50	50
H45P55	45	55
H40P60	40	60
H35P65	35	65
H30P70	30	70
H25P75	25	75
H20P80	20	80
H15P85	15	85
H10P90	10	90
H5P95	5	95
P100	0	100

Next, Fourier transform infrared spectroscopy (FTIR) was performed on the compression moulded samples, along with differential scanning calorimetry. Both single bounce diamond attenuated total reflectance (ATR) and a single bounce silicon ATR objective fitted to a Thermo-Nicolet Continuum FTIR microscope were used. However, it was found that the single-bounce silicon ATR FTIR was too sensitive and returned IR spectra for only the surface layers of the analysed sample. Therefore it is worth noting that the FTIR spectra discussed in this thesis were produced using the single-bounce diamond ATR method as described in Section 2.5.4.

2.4.2 Composites based on virgin polymers

Composites were produced (as per Section 2.3.2) using virgin polymers with increasing levels of both untreated (U) and C800 treated fillers (M), as shown below (Table 8).

Table 8: Details of the virgin material composites produced.

Polymer	Sample ID	Untreated Filler level (% wt)
HDPE*	H100	0
	H100-33U	33
	H100-50U	50
	H100-60U	60
PP**	P100	0
	P100-33U	33
	P100-50U	50
	P100-60U	60
Polymer	**Sample ID**	**C800 Treated Filler level (% wt)**
HDPE*	H100	0
	H100-33M	33
	H100-50M	50
	H100-60M	60
PP**	P100	0
	P100-33M	33
	P100-50M	50
	P100-60M	60
*Borealis MG7547S / **Borealis HD120MO		

2.4.3 Composites based on post-industrial polymer waste

Composites were also produced (as per Section 2.3.2) using the post-industrial polymer waste (PIPW) with increasing levels of both untreated filler (U) (Table 9), and C825 treated filler (M) (Table 10).

Table 9: Details of the composites produced using PIPW and untreated filler.

PIPW Sample	Composite ID	Untreated Filler level (% wt)
A	A	0
	A-33U	33
	A-50U	50
	A-60U	60
B	B	0
	B-33U	33
	B-50U	50
	B-60U	60
C	C	0
	C-33U	33
	C-50U	50
	C-60U	60

Table 10: Details of the composites produced using PIPW and C825 treated filler (M).

Polymer	Sample ID	C800 Treated Filler level (% wt)
A	A	0
	A-33M	33
	A-50M	50
	A-60M	60
B	B	0
	B-33M	33
	B-50M	50
	B-60M	60
C	C	0
	C-33M	33
	C-50M	50
	C-60M	60

2.4.4 Composites based on post-consumer polymer waste

Upon initial investigation, it was found that the as-supplied PCPW was not completely free from undesirable non-polyolefinic materials. These presented themselves as unmelted defects in the final pellets, mainly of either PET or Nylon materials with a melt temperature substantially higher than that used for processing the polyolefin blend.

Such material was removed by performing a second floatation step on the material, where a further 5% was found to have a density greater than unity. The floating fraction was then dried at 50°C for 12 hours. Upon removal from the oven, it is worth noting that a strong musty odour was emitted on opening. This suggests that the PCPW was not thoroughly cleaned and devoid of all residues, resulting in obvious microbial growth.

After drying, the flakes were then compounded using a Betol single screw extruder with a 1mm mesh filter pack to further remove any remaining non-polyolefinic materials.

Table 11: Details of the composites produced using PCPW and both untreated (U) and C825 treated fillers (M)

Polymer	Sample ID	Untreated Filler level (% wt)
PCPW	PCPW	0
	PCPW-33U	33
	PCPW-50U	50
	PCPW-60U	60
Polymer	**Sample ID**	**C825 Treated Filler level (% wt)**
PCPW	PCPW	0
	PCPW-33M	33
	PCPW-50M	50
	PCPW-60M	60

2.4.5 Synthesis of novel coupling agent molecules

The new compounds were synthesised with the help of Lubrizol Ltd, the industrial partners in the project at Blackley, as part of the industrial placement aspect of the project. Two new and novel compounds were synthesised. The effectiveness and characteristics of these compounds are explored in Section 3.6.

2.5 Testing and characterisation

Examples of the raw data obtained from the methods employed in this section are given in Appendix 3.

2.5.1 Melt flow rate determination

Melt-flow rates (MFR) were obtained according to BS1133, using a Ray-Ran melt-flow indexer set at 200 °C with a 10 kg mass. The 10 kg mass was chosen due to the highly viscous nature of the composites tested, as a 2.16 kg mass did not produce cut-offs of an acceptable length. A small quantity of the sample to be tested was fed as chips into the barrel and the unloaded piston placed into the barrel, to allow the sample to heat for 5 minutes. After this time, the full 10 kg

mass was applied and cut-offs taken at suitable regular intervals between the two marks on the piston rod. The volume melt flow rate (VMFR) was calculated using the density of the polymer (or composite) and was quoted as the number of cm^3 of material extruded in 10 minutes. VMFR is a better comparison for filled composites, as density is taken into account. Furthermore, an error of 10% is assumed with this test method, and is expressed as such in Section 3 by the error bars.

2.5.2 Determination of mechanical properties

2.5.2.1 Tensile and flexural testing

Six moulded tensile test pieces (BS2782, 10 mm x 4 mm nominal cross sectional dimensions) per formulation were left for 1 week at 20 °C after injection moulding in order to stabilise. Testing was then carried out on a Hounsfield H10KS tensometer at 50 mm min^{-1} using the 100S/100R extensometer and a 10 kN load cell, which gives an error value of ± 0.1 MPa.

This machine was also used to test flexural properties at 5 mm min^{-1} to an end point of 16mm, using a three point bend attachment with a 64mm span width and a 1 kN load cell.

2.5.2.2 Impact testing

Impact testing was performed according to BS EN ISO 179-2:1999, on seven replicates of both notched and unnotched test pieces per sample. Notches were made using a 45° “v” notch broach. Notch depths and tip radii were 2 mm and 0.5 mm respectively. One of two Zwick impact testing machines was used, one with a 4 J tup and the other with a 50 J tup. For samples where the first test piece was unable to be fractured using the machine with the 4 J tup, subsequent samples were tested using the machine with the 50 J tup. Both machines have a margin of error of ± 0.05 J in their respective readouts, which combined with sample dimension measurement error of ± 0.01 mm gives an impact strength error of ±

0.01 kJm^{-2}. E.g. an average impact strength was obtained for five replicates and standard deviation was calculated.

If the sample was still not fractured using the machine with the larger tup, the value was noted as an energy of deformation rather than an impact strength.

2.5.3 Differential Scanning Calorimetry (DSC)

Differential scanning calorimetry (DSC) analysis was carried out using a Perkin Elmer DSC-7, with a heat-cool-heat cycle run at 20 °C min^{-1} under nitrogen. The initial starting temperature was set at 20 °C, increasing to 240 °C then held at this temperature for 5 minutes.

The sample was then cooled to 20 °C, and held at this temperature for 2 minutes, before being heated again to 240 °C. The DSC has a heat measuring accuracy of ± 1 %, which is insignificant in relation to the sample weighing error of ± 0.1 mg. The latter error gives a fusion enthalpy error of ± 0.11 J g^{-1}.

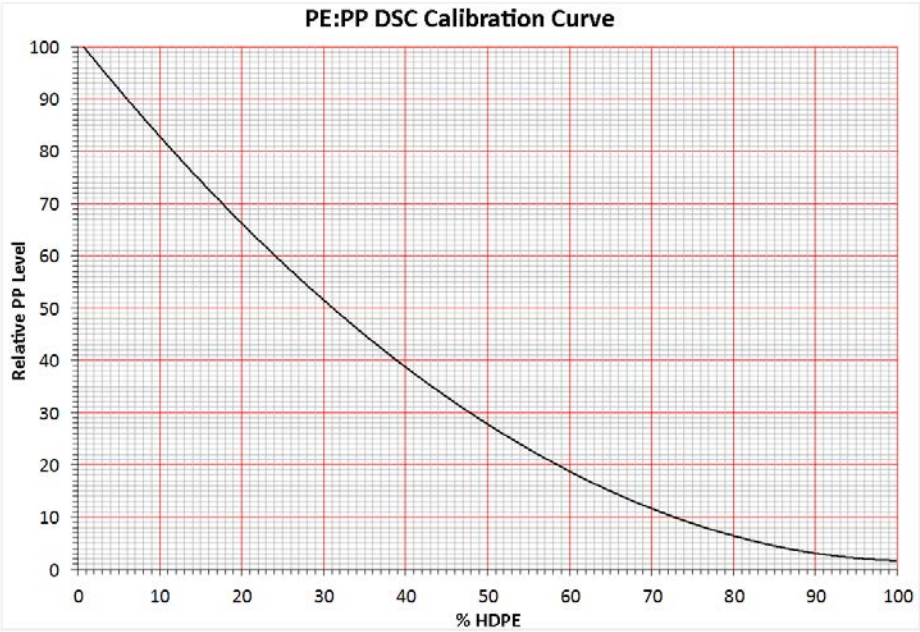

Figure 22: The DSC calibration curve generated from DSC data obtained from the virgin polymer blends.

DSC data was gathered from the blends produced in Section 2.4.1 to determine a relative percentage of PP in the blends using Equation 3, where the ΔH values are

the areas of the peaks observed. This relative percentage of PP was then plotted against the known level of HDPE in the blends to produce the calibration curve shown in Figure 22.

$$\text{Relative percentage of PP in blend} = \frac{(\Delta H_f)_{PP}}{(\Delta H_f)_{PP} + (\Delta H_f)_{HDPE}} x100 \qquad \textbf{Equation 3}$$

Where ΔH_f is the heat of fusion (determined from the peak areas as shown in Figure 23) and the subscripts PP and HDPE refer to the polypropylene and high density polyethylene fusion peaks, respectively. It is worth noting that the individual peaks were separate and well-defined with no observable overlapping.

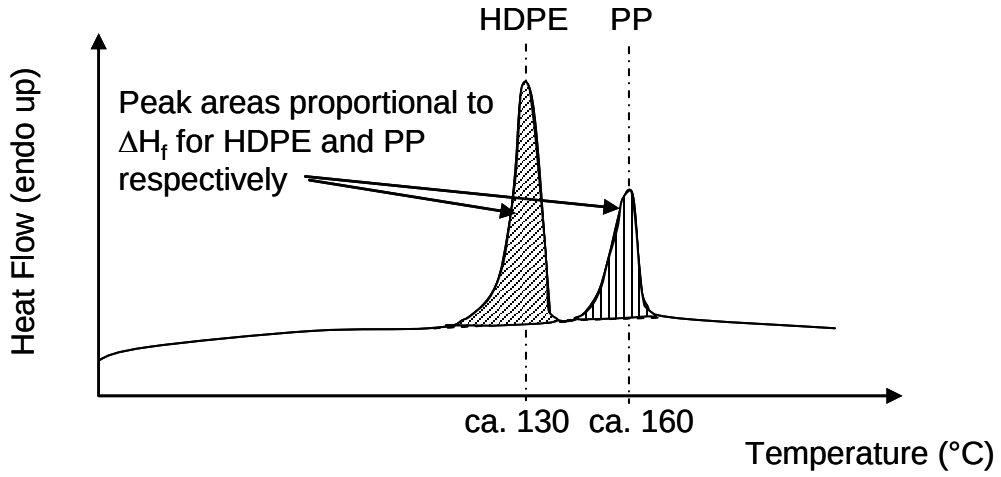

Figure 23: Schematic DSC data showing fusion endotherm peaks for HDPE and PP.

Samples of an unknown composition were then analysed using the DSC thermal cycle discussed earlier in this section, and the subsequent data was processed using Equation 3. The values produced by Equation 3 were then transcribed onto the calibration curve (Figure 22) to provide a ratio of PP and HDPE in the blends. This is possible due to the fact that the sample masses and ratios of polymers were known during the construction of the calibration curve. In turn, this permits the use of a simple ratio of peak areas to calculate the value which is transcribed.

2.5.4 Fourier Transform Infrared Spectroscopy (FTIR)

For the characterisation work, standard FT-IR was carried out using a Thermo Nicolet 380 FT-IR Spectrometer with a Smart Diamond ATR attachment. The micro FT-IR was carried out using a Thermo Nicolet Nexus 670. The instrument was run in reflectance mode using a Continuum microscope with a single-bounce objective ATR silicon crystal and an aperture size of 400 μm^2 (i.e. 200x200 µm). In both instances scanning rates were set at 160 scans at 4-bit resolution.

Spectra were collected and processed through the macro tool that was supplied within the instrument's OMNIC software, allowing exact peak values and areas to be obtained and calculated.

To produce the calibration curves used to obtain the data in Section 3.4.4, the intensity of the methylene C-H stretching (2915cm^{-1}) and methyl C-H stretching (2950 cm^1) peaks (see Appendix 3, Section VI) were determined from the spectra for the un-extracted samples (Figure 24). The composites and blends were then analysed and using the calibration curve data the relative PE level and percentage by weight PP content were calculated.

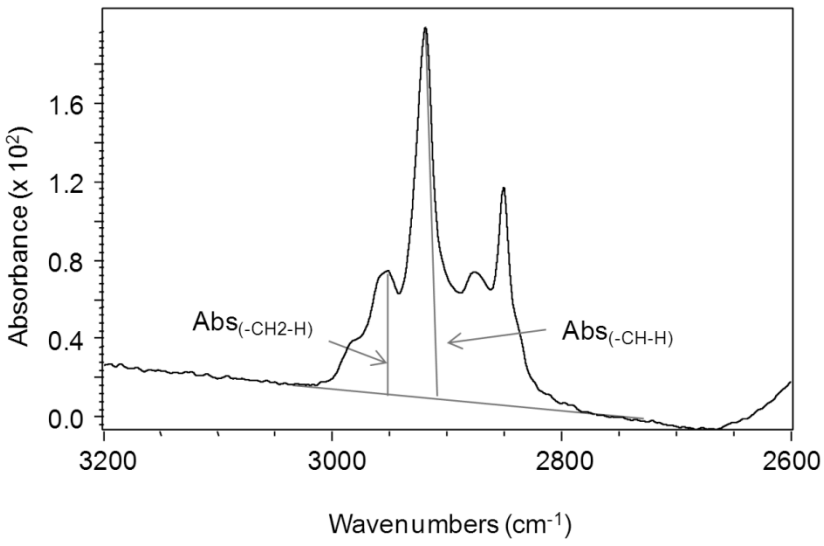

Figure 24: Schematic FT-IR spectrum of a composite, illustrating the peak values analysed.

After determining the peak height values, Equation 4 was used to calculate the relative PE level.

$$\text{Relative PE level} = \frac{I(>CH-H)_s}{I(>CH-H)_s + I(-CH_2-H)_s}$$ **Equation 4**

Where:

$I(>CH-H)_s$ = intensity of the methylene CH stretching peak

$I(>CH_2-H)_s$ = intensity of the methyl CH stretching peak

The relative PE level was then plotted against the known percentage of PP present in the blends and composites, to produce a calibration curve (Figure 25). Using the equation of the calibration curve (Figure 25), the percentage level of PP could be calculated (Equation 5).

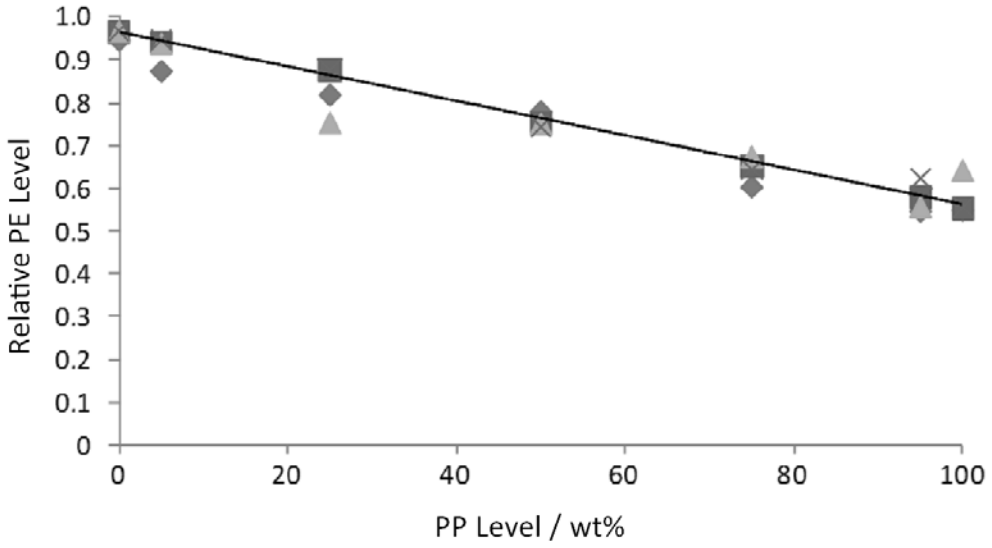

Figure 25: Calibration curve, where ◆ represents the unfilled blends, ■ represents the blends with the additive only, ▲ represents the blends with unmodified filler and ✕ represents the blends with modified filler.

$$y = -0.004x + 0.9647$$ **Equation 5**

Where:

y = Relative PE level

x = %PP

For example, the H25P75U TR sample gave peak values of:

- Left peak (2950cm^{-1} CH_2-H):0.0456
- Right peak (2915cm^{-1} CH-H): 0.0897

Therefore, using the formula the relative PE level is 0.6630. Thus using the equation of the calibration curve, the percentage of PP present is 75.43%.

Conversely, for the bound polymer content the peak areas at 3025-2775 cm^{-1} (C-H) and 892-829 cm^{-1}(CO_3) illustrated in Figure 26 were ratioed ($A_{(C-H)}/A_{(CO3)}$) and then plotted against the TGA values obtained for the samples.

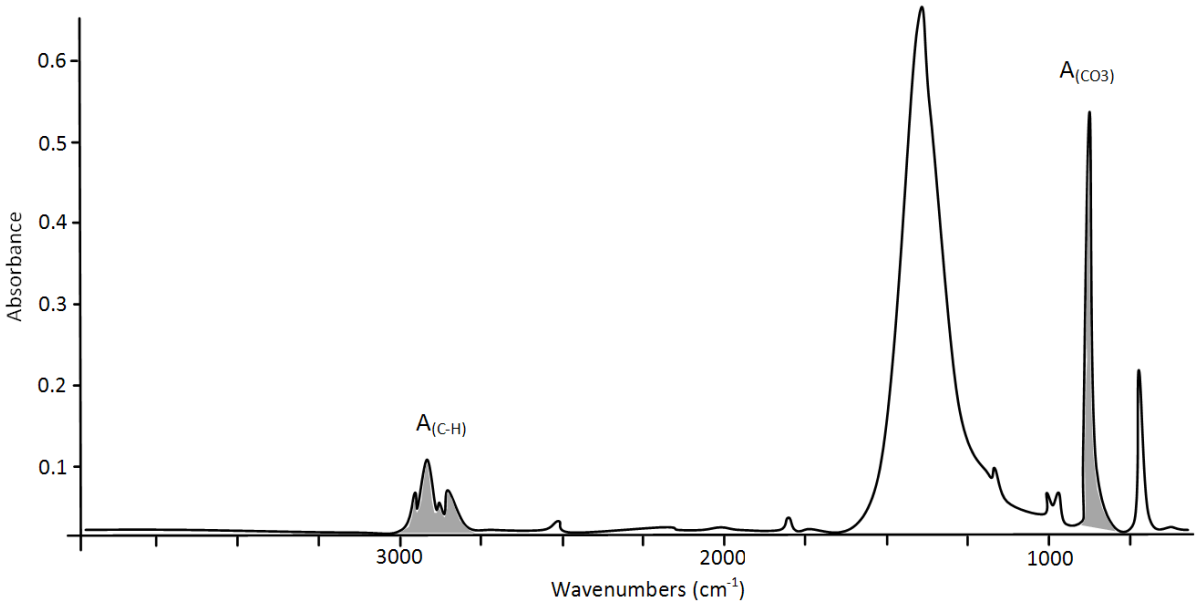

Figure 26: Schematic FTIR spectrum highlighting the peak areas for the C-H and CO_3 peaks.

2.5.5 Dynamic Mechanical Thermal Analysis (DMTA)

As an alternative approach to using FTIR to create a calibration curve, dynamic mechanical thermal analysis (DMTA) was investigated using a Perkin Elmer DMA 7e mechanical analyser. 2mm thick samples were fashioned into strips that fit into the grips of the machine. Samples were then heated from -70°C to 150°C at a rate of 20°C/min whilst being subjected to a dynamic force of 5N at frequency 10Hz.

2.5.6 Solvent extraction of unbound matrix

To investigate the percentage of bound matrix in the composites a Sohxlet extraction was carried out. Samples were pre-extracted in hexane for 8 hours at 140°C to remove any peroxide and/or anti-oxidants that were present in the polymers. Next, the samples were extracted for 16 hours in decane at 185°C, but upon investigation it was found that the lagged extractors were not reaching the required temperature. Subsequently, the samples were enclosed in small packets constructed from filter paper and submersed directly into boiling xylene rather than in the usual Soxhlet thimble arrangement. The samples were weighed before and after to assess the percentage mass loss. Furthermore, the remaining residues were subjected to thermo-gravimetric analysis to determine the levels of polymer present after extraction (see Section 2.5.7).

2.5.7 Thermo-Gravimetric Analysis (TGA)

To perform thermo-gravimetric analysis, a Netzsch TG 209 cell was used in conjunction with a TASC 414/3 controller. Samples were heated from room temperature (c.a. 20°C) to 700°C at 20° min^{-1} and the data logged via a connected PC. Printouts were then produced via the logging software (Figure 27).

In order to calculate the percentage of bound polymer matrix, sample weights were recorded before and after each TGA run. The final mass (before the subsequent decomposition of the $CaCO_3$) was then divided by the initial mass and multiplied by 100 to give the percentage of bound polymer.

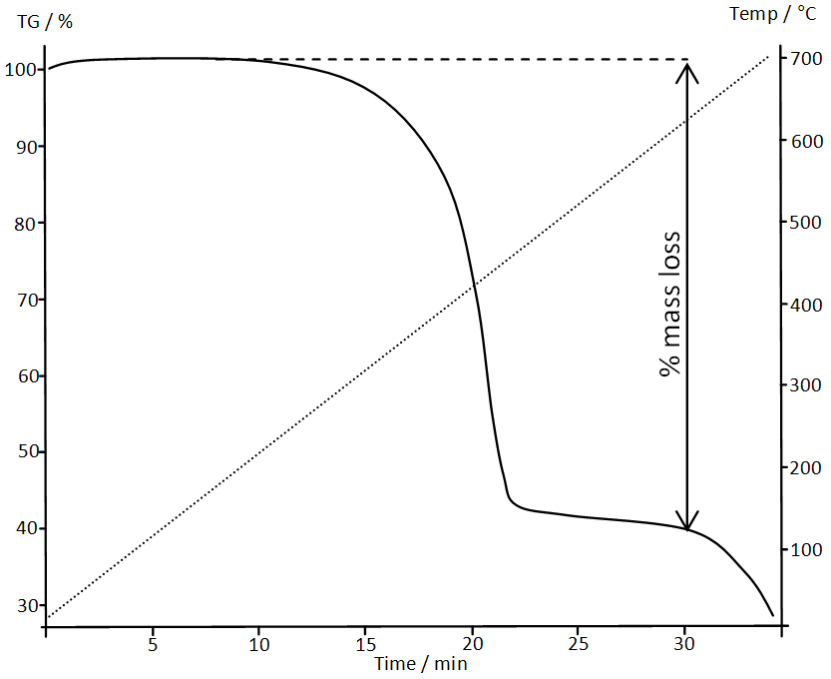

Figure 27: Schematic representation of a TGA plot.

Furthermore, as Figure 27 shows that the $CaCO_3$ began to decompose at around 650°C, the percentage of mass lost during this decomposition was taken into account when calculating the percentage of bound polymer.

3 RESULTS AND DISCUSSION

This section presents the progression of work and results as follows.

Firstly, Section 3.1 discusses the effects of C800 in post-consumer polymer waste.

Due to the observation that the post-consumer polymer waste was significantly degraded and contaminated, work progressed to better understand the effects of the coupling agent on individual polymers by incorporating differing levels of filler, which is discussed in Section 3.2.

A much-less degraded series of uncontaminated post-industrial polymer waste samples were then analysed and processed to again attempt compatibilisation of 'real-world' examples of mixed polyolefin waste. Section 3.3 details this work and highlights trends that suggest the ratio of the HDPE to PP component plays an important role in determining properties in the final material, and that there are a series of complex interactions taking place within the composites.

To better understand the complex interactions and their effects on the final materials, a series of polyolefin blends and composites were produced. Section 3.4 details these effects by investigating the properties of:

- unfilled polyolefin blends
- polyolefin blends with C800 and peroxide (i.e. the additive package)
- polyolefin blends with unmodified filler
- polyolefin blends with modified filler (filler treated with the additive package)

Section 3.5 then goes on to discuss the limitations associated with the C800 modification system, while Section 3.6 details the attempts at overcoming the aforementioned limitations.

3.1 Effect of Solplus C825/GCC on compatibilisation of post-consumer polyolefin waste

Initial work was carried out on a sample of flaked post-consumer polymer waste (PCPW). The material was supplied as the floating fraction of a float-sink process (in water), and was assumed to comprise solely of polyolefin material. This was brought into question when the material was processed alone, and with both unmodified and modified filler. During testing, the composites produced had poor mechanical properties compared to those of the PIPW samples produced (Section 3.3). It was found however, that this was due to defects in the material that were acting as failure points (Figure 28). These defects were in fact small particles of unmelted material, assumed to be denser polymers (such as polyethylene terephthalate, polyamides or styrenics) that had evaded the float-sink separation process.

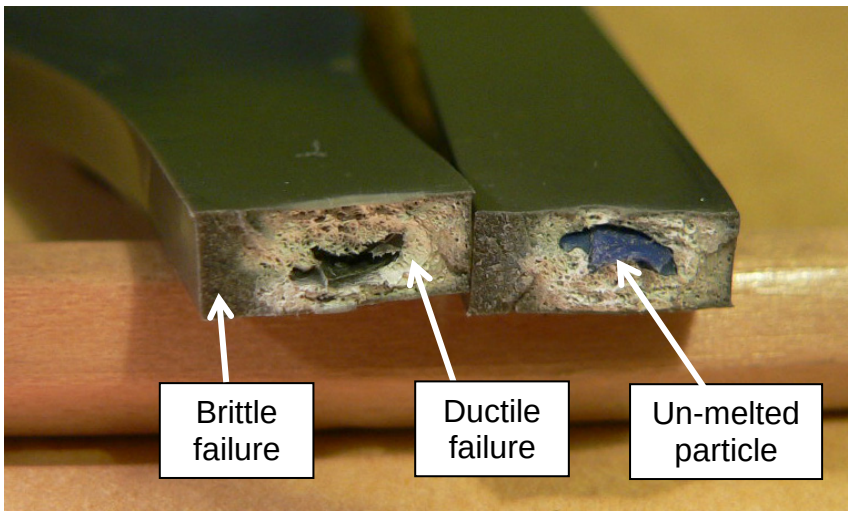

Figure 28: An un-melted particle that has acted as a stress concentrator in a tensile test specimen.

To investigate this problem, a second float-sink procedure was performed in water using a small amount of surfactant, which verified that this was indeed the case (Figure 29). It is evident that unless an improved separation is used, defects in the mouldings will adversely affect the properties of the composites formed regardless of the effectiveness of the compatibilising system used.

Figure 29: Image of a second float-sink separation process. The denser, non-polyolefinic fraction can be seen at the bottom of the beaker.

When comparing the results from the primary and secondary float-sink separation process, it can be seen that further removal of any non-polyolefinic material has a mostly marginal effect on the mechanical properties. Where tensile strength is concerned, a slight improvement of around 2 MPa can be observed (Figure 30).

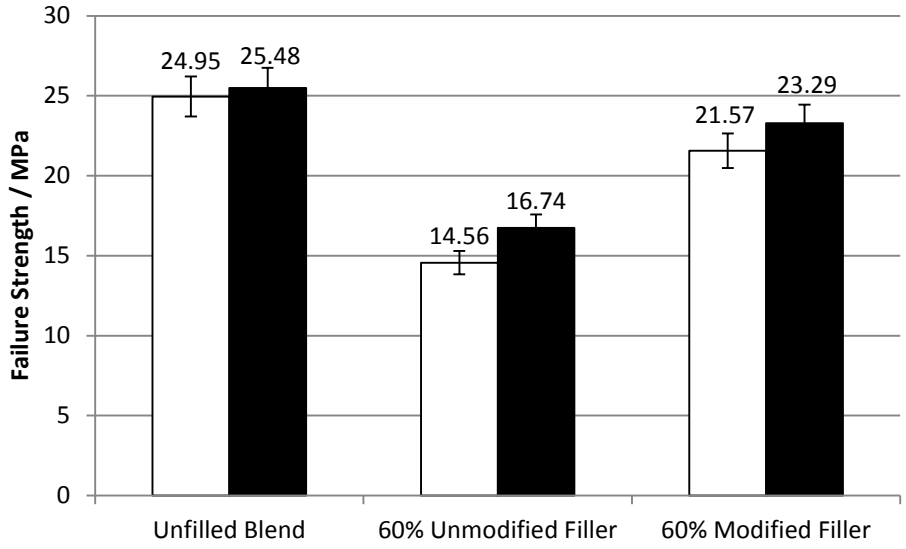

Figure 30: Failure strength of PCPW composites, where the white bars represent the primary float-sunk material and the black bars represent the secondary float-sunk material.

Furthermore, the percentage elongation (Figure 31) is almost doubled for the unfilled and unmodified filler blends, but only increased by around 1% for the blend incorporating the modified filler.

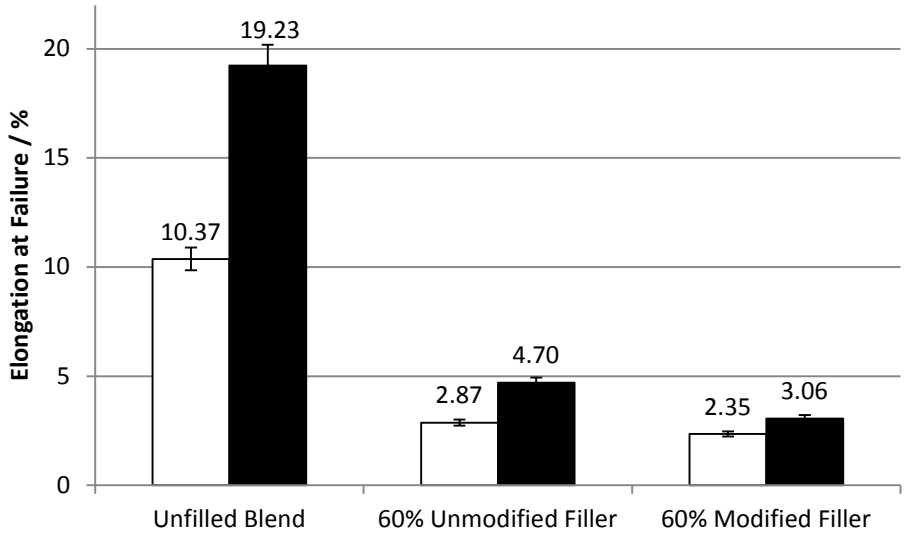

Figure 31: Elongation at failure of PCPW composites, where the white bars represent the primary float-sunk material and the black bars represent the secondary float-sunk material.

It is interesting to note the effect that the secondary separation had on the flexural modulus of the filled blends (Figure 32), where it appears to have resulted in a slight reduction in modulus. However, in the case of the unfilled blend, the modulus has been slightly increased.

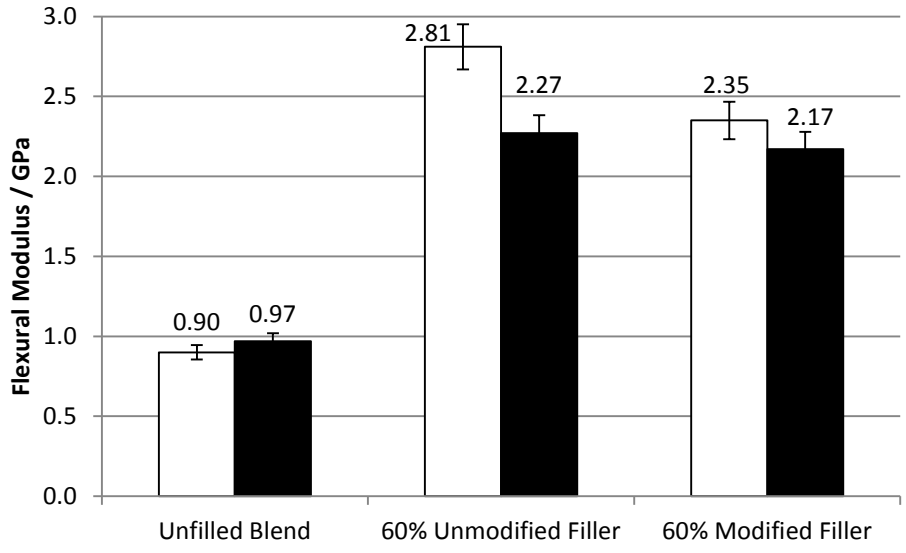

Figure 32: Flexural modulus of PCPW composites, where the white bars represent the primary float-sunk material and the black bars represent the secondary float-sunk material.

As is to be expected, an increase is observed upon adding filler, with the surface treatment having the effect of maintaining the stiffness observed for the unmodified filler.

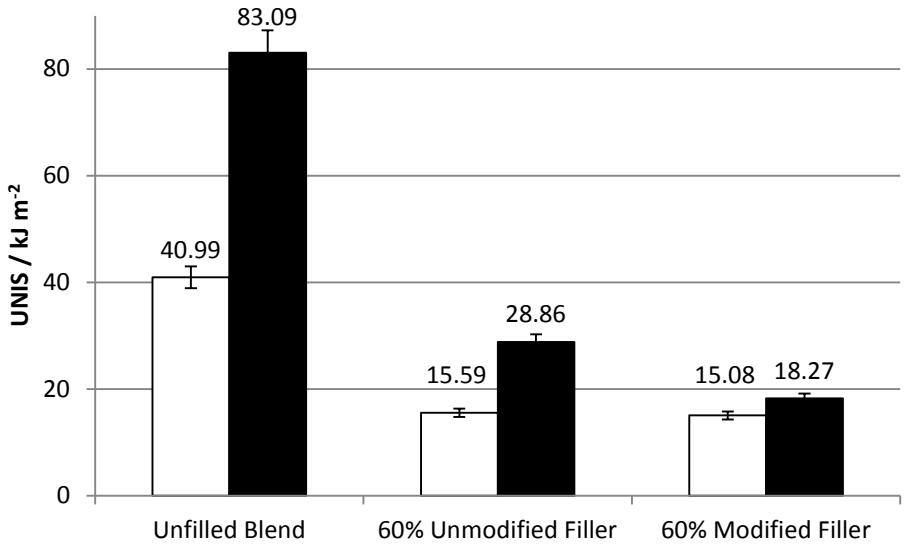

Figure 33: Un-notched impact strength of PCPW composites, where the white bars represent the primary float-sunk material and the black bars represent the secondary float-sunk material.

Un-notched impact properties were mostly doubled by performing the secondary separation process (Figure 33). This resulted in an impact strength of 80 kJ m^{-2} for the unfilled blend and around 30 kJ m^{-2} for the blend using unmodified filler. The increase was less pronounced when the modified filler was used, as an improvement of only 3 kJm^{-2} was recorded.

3.1.1 Comprehensive classification of PCPW

3.1.1.1 Separation method and results

The post-consumer polymer waste (PCPW) was sequentially float-sink separated as described in Section 2.2. After the separations, all of the fractions were weighed to determine the percentage of each fraction compared with the initial mass of the PCPW. Each fraction was expected to contain a majority of a given polymer. For instance, the second fraction was expected to be composed mainly of LDPE. There are however several caveats which could go some way to explain the dependability of the separation process:

- The small plastic flakes (regrind) may be coagulated; hence two different polymers could be present in the same fraction.
- The polymer wastes were not pure polymer and so their densities might not be the expected value.
- The experimental error associated with creating the density solutions may somewhat compromise the separation process results.

The initial mixture was first placed in water ($\rho = 1$) which produces a floating polyolefin fraction (Fraction i) and a sinking fraction (Fraction ii), which consists of PVC, PET and PS. Fraction i was then placed in a water/ethanol solution of density 0.93, which produced a PP/LDPE floating fraction (Fraction iii) and a HDPE sinking fraction (Fraction 3).

Fraction iii was then placed in a water/ethanol solution of density 0.91, where the PP fraction floated (Fraction 1) and the LDPE fraction sank (Fraction 2). Finally, Fraction ii was placed in a NaCl/water solution of density 1.2 to produce a floating PS fraction (Fraction 4) and a sinking fraction composed of PET and PVC (Fraction 5). This procedure is summarised in Figure 34 and the results are presented in Table 12.

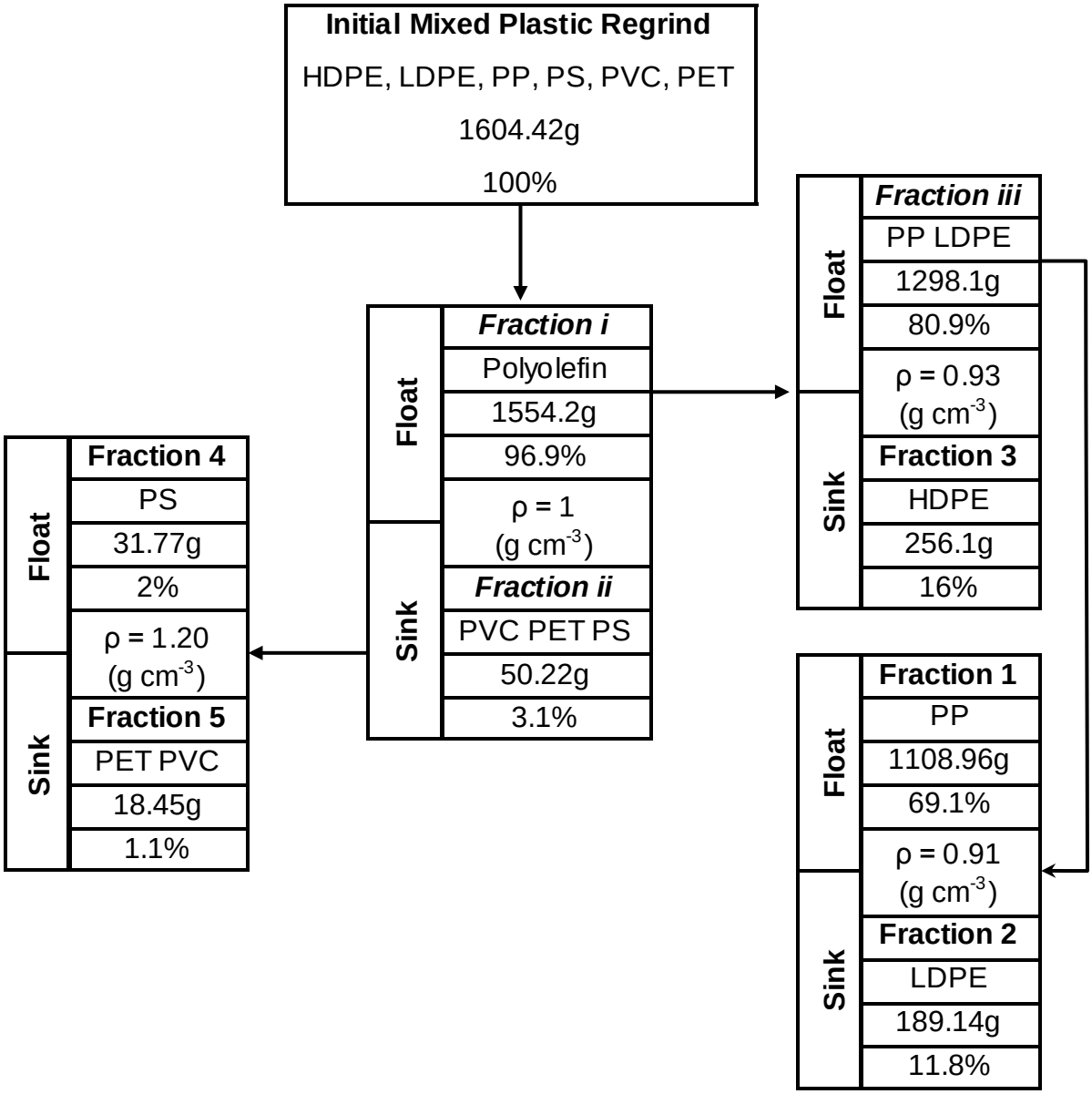

Figure 34: Schematic overview of the sequential float-sink separation process.

Table 12: Sequential float-sink separation fraction results.

Fraction	Fraction 1	Fraction 2	Fraction 3	Fraction 4	Fraction 5	Total
Expected polymer	PP	LDPE	HDPE	PS	PET/PVC	
% w/w	69.1	11.8	16	2	1.1	100

For all of the separations the main polymer constituent floated. The post-consumer polymer waste was mainly composed of polyolefinic materials; the non-polyolefin fractions represented just 3.13 % w/w of the post-consumer waste. The

polypropylene fraction was the most notable fraction, as it was significantly higher than would be expected based on the WRAP data presented in Table 1.

In order to confirm that the samples obtained via the separation process were indeed those expected, FTIR was used to confirm that these expected polymers had in fact been obtained.

3.1.1.2 FTIR results

A selection of regrind flakes were taken from each fraction and their infra-red spectra obtained. It was important that the selected regrind flakes were representative of the expected fraction composition. Therefore the flakes were closely scrutinised and sorted by colour and appearance. The different spectra were classified according to their corresponding expected polymers. Only the polyolefin fractions were analysed extensively to assess their actual compositions.

The polypropylene regrind flakes from the separation process gave the expected PP spectrum as shown in Figure 35.

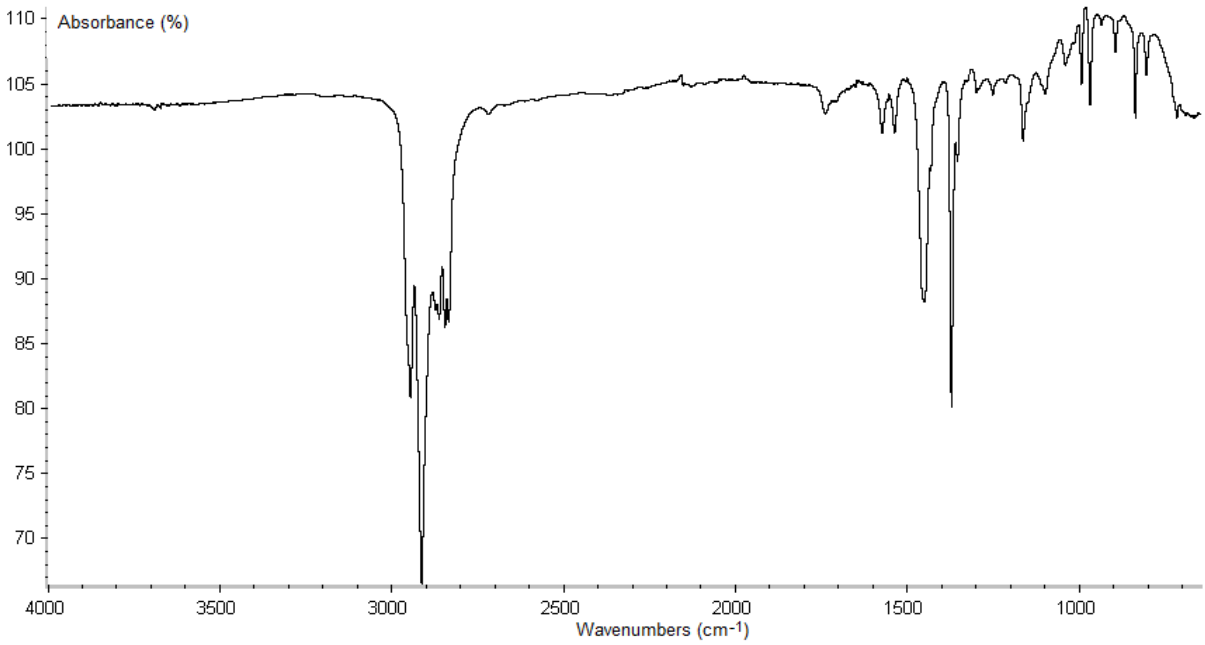

Figure 35: A selected PP regrind FT-IR spectrum.

Table 13: The associated interpretations for an FT-IR spectrum for PP.

Frequency range (cm^{-1})	Vibration	Intensity
2950	CH_3 Stretching	Strong
2915	CH_2 Asymmetrical stretching	Strong
2837	CH_2 Symmetrical stretching	Medium to strong
1460	CH_2 Scissoring	Medium to strong
1380	CH_3 Bending	Strong

The presence of the CH_3 branching in the repeat unit of the polypropylene led to the appearance of the characteristic strong peaks of the methyl group. It was therefore concluded that this fraction was PP.

The LDPE regrind flakes from the separation also gave the expected associated spectrum (Figure 36).

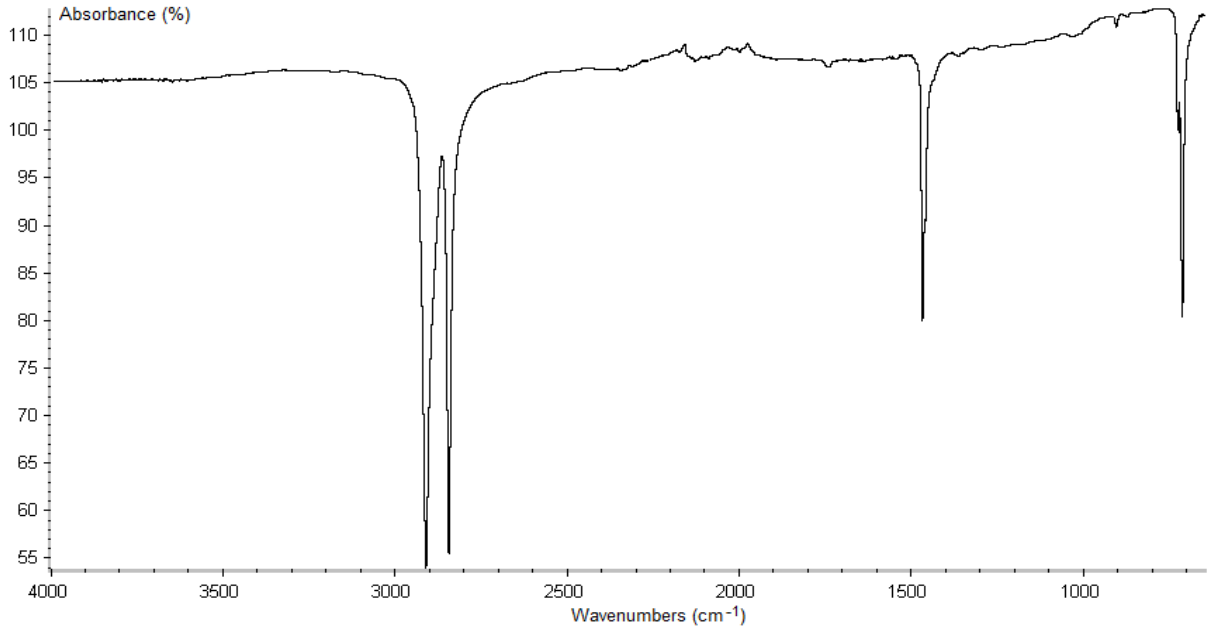

Figure 36: A selected LDPE regrind FT-IR spectrum.

Table 14: The associated interpretations for an FT-IR spectrum for LDPE.

Frequency range (cm^{-1})	**Vibration**	**Intensity**
2915	CH_2 Asymmetrical stretching	Strong
2850	CH_2 Symmetrical stretching	Strong
1470	CH_2 Scissoring	Medium
720	CH_2 Rocking	Medium to weak

Due to the relatively basic structure of polyethylene, the infrared spectrum of LDPE is very straight forward. It has only the peaks present corresponding to the associated CH_2 groups (Figure 36).

Finally, the HDPE regrind flakes from the separation gave a spectrum similar to HDPE (Figure 37).

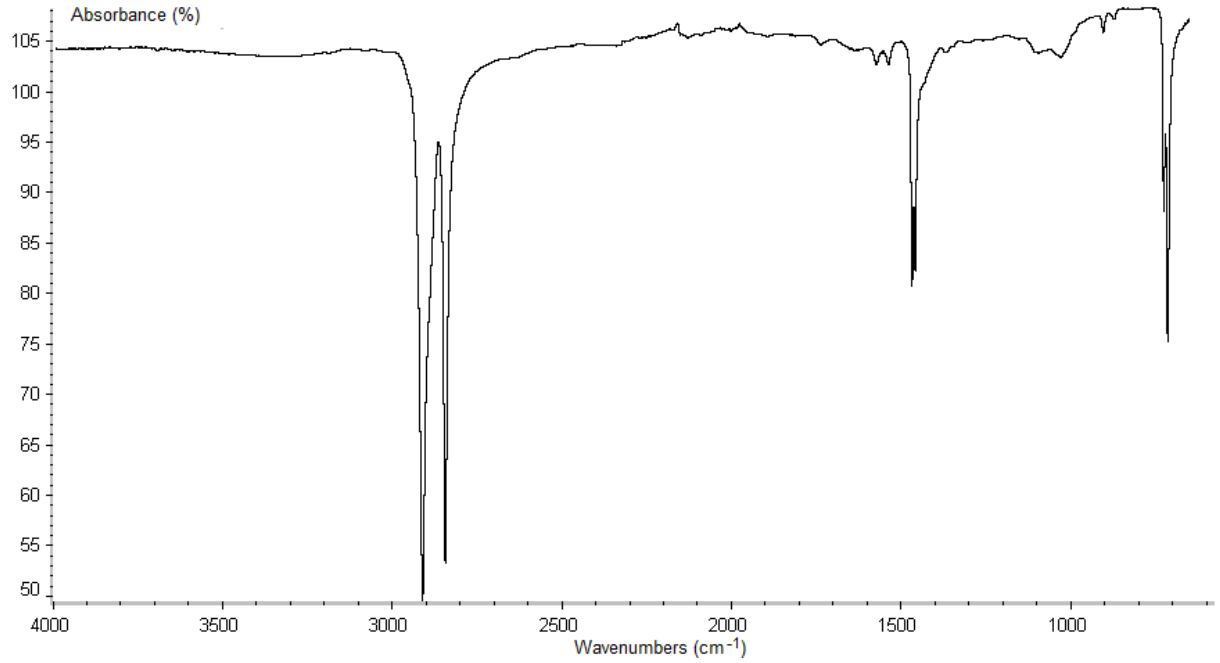

Figure 37: A selected HDPE regrind FT-IR spectrum.

Table 15: The associated interpretations for an FT-IR spectrum for HDPE.

Frequency range (cm^{-1})	Vibration	Intensity
2915	CH_2 Asymmetrical stretching	Strong
2850	CH_2 Symmetrical stretching	Strong
1470	CH_2 Scissoring	Medium
720	CH_2 Rocking	Medium to strong

The IR spectra of HDPE and LDPE looked alike. Indeed, it appeared just four significant peaks related to the repeat unit of polyethylene, the CH_2 group. The difference between the HDPE and LDPE spectra was linked to the intensity of two peaks: in HDPE, the 1470 cm^{-1} peak was weaker than the 720 cm^{-1} peak. On the

contrary, in LDPE, the 1470 cm^{-1} peak was stronger than the 720 cm^{-1} peak. It was mainly the intensity of the peak at 720 cm^{-1} which changed. In LDPE, the high level of branching reduced the possibility for the CH_2 groups to rock; thus the intensity of the CH_2 rocking peak was lower than the HDPE. The HDPE was more linear and more crystalline than the LDPE, thus there were more CH_2 groups which could rock in HDPE than LDPE. The intensity of CH_2 rocking peak was more prevalent in HDPE than LDPE.

In order to quantify the effectiveness of the separations, a cross section of regrind flakes was analysed to verify the percentage of each polymer in the five fractions (Table 16). For each of the first three fractions, eighty regrind flakes were analysed. For each of the two remaining fractions, only 20 flakes were analysed due to the reduced sample sizes.

Table 16: FTIR Results.

Fraction	N°1	N°2	N°3	N°4	N°5
Expected polymer	PP	LDPE	HDPE	PS	PVC/PET
Number of spectra	80	80	80	20	20
PP (%)	95	48.8	18.8	30	0
LDPE (%)	1.3	25	23.8	0	0
HDPE (%)	3.8	26.3	57.5	20	0
PS (%)	0	0	0	0	0
PVC (%)	0	0	0	10	30
PET (%)	0	0	0	40	70

As Table 16 shows, the separation was not as effective as expected due to the fact that each fraction contains a percentage of unexpected polymers. Only the polypropylene fraction was composed of mostly polypropylene (95%), and a high proportion of what was supposed to be the LDPE fraction appears to be PP (48.75%). Furthermore, the HDPE and PS fractions contained 18.75% and 30% PP respectively. The second fraction (LDPE) was composed of only 25% LDPE with the remaining 26.25% being HDPE. The HDPE fraction was only 57.5%

HDPE with 23.75% LDPE and the remainder being PP. Table 16 also suggests that the post-consumer waste did not actually contain any polystyrene, but that the supposed PS fraction was instead a combination of PVC and PET. It could be argued that the composition of the non-polyolefin fraction was not as accurate as the compositions of the other fractions due to the reduced number of spectra recorded.

These results confirmed the presence of a majority proportion of polypropylene in the initial post-consumer waste. These results have been verified by DSC in Section 3.1.1.3, where several selected regrind flakes were analysed to confirm the FTIR results.

Whilst the separation was far from ideal, it did identify that the sample of post-consumer waste contained far more PP than would have been expected from the WRAP figures given in Table 1 on page 15. This illustrates the potential difficulties in trying to use post-consumer waste in that besides the presence of non-polyolefinic contaminants, there is likely to be a wide variation in composition of wastes from different sources.

3.1.1.3 Differential Scanning Calorimetry Results

To support the data gathered by FT-IR, DSC was used to further identify a selection of the regrind flakes analysed previously in Section 3.1.1.2. Of the eighty regrind flakes analysed from the first fraction, ten random supposed PP flakes were selected and assigned sample numbers 1-10 (Table 17). Next, of the eighty regrind flakes analysed from the third fraction, seven random supposed HDPE flakes were selected and assigned sample numbers 11-17 (Table 17). Furthermore two control samples were run to provide comparative baseline data – the first being virgin PP and the second being virgin HDPE.

Table 17: DSC data gathered for the selected PP and HDPE regrind flakes.

Sample	Suggested Polymer (by FT-IR)	T onset (°C)	Enthalpy (J/g)	Actual Polymer (by DSC)	Crystalline content (%)
1	Polypropylene	156.2	106.0	Polypropylene	50.7
2	Polypropylene	152.1	95.4	Polypropylene	45.7
3	Polypropylene	153.9	98.5	Polypropylene	47.1
4	Polypropylene	151.2	85.7	Polypropylene	41.0
5	Polypropylene	154.2	98.2	Polypropylene	47.0
6	Polypropylene	154.0	88.2	Polypropylene	42.2
7	Polypropylene	148.1	80.6	Polypropylene	38.6
8	Polypropylene	149.8	90.4	Polypropylene	43.2
9	Polypropylene	153.2	95.6	Polypropylene	45.7
10	Polypropylene	152.7	77.7	Polypropylene	37.2
11	Polyethylene	126.9	165.0	Polyethylene	59.6
12	Polyethylene	121.8	167.9	Polyethylene	60.6
13	Polyethylene	128.1	201.2	Polyethylene	72.6
14	Polyethylene	124.6	183.9	Polyethylene	66.4
15	Polyethylene	124.4	172.7	Polyethylene	62.3
16	Polyethylene	124.7	146.7	Polyethylene	53.0
17	Polyethylene	121.5	183.4	Polyethylene	66.2
Virgin PP	**Polypropylene**	**150.4**	**78.6**	**Polypropylene**	**37.6**
Virgin HDPE	**Polyethylene**	**124.2**	**162.2**	**Polyethylene**	**58.6**

Each regrind flake sample was identified as a specific polymer prior to the DSC analysis (according to its FT-IR spectra). The DSC analysis was carried out and the parameters of interest, namely enthalpy and melting point of the sample, were compared to the properties of the virgin polymer control samples (PP and HDPE); therefore the definitive identification of the regrind flake sample could be determined. From this, the crystalline content of the sample could be found from the appropriate peak area.

With regards to Table 17, all of the DSC results fully confirm the interpretation of the FT-IR spectra. Firstly, all of the samples which the FT-IR suggested were polyethylene were in fact polyethylene; secondly all the samples which were suggested to be polypropylene were in fact polypropylene. Therefore, the ratios shown in Table 16 are considered valid even though they differ from the WRAP data by a wide margin.

3.1.1.4 Result synthesis and following approach

The traces from the DSC confirmed the FTIR spectra results, and by combining these with the sequential separation results the actual proportions of each polymer in the post-consumer polymer packaging waste could be calculated, resulting in a 'corrected' value.

An example of the equation used to calculate the percentage of PP in the post-consumer polymer packaging waste is shown in Equation 6 (see Table 12 and Table 16).

$$\frac{69.1\times95 + 11.8\times48.8 + 16\times18.85 + 1.1\times30}{100} = 74.7\ \%\ \text{PP} \qquad \textbf{Equation 6}$$

The same calculation was performed for HDPE and LDPE. Table 18 shows these results along with the published WRAP composition.

Table 18: Composition of post-consumer *polymer* packaging waste.

	PP (wt%)	LDPE (wt%)	HDPE (wt%)	Other (wt%)
Experimental post-consumer waste (corrected composition)	74.7	7.6	15.3	2.1
WRAP published post-consumer waste composition	17	38	13	32

The data in Table 18 was then analysed to calculate the relative compositions of the polyolefin fractions of the polymer packaging waste (Table 19).

Table 19: Composition of post-consumer *polyolefin* packaging waste.

	PP (wt%)	LDPE (wt%)	HDPE (wt%)
Experimental post-consumer waste	76.5	7.8	15.7
Classic post-consumer waste	25	55.9	19.1

The two PCPW compositions (published and experimental) are very different. In the experimental post-consumer waste, polypropylene is the main constituent, whereas the WRAP post-consumer waste is mainly composed of polyethylenes. It is possible that the experimental post-consumer waste had been recovered after an initial sorting step had taken place, so the polymer ratios may have been changed significantly compared to the published WRAP results. Alternatively, the results may simply indicate the wide variability that will be found in PCPW.

In order to investigate the mechanical and rheological properties of the two compositions, test pieces were produced based on both the experimental and the published WRAP composition. These blend compositions were also used to undertake a comparative study by producing composites to investigate the effect of adding untreated and surface-treated fillers to produce a compatibilised composite and assess the effectiveness of the surface treatments used.

The blends and composites (see Table 20) were produced using a HAAKE Polydrive (see Section 2.3.1) and subsequently compression moulded.

Table 20: Composition of the filled blends.

Blend ID	Details	%wt polymer blend**	%wt $CaCO_3$	%wt C800	%wt BMI	%wt $CaCO_3$(st)*
N°1	Unfilled blend	100	0	0	0	0
N°2	Untreated filler	40	60	0	0	0
N°3	C800 treatment	39,28	60	0,72	0	0
N°4	BMI treatment	37	60	0	3	0
N°5	Stearic acid treatment	39	0	0	0	61
* $CaCO_3$ treated with stearic acid						

Two sets of blends were produced – one utilising the PCPW as the base polymer, the other using virgin polymers to simulate the published WRAP composition (Table 19), i.e. 10 samples in total.

Furthermore, due to a shortfall in the required quantity of the experimental post-consumer waste, polymer blends were simulated utilising virgin polymers according to the composition data in Table 19.

Once produced, the effects and effectiveness of the surface treatments were investigated and are discussed in the following sections.

3.1.2 Effect of different surface treatments on the PCPW blends

The filled blends investigated corresponded to the blends composed of the two different compositions (experimental and WRAP published) both with and without filler and coupling agent. The two polymer blends were treated equally in order to compare the effects of the different filler surface treatments.

3.1.2.1 Volume Melt Flow Rate (VMFR)

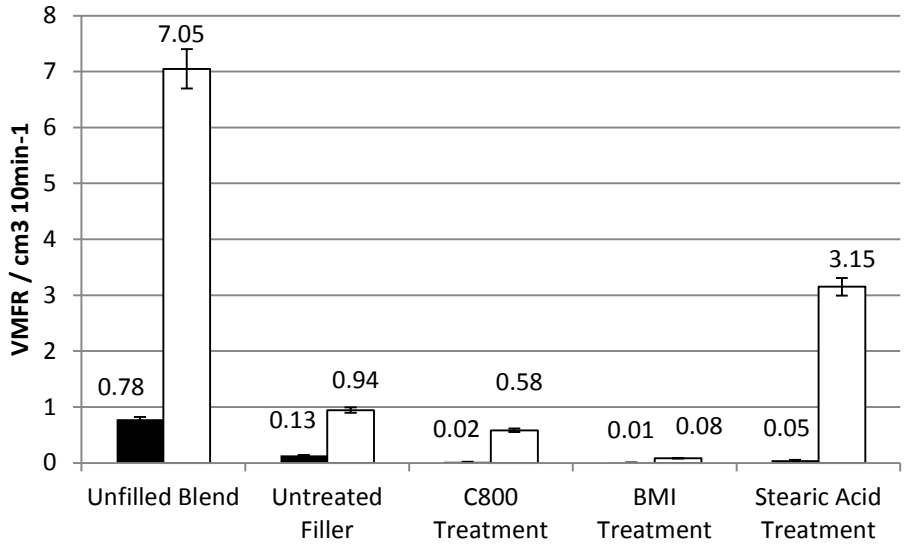

Figure 38: Volume melt flow rate for the composites produced, where the black bars denote the WRAP published composition and the white bars denote the experimental composition.

As discussed previously, surface treatment significantly reduces the VMFR. The unfilled blends had a higher VMFR compared to the filled blends. The VMFR decreased when filler was added, as the filler hindered the flow of the polymer molecules resulting in a more viscous melt. Furthermore, the VMFR decreased when a coupling agent was added due, most likely, to the strong interface which forms between the filler and the matrix. The VMFR of the experimental compositions were higher than those for the WRAP published compositions. This may be due to the fact that the experimental composition was mainly composed of polypropylene, which is contrary to the WRAP published composition which has a greater proportion of polyethylene. Due to the dispersive action of the stearic acid treatment, the polymer chains are not coupled to the filler surface, which may have manifested as a lubricating effect in the composites, thus facilitating flow. This in

turn led to a higher VMFR in the composite using the experimental composition; however this was not valid for the WRAP published composition.

3.1.2.2 Flexural testing

The flexural modulus increased when filler was added to the unfilled polymer blend, which is due to the stiffening effect of adding a particulate filler. Figure 39 shows that in some instances the addition of coupling agents improved the flexural modulus (WRAP published compositions plus C800 treated filler and BMI treated filler), and maintained or slightly reduced it in other instances (stearic acid treatment).

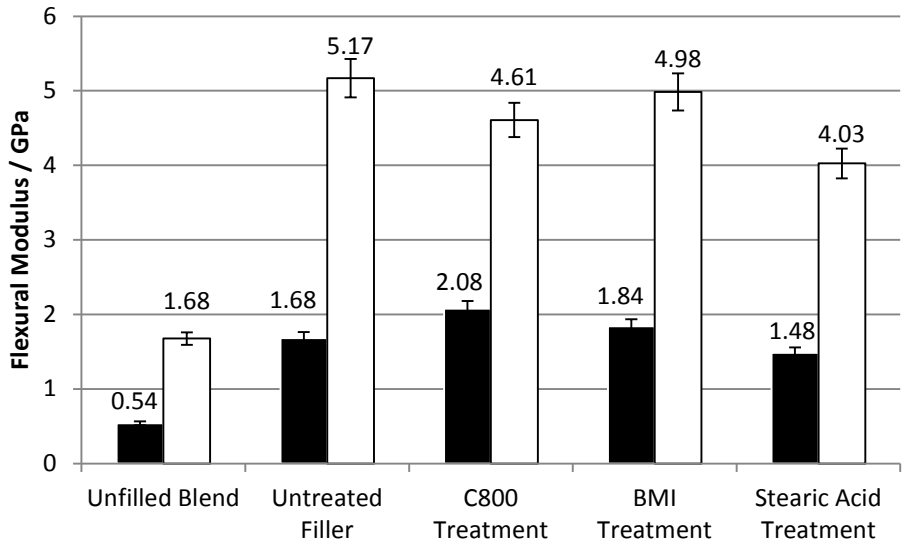

Figure 39: Flexural moduli for the composites produced, where the black bars denote the WRAP published composition and the white bars denote the experimental composition.

The blends formulated using the WRAP published composition had lower flexural moduli than those utilising the experimental composition due to the fact that the WRAP published composition blends were mainly composed of PE. Thus, due to effects mentioned previously, the PE may have cross-linked resulting in a highly flexible rubbery interphase both surrounding and coupling to the filler surface. Conversely, the composites produced using the experimental composition show a significantly higher flexural modulus than their associated composites using the WRAP published compositions. While PP is a stiffer material than HDPE, this may

also be due to increased levels of PP which has undergone chain scission, facilitating crystallisation in the composites to create a stiffer material.

Again, as the stearic acid treatment results in dispersion rather than adhesion or coupling, the composites utilising this additive resulted in an overall reduction in flexural modulus values when compared to the other composites produced.

This hypothesis may be further supported by the differences in the deflection at break values obtained (Figure 40). While the unfilled blend did not break, the untreated filler blend based on the experimental composition highlights the reinforcing effect of a particulate filler. However, for the WRAP published composition this value is halved.

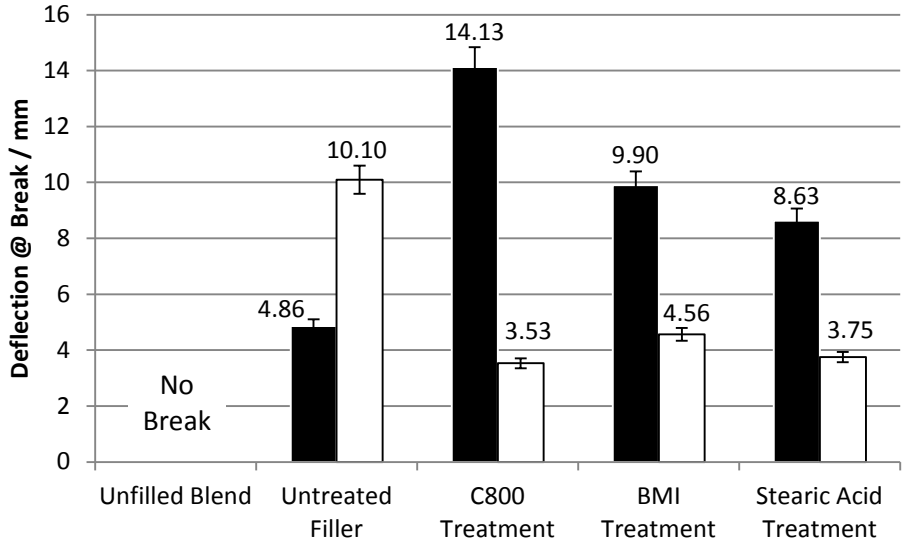

Figure 40: Deflection at break values for the composites produced, where the black bars denote the WRAP published composition and the white bars denote the experimental composition.

Furthermore, as the composites based on the WRAP published compositions have a higher level of PE, increased levels of a rubbery interfacial region would result in a more flexible sample. Figure 40 illustrates this due to higher values for deflection at break when compared to the composite using untreated filler (black bars).

3.1.2.3 Impact testing

The unfilled blend based on the WRAP published composition was not broken on impact, so the value of its impact strength was recorded as no break for this test. As expected, the impact strength decreased when untreated filler was added to the polymer blends; but the impact strength increased with coupling agent treatments presumably due to the formation of the interface (Figure 41).

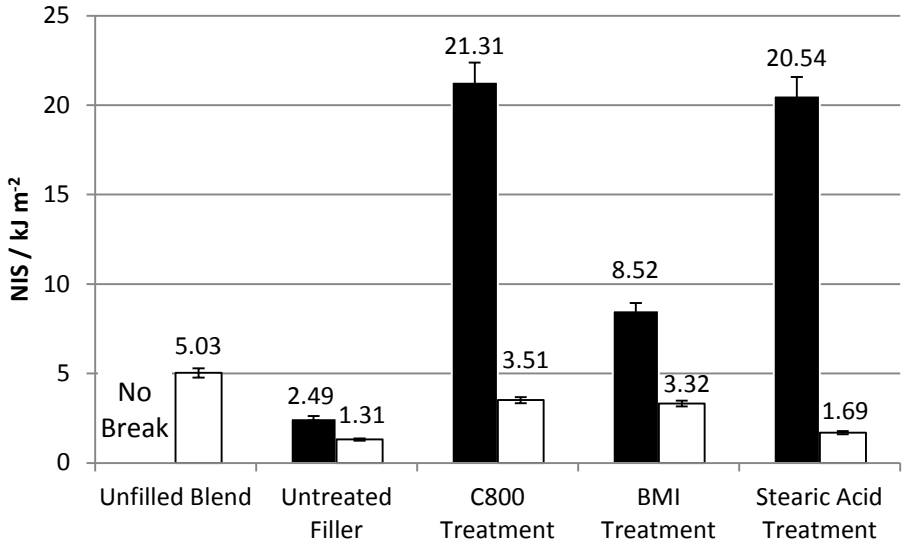

Figure 41: Notched impact strength values for the composites produced, where the black bars denote the WRAP published composition and the white bars denote the experimental composition.

The composites using the WRAP published composition appear to have benefitted most from the C800 and steric acid treatment, while the BMI treatment shows a less marked improvement. When comparing these with the experimental compositions, the impact strength appears to be reduced to less than that for the unfilled blend. As the WRAP published composition has a greater level of PE, this further suggests the formation of a rubbery amorphous region which can absorb the impact energy more sufficiently than in the untreated filler sample. Furthermore, the data in Figure 41 suggest that the PP may have undergone chain scission and promoted higher levels of crystallisation, resulting in less rubbery material at the interface and thus a more brittle material overall, which is presented as a reduction in impact strength. It appears that the C800 treated filler had the greatest effect overall when incorporated into the WRAP published composition blend.

3.1.2.4 Differential Scanning Calorimetry

DSC traces of the ten samples were obtained to compare the crystalline contents and melting onset temperatures of each polymer phase (PP and PE) in the blends and composites.

It is interesting to note that the BMI seems to have reduced the melting temperature onset somewhat for both the PE and PP phases (Figure 42 and Figure 43), whereas the other blends and composites show little to no change. This suggests that the BMI treatment is having a major effect on the structure/morphology of the systems – i.e. changing the characteristics of the bulk material rather than changing the interphase.

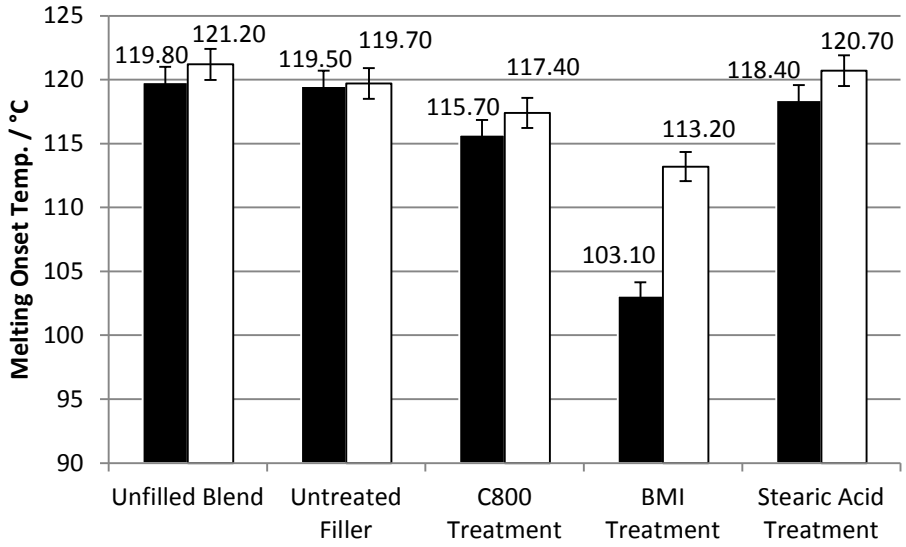

Figure 42: Melting onset temperatures for the PE phase in the blends and composites produced, where the black bars denote the WRAP published composition and the white bars denote the experimental composition.

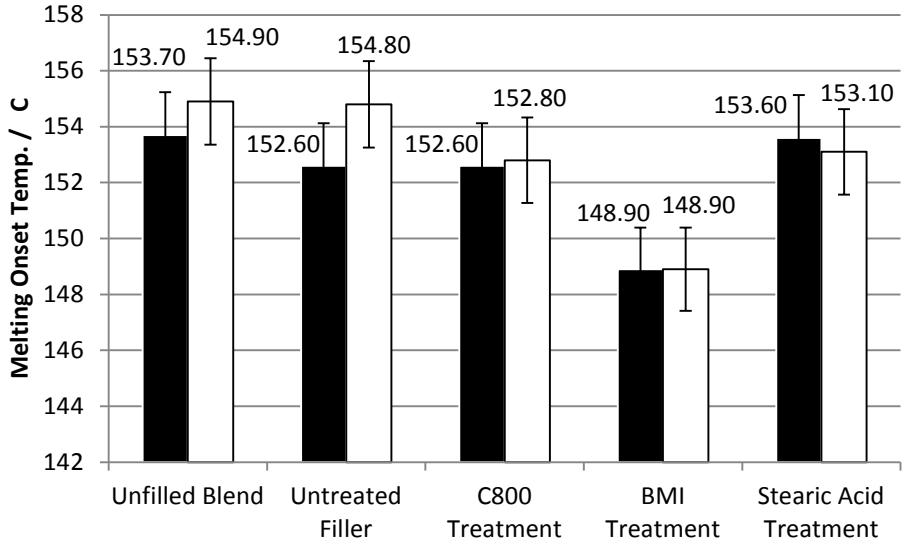

Figure 43: Melting onset temperatures for the PP phase in the blends and composites produced, where the black bars denote the WRAP published composition and the white bars denote the experimental composition.

Considering the levels of crystallinity in the PE phase, Figure 44 shows that both of the coupling agent treatments have reduced the levels of crystallinity when compared to the unfilled blend, which is the case for both of the compositions. This seems to support the suggestions made in the previous sections whereby the PE phase contributes to the creation of a rubbery interface in the composites. However, the stearic acid treatment has not resulted in such a reduction, reflecting the fact that it is a dispersant and will not be causing structural change due to interphase formation.

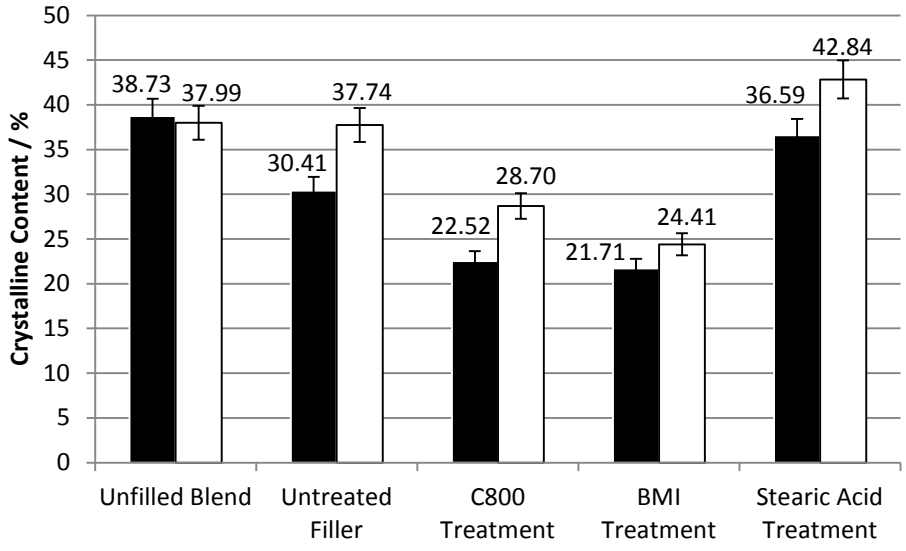

Figure 44: Crystalline content of the PE phase for the composites produced, where the black bars denote the WRAP published composition and the white bars denote the experimental composition.

However, when compared to the levels of crystallinity in the PP phase, Figure 45 shows that only the C800 treatments in the experimental composition composite, and the stearic acid treatments in both the WRAP published and experimental composites increased the levels of crystallinity. The latter effect may be expected as the stearic acid does not couple the filler to the matrix, but disperses it perhaps leading to a nucleation type effect.

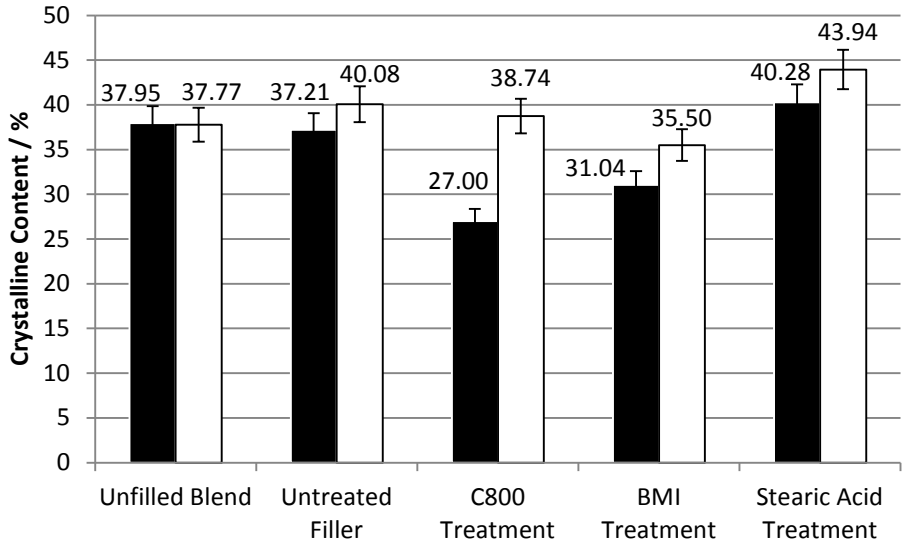

Figure 45: Crystalline content of the PP phase for the composites produced, where the black bars denote the WRAP published composition and the white bars denote the experimental composition.

Conversely, both the C800 and the BMI treatments had somewhat reduced the crystallinities in the WRAP published composition composites by a factor of around 10 and 6 percent respectively.

3.2 Effect of Solplus® C800 on composites based on HDPE and PP

3.2.1 Volume melt flow rate

The VMFR data shows interesting trends (Figure 46 and Figure 47). It is evident that in HDPE based composites, (Figure 46), there is a significant reduction in VMFR with C800 modification relative to the respective unmodified composites. In PP, the data suggests that at the lower levels of modified filler the coupling reaction dominates (VMFR value falls indicating increasing melt viscosity), whereas once the crossover point is reached (at around 50 % filler level) the VMFR significantly increases.

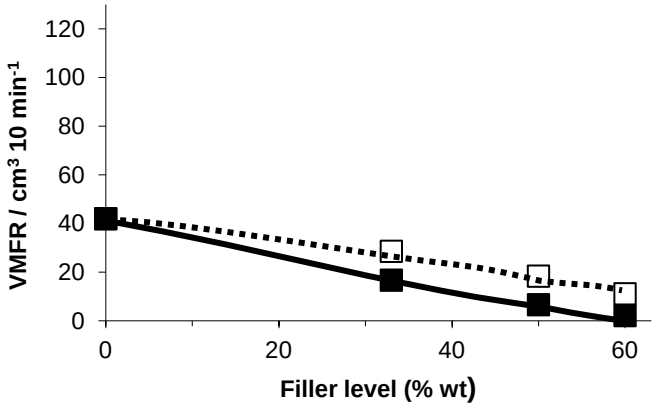

Figure 46: Plot of volume melt-flow rate vs filler level for HDPE based composites, where □ represents unmodified filler, and ■ represents modified filler.

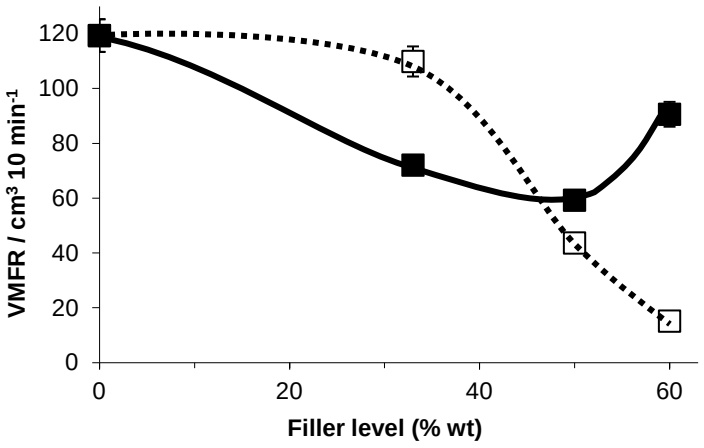

Figure 47: Plot of volume melt-flow rate vs filler level for PP based composites, where □ represents unmodified filler, and ■ represents modified filler.

As it is widely accepted that under the action of a peroxide, HDPE undergoes a crosslinking reaction and PP undergoes a chain scission reaction [84], it is considered that the peroxide, besides promoting the coupling reaction, may be attacking the polymer chains. In the case of HDPE, a peroxide can cause crosslinking of the polymer which will increase the melt viscosity. Then what may appear to be an effect of extensive coupling is a combination of coupling and crosslinking with both effects resulting in an increase in melt viscosity (Figure 46). However, as can be seen in the VMFR data for PP based composites in Figure 47 where at the higher treated filler levels the increased amount of peroxide present appears to drive chain scission to dominate over the coupling reaction, thus reducing the molecular mass of the polymer and hence decreasing the melt viscosity (Figure 47).

It can be argued that these reactions are not detrimental, as in the case of HDPE composites the crosslinks may aid the formation of an amorphous rubbery interfacial region around the filler particles to which the chains themselves are coupled by preventing / restricting crystallisation. This is illustrated by the subsequently described trends in the elongation and impact strength of the HDPE based composites, which show significant improvement upon C800 modification. Whilst with the PP composites, the chain scission reactions are, at least, not detrimental to the elongation and impact strength. The composite may in fact benefit from chain scission, as a consequence of the VMFR trends (Figure 47). This is due to the fact that a decrease in melt viscosity can be of significant benefit to melt processing and so when blends of PP and PE are combined, manipulation of the PE/PP ratio may be used to alter beneficially specific properties.

3.2.2 Mechanical properties

Mechanical failure can occur in either a brittle or a ductile fashion, whilst sometimes mixed-mode failure can occur. Brittle failure results in a clean break of the sample at a relatively low extension value, whereas ductile failure results in yielding and cold-drawing of the sample, often giving a higher extension value. Where samples have failed in a brittle manner, the break values recorded by the test apparatus are used, and where the failure mode is ductile, the yield values are used.

As is to be expected when incorporating an untreated particulate filler, a reduction in mechanical properties occurs; the reduction increasing with increasing filler level. This is a consequence of the filler particles acting as defect points, which has also been shown theoretically by Turczanyi et al [85]. This effect can be clearly seen by the trends shown in Figure 48 and Figure 49 by the reduction in failure strength.

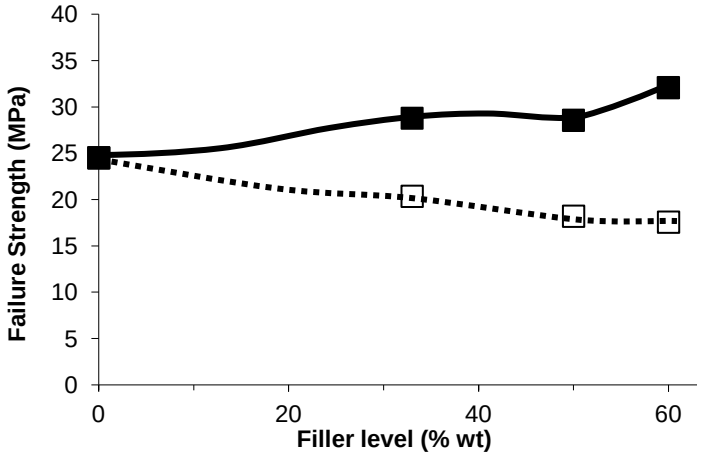

Figure 48: Plot of failure strength vs filler level for HDPE based composites, where □ represents unmodified filler, and ■ represents modified filler.

Generally, the mechanical properties of both composites respond well to the addition of the C800/peroxide treatment. Considering the tensile test results, the HDPE based composites increase in strength from 25 MPa (unfilled matrix) to 30 MPa (at 60 % wt. filler) with C800 modification, which implies good coupling. However, with unmodified filler the tensile strength falls with increasing filler loading. Similar effects are also noted for the PP based composites, though in this case the tensile strength is maintained at around the level of the unfilled matrix as filler level increases.

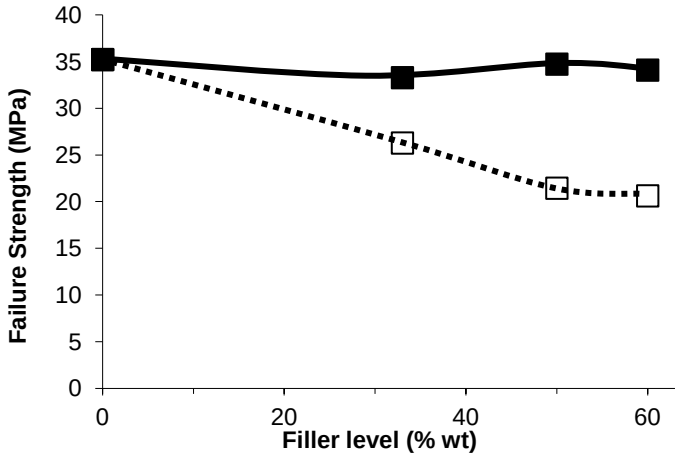

Figure 49: Plot of failure strength vs filler level for PP based composites, where □ represents unmodified filler, and ■ represents modified filler.

The elongation (at failure) results for HDPE based composites show that the C800 modification leads to an increased elongation at failure over the respective unmodified composites (Figure 50). With the PP based composites elongation continuously falls but stays slightly above the respective unmodified composites. This becomes increasingly true of filler levels above 33 % wt (Figure 51).

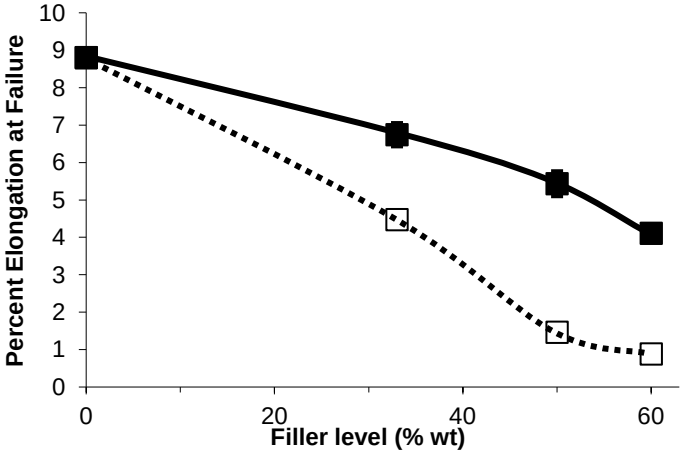

Figure 50: Plot of percent elongation at failure vs filler level for HDPE based composites, where □ represents unmodified filler, and ■ represents modified filler.

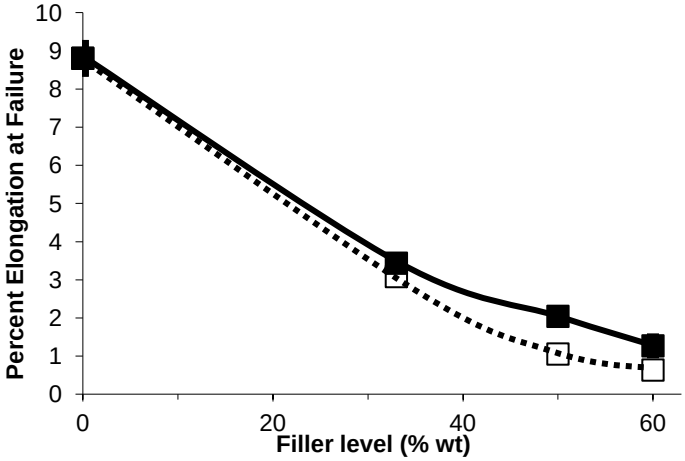

Figure 51: Plot of percent elongation at failure vs filler level for PP based composites, where □ represents unmodified filler, and ■ represents modified filler.

The unnotched impact strength data shows that C800 coupling provides some benefit throughout the filler level range, though again the greatest benefit is seen in the HDPE based composites (Figure 52 and Figure 53). The greater improvement in elongation and unnotched impact strength observed in the case of HDPE based composites is likely to be due to peroxide related crosslinking that may be concentrated mainly within the interfacial regions between filler and matrix. This effect will lead to an interfacial region with reduced crystallisation content and therefore increased elastomeric character. These aspects will be discussed in the following section.

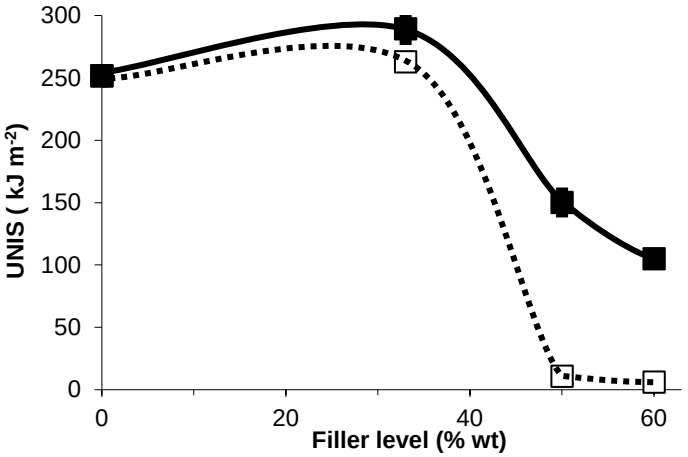

Figure 52: Plot of un-notched impact strength vs filler level for HDPE based composites, where □ represents unmodified filler, and ■ represents modified filler.

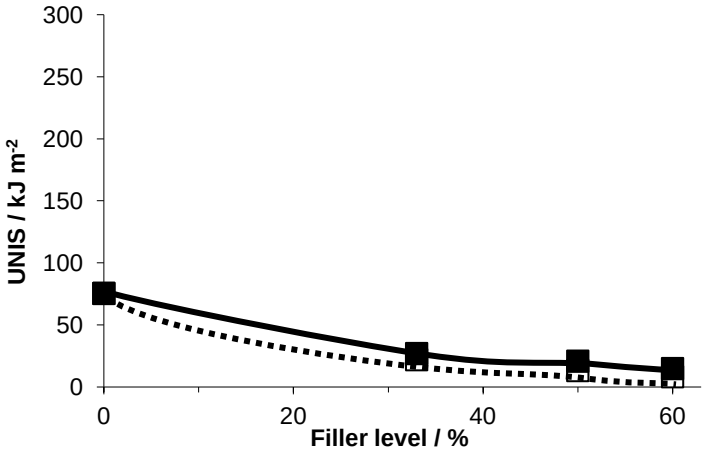

Figure 53: Plot of un-notched impact strength vs filler level for PP based composites, where □ represents unmodified filler, and ■ represents modified filler.

3.3 Effect of Solplus C825/GCC on compatibilisation of post-industrial polyolefin waste

3.3.1 Preliminary characterisation of post-industrial polymer waste (PIPW) samples

Work began by investigating a method to characterise the PE / PP blend ratio in the mixed polymer waste by means of a calibration curve created by analysing a set of samples with known blend composition. The analysis commenced with micro-attenuated total reflectance (ATR) FT-IR, however as this method analysed an area of only 200 x 200 µm, the data was not always considered to be representative of the bulk of the sample. Work then moved to the diamond compression cell ATR FT-IR method, which analyses a much larger area (c.a. 3 x 3 mm) compared to the previous method. Although both of these methods use infrared spectroscopy, it should be noted that analysis of the samples required contact with the instrument, whereas an in-stream process would require a continuous non-contact analysis method such as laser Raman spectroscopy. Construction of a calibration curve was attempted using the gathered infrared spectra, but proved less useful than that generated from differential scanning calorimetry (DSC) described below.

DSC analysis was then performed on a range of control samples (as detailed in Section 2.5.3). By using the crystalline fusion peak areas from the DSC traces, ΔH values for HDPE and PP were calculated, allowing the construction of a DSC calibration curve (Figure 54).

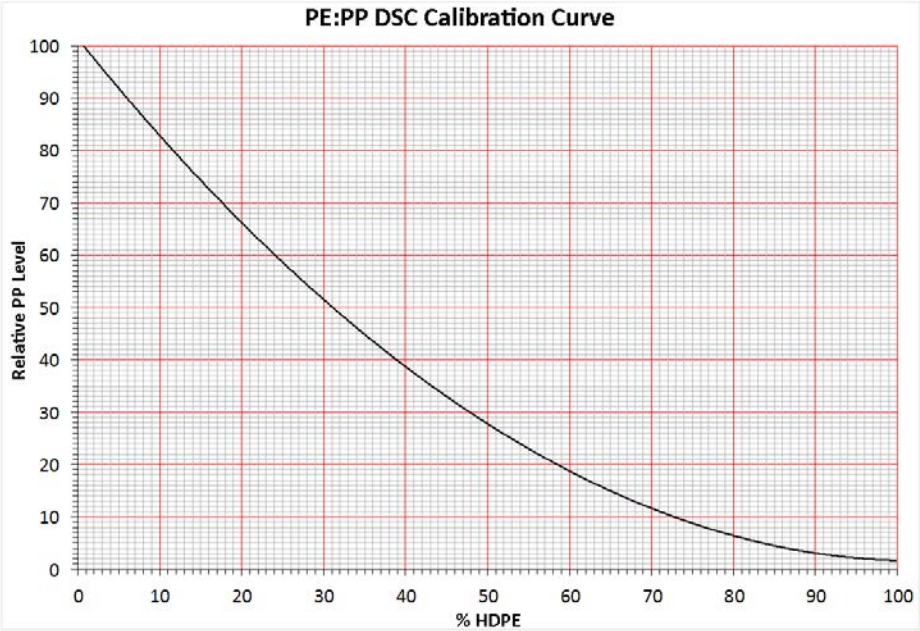

Figure 54: The DSC calibration curve.

By relating fusion peak areas in the PIPW to those of HDPE/PP blends of known composition (as per the method detailed in Section 2.5.3), the three samples were all found to be polyolefin blends, giving the ratios shown in Table 21. It is to be noted, however, that although the ratio of polyethylene to polypropylene was obtained, distinguishing between the different polyethylene types (i.e. high, medium, low and linear low density) by DSC is very difficult. From the melting point of the PE sample it should be possible to identify HDPE from LDPE, but if a blend of PE types is present then distinguishing a given type would not be possible. Furthermore, as an on-stream process, DSC is not very practical, as it would require samples to be taken of the waste polymer feedstock at regular intervals. However, for batch sampling it would be extremely useful.

Table 21: Calculated composition of PIPW samples.

Sample	PE (%wt)	PP (% wt)
A	100	0
B	76	24
C	38	62

Also, as a typical DSC run can take anything from forty minutes to two hours, a time lag effect will occur, where the analysed sample may be processed before any composition data could be produced. Therefore it would be much more effective to use DSC analysis to verify the efficiency of the float/sink separation process which is described in Section 3.1.1.

The following results show the influence of the C800/calcium carbonate system on the three samples of post-industrial polymer waste, and as a function of filler level.

3.3.2 Melt flow rate of PIPW based composites

The variations in MFR are shown in
Figure 55. Sample A shows a continuing decrease with increase in filler level, with treated filler showing the most significant decrease. This, as previously explained, is due to the combination of coupling and the cross-linking reaction of the PE in the blend. With higher PP levels, the increase in viscosity is less pronounced. It is worth noting that sample C shows no difference in MFR values at both untreated and treated filler levels greater than 50%. This is due to the chain scission reactions of the PP component in the treated filler system cancelling out the effects of both the coupling reaction between the polymer and the filler surface, and the crosslinking of the PE component. These trends indicate that manipulation of the PE/PP ratio is a means of property modification.

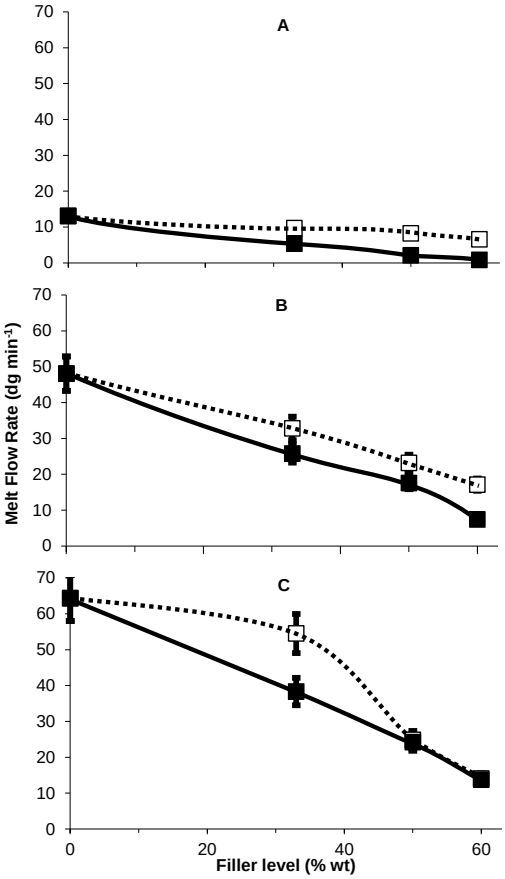

Figure 55: Plots of melt-flow rate vs filler level for the three PIPW based composites (A, B and C), where □ represents unmodified filler, and ■ represents modified filler.

3.3.3 Mechanical properties

Figure 56 shows the trends in tensile strength for the three PIPW samples with increase in filler level. In all cases the treated filler improves the tensile strength in relation to the untreated filler. It is particularly significant that the tensile strength is greater than the respective unfilled samples at all filler levels. It can also be noticed that with higher PP levels the rate of increase reduces.

Figure 57 shows the trends in relation to elongation at failure. It is significant here that whilst samples B and C give higher elongation at all filler levels than the untreated samples, sample A does not until the filler level exceeds 50%. It is considered that this is a direct result of sample A having a very high PE level and

the cross-linking reaction dominating the property at filler levels below 50%. However, while Figure 50 on page 104 presents a differing trend for HDPE, the trend observed in Figure 57 A may be due to the fact that this sample contains mainly LDPE.

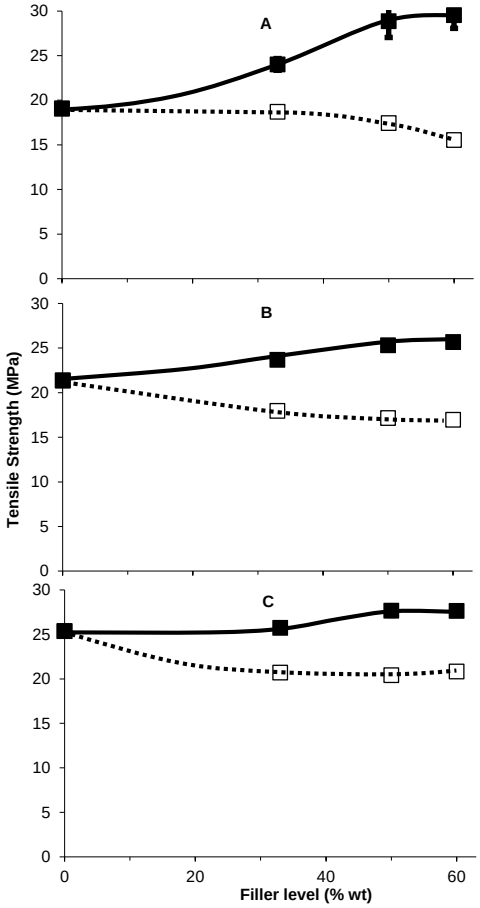

Figure 56: Tensile strength vs filler level for PIPW based composites.

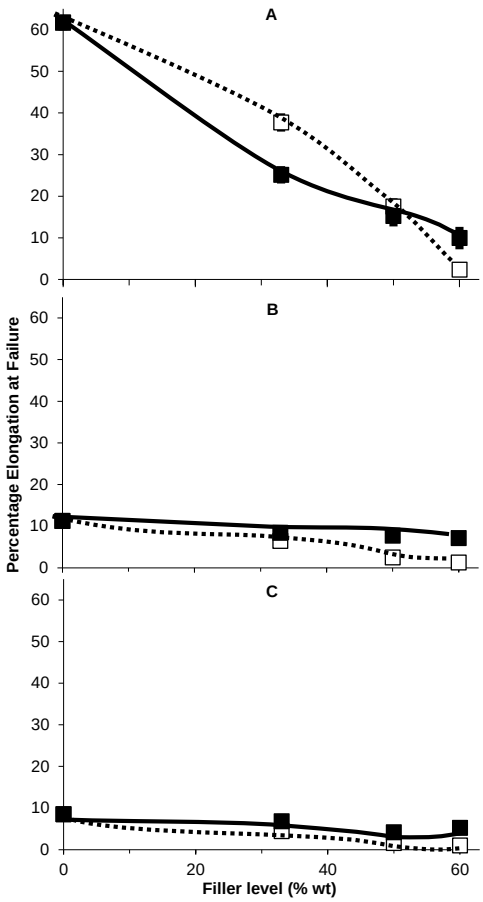

Figure 57: Elongation* vs filler level for PIPW based composites.

□ represents unmodified filler, and ■ represents modified filler

***Elongation values are recorded at yield for composites showing yield behaviour, and at break for composites showing no yield behaviour.**

The trends for the PIPW samples in relation to un-notched impact strength (UNIS) (Figure 58) are similar to those shown for elongation in that samples B and C have high UNIS at all filler levels for the modified filler. With sample A the UNIS collapses above 50% untreated filler but the modified filler, whilst falling, does so to a much lesser extent.

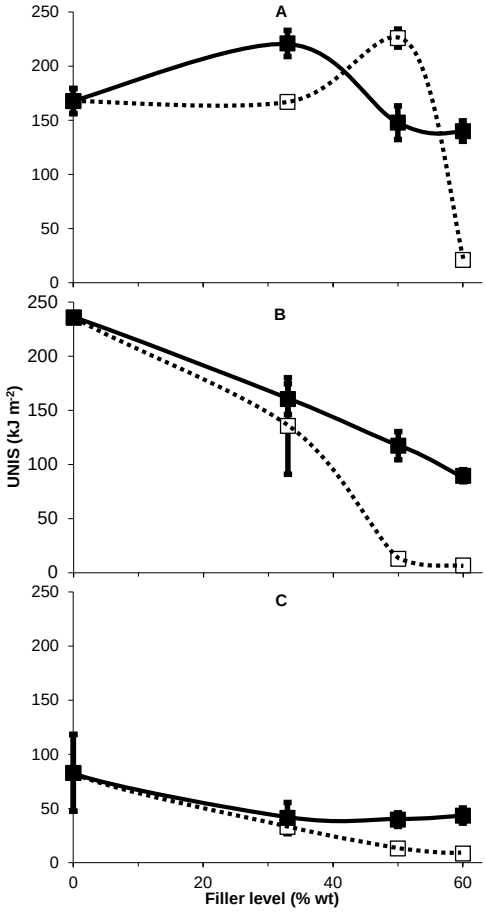

Figure 58: Plots of un-notched impact strength vs filler level for PIPW based composites, where □ represents unmodified filler, and ■ represents modified filler.

The elongation and impact strength data for the PIPW based composites indicate a potential toughening mechanism that involves the co-interactions of PE and PP with the filler surface. As filler level increases, the amount of interfacial area in the composite increases, which explains the increasing relative improvement observed with the modified composite at high filler level. It is envisaged that the co-interaction of the PE and PP with the C800 modified filler system, together with crosslinking of the PE component may lead to a reduction in crystallinity in the filler-matrix interfacial region, therefore giving an elastomeric inter layer. These conclusions have been examined and discussed in Section 3.4.4.

3.4 Effect of Solplus® C800 on composites based on Blends of HDPE & PP

The following results show the influence of variation in the blend ratio of HDPE to PP polymer blends and the equivalent composite blends with either unmodified or modified filler present at 60% by weight.

3.4.1 Mechanical properties

Comparison of the tensile properties of the unfilled blends and the unmodified filler composites reflect the brittle properties introduced by addition of unmodified particulate filler to a polymer system. While the tensile strength of the unmodified filler composite may be reduced in relation to the other composites, it remains relatively constant across the blend composition range. However the two extremes of these graphs (Figure 59 – Figure 61) show that the modification has a marginally greater effect when only one polymer is present, and particularly at high HDPE levels.

Where no filler is present, there appears to be a point between 50 and 75% HDPE where the strength begins to reduce. Furthermore, it is interesting to note that there are two distinct crossover points at each extreme of the graphs for the polymer blend with and without the additive package. The plot for the blend with the additive package present mirrors (to a certain extent) the trend shown in the plot where the modified filler is present. What is striking is the considerable improvement in tensile strength for the modified filler composite, at all blend ratios in comparison to the unmodified filler composite.

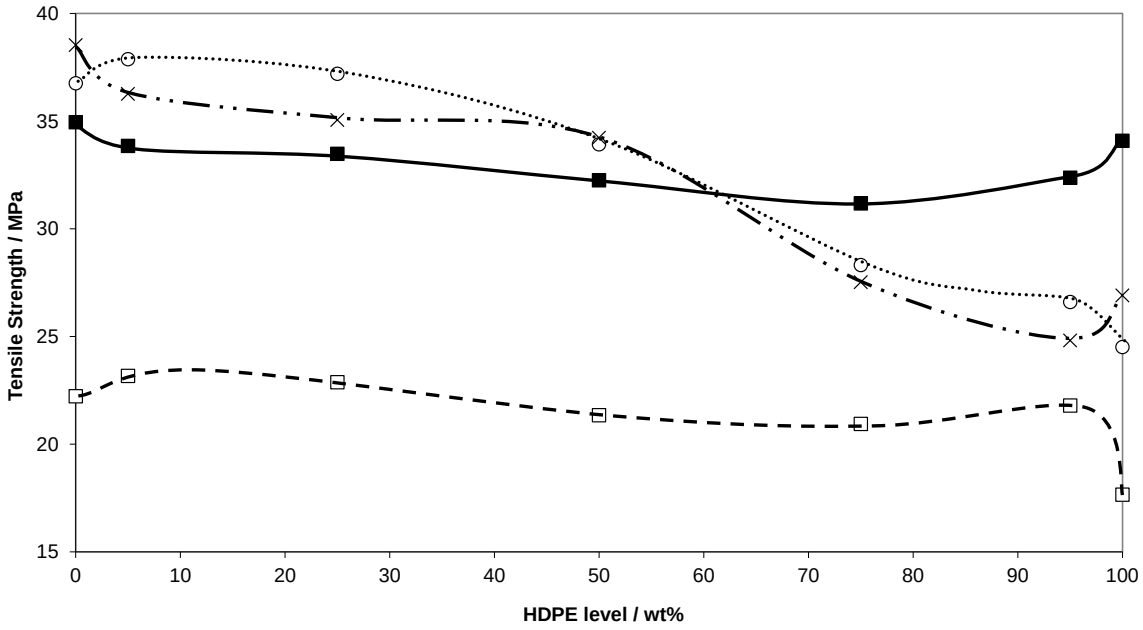

Figure 59: Plot of tensile strength vs blend composition for HDPE/PP based composites, where o represents blend only, x represents blend with additive only, □ represents unmodified filler composite, and ■ represents modified filler composite.

Further to the trends shown by the tensile strength data, the Young's modulus data for these composites shows that addition of the unmodified filler produces a generally stiffer composite. This stiffness is reduced when adding the surface modification, but a similar trend over the blend composition range is followed. Introducing only the additive package has little effect on the modulus when comparing with the unmodified polymer blends. Looking at PP alone, the additive seems to reduce the modulus, while in HDPE it appears to be maintained. The difference between the modified and unmodified filler blends shows the coupling system is having a marked effect on the composite system. This suggests formation of an interphase region which is rubbery in character.

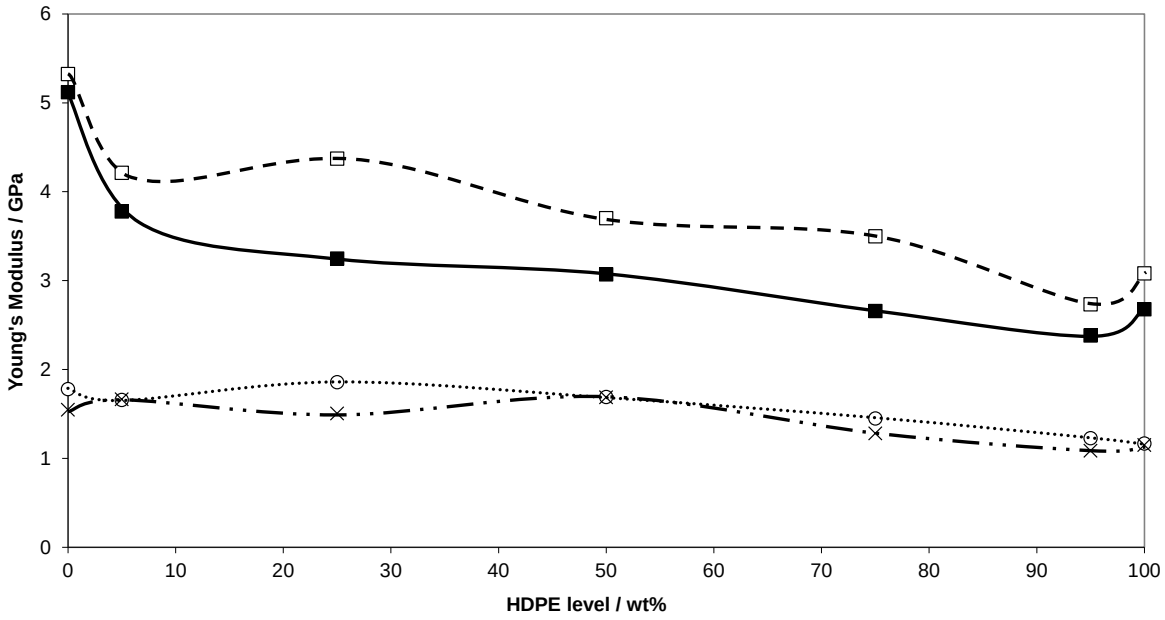

Figure 60: Plot of Young's modulus vs blend composition for HDPE/PP based composites, where o represents blend only, x represents blend with additive only, □ represents unmodified filler, and ■ represents modified filler.

In addition to the trends presented by the Young's modulus data, the elongation at break data appears to support the theory of the formation of a rubbery interphase. Again, the unmodified filler presents a composite with poor elongation due to the defects introduced by the particulate nature of the filler. The elongation values of the unfilled blend slowly increase from 100% PP to 100% HDPE, and the blend plus additives show a similar trend with some variation at the extremes. However, while the modified composite initially follows an albeit lower similar trend, there is a significant increase in percent elongation from 50% HDPE to 95% HDPE. This trend peaks at 95% HDPE before falling again at 100% HDPE, suggesting that the 5% PP present is having an effect on the morphology of the system.

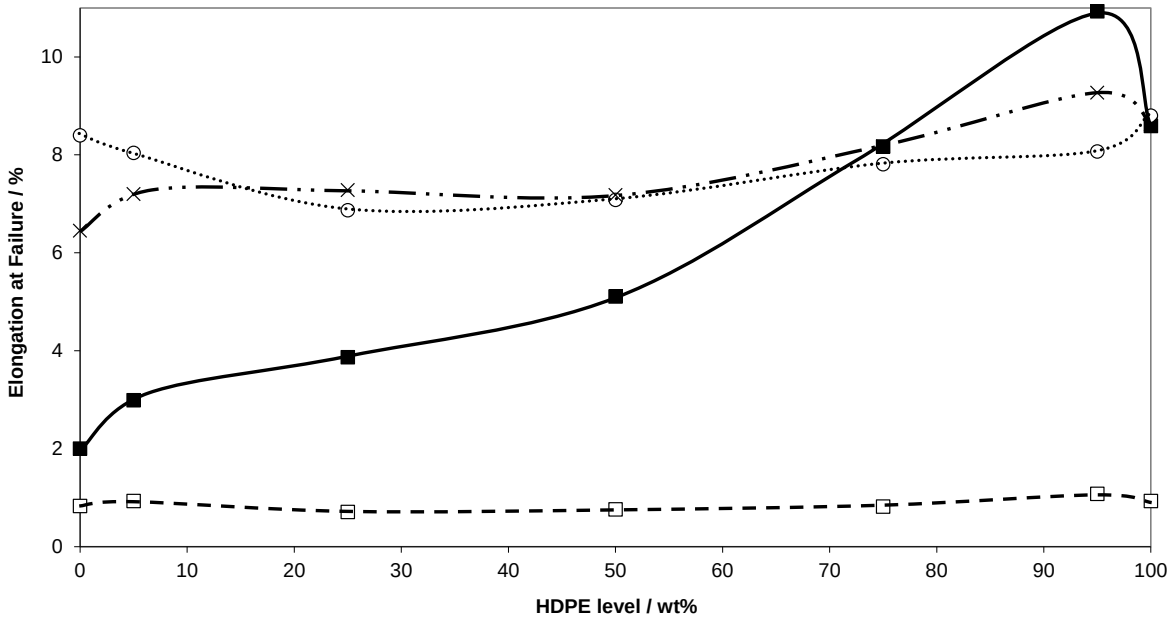

Figure 61: Plot of elongation at failure vs blend composition for HDPE/PP based composites, where o represents blend only, x represents blend with additive only, □ represents unmodified filler, and ■ represents modified filler.

As with the values for Young's modulus, the flexural modulus data shows that addition of filler creates a stiffer composite. While the unmodified filler produces the stiffest composite, the values for the modified filler follow a similar trend at lower values. This trend suggests that an increase in HDPE level results in a decrease in stiffness, which is also the case with the polymer-only blends and the polymer blends with the additive package. A reduction in stiffness may be caused by the formation of an amorphous rubbery interphase.

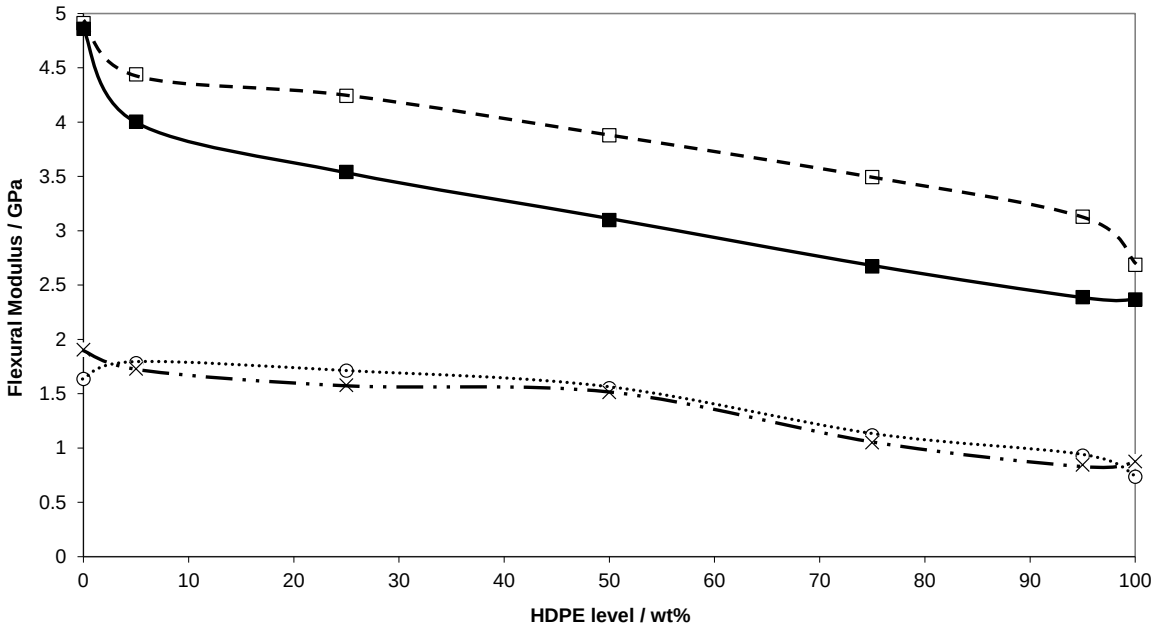

Figure 62: Plot of flexural modulus vs blend composition for HDPE/PP based composites, where o represents blend only, x represents blend with additive only, □ represents unmodified filler, and ■ represents modified filler.

Again, the untreated calcium carbonate greatly reduces the un-notched impact strength of the composites across the blend composition range (Figure 63). While the modification improves this, it is not increased to the level of the polymer blend or the individual polymers. However in this composite un-notched impact strength continuously rises as HDPE level increases with a climbing rate of improvement observed at 75% HDPE in the blend. Similar trends are observed for the unfilled polymer blends with the rising rate of increase observed at around 50% for the blends with the additive and at 25% HDPE for the blends alone.

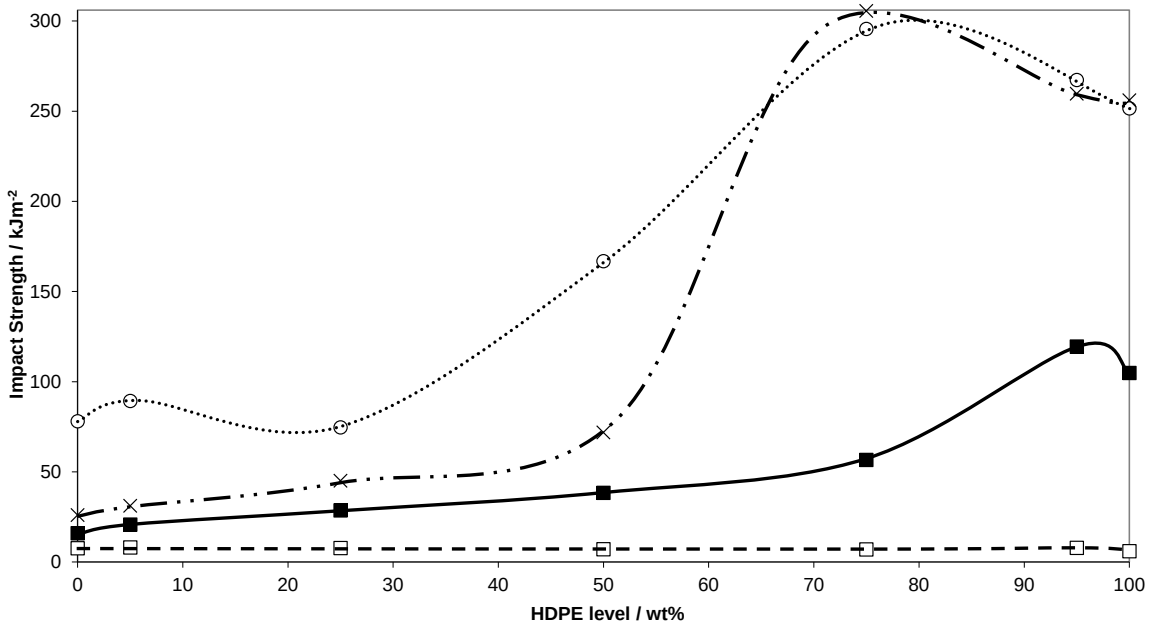

Figure 63: Plot of un-notched impact strength vs blend composition for HDPE/PP based composites, where o represents blend only, x represents blend with additive only, □ represents unmodified filler, and ■ represents modified filler.

Notched impact strength results (Figure 64) show that the C800 treatment of the filler has a toughening effect on the blend composites, and increasingly so towards the higher HDPE levels. The effect is very noticeable compared to composites formed with untreated filler, and there is also a similar trend in the blends where only the additive package is present. Thus, as is to be expected, the blend composites with 60% untreated filler are the worst performing due to their brittle nature.

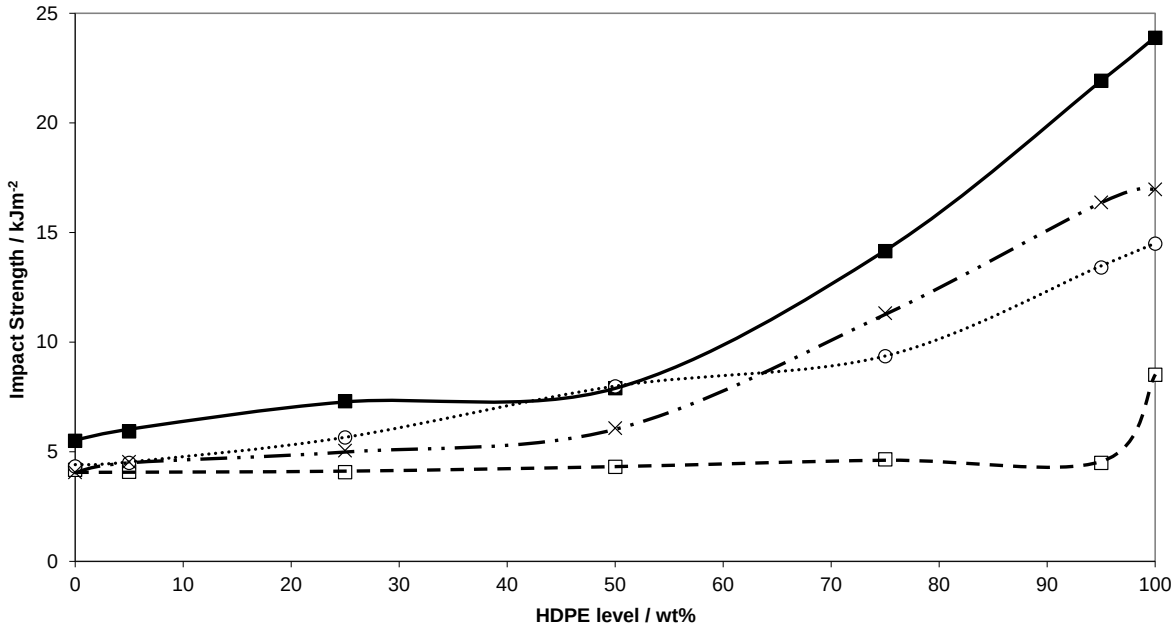

Figure 64: Plot of notched impact strength vs blend composition for HDPE/PP based composites, where o represents blend only, x represents blend with additive only, □ represents unmodified filler, and ■ represents modified filler.

Instrumented impact testing will provide force versus time data which will afford deeper insight into the failure modes.

For many of the mechanical properties, it appears that there is trade-off between the property investigated and the level of PP present. When applying this additive system to waste polymer blends, it may be possible to modify the properties by controlling the level of PP present.

3.4.2 Rheological properties

The melt flow rate data presents some interesting trends when compared to those discussed in Section 3.2.1, in that in the presence of the additive the MFR increases for PP and decreases for PE composites. In the case of the unmodified filler, there is little change in melt flow rate across the blend range. Yet for the other composite blends there is a marked decrease when moving from 100% PP to 100% HDPE, particularly in blends where only the additive is present.

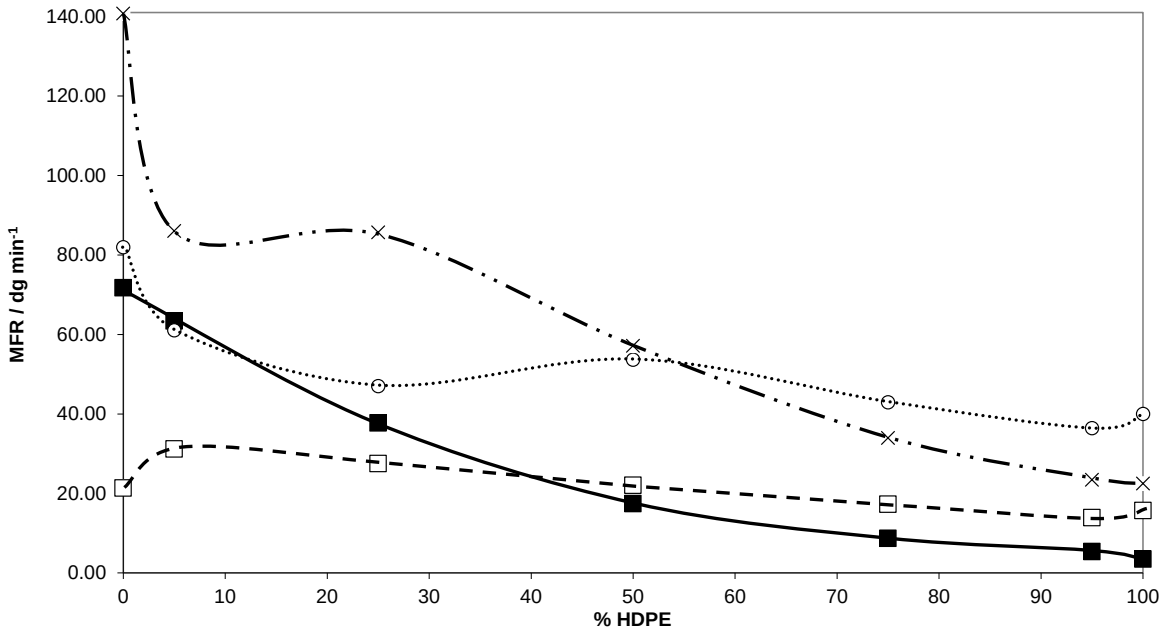

Figure 65: Plot of melt-flow rate vs blend composition for HDPE/PP based composites, where o represents blend only, x represents blend with additive only, □ represents unmodified filler, and ■ represents modified filler.

This can be seen in Figure 65, where the MFR for PP with the additive package alone is 140 dg min^{-1}, and falls to around 24 dg min^{-1} at 100% HDPE. A similar trend is also noticeable in the composites employing the treated filler, where the equivalent values are 75 dg min^{-1} for the PP composite and around 5 dg min^{-1} for the HDPE composites.

3.4.3 Morphological properties

The percentage crystallinity of each phase in each sample was calculated as per Section 2.5.3. Figure 66 shows that there is a marked increase in crystallinity in the HDPE phase from 0% HDPE to 30% HDPE then a levelling off from 40% to 80% and then potentially another increase to 100% HDPE. This trend is shown for all the samples but for the most part, the modified composite systems appear to have the lowest level of crystallinity. This may relate to a level of coupling to the filler and/or crosslinking at the interphase. The unfilled, unmodified blend has the highest levels of PE crystallinity from 25% HDPE to 75% HDPE blend ratios. The highest level of crystallinity is presented at 100% HDPE with unmodified filler, which may be due to nucleation effects of the filler [86 - 88].

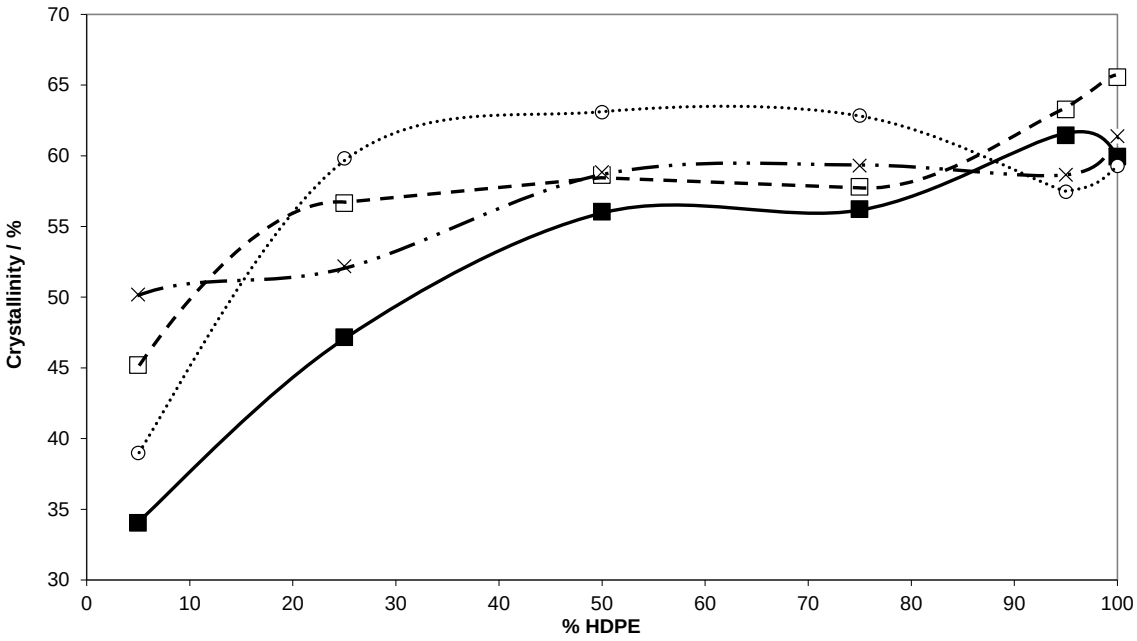

Figure 66: Plot of % crystallinity of the HDPE phase vs blend composition for HDPE/PP based composites, where o represents blend only, x represents blend with additive only, □ represents unmodified filler, and ■ represents modified filler.

Where the PP phase crystallinities are concerned (Figure 67), the trends are less distinct and it may be argued that an almost linear reduction is followed. Furthermore, generally lower percentage crystallinity values are observed, with the majority falling in the range of 20-45%. Overall, both plots suggest a reduction in crystallinity between the composites with the untreated filler and with the treated filler.

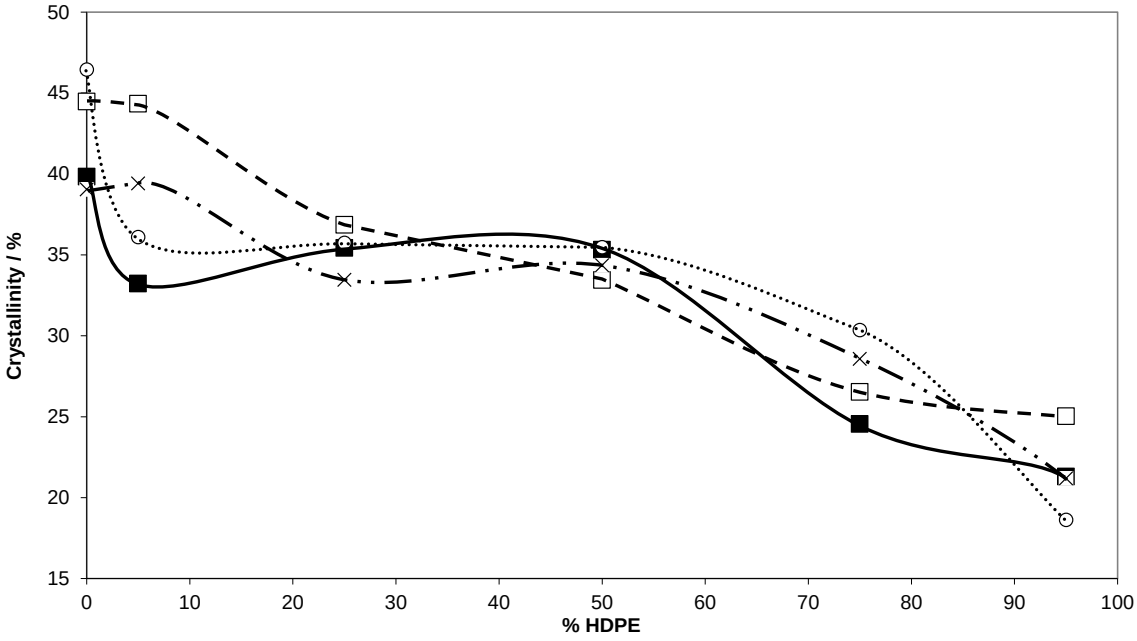

Figure 67: Plot of percent crystallinity of the PP phase vs blend composition for HDPE/PP based composites, where o represents blend only, x represents blend with additive only, □ represents unmodified filler, and ■ represents modified filler.

3.4.4 Solvent extraction – morphological properties

The composites were solvent extracted as detailed in Section 2.5.6, then the subsequent flask and thimble residues were analysed using DSC, TGA and ATR FT-IR.

The composites were designated the following identification labels:

- Unfilled blend (B series)
- Unfilled blend with additive package (A series)
- Filled blend (U series)
- Filled blend with additive package (M series)

Both the insoluble fractions, recovered from the paper cartridges, and the soluble fractions of the matrix were analysed as follows:

1. TGA (see Section 2.5.7) to ascertain the overall level of bound matrix in the case of the insoluble residues (see Section 3.4.4.1 for additional information)
2. FTIR (see Section 2.5.4) to determine the relative level, in the insoluble matrix, of PE to PP (via measurement of A(C-H) to A(CO_3) peak area ratios).
3. DSC (see Section 2.5.3) to determine the crystalline contents of the PP and HDPE components of the samples. The masses of these components were determined using the TGA and FTIR data which allows determination of the mass of PE and PP in the samples being analysed.

3.4.4.1 Insoluble matrix content by TGA

It was decided to record the mass change before loss of CO_2 from the calcium carbonate. Each of these values was plotted against the initial PP level in the sample. The values of insoluble matrix content are given in Table 22. Please note only thimble residues of composite samples were analysed as the unfilled (B and A series) samples did not yield any obvious insoluble fraction, though insoluble matrix may be soaked into the paper cartridges themselves as a “soft” gel.

Due to the potential variability in the results, a number of samples were analysed in duplicate and some in triplicate. Where measurements were repeated, the final value used for producing the graphs is given in the third column together with how the value was obtained. In some cases where three samples were run, the value showing the greatest deviation has not been included in the average calculation.

Table 22: Samples and the corresponding bound polymer content.

Samples*	Bound polymer content (% wt of residue)	Selected or averaged value (% wt)
P100 U TR (1)	5.69	5.60 (Average)
P100 U TR (2)	5.50	
H5P95 U TR	4.28	4.28
H25P75 U TR	9.38	9.38
H50P50 U TR (1)	1.59	0.95 (Average)
H50P50 U TR (2)	0.30	
H75P25 U TR	3.82	3.82
H95P5 U TR	81.02**	81.02
H100 U TR (1)	30.81**	32.11 (Average)
H100 U TR (2)	33.40	
P100 M TR (1)	3.41	3.26 (Average)
P100 M TR (2)	3.10	
H5P95 M TR	4.90	4.90
H25P75 M TR (1)	5.22	5.00 (average of 1 and 2 only)
H25P75 M TR (2)	4.78	
H25P75 M TR (3)	0.95**	
H50P50 M TR (1)	4.60	4.05 (Average)
H50P50 M TR (2)	3.50	
H75P25 M TR (1)	9.48	8.45 (Average of 1 and 3 only)
H75P25 M TR (2)	3.26**	
H75P25 M TR (3)	7.41	
H95P5 M TR	9.69	9.69
H100 M TR (1)	5.70	5.35 (Average)
H100 M TR (1)	5.00	
**where TR is an abbreviation of 'thimble residue'*		

****<u>Note</u>:** It is considered reasonable to ignore H25P75 MTR3 and H75P25 TR2 but to accept that H95P5 UTR and H100 UTR are valid as is H100 UTR has been done in duplicate and confirmed high values of bound polymer content in this blend range.

The bound insoluble matrix content was plotted against the initial PE level in the blend (Figure 68).

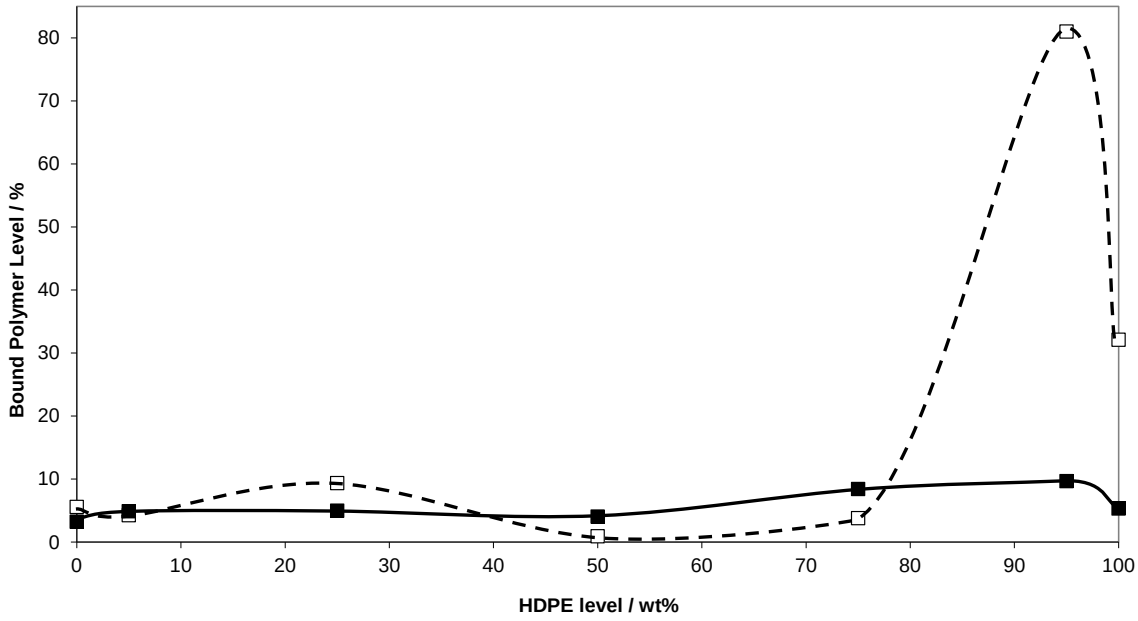

Figure 68: Insoluble matrix content against initial HDPE level; □ unmodified composites, ■ C800-DCP modified composites.

For the unmodified composites the insoluble matrix level started at a low percentage, and resulted in a high percentage at higher PE levels in the blend above 70% HDPE. This may be due to crosslinking of the PE matrix which is initiated by mechano-oxidative degradation resulting from the melt viscosities associated with use of a high filler content. As PE content of the matrix decreases beyond 75 % wt the bound polymer level falls sharply to a level below that for the equivalent C800-DCP modified composites. This may be due to chain scission related effects in the PP fraction that may also initiate chain scission at the few deliberately introduced branch points in the HDPE component. Beyond approximately 25% PE (i.e. 75 % wt PP) in the matrix, there are suggestions that the peroxide in the C800-DCP system dominates, leading to chain scission (in the PP phase) and an indication of a reduction in insoluble matrix content to a level below that in the equivalent unmodified composites. The low insoluble matrix content observed at low PP levels in the C800-DCP modified composites may be related to dominance of chain scission. However at 50 and 75 % wt PE in the matrix, the insoluble matrix content of the C800-DCP modified composites is higher than the equivalent unmodified composites, an effect that may be related to

the PP/HDPE ratio being conducive to coupling of matrix to the filler via adsorbed C800. Due to the low values recorded and the associated levels of error, the accuracy of these results would be significantly improved if all of the associated data sets were repeated in at least triplicate. However it is considered that the overall trends are valid.

3.4.4.2 Determination of the HDPE and PP content in the insoluble fractions (Thimble residues) using FTIR:

The compositions of the thimble and flask residues were determined using ATR-FTIR as described in Section 2.5.4. The relative HDPE content was then determined from the absorbancies of the methylene and methyl asymmetric stretching bands using Equation 4 (Section 2.5.4). The equation for the calibration curve, made up from the samples before extraction (Equation 5), was then used to determine the composition of the residues.

The PP content of the thimble residues of the U and M series composites is given in Table 23 and Table 25, and PP content in the thimble residues is plotted against the initial PP level in the matrix in Figure 69.

It is evident that the extraction behaviour (in terms of thimble residue composition) of the U and M series composites at PP levels greater than 50 % wt in the matrix is sensibly identical. However, at PP levels less than 50 % wt in the matrix, some interesting differences are apparent; the PP content is higher in the thimble residue of the unmodified composites. This observation is likely to be due to reduced chain scission of PP relative to that in the equivalent C800-DCP modified samples. The dicumyl peroxide in the M series composites is likely to lead to rapid chain scission of the relatively small amount of PP present. The insoluble matrix content versus initial PP level plot (Figure 68) also indicates some crosslinking (most probably of HDPE within the bulk matrix); the latter will trap PP chains both via physical entrapment and grafting. In the C800-DCP modified composites, the rate of PP chain scission is likely to be greater than the rate of PP and HDPE macroradical addition to the active double bond of C800, and greater than the rate of peroxide induced crosslinking of HDPE (it is also likely that chain scission of the PE occurs as well, particularly at any branch points). Therefore possibly only a

very small fraction of the broken PP chains are bound to the filler or to HDPE sequences, the remainder is extractable as a result of being unattached.

Table 23: PP content in the thimble residues for the unmodified (U series) and C800-DCP modified (M series) composites.

%PP initial composition	U series %PP in TR	M series %PP in TR
100	100	100
95	91.24	81.42
75	67.63	72.92
50	34.15	28.04
25	29.26	3.78
5	33.22	4.37
0	0.245	2.77

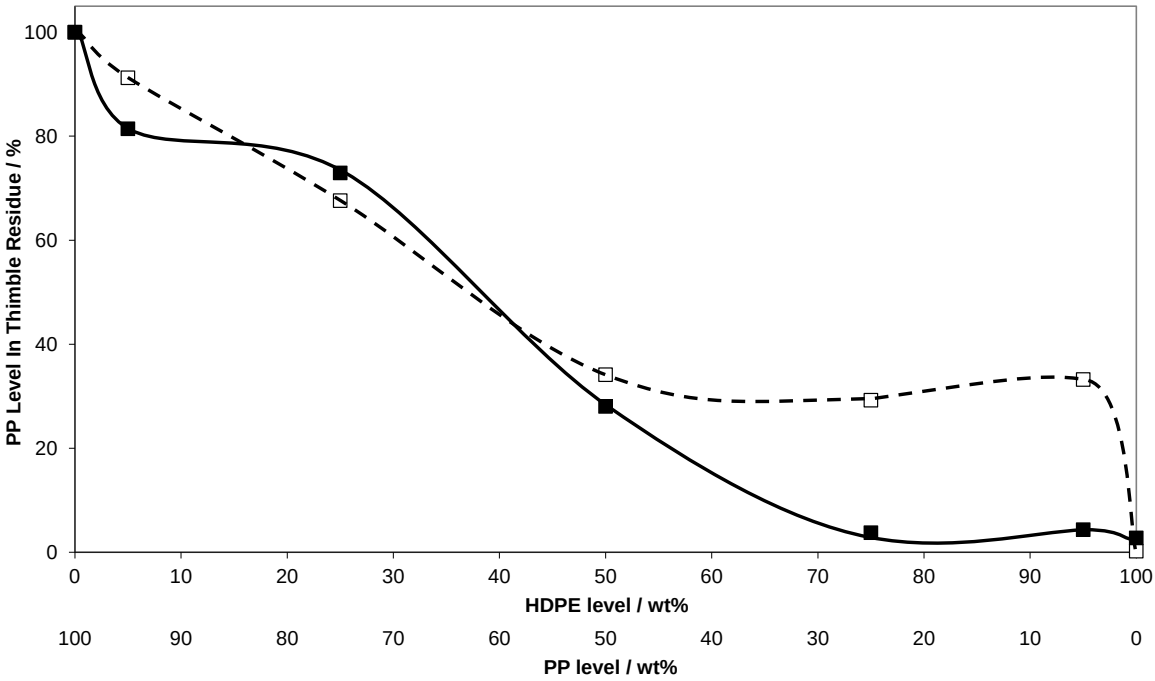

Figure 69: %PP in thimble residue vs %PP initial composition. □ unmodified composites, ■ C800-DCP modified composites.

3.4.4.3 Determination of the HDPE and PP content in the soluble fractions (Flask residues) using FTIR:

The PP content found in the flask residues of the unfilled PP/HDPE blends (B series), C800-DCP modified unfilled PP/HDPE blends (A series), 60 % wt GCC filled PP/HDPE blends (U series) and C800-DCP modified 60 % wt GCC filled PP/HDPE blends (M series), are given in Table 24. PP content in the flask residues are plotted in Figure 70 and Figure 71 for the B and A series and U and M series samples, respectively.

Table 24: PP content in the B, A, U and M series in the flask residues.

%PP initial composition	B series %PP in FR	A series %PP in FR	U series %PP in FR	M series %PP in FR
100	100	100	100	100
95	89.35	98.41	88.69	87.81
75	55.65	74.67	62.04	70.93
50	81.45	50.92	29.67	49.26
25	20.56	30.38	19.47	25.90
5	4.11	3.41	5.51	6.58
0	9.32	8.05	7.34	5.49

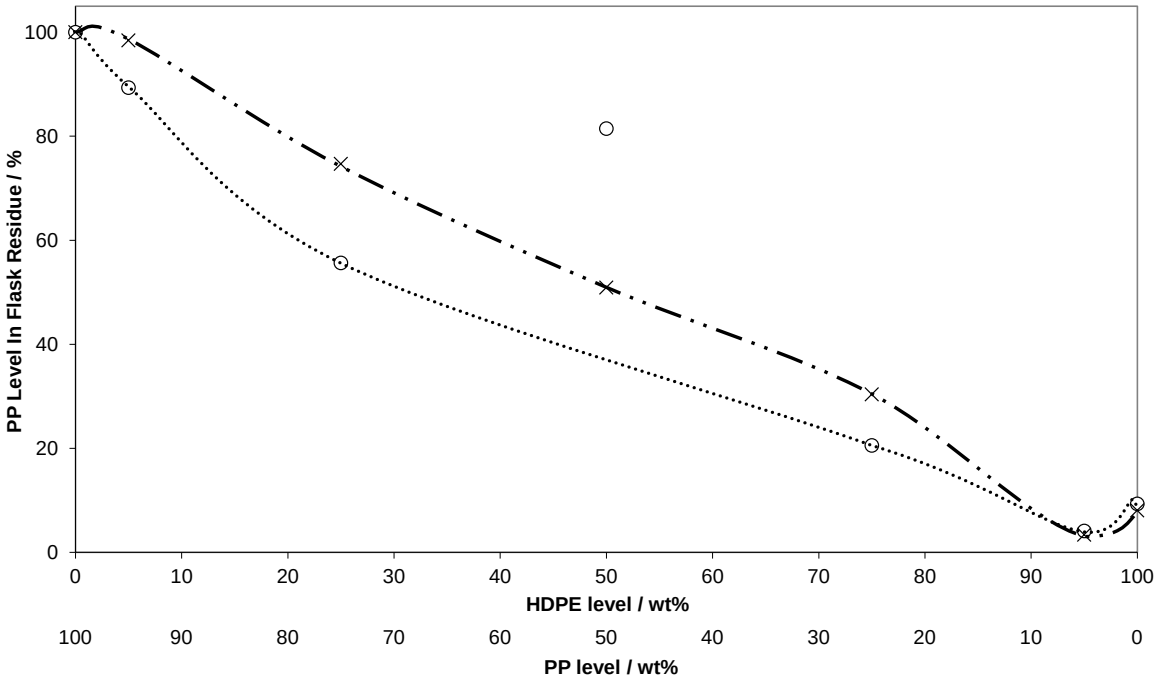

Figure 70: %PP in flask residue vs %PP initial composition in B and A series. ○ unfilled composites, x unfilled with additive composites.

Interestingly the flask residues of the samples modified with C800-DCP (M and A series) show a linear composition dependence, this is not surprising bearing in mind the small (insignificant) amount of insoluble matrix in relation to the soluble component. However, a negative deviation from linear composition dependence is observed with samples that are not C800-DCP modified. This smaller than expected level of PP in the flask residue for the latter samples is likely to be due to entrapment/grafting of PP within the insoluble crosslinked network of HDPE which is initiated as a result of mechano-oxidative degradation. Whilst an insoluble residue was not observed in the A series samples some lightly crosslinked HDPE may have become trapped within the filter paper from which the extraction thimbles were made. For the U series samples at least both the insoluble matrix content and PP level in the thimble residue was high (Figure 68) when the initial PP level in the matrix was low.

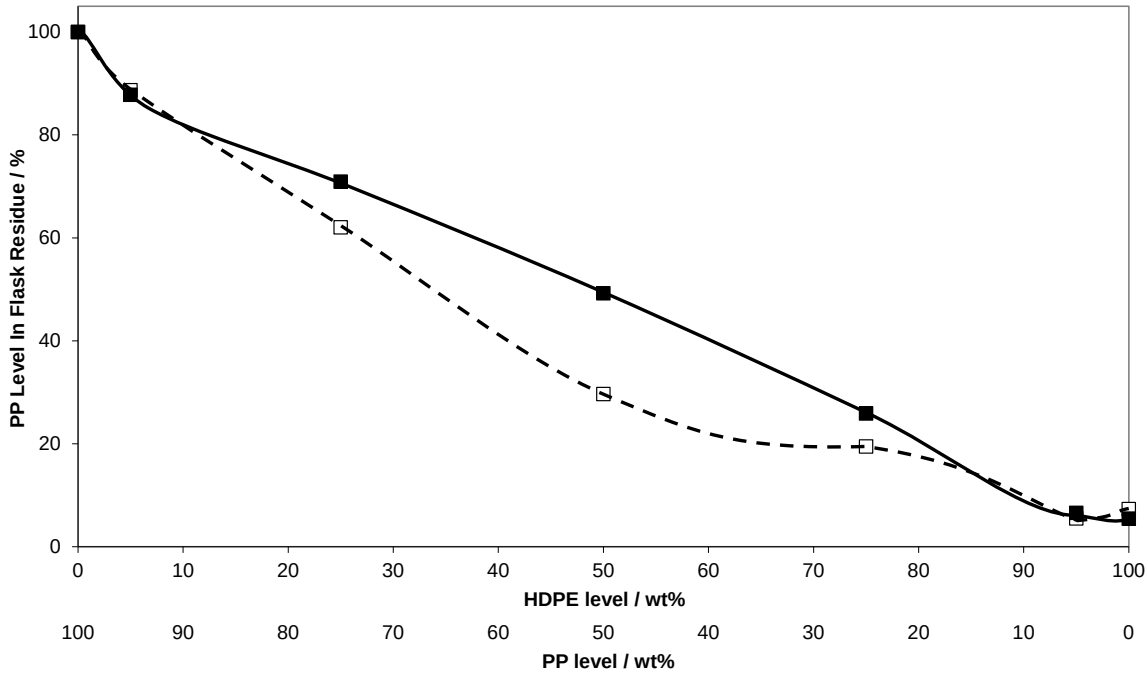

Figure 71: %PP in flask residue vs %PP initial composition in U and M series. □ unmodified composites, ■ C800-DCP modified composites.

3.4.4.4 Crystalline content of thimble and flask residues:

The crystalline content of the HDPE and PP components in the thimble residue and the flask residue samples were determined using DSC (see Section 2.5.3). As stated, the overall mass of polymer in the thimble residue samples was determined using the TGA data (Section 2.5.7) and the ratio of PP to HDPE was determined using the ATR-FTIR data (Section 2.5.4).

3.4.4.5 Thimble residues:

The crystalline content (X_c) in the PP and HDPE components ($(X_c)_{PP}$ and $(X_c)_{PE}$, respectively) in the thimble residues of the U series samples are shown in Table 25. $(X_c)_{PP}$ and $(X_c)_{PE}$ are plotted as a function of initial PP level in matrix in Figure 72.

Table 25: Crystallisation of PP and HDPE in U series in TR.

%PP in initial composition	$X_{c\ PP}$(U)	$X_{c\ PE}$(U)
100	16.5	0
95	17.4	14.7
75	22	21.6
50	0	57
25	26	19.9
5	1.4	43.5
0	0	67

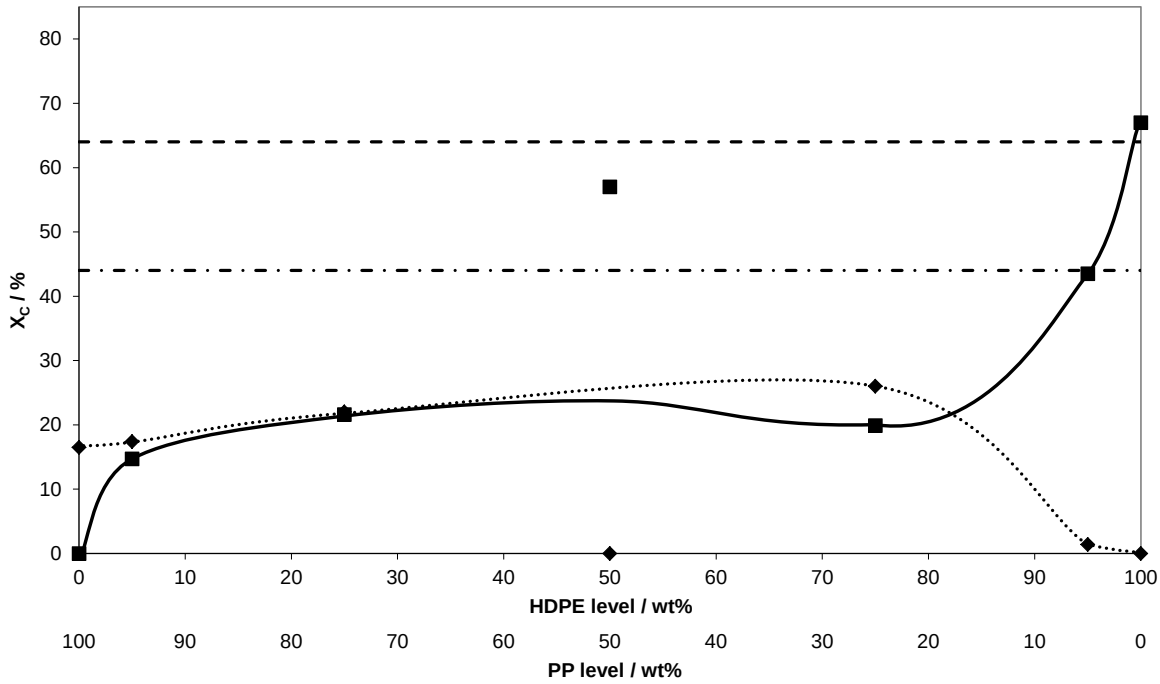

Figure 72: X_c against PP level in initial composition for thimble residues (insoluble fractions) of unmodified filled blends (U series samples). ◆ $(X_c)_{PP}$, ■ $(X_c)_{PE}$. The dashed line denotes the crystalline content of an injection moulded sample of HDPE and the dot-dashed line denotes the crystalline content of an injection moulded sample of PP.

The data point for the 50:50 PP/HDPE blend is considered erroneous. If the latter point is ignored, $(X_c)_{PE}$ decreases quickly from 67% to a limiting value of ca 20% at matrix PP levels between 25 % wt and 75 % wt. Beyond the latter, $(X_c)_{PE}$ decreases to about 15 % at 95 % wt PP and then finally to zero at 100 % wt PP. Again ignoring the data point for the 50:50 U series composite, $(X_c)_{PP}$ increases initially rather slowly to a maximum of 26 % at 25 % wt PP and then slowly, almost linearly, decreases to about 17% at 100 % wt PP. The very low value of $(X_c)_{PP}$ and reduced value of $(X_c)_{PE}$ at 5 % wt PP is consistent with the high insoluble matrix content which can be explained by crosslinking and entrapment of PP, the low $(X_c)_{PP}$ implies that the PP is entrapped by grafting with PP block lengths that are too short to enable crystallisation to occur. The latter argument is true but to a lesser extent for all the U series samples – the crystalline content of both components are reduced relative to the respective bulk, unbound polymers.

The crystalline content (X_c) in the PP and HDPE components ($(X_c)_{PP}$ and $(X_c)_{PE}$, respectively) in the thimble residues of the M series samples are shown in Table

26. $(X_c)_{PP}$ and $(X_c)_{PE}$ are plotted as a function of initial PP level in matrix in Figure 73.

Table 26: Crystallisation of PP and HDPE in M series in TR.

%PP initial composition	$X_{c\ PP}$(M)	$X_{c\ PE}$(M)
100	4.3	0
95	10	23
75	8	47
50	0	41
25	15.6	12.6
5	16.3	11
0	0	33

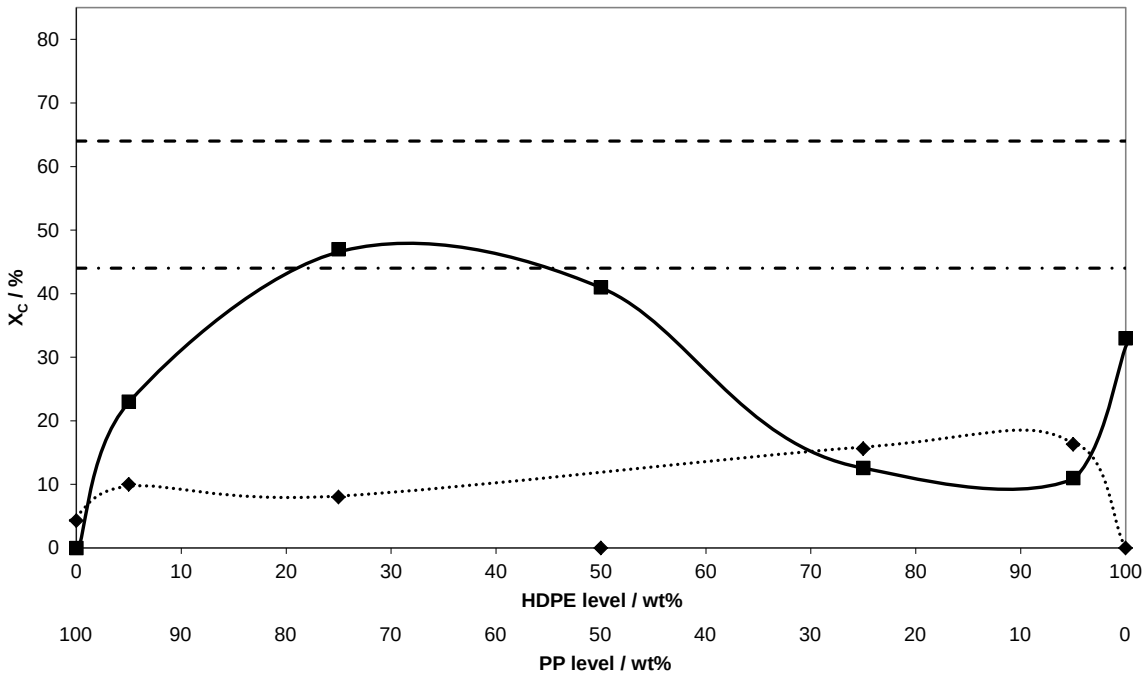

Figure 73: X_c against PP level in initial composition for thimble residues (insoluble fractions) of modified filled blends (M series samples). ◆ $(X_c)_{PP}$, ■ $(X_c)_{PE}$. The dashed line denotes the crystalline content of an injection moulded sample of HDPE and the dot-dashed line denotes the crystalline content of an injection moulded sample of PP.

If the 50:50 HDPE/PP data point is ignored, $(X_c)_{PP}$ undergoes a slow reduction from about 16 % at 5 % wt PP to about 10 % at 95 5 wt PP and a drop to below 5 % at 100 % wt PP. $(X_c)_{PE}$ is at a low level (33 %) at 0 % wt PP at reduces quickly to about 9 % from 5 % wt to 25 % wt PP. Beyond 25 % wt PP, $(X_c)_{PE}$ increases to

41 % at 50 % wt PP and then increases further to a maximum at 75 % wt PP, followed by a reduction to 23 % at 95 % wt PP. The reduced X_c of both components up to 25 % wt PP indicates formation of a block copolymer of consisting of short PP and HDPE sequences. The latter appears to be formed more readily in the presence of C800-DCP. The increase in $(X_c)_{PE}$ at the higher PP levels may be due to separation of branched from relatively linear sequences of HDPE as a result of beta-scission at the branch points. Liberation of the linear sequences of HDPE will allow them to crystallise relatively un-hindered. The low $(X_c)_{PP}$ in this region suggests that a block copolymer type structure is still present, which is perhaps bonded to the filler surface via the adsorbed C800. Furthermore, the more crystalline HDPE component is perhaps on the extremity of the interfacial region.

3.4.4.6 Flask residues:

3.4.4.6.1 B Series Samples – unfilled polyolefin blends

The crystalline content (X_c) in the PP and HDPE components ($(X_c)_{PP}$ and $(X_c)_{PE}$, respectively) in the flask residues of the unfilled blends (B series samples) are shown in Table 27. $(X_c)_{PP}$ and $(X_c)_{PE}$ are plotted as a function of initial PP level in matrix in Figure 74.

Table 27: Crystallinity of PP and HDPE of B series in FR.

%PP initial composition	X_{cPP} (B)	$X_{C\ PE}$ (B)
95	44.3	64
75	41.4	64
25	12.3	40.8
5	27.4	58.9

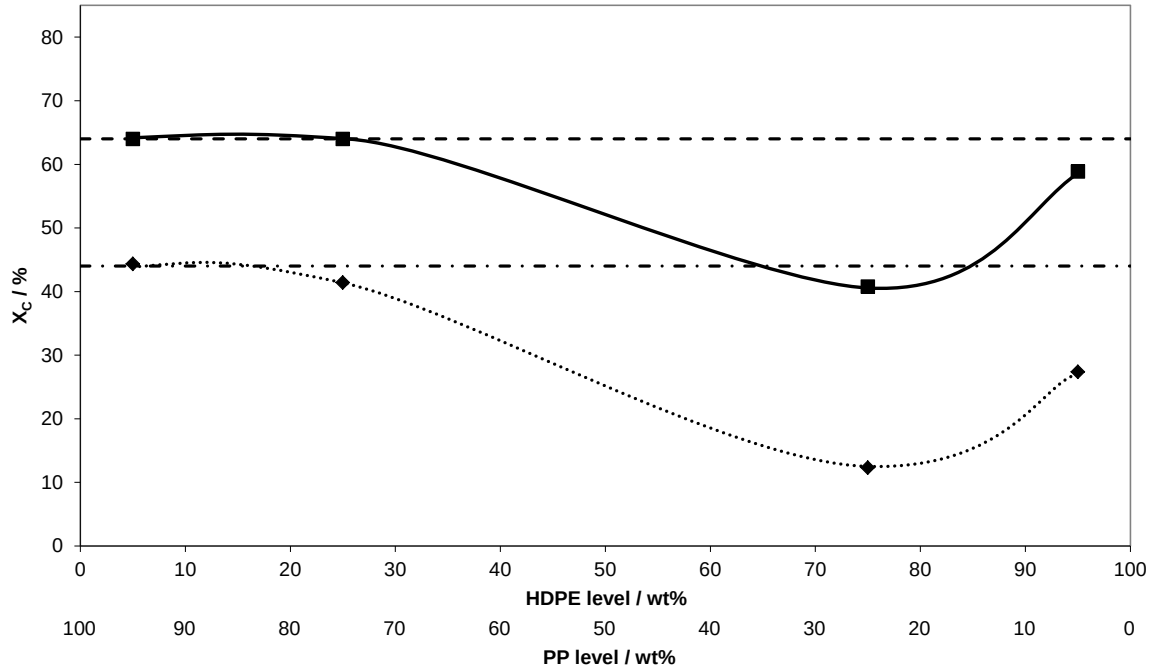

Figure 74: X_c against PP level in initial composition for flask residues (soluble fractions) of unfilled blends (B series samples). ◆ $(Xc)_{PP}$, ■ $(Xc)_{PE}$. The horizontal dashed and dot-dashed lines have been defined previously (see Figure 70).

Firstly considering the $(X_c)_{PP}$ trends, at low PP levels $(X_c)_{PP}$ is slightly lower than expected based on the value for the bulk composite (ca. 45 %), this may be due to degradation (and possible grafting to HDPE) of this small amount of PP during extraction. As PP level increases its crystalline content reaches the expected value. The $(X_c)_{PE}$ data shows some obvious errors at higher PP levels though at 5 and 25 % wt PP $(X_c)_{PE}$ values are only slightly lower than that in bulk sample (ca. 64 %).

3.4.4.6.2 A Series Samples – polyolefin blends with C825 & DCP only

The crystalline content (X_c) in the PP and HDPE components ($(X_c)_{PP}$ and $(X_c)_{PE}$, respectively) in the flask residues of the unfilled blends modified with C800-DCP (A series samples) are shown in Table 28. $(X_c)_{PP}$ and $(X_c)_{PE}$ are plotted as a function of initial PP level in matrix in Figure 75.

Table 28: Crystallinity of PP and HDPE of A series in FR.

%PP initial composition	X_{CPP} (A)	X_{cPE} (A)
95	51.6	250*
75	39.9	49.9
25	29.7	76.3
5	40.6	75.8
*Erroneous value not included in graph but replaced with the X_C value for an injection moulded sample of HDPE which was 64%.		

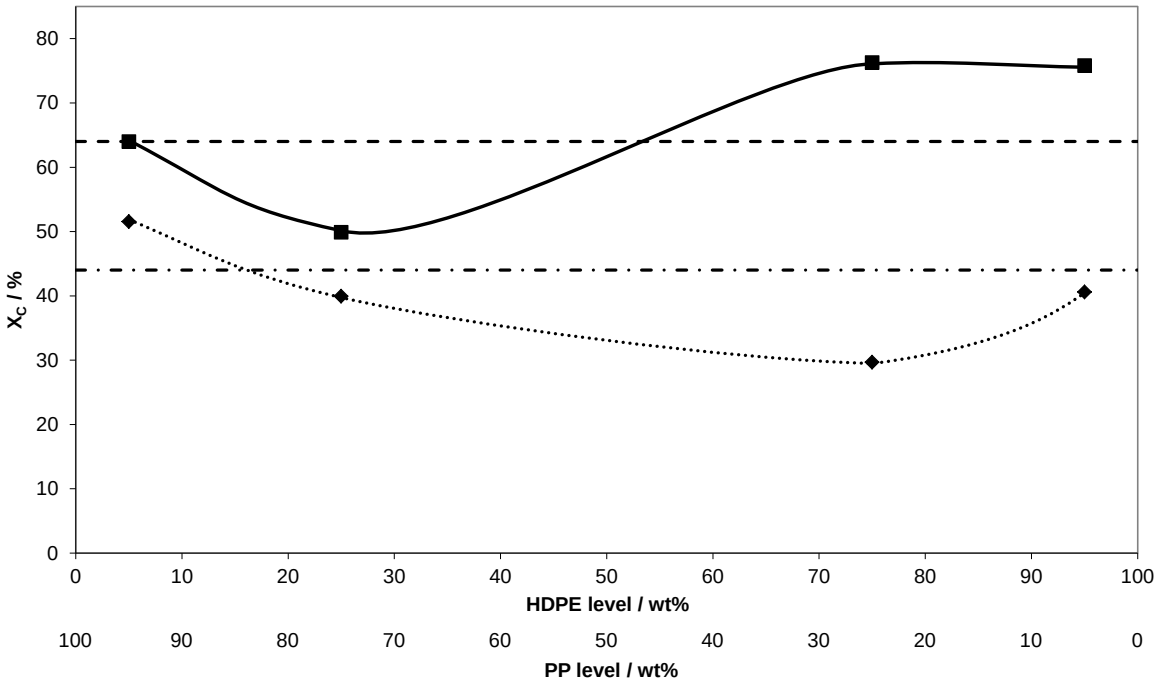

Figure 75: X_c against PP level in initial composition for flask residues (soluble fractions) of unfilled with additive blends (A series samples). ◆ $(X_c)_{PP}$, ■ $(X_c)_{PE}$. The horizontal dashed and dot-dashed lines have been defined previously (see Figure 72).

$(X_c)_{PP}$ remains between 30 and 50% throughout the PP level range, the reduction to around 30 % (at 25 % wt PP) may be indicative of some short-block copolymer formation. $(X_c)_{PE}$ for the 95 % wt PP composite is obviously erroneous, however, the values at 5 and 25 % wt PP are rather high, but not unrealistically so considering possible incorporation of the branched components within the insoluble fraction and liberation of the more linear fractions.

3.4.4.6.3 U Series Samples – polyolefin blends with untreated filler

Table 29: Crystallinity of PP and HDPE of U series in FR.

%PP initial composition	X_{cPP} (U)	X_{cPE} (U)
95	56.67	34.08
75	56.70	49.89
25	46.30	81.61
5	40.64	81.83

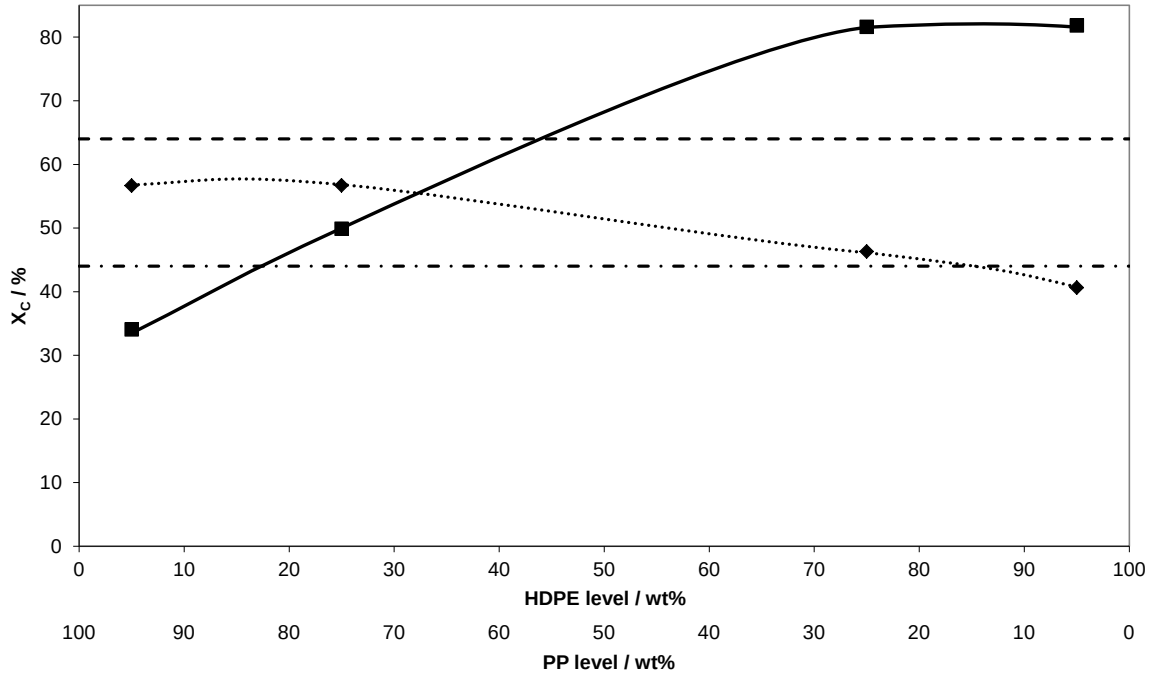

Figure 76: X_c against PP level in initial composition for flask residues (soluble fractions) of unmodified filled blends (U series samples). ◆ $(X_c)_{PP}$, ■ $(X_c)_{PE}$. The horizontal dashed and dot-dashed lines have been defined previously (see Figure 70).

The crystalline content (X_c) in the PP and HDPE components ($(X_c)_{PP}$ and $(X_c)_{PE}$, respectively) in the flask residues of the filled blends (U series samples) are shown in Table 29. $(X_c)_{PP}$ and $(X_c)_{PE}$ are plotted as a function of initial PP level in matrix in Figure 76. Addition of filler to the HDPE/PP blends brings about some interesting changes, perhaps due to the higher shear experienced by the polymer chains in the melt and the associated mechano-oxidative degradation processes. Considering the $(X_c)_{PP}$ data first of all; there is a steady increase from ca 40 % at 5 % wt PP to a limiting value close to 60 % at 75 % wt PP. In contrast $(X_c)_{PE}$ reduces

from perhaps rather high values just over 80 % at 5 and 25 % wt PP down to 34 % at 95 % wt PP. The increase in $(X_c)_{PP}$ may be related to chain scission within the bulk matrix; shorter chains will crystallise more rapidly to a higher crystalline content. The high $(X_c)_{PE}$ observed at 5 and 25 % wt PP may be related to segregation of the more linear HDPE chains at low PP levels. As the PP level increases such that HDPE becomes the minor component the probability of incorporation within short block structures formed via collision of PP and HDPE macro-radicals increases, leading to the reduction in $(X_c)_{PE}$.

3.4.4.6.4 M Series Samples – polyolefin blends with treated filler

The crystalline content (X_c) in the PP and HDPE components ($(X_c)_{PP}$ and $(X_c)_{PE}$, respectively) in the flask residues of the C800-DCP modified filled blends (M series samples) are shown in Table 30. $(X_c)_{PP}$ and $(X_c)_{PE}$ are plotted as a function of initial PP level in matrix in Figure 77.

Table 30: Filled blend with additive.

%PP initial composition	X_{cPP} (M)	X_{cPE} (M)
95	46.58	24.84
75	55.28	42.63
25	36.93	55.88
5	32.69	73.08

The C800-DCP modified filled blends show very similar trends to the unmodified filled blends but at a generally lower level of crystalline content. In very general terms the data has been shifted down the y- axis, though the $(X_c)_{PE}$ / $(X_c)_{PP}$ crossover point appears to be shifted slightly to a lower PP level. The overall reduction in X_c for all components is likely to be related to the enhanced level of degradation (and possibly increased level of short-block HDPE – PP block copolymer and possibly loose HDPE gel) associated with the DCP.

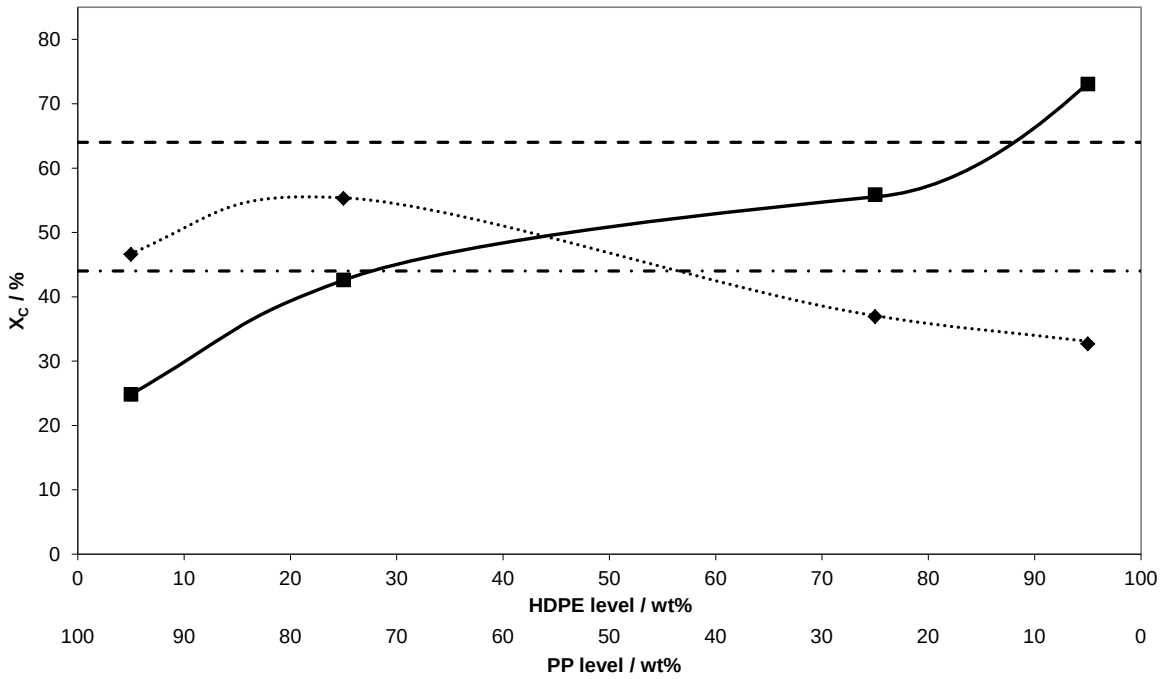

Figure 77: X_c against PP level in initial composition for flask residues (soluble fractions) of modified filled blends (M series samples). ◆ $(X_c)_{PP}$, ■ $(X_c)_{PE}$. The horizontal dashed and dot-dashed lines have been defined previously (see Figure 70).

3.5 Discussion of problems with C800 as a compatibiliser for PCPW

Whilst in PCPW the results from the preliminary work suggested that C800 seemed to be less effective than when used in PIPW, this could be due to several factors, including (but not limited to):

- the different ratio of polymers present
- different grades of polymer present
- the level of degradation of the polymer waste
- the amount of contamination by denser polymers
- how effective the washing process is

As with the PIPW, the action of the peroxide will have the effect of crosslinking the PE component and causing chain scission of the PP component [84]. However, as the PCPW was composed of a majority of PP (c.a.70%), much of this would undergo the chain scission reaction, therefore reducing the effect that the C800 would normally have. The potentially rapid peroxidation of fatty residue contamination on PCPW may also accelerate degradation in the melt state [89]. To overcome this problem, active repair of the 'damaged' (degraded) PP matrix is required, which would be achieved by re-bonding the smaller fragments of the PP chains back together. Various approaches may be taken, including increasing the functionality of C800, or the use of a co-agent such as trimethylol propane triacrylate (TMPTA).

From the observations made in Sections 3.1 to 3.4, it can be seen that whilst network formation may be evident in composites with a higher proportion of HDPE, chain scission leads to a reduction in molecular weight of the PP. This is manifested as an increase in MFR values, accompanied by a reduced improvement in mechanical properties. One such method of overcoming the issue of chain scission is to attempt to crosslink the reduced molecular weight fragments of PP using a multifunctional monomer such as TMPTA.

3.6 Overcoming the limitations of C800

3.6.1 TMPTA

Trimethylol propane triacrylate (TMPTA, Figure 78) is a tri-functional monomer that has been used to crosslink PP [90]. It was envisaged that TMPTA could be utilised as a co-agent with the C800 coupling agent to actively repair the matrix while also coupling it to the filler surface.

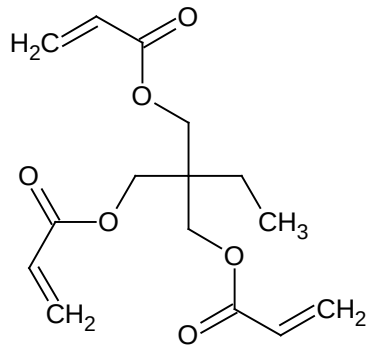

Figure 78: Structural formula for TMPTA. Tri-functionality is achieved via the three active double bonds present.

Overall, the addition of TMPTA appears to have reduced the flexural moduli of the PCPW (black bars), yet increased it in the PIPW samples (white bars). Furthermore, Figure 79 shows that adding peroxide with the TMPTA increases the modulus of the PCPW sample, yet reduces the value for the PIPW sample.

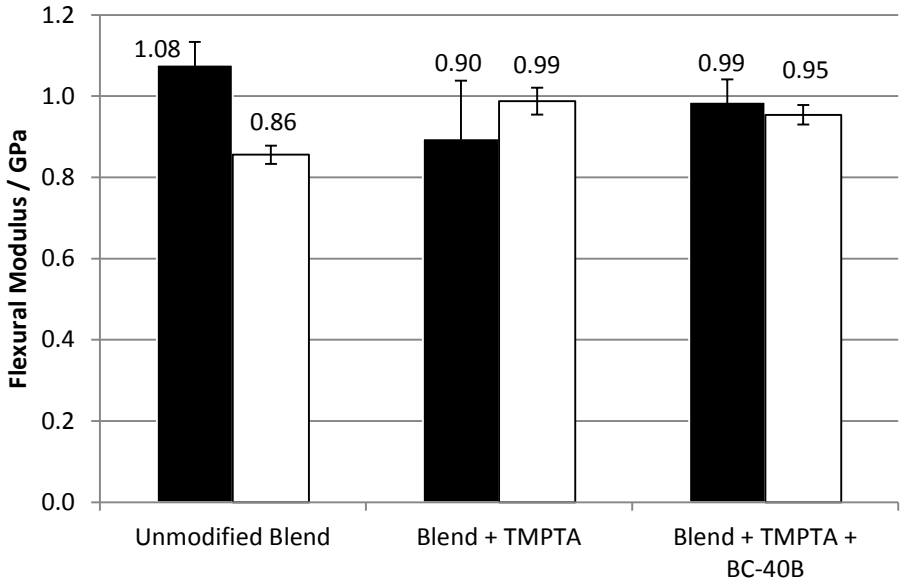

Figure 79: Flexural modulus data for composites incorporating TMPTA where the black bars represent the PCPW and the white bars represent the PIPW.

This effect is interesting considering that the PP level for the PIPW (Sample C) is 62% and the level for the PCPW is around 74%, a difference of only 12%.

When reviewing the un-notched impact data, the PCPW (black bars) utilising the TMPTA without the peroxide gives the highest value, and gives the second highest value with the peroxide. The PIPW (white bars) utilising the TMPTA with the peroxide gives the lowest value at 21.92 kJm^{-2}.

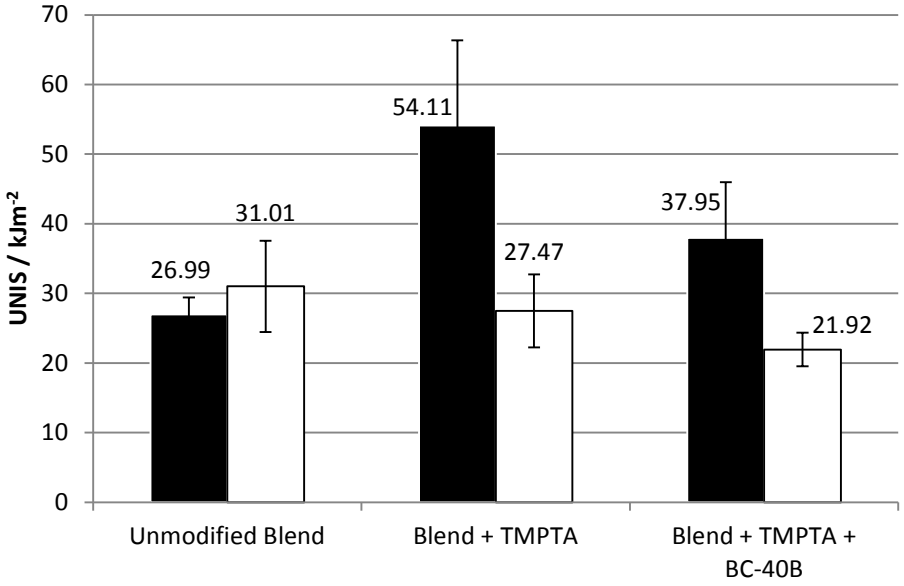

Figure 80: UNIS data for composites incorporating TMPTA where the black bars represent the PCPW and the white bars represent the PIPW.

The PIPW samples also show a less marked difference in values when compared to those for the PCPW samples. This may be due to the fact that the PP fraction of the blend is more degraded in the PCPW and is thus more extensively 'repaired', while the TMPTA has little to no effect on the less degraded portion of the PIPW samples.

3.6.2 New compounds

In order to overcome some of the limitations of the C800® additive, two new compounds were synthesised. It was envisaged that increased functionality towards both the polymer matrix and the filler surface would promote more extensive coupling. This would be achieved firstly via two filler reactive functional groups to provide stronger, two-point anchorage to the filler surface, and ideally orientate the molecule in such a way that the polymer reactive groups would be directed into the matrix. Secondly, two polymer reactive groups (acrylic double bonds) will boost the functionality from two (in the case of C800) to four, thereby increasing the probability of 'active matrix repair' and thus facilitate network formation. In previous work conducted on 1, 3-phenylene dimaleimide (BMI) modified PP/magnesium hydroxide based composites [91], mixing torque versus time data shows that BMI can at least chain extend unfilled PP. It is anticipated that the new compounds could act in the same manner as they have the same functionality and similar double bond reactivity to BMI. Furthermore, Pukanzsky has shown that increased penetration of the hydrocarbon chains of the coupling agent molecule into the bulk polymer matrix can improve mechanical properties [92].

Compounds A and B in Figure 81 have been synthesised by Lubrizol Ltd and satisfy the above requirements. Compound A (Figure 81 [i]) has just one spacer group between the anchor group and the acrylic double bond. However, compound B (Figure 81 [ii]) has effectively four spacer groups. Variation in the distance between the anchor group and the double bond may affect the access of matrix macro-radicals to the double bonds.

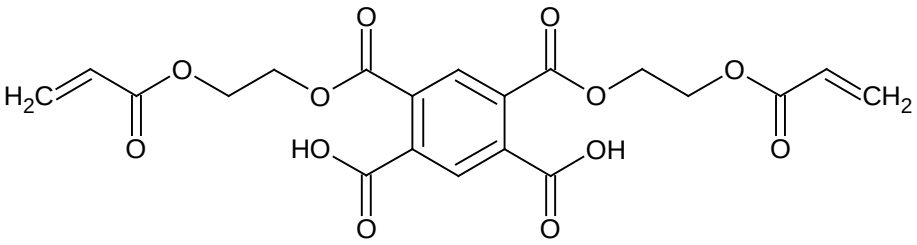

(i)

4,6-bis({[2-(prop-2-enoyloxy)ethoxy]carbonyl})benzene-1,3-dicarboxylic acid

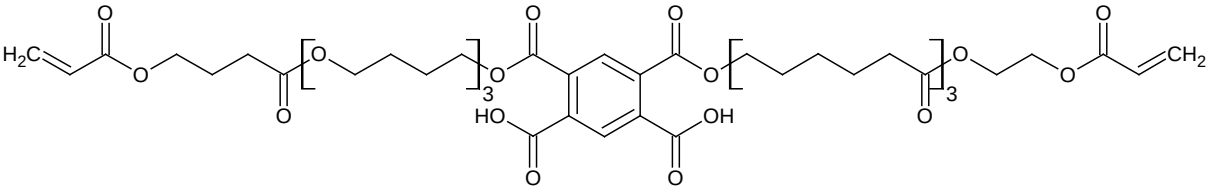

(ii)

4-({4-[4-(4-{[4-(prop-2-enoyloxy)butanoyl]oxy}butoxy)butoxy]butoxy}carbonyl)-6-[({6,12,18-trioxo-18-[2-(prop-2-enoyloxy)ethoxy]octadecyl}oxy)carbonyl]benzene-1,3-dicarboxylic acid

Figure 81: Structural formulae and names of the two oligomers produced for Compound A (i) and Compound B (ii).

3.6.3 Effect of the new compounds on a sample of post-industrial polymer waste

The new compounds were each dissolved in acetone and slurried with Ultrasil VN3 silica for 18 hours. This was then dried for 72 hours at 24°C to evaporate the acetone and produce a 50% wt active form of the compounds that were easier to handle and dose than their native highly viscous forms. A 50% wt active form of Solplus® C800 exists in which the latter is supported on a gel silica and is commercially known as Solplus C825®. For the following work, C800 has been used in the C825 form as a control to evaluate the effectiveness of the new compounds produced.

The graphs that follow compare the effect of both compounds A and B at three different loading levels. The first is the same mass loading level as C825 (i.e. 1.2 wt % calculated on the mass of the filler giving 0.6 wt % of C800 on the mass of

filler), the second uses the same number of moles of the compound as that of C800. The third and final level uses half the number of moles of the original C800 level. These were devised as a means of assessing the effectiveness of the compounds as follows:

- The same loading level results in less coupling groups present due to the higher molecular weight of the compounds A and B relative to C800
- The same number of moles as C800 results in double the number of moles of coupling groups present, taking into account the tetra- functionality of the new compounds.
- Half the number of moles of A and B results in the same amount of coupling groups present as in 0.6 wt % on filler of C800 due to the tetra-functionality of the new compounds; i.e. an equimolar amount.

Figure 82 shows that compound A appears to perform better than compound B in terms of failure strength, while C800 still gives the highest value. This may be due to the fact that there is less coupling of compound B to the filler and/or the matrix. Furthermore, compound A almost matches C800 if added at the same molar level.

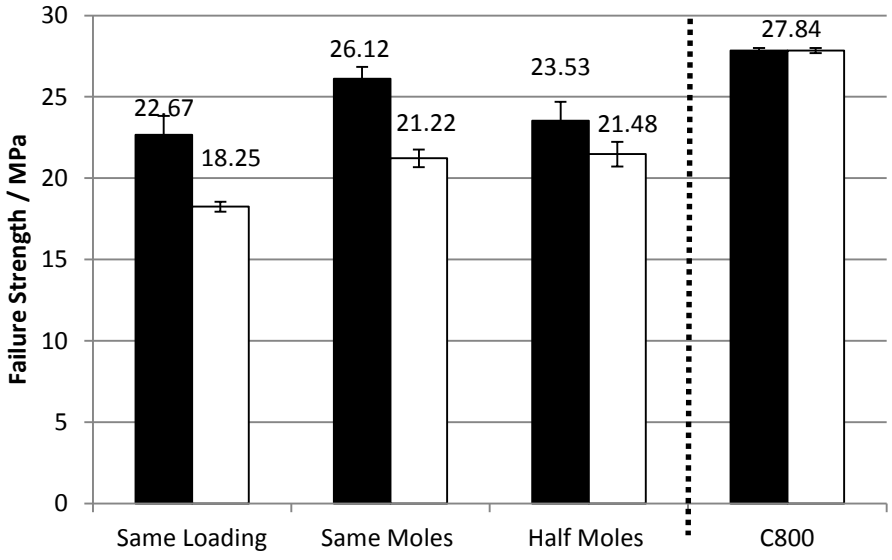

Figure 82: Failure strength for composites incorporating compound A (black bars) and compound B (white bars) using loading levels relative to that of C800 (far right).

Again, compound A performs better than compound B in terms of elongation at failure, with the same molar level giving the best result – albeit still slightly lower

than that for C800. The elongation at failure data (Figure 83) reveals the superiority of C800. Use of compound A at the same molar dosage as C800 gave the best result.

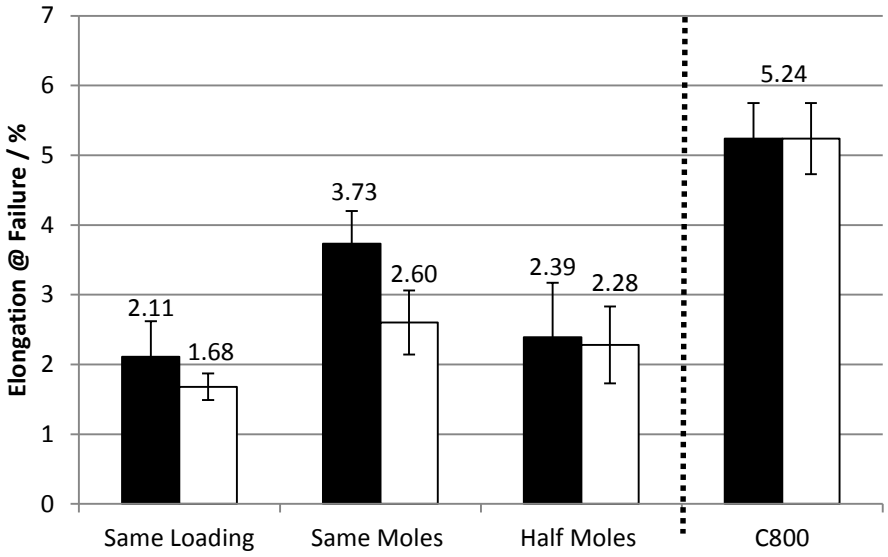

Figure 83: Elongation at failure for composites incorporating compound A (black bars) and compound B (white bars) using loading levels relative to that of C800 (far right).

The flexural modulus results present a different trend, where the same loadings of both compounds produce composites of a similar modulus to that produced using C800 (Figure 84). However, when using the same molar level as C800, both compounds result in a lower flexural modulus which suggests a more flexible and perhaps more rubbery composite. This alludes to the formation of a rubbery interphase or interfacial region within the final composites.

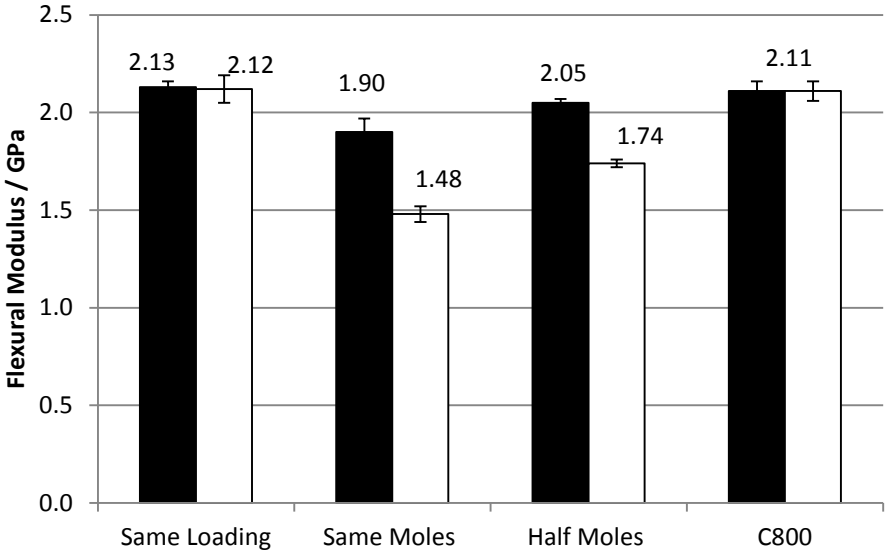

Figure 84: Flexural modulus for composites incorporating compound A (black bars) and compound B (white bars) using loading levels relative to that of C800 (far right).

Finally, the values for un-notched impact strength in Figure 85 show that compound A at the same molar level as C800 gives the best result after C800 itself.

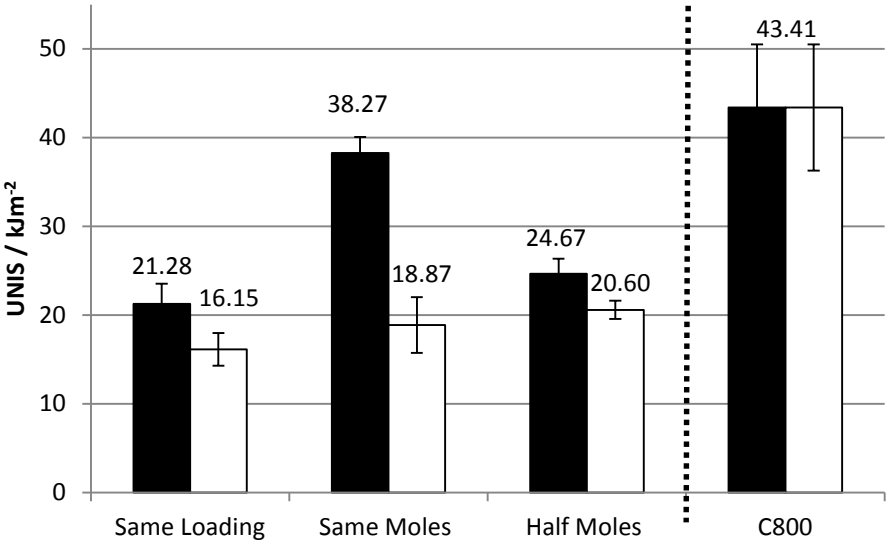

Figure 85: Un-notched impact strength for composites incorporating compound A (black bars) and compound B (white bars) using loading levels relative to that of C800 (far right).

The previous discussion suggests that compound A performs better than compound B, yet neither out-performs C800 which affords the best properties in all instances. Further work would be required to investigate why A and B did not

perform as well as C800. It is certain however, that in the case of A, B and C800 that a matrix macro-radical will see the same species in all cases, i.e. the CH_2= of an acrylic double bond. There may however, be differences in the accessibility of the group, though in the case of C800 there is no provision in the molecular structure to ensure that the CH_2= is held away from the filler surface; though it has to be said that C800 has a rather more linear structure. The rigid planar aromatic central structure of A and B however may result in the molecules taking up too much space on the filler surface and that the packing arrangement on the filler may result in reduced macro-radical access to the CH_2=. These factors may explain the poorer than expected performance. To a degree this argument is supported by the fact that A performed better than B. Due to the increased length of the flexible spacer group between the anchor group and the acrylic double bond in B, there is a greater probability that the CH_2= will be able to adsorb on the filler surface and perhaps be trapped by other adsorbed B molecules. Furthermore, if B is adsorbed flat it will take up more space on the surface than A, thus reducing the density of coupling. In contrast the “linearity” of the C800 molecule will ensure that the molecules pack closely on the surface such that the concentration of CH_2= at the surface compensates for its lower functionality.

4 CONCLUSIONS

The studies have shown that Solplus C800 has the ability to couple both polyethylene and polypropylene to a calcium carbonate filler surface. As a result C800 successfully enhanced the “interfacial compatibilisation” activity of the filler in blends of high density polyethylene and polypropylene. A side effect of the coupling reaction is scission of PP matrix chains and crosslinking of chains in PE based matrices. This is suggested by the reduction in MFR of composites rich in PE, and an increase in MFR of composites rich in PP. Despite the latter, significantly enhanced properties could be obtained in composites based on post-industrial polymer waste and ground calcium carbonate filler.

4.1 Effect of C800-DCP modification of PP/GCC & HDPE/GCC composites

Whilst an increasing level of untreated filler has the expected effect of reducing the melt flow rate (MFR) in composites based on HDPE and PP, C800-DCP modification reduces the MFR of the HDPE based composites, however in the PP based composites MFR is increased. Furthermore, an increase in failure strength relative to the unfilled polymer and higher elongation at failure resulting from C800-DCP modification, suggests formation of an amorphous rubbery interphase between the filler and bulk polymer matrix in the HDPE based composites. However, in the PP based composites, failure strength is maintained across the filler level range, therefore the improvement when using the modified filler is less marked than with the equivalent HDPE based composites. Impact strength data (particularly un-notched) revealed similar trends.

4.2 Effect of C800-DCP modification of PP/HDPE blend based composites

Where the PP/HDPE blends (containing a fixed calcium carbonate level of 60 % wt) are concerned, there are some interesting trends presented, as it appears that at certain PP/HDPE ratios certain properties are enhanced. In the case of unmodified composites based on the PP/HDPE blends, the tensile strength showed only a small variation across the composition range. However, the unfilled blend and unfilled blend containing C800-DCP show a reduction in tensile strength

when the PP level exceeds 50 % wt. The tensile modulus versus blend composition data shows that the C800-DCP modified composite blends show reduced modulus relative to the equivalent unmodified composites. Interestingly the stiffness of the unfilled blends is not affected by C800-DCP modification. These observations point to formation of a filler-matrix interfacial region of reduced stiffness (i.e. reduced crystalline content) in C800-DCP modified composites. This is consistent with mixed coupling of PP and HDPE to the filler surface; DSC measurements indicate reduced crystalline content in the HDPE component, which to a degree, supports this explanation. The chain scission and crosslinking reactions are highlighted by the rheological properties of the composites, due to a reduction in MFI from 100% PP to 100% HDPE. The latter observation is more marked in the unfilled blends containing C800-DCP because the PP and PE macro-radical grafting reactions are not confined to the filler-matrix interfacial regions. Studies focussed on analysis of the interfacial regions are summarised below.

4.3 Study of the interfacial effects in composites based on virgin blends

The interfacial properties of the composites (60 wt % calcium carbonate) based on the virgin blends (and the unfilled blends) were investigated by extraction of the bulk matrix from the composites using hot xylene. The level of insoluble matrix was determined using TGA and the PP/PE ratio in the insoluble matrix component was determined via ATR-FTIR. From the latter, the level of insoluble matrix and DSC data for the insoluble residues, the crystalline contents of the PP and PE fractions of the residues were estimated. The unfilled blends were also extracted with hot xylene. The soluble fractions of the composites / unfilled blends were characterised in the same manner as the insoluble residues.

The most significant conclusion of this study is that C800-DCP modification does result in an interfacial region of reduced crystalline content. This was considered to arise from mixed PE and PP macro-radical additions to the C800 double bond together with random collisions of PP and PE macro-radicals. Similar effects, however, also apparently occurred, albeit to a lesser extent, in the unmodified composites; in the latter macro-radicals were mainly generated by thermo-

oxidative degradation and mechanical rupture of chains during melt blending. Examination of the soluble matrix residues however, revealed that in the case of the unmodified composites macro-radical reaction were not mainly confined to the interfacial region.

4.4 Conclusions associated with characterisation of the PCPW and the PIPW

The compositions of the post-consumer (PCPW) and post-industrial (PIPW) plastic wastes were determined using various analytical methods. While these methods would be unsuitable for use in a 'live' or 'on stream' environment, they highlight an unexpected discrepancy from published results for post-consumer waste. As discussed in Section 3.1.1, the published results suggest that the PCPW has a higher proportion of LDPE. Furthermore, the proportion of HDPE may be lower due to the closed-loop process of recycling HDPE milk bottles, which suggests that the HDPE wastes had already been segregated from the post-consumer waste stream. Despite this, there was still a discrepancy between the PP level in the obtained sample of PCPW (around 75% PP) which is vastly greater than the 17% suggested by WRAP.

This variation is not limited to the PCPW, as the three samples of PIPW were also different in composition. While sample A was calculated to be 100% PE, samples B and C had increasing levels of PP (24 and 62% respectively). This further highlighted the effect of the coupling system, as a reduction in effectiveness was observed when progressing from samples A-C. Nevertheless respectable results were still obtained for sample C.

4.5 Conclusions associated with the effect of C800-DCP modification of composites based on the PIPW and PCPW

Blends of PE and PP in the form of post industrial waste have benefited enormously from addition of Solplus C800 and ground calcium carbonate. In the case of material B (76% PE and 24% PP), a very good strength-toughness balance was obtained. The increase in impact strength and elongation obtained

indicates successful compatibilisation of this blend, certainly within the filler-matrix interfacial region.

The presence of PP in the blend has an important role in terms of mediating the crosslinking of the PE component, which can give rise to unacceptably high melt viscosity. PP may also act to restrain/prevent crystallisation within the interfacial region due to the inability for PP to be incorporated into the crystal structure of PE and vice versa.

Although C800 provides significant improvement in composites based on PIPW samples B and C, the results obtained with the samples of mixed post-consumer polyolefin waste indicate that the system requires further optimisation.

The test results demonstrated the efficiency of the coupling agent treatment, notably the Solplus® C800 significantly improved the properties of the composites, as it appears that compatibilisation of the polymers has occurred at the matrix-filler interface. The composites produced using the experimental blend composition had properties different to those of the WRAP published blend composition, yet the effects of the coupling agent showed promising results for the two blend compositions, notably in terms of an increase in impact strength (albeit more marked for the WRAP published composition).

The results suggest that the blends treated with the coupling agent had low crystallinity, low VMFR, high impact strength and increased flexural modulus. Furthermore, the coupling agents had improved the impact strengths of the composites when compared to those using untreated filler. Thus, the materials (with the coupling agents) had interesting properties, as the behaviour was linked to the structure of the materials and particularly the composition of the interface between filler and polymer matrix. The amorphous areas near the filler particle were responsible of the low crystallinity, but the strong interactions (e.g. cross-linking) between the polymer chains (near the filler) improved the mechanical properties such as the impact strength, suggesting that some compatibilisation between the two phases may have occurred. The Solplus® C800 treatment was very effective for the WRAP published composition blends, while the unmodified PCPW demonstrated poor mechanical properties.

The WRAP published composition blends had better impact strengths than the experimental composition blends, yet also had reduced flexural moduli which suggest the presence of an increased proportion of an amorphous rubbery phase within the composites.

While there are some limitations associated with polymer wastes that have a high proportion of PP, it can be suggested from the results so far that compatibilisation of the polyolefin post-consumer polymer waste via a C800 activated filler surfaces is a potentially viable solution that would make much more economic sense than separation. Furthermore, the resulting composites are also likely have an attractive set of properties including a good balance of strength and toughness.

4.5.1 Limitations of the C800-DCP modification when the PP level in the blend is too high or too low

As shown previously, higher levels of PP in the polyolefin blends results in a reduction in various mechanical properties and an increase in MFR due to chain scission of the PP phase. This degradation produces material which is difficult to process and has disappointing brittle impact properties. Furthermore, crosslinking of the PE phase appears to lead to an increase in elongation at failure, yet a decrease in MFR. While the increase in impact and tensile strengths are by no means detrimental, a reduction in MFR may present processing issues, as the material produced would be limited to forming methods solely employing extrusion processes such as pipe, sheet or profiles.

4.5.2 Solutions to the limitations of the C800-DCP modification system

In order to overcome the aforementioned limitations, a coupling agent featuring increased functionality would be required to promote active repair of the PP phase within the polyolefin blend. Ideally, the system would not require peroxide as this would reduce the level of crosslinking in the PE phase.

Section 3.6 details the initial work that has been done to overcome the problem of chain scission within the composites with some promising results. However,

further work is needed to optimise both the coupling agent and also the dosage levels required.

Finally, if a method of chain scission were possible for the PE phase, a system may perhaps be developed which gives control over chain scission *and* crosslinking in both the PP *and* the PE phases whilst also providing a coupling and compatibilising mechanism to create a truly bespoke system.

5 FURTHER WORK

Whilst every effort has been made to make this study as comprehensive as possible, time constraints have placed limits on the depth of investigation of some aspects.

The new high functionality coupling agents that have been produced (see Section 3.6.2) showed a degree of promise. However, further optimisation of the correct balance between the number of reactive double bonds present and the overall size of the molecule is needed if the potential relating to the higher functionality is to be realised. The levels of addition and incorporation methods also require further refinement too. These further studies could afford a more comprehensive insight in to the structure / performance relationships of such species which could lead to a commercially viable product.

An alternative approach which may also be considered is that of blending of the high functionality coupling agents with C800 to balance functionality in relation to blend composition. Due to the fact that C800 seems to be more effective at coupling HDPE to GCC, a PP specific coupling agent may be required which can also be blended to produce an effective coupling compatibiliser additive package.

Furthermore, if addition of a peroxide is necessary, the deployment method for the coupling agent and peroxide initiator system may need to be developed in order to produce a more user friendly system, i.e. pre-blending with a filler to a give an “enhanced compatibilising filler” that can be added to the mixed polymers prior to compounding, or via a form of highly filled masterbatch.

Whilst the masterbatch route has not yet been investigated, there is commercial interest and active product development currently underway (as of 2012) by one of the world’s largest filler producers. The author is actively collaborating to produce a commercial product.

6 REFERENCES

1. Direct Gov, Landfill tax: increase to standard rate, Available at http://webarchive.nationalarchives.gov.uk/20110314113412/http:/hmrc.gov.uk/pbr2006/pbrn26.htm (2006).
2. Kollewe, J., We must end our oil dependency, says chancellor, Available at http://www.guardian.co.uk/business/2008/jul/03/oil.alistairdarling (2008).
3. Messe Düsseldorf GmbH, Plastics - A Sucess Story, Available at http://www.interpack.com/cipp/md_interpack/custom/pub/content,lang,2/oid,10344/ticket,g_u_e_s_t/local_lang,2/~/Plastics._A_success_story.html (2009).
4. Foster, S., *Domestic Mixed Plastics Packaging Waste Management Options Report* (Waste Resource Action Programme, 2008).
5. Last, S., Materials Recovery Facility (Clean MRF), Available at http://www.mbt.landfill-site.com/MRF/mrf.html (2011).
6. Last, S., Unsorted / residual waste Materials Recovery Facility (Dirty MRF), Available at http://www.mbt.landfill-site.com/Dirty_MRF/dirty_mrf.html (2011).
7. Brown, R., Garbage & Recycling - Materials Recovery Facility (MRF), Available at http://www.sjrecycles.org/residents/mrf.asp (2010).
8. Cardiff Council, MRF at Lamby Way, Available at http://www.cardiff.gov.uk/content.asp?nav=2870,4049&parent_directory_id=2865&id=2931 (2011).
9. Closed Loop Recycling, AAbout Us, Available at http://www.closedlooprecycling.co.uk/information/ (2011).
10. BSI, BS EN 15343:2007 Plastics. Recycled plastics. Plastics recycling traceability and assessment of conformity and recycled content (2008).
11. Closed Loop Recycling, Our Plant & Process Technology, Available at http://www.closedlooprecycling.co.uk/information/our-plant-process-technology (2011).
12. Erema Technologies, The Vacumera® Process, Available at http://www.erema.at/en/vacurema_general/ (2011).
13. Rutledge, S., Biffa Polymers opens UK's first Mixed Plastic Sorting & Processing Facility, Available at http://www.biffa.co.uk/assets/files/News/2011/Biffa%20Polymers%20press%20release%2018-03-11.pdf (2011).
14. Quinault, C., Powys "dirty" MRF to form part of recycling stategy, Available at http://www.letsrecycle.com/news/latest-news/general/powys-dirty-mrf-to-form-part-of-recycling-strategy (2001).
15. Last, S., Unsorted / Residual Waste materials recovery facility (Dirty MRF), Available at http://www.mbt.landfill-site.com/Dirty_MRF/dirty_mrf.html (2011).
16. Buhler Ltd, Sortex Z+ Optical Sorting System, Available at http://www.buhlergroup.com/global/en/products/sortex-z-optical-sorter.htm (2011).
17. Best Sorting Recycling, Genius Optical Scanner, Available at http://www.bestsorting.com/recycling/sorters/genius-optical-sorter/ (2011).
18. Pellenc Selective Technologies, Air Knife Ejection Unit, Available at http://www.pellencst.com/en/23/15/ejection-unit (2011).

19. Alibaba Ltd, Optical Sorting Machines, Available at http://www.alibaba.com/showroom/optical-sorting-machine.html (2011).
20. Fraunhofer UMSICHT & EcoProg Consultancy, *The World Market for Waste Incineration Plants* (EcoProg GmbH, 2010).
21. Bontoux, L., *The Incineration of Waste In Europe: Issues And Perspectives* (Institution For Perspective Technological Studies, Seville, 1999).
22. Industry Council for Packaging & the Environment, Energy From Waste Factsheet, Available at http://www.incpen.org/displayarticle.asp?a=14&c=2 (2010).
23. The University of Tennessee, Waste-to-Energy Incineration Student Handout, Available at http://www-tnswep.ra.utk.edu/activities/pdfs/mu-W.pdf (2010).
24. Herington, E. F. G., Calorific Values of Solid, Liquid and Gaseous Fuels, Available at http://www.kayelaby.npl.co.uk/chemistry/3_11/3_11_4.html (2011).
25. Plastenergo, Our Technology, Available at http://plastenergo.com/our_technology.html (2011).
26. Coxworth, B., New Technique Recycles 100% of Household Plastic, Available at http://www.gizmag.com/fluidized-bed-reactor-recycles-plastic-waste/17281/ (2010).
27. Mrabet, Y., File:Fluidized Bed Reactor Graphic.svg, Available at http://commons.wikimedia.org/wiki/File:Fluidized_Bed_Reactor_Graphic.JPG (2009).
28. Coxworth, B., Plastic2Oil process turns plastic waste into fuel, Available at http://www.gizmag.com/plastic2oil-converts-plastic-to-fuel/19108/ (2011).
29. JBI Inc., Plastic2Oil: Our Process, Available at http://www.plastic2oil.com/plastic2oil-business/process.aspx (2011).
30. JBI Inc., The Plastic2Oil Business, Available at http://www.plastic2oil.com/plastic2oil-business/business-model.aspx (2011).
31. UNFCCC, Glossary of Climate Change Acronyms, Available at http://unfccc.int/essential_background/glossary/items/3666.php#C (2011).
32. Biello, D., Enhanced Oil Recovery: How to Make Money from Carbon Capture and Storage Today, Available at http://www.scientificamerican.com/article.cfm?id=enhanced-oil-recovery (2009).
33. Mick, J., Massive $84M USD Carbon Burial Experiment Begins, Available at http://www.dailytech.com/article.aspx?newsid=14296 (2009).
34. O'Brien, C., Success for carbon dioxide burial, Available at http://www.newscientist.com/article/dn2779-success-for-carbon-dioxide-burial.html (2002).
35. Statoil, Leading the world in carbon capture, Available at http://www.statoil.com/en/TechnologyInnovation/NewEnergy/Co2Management/pages/carboncapture.aspx (2009).
36. Abatzoglou et al, US Patent No. US7794690 - Carbon sequestration and dry reforming process and catalysts to produce same (September 2010).
37. Steinfeld, A. & Weimer, A. W., Thermochemical Production of Fuels with Concentrated Solar Energy. *Optics Express* **18** (S1), 100-111 (2010).
38. Matare et al, US Patent No. US2010/0300892 - Apparatus and Method for

Solar Hydrogen Synfuel Production (December 2010).
39. Bullis, K., Making gasoline from carbon dioxide, Available at http://www.technologyreview.com/energy/18582/page1/ (2007).
40. Squatriglia, C., Scientists use sunlight to make fuel from CO2, Available at http://www.wired.com/science/discoveries/news/2008/01/S2P (2008).
41. Stamatiou, A., Steinfeld, A. & Loutzenhiser, P., Solar Syngas Production via H_2O/CO_2-splitting Thermochemical Cycles with Zn/ZnO and FeO/Fe_3O_4 Redox Reactions. *Chemistry of Materials* **22** (3), 851-859 (2010).
42. Holton, C., Dissolving The Plastics Problem. *Envoronmental Health Perspectives* **105** (4), 388-390 (1997).
43. Naumant et al, US Patent No. US5198471 - Polymer recycling by selective dissolution (March 1993).
44. Nauman et al, US Patent No. US5278282 - Polymer recycling by selective dissolution (Jan 1994).
45. Associated Newspapers Limited, Historic Inflation Calculator, Available at http://www.thisismoney.co.uk/money/bills/article-1633409/Historic-inflation-calculator.html (2011).
46. Crain Communications, Resin Pricing - Recycled Plastics, Available at http://plasticsnews.com/resin-pricing/recycled-plastics.html (2011).
47. The Plastics Exchange, The Plastics Exchange, Available at http://www.theplasticsexchange.com/ (2011).
48. Khunová et al, Elimination of Separation Processes for Post-Consumer Polyolefin Waste: Reactive Blending Using 1,3-Phenylene Dimaleimide in Presence of Filler. *Macromolecular Materials and Engineering* **294** (8), 502-509 (2009).
49. Bussi, P., France Patent No. US6093772 - Immiscible polymer compatibiliser system (July 2000).
50. Parsy et al, France Patent No. US5055521 - Agent for rendering compatible at least two incompatible thermoplastic polymers, process for the preparation and thermoplastic alloys obtained therefrom (October 1991).
51. Mylonakis et al, US Patent No. US4866126 - Polymer blend compositions including copolymer compatibilizing agents (September 1989).
52. Dang et al, US Patent No. US6887940 - Compatibilizing agent for engineering thermoplastic/polyolefin blend (May 2005).
53. Japon, S., Leterrier, Y. & Månson, J. E., Recycling of poly(ethylene terephthalate) into closed-cell foams. *Polymer Engineering & Science* **40** (8), 1942-1952 (2000).
54. Oromiehie, A. & Mamizadeh, A., Recycling PET beverage bottles and improving properties. *Polymer International* **53** (6), 728-732 (2004).
55. Torres, N., Robin, J. & Boutevin, B., Chemical modification of virgin and recycled poly(ethylene terephthalate) by adding of chain extenders during processing. *Applied Polymer Science* **79** (10), 1816-1824 (2001).
56. Sombatsompop, N. & Sungsanit, K., Processability, rheology, and thermal, mechanical, and morphological properties of postconsumer poly(vinyl chloride) bottles and cables. *Applied Polymer Science* **89** (10), 2738-2748 (2003).
57. Wenguang, M. A. & Mantia, F., Processing and mechanical properties of recycled PVC and of homopolymer blends with virgin PVC. *Applied Polymer*

Science **59** (5), 759-767 (1996).

58. Nowaczyk, G., Glowinkowski, S. & Jurga, S., Rheological and NMR studies of polyethylene/calcium carbonate composites. *Solid State Nuclear Magnetic Resonance* **25** (1-3), 194-199 (2004).
59. Vasile, C. & Pascu, M., in *Practical Guide to Polyethylene* (Rapra Technology Limited, Shrewsbury, 2005), pp. 5, 19.
60. Vasile, C. & Pascu, M., in *Practical Guide to Polyethylene* (Rapra Technology Limited, Shrewsbury, 2005), pp. 31-32.
61. The Open University, Section 5.6.1 - Morphology of polymer crystallites, Available at http://openlearn.open.ac.uk/mod/oucontent/view.php?id=397829&section=5.6.1 (2011).
62. Gaylord, N. G., *Linear and stereoregular addition polymers: Polymerization with controlled propagation* (Interscience, New York, 1959).
63. Dikobe, D. G. & Luyt, A. S., Comparative study of the morphology and properties of PP/LLDPE/wood powder and MAPP/LLDPE/wood powder polymer blend composites. *eXPRESS Polymer Letters* **4** (11), 729-741 (2010).
64. Bertin, S. & Robin, J.-J., Study and characterization of virgin and recycled LDPE/PP blends. *European Polymer Journal* **38** (11), 2255-2264 (2002).
65. Fortelný, I., Michálková, D. & Kruliš, Z., An efficient method of material recycling of municipal plastic waste. *Polymer Degradation and Stability* **85** (3), 975-979 (2004).
66. Nedkov, T., Lednický, F. & Mihailova, M., Compatibilization of PP/PE blends and scraps with Royalene: Mechanical properties, SAXS, and WAXS. *Journal of Applied Polymer Science* **109** (1), 226-233 (2008).
67. Choudhury, A. & Adhikari, B., Dynamic vulcanization of recycled milk pouches (LDPE-LLDPE) and EPDM blends using dicumyl peroxide. *Polymer International* **56** (10), 1213-1223 (2007).
68. Rosato, D. V., Rosato, D. V. & Rosato, M. G., *Injection Moulding Handbook*, 3rd ed. (Springer, 2001).
69. DeArmitt, C. & Breese, K. D., Filled polypropylene: a cost - performance comparison of common fillers. *Plastics Additives & Compounding* **3** (9), 28-33 (2001).
70. Nachtigall, S., Mioto, M., Schneider, E., Mauler, R. & Forte, M., Macromolecular coupling agents for flame retardant materials. *European Polymer Journal* **42** (5), 990-999 (2006).
71. Rothon, N., *Particulate-Filled Polymer Composites*, 2nd ed. (Rapra, Shrewsbury, 2003).
72. Wypych, G., *Handbook of Fillers*, 1st ed. (ChemTec, Toronto, 2010).
73. Plastic Products Inc, Nylon physical properties, Available at http://www.plastic-products.com/spec1.htm (2012).
74. Boszor, S. M., US Patent No. US3930130 - Carbon fibre strengthened speaker cone (December 1975).
75. Kiss, A., Fekete, E. & Pukánszky, B., Aggregation of $CaCO_3$ particles in PP composites: Effect of surface coating. *Composites Science & Technology* **67** (7-8), 1574-1583 (2007).
76. Osman, M., Atallah, A. & Suter, U., Influence of excessive filler coating on

the tensile properties of LDPE–calcium carbonate composites. *Polymer* **45** (4), 1177-1183 (2004).

77. Kwon, S. *et al.*, Tensile property and interfacial dewetting in the calcite filled HDPE, LDPE, and LLDPE composites. *Polymer* **43** (25), 6901-6909 (2002).
78. Rothon, R., *Particulate-Filled Polymer Composites*, 2nd ed. (Rapra Technology Ltd, 2003).
79. Xanthos, M., *Functional Fillers for Plastics*, 1st ed. (Wiley-VCH, Verlag, 2005).
80. Schreiber, H. P. & Germain, F. S., Specific interactions and their effect on the properties of filled polymers. *Journal of Adhesion Science and Technology* **4** (1), 319-331 (1990).
81. Keene, E., Ellen Keene-SEM, Available at http://www.ccmr.cornell.edu/facilities/winners07feb/images/20070123145929.jpg (2012).
82. Roskill Information Services, The Economics of Ground Calcium Carbonate Report No. 9780862148744, 2008.
83. Schofield, J. D., A novel coupling agent technology. *Polymer & Polymer Composites* **2** (11), 71-79 (2003).
84. Grassie, N., *Polymer Degradation and Stabilisation* (Cambridge University Press, 1985).
85. Turczanyi, B., Pukanzsky, B. & Tudos, F., Composition Dependence of Tensile Yiled Stress in Filled Polymers. *Journal of Materials Science Letters* **7**, 160-162 (1988).
86. Minkova, L. & Magagnini, P. l., Crystallization behaviour and thermal stability of HDPE filled during polymerization. *Polymer Degradation and Stability* **42** (1), 107-115 (1993).
87. Valadez-Gonzalez, A. & Veleva, L., Mineral filler influence on the photo-oxidation mechanism degradation of high density polyethylene. Part II: natural exposure test. *Polymer Degradation and Stability* **83** (1), 139-148 (2004).
88. Addiego, F. *et al.*, Cavitation in unfilled and nano-$CaCO_3$ filled HDPE subjected to tensile test: revelation, localization, and quantification. *Polymer Engineering and Science* **50** (2), 278-289 (2010).
89. Hoang, E. M., Liauw, C. M., Allen, N. S., Fontan, E. & Lafuente, P., Effect of metal stearates on the melt stabilisation performance of ohenolic/phosphite antioxidants in metallocene LLDPE: Part 1 Melt processing stability. *Journal of Vinyl and Additive Technology* **10** (3), 137-143 (2004).
90. An, Y. . Z. Z. . W. Y. . Q. J. a. T. T., Structure and properties of high melt strength polypropylene prepared by combined method of blending and crosslinking. *Journal of Applied Polymer Science* **116** (3), 1739-1746 (2010).
91. Liauw, C. M., Khunová, V., Lees, G. C. & Rothon, R. N., The role of m-phenylene bismalaeimide (BMI) in reactive processing of PP/$Mg(OH)_2$ composites: Part 3 The effect of formulation on interactions within composites. *Macromolecular Materials and Engineering* **279** (6), 34-41 (2000).
92. Pukanszky, B., Tudos, F., Jancar, J. & Kolarik, J., The possible mechanisms of polymer-filler interaction in polypropylene-CaCO3 composites. *Journal of Materials Science Letters* **8** (9), 1040-1042 (1989).

APPENDICES

APPENDIX 1 – Conference papers presented at various international conferences during the duration of the PhD program.

I – Conference paper presented at the High Performance Fillers Conference, Barcelona, 2009

FILLER-BORN REACTIVE COMPATIBILISATION OF MIXED POLYOLEFIN POST-CONSUMER POLYMER WASTE: A MORE VIABLE ALTERNATIVE TO SEPARATION?

Clint Bainbridge, Christopher Liauw, Graham Lees, Roger Rothon, Dean Thetford*, Patrick Sunderland*, John Schofield*

Manchester Metropolitan University, Centre for Materials Research, Faculty of Science and Engineering, Chester Street, Manchester, M1 5GD, UK

e-mail: *c.m.liauw@mmu.ac.uk* Telephone: +44 (0)161 247 3325

* Lubrizol Limited, Hexagon Tower, Delauneys Road, Blackley, Manchester, M9 8ES, UK

e-mail: *Dean.Thetford@lubrizol.com* Telephone: +44 (0)161 721 1401

BIOGRAPHICAL NOTE

Clint Bainbridge was awarded his honours degree in Plastics and Rubber Materials from the Manchester Metropolitan University (MMU) in June 2007. Clint is the last full time Plastics and Rubber student to graduate from MMU due to the unfortunate demise of the course in 2007. For his final year project he studied the interfacial modification of ethylene vinyl acetate / aluminium hydroxide composites using a novel coupling agent system (Solplus® C800) from Lubrizol. After graduating, Clint successfully applied for a CASE award PhD position at MMU which is funded by Lubrizol Limited and the Engineering and Physical Sciences Research Council. Results from this PhD study on compatibilisation of post-consumer polymer waste are to be reported in this presentation.

ABSTRACT

Increasing tax on landfill and general environmental pressure has increased the need to recycle polymer waste. The unfilled/lightly filled polyolefin fraction of post-consumer polymer waste is relatively easily separated from the denser polymers by floatation. The complexity does not end here because the polyolefin fraction itself consists of dissimilar materials that when melt blended would form an immiscible blend with generally poor and inconsistent properties. The work presented will explore the use of activated filler (ground calcium carbonate (GCC)) surfaces as compatibilising interfaces for polyolefin blends. The activation is in the form of Lubrizol Solplus® C800 coupling agent, which has been found to effectively activate GCC and lead to a property enhancing interphase structure in post-industrial polypropylene (PP)/high density polyethylene (HDPE) blends.

INTRODUCTION

The increasing tax on land-fill[(1)], along with mounting environmental pressure to recycle has provided significant drive for serious attempts at recycling of post-consumer polymer waste. Furthermore, with political pressure to reduce our dependency on oil[(2)], and an increasing volume of plastics production, recycling is seen as both an environmentally friendly and a politically attractive option.

Current trends in recycling of post-consumer polymer waste involve collection, sorting, shredding, washing, and further sorting to produce reclaimed feedstocks with varying purities. However, with each additional step additional costs are incurred and this may therefore not be the most economically appealing option.

Table 1 – Composition of post-consumer polymer waste stream, based on WRAP 2006 figures[3] and extrapolated to 2008 assuming 2% growth.

Polymer	% wt of wastestream*	S.G.
LLDPE + LDPE	38	0.91-0.94
HDPE	13	0.94-0.96
PP	17	0.91
Other Polyolefin	4	ca. 0.92
PS	5	1.05
PVC	5	1.4
PET	16	1.4
Other	2	>1

An alternative method is a selective dissolution process, where a co-mingled waste stream is fed through an apparatus and treated with various solvents at differing temperatures to yield the original materials[4]. However, this process may be easily dismissed by the industry, due to its associated costs and solvent related hazards.

Hence, is sorting to such a high degree the most viable method of processing recovered polymer waste?

Table 1 gives the composition of the post-consumer polymer waste stream. These figures show that polyolefins constitute the major proportion of this waste stream. As polyolefins generally have a density of less than unity, they can easily be float-separated from the denser polystyrene (PS), polyethylene terepthalate (PET) and polyvinylchloride (PVC) fraction. Whilst polyolefins are of a similar nature in terms of polarity, they will not form a miscible blend with useful mechanical properties, due to the different chain conformations that each polymer adopts. Whereas polyethylene adopts a planar zigzag conformation, polypropylene adopts a helical conformation in the crystal lattice and hence co-compatibilisation is impossible as co-crystallisation cannot occur and phase separation of the two materials results. Furthermore, branching in low density polyethylene adds further complexity which needs to be considered in relation to miscibility of other polyethylenes.

Another route that is not often considered is that of compatibilisation, where a filler is treated with a suitable coupling agent and can thus act as a compatibilising surface in the final composite, resulting in interactions between otherwise immiscible phases. This will be explored in this paper, initially in composites comprising of one virgin polymer type, and then in real-world post-industrial polymer waste (PIPW) samples. This appears to be a practical solution to an otherwise labour and resource intensive separation procedure.

EXPERIMENTAL

Materials

The virgin polymers used for the initial part of the study were Borealis MG7547S (4 dg min^{-1}; 190°C / 2.16 kg) high density polyethylene (HDPE) and BP HV001PF (10 dg min^{-1}; 230°C / 2.16 kg) polypropylene homopolymer (PP). The filler used for both parts of the study was Imerys Carbital 110 (average particle size: 3 µm), and the coupling agent was Lubrizol Solplus® C825, which is the supported 50% active form of Solplus C800®. Finally Akzo Nobel Perkadox BC-40B, a supported 40% active form of dicumyl peroxide was used as an initiator for the coupling reaction.

Three samples of post-industrial polymer waste (PIPW) were examined. All three were polyolefin blends. Sample A was mainly polyethylene with less than 10% polypropylene present. The polyethylene component was predominantly low density polyethylene. Sample B was richer in polypropylene (c.a. 25%), whilst sample C was even richer in polypropylene (60% wt). These ratios were determined experimentally using differential scanning calorimetry, and relating fusion peak

areas in the PIPW to those of HDPE/PP blends of known composition. These samples will be referred to as PIPW A, PIPW B and PIPW C, respectively.

Preparation of the filler

In both cases, 8 kg of filler was mixed with 1.2 % by weight (on the filler) Solplus® C825 (the active level of Solplus® C800 was 0.6 % by weight on filler), and 5% by weight (on Solplus® C800) Perkadox® BC-40B. The filler was prepared in two 4 kg batches by tumble blending is a large screw-top container.

Processing of composites

The PIPW was initially supplied in a washed, flaked form which was then extruded on a 40mm Betol twin screw extruder to form granules. The composites were compounded on a Thermo-Electron HC24 twin screw extruder (L:D ratio 28:1) at filler levels of 0% wt, 33% wt, 50% wt and 60% wt, both with and without C800 and peroxide. The set barrel temperature was 200 °C. After compounding, the composites were injection moulded into tensile and impact test pieces using a Battenfeld BA 230 CD plus injection moulding machine, set at 50 °C mould temperature and 200°C barrel temperature.

Testing of composites

The moulded tensile test pieces (BS2782, 10 mm x 4 mm nominal cross sectional dimensions) were tested on a Hounsfield H10KS tensometer at 50 mm min^{-1}. Impact testing was performed on unnotched test pieces using a Zwick impact testing machine with 4 J and 50 J tups. The melt-flow rate was obtained at 200 °C using a Ray-Ran melt-flow indexer with a 10 kg mass.

RESULTS AND DISCUSSION

As is to be expected when incorporating a particulate filler, a higher untreated filler level results in a reduction in properties, as the particulate nature of the filler presents itself as defects in the final composite. This can be clearly seen by the trends shown in figures 3 to 8.

Composites Based on virgin High Density Polyethylene & Polypropylene

Generally, the mechanical properties of both composites respond well to the addition of the C800/peroxide treatment. It can be argued that larger improvements are found for HDPE composites than in PP composites, as per figures 3 and 4.

Considering the tensile test results, with the HDPE based composites the increase in strength from 25 MPa (unfilled matrix) to 30 MPa (at 60 % wt. filler) with C800 modification implies good coupling, however, with unmodified filler the tensile strength falls with increasing filler loading. Similar effects are also noted for the PP based composites, though in this case the tensile strength is maintained at the level of the unfilled matrix on increasing filler level.

The elongation results show that the C800 modification leads to an increase throughout the filler loading range explored, this is particularly true of the HDPE based composites. The unnotched impact strength data shows that C800 coupling provides some benefit throughout the filler level range though again the largest improvement is seen in the HDPE based composites.

The MFR data shows some interesting trends, it is evident that in HDPE based composites, (Figure 3), there is a significant reduction in MFR with C800 modification relative to the respective unmodified composites. In PP the data suggests that at the lower level of modified filler it is evident that the coupling reaction dominates, whereas once the crossover point is reached the MFR is significantly increased. As it is widely accepted that under the action of a peroxide, HDPE undergoes a crosslinking reaction and PP undergoes a chain scission reaction (Figure 1), it is possible that the peroxide is further reacting beyond the coupling agent and attacking the polymer chains. This can be seen in the MFR data for PP in Figure 4 where at the higher treated filler levels the increased amount of peroxide present causes chain scission to dominate over the coupling reaction, reducing the molecular weight of the material and hence the viscosity. Conversely, in HDPE what may appear as extensive coupling may be a mixture of coupling and crosslinking of the bulk matrix.

Nevertheless, it can be argued that these reactions have no detrimental effect on the mechanical properties of the composites, as in the HDPE composites they may aid in the formation of a rubbery interphase around the filler particles to which the chains themselves are coupled. This is manifested in the elongation and impact strength of the HDPE based composites, showing significant improvement on C800 modification, as shown in Figure 3. Crosslinking of PE chains in the filler-matrix interfacial region (schematically represented in Figure 2) will prevent crystallisation, creating rubber like properties in this region.

Post-Industrial Waste

In Figure 5, the downward deviation in MFR data of C800 modified PIPW composites in relation to the equivalent unmodified composite is an indication of the level of PE in the blend. Therefore in PIPW A the downward deviation is greatest due to significant crosslinking, whereas in PIPW C the high PP content and associated chain scission cause a downward deviation only at 33% wt filler. At 50% wt and 60% wt filler, MFR is the same for both unmodified and C825 modified composites. This data indicates that PP in the PIPW mediates reduction in MFR caused by crosslinking of the PE.

In relation to the mechanical properties, the C800 coupling in PIPW B and PIPW C improves all the properties, particularly at the highest filler levels. The improvements in impact strength (Figure 6) and elongation (Figure 8) are particularly significant. In the PIPW A based composites tensile strength is improved at all filler levels (Figure 7), though due to the significant crosslinking elongation and impact strength decrease on C825 modification of intermediate filler levels though at 60% wt an increase is evident.

CONCLUSIONS/PROSPECTS

In the filled PIPW, C800 shows promising improvements to mechanical properties, with composites based on PIPW samples B and C showing the best overall response to the treatment. The PP fraction of the PIPW is important as chain scission of the latter mediates the decrease in MFR associated with crosslinking of the polyethylene components. Probable attachment of both polyethylene and PP chains to the filler surface and crosslinking between these chains within the interfacial region (interphase) is likely to assist in the formation of an amorphous interfacial region with a low Tg. Both these factors will cause the interphase to be elastomeric in nature and somewhat thicker than in the unmodified composite. Whilst further ongoing experimental work is required for proof of this concept, the large increases in impact strength and elongation at failure are most likely to be a manifestation of it.

Although C800 provides significant improvement in composites based on PIPW samples B and C, the preliminary results obtained with some mixed post-consumer polyolefin waste indicate that the system requires further optimisation. The latter will require a detailed understanding of the role of C800 in filled binary and ternary polyolefin blends, such studies form the stages of the project.

It can however be suggested from the encouraging results so far that compatibilisation of the polyolefin fraction of post-consumer polymer waste via C800 activated filler surfaces is a viable solution that will make much more economic sense than separation. Furthermore the resulting composites are also likely have an attractive set of properties including a balance of stiffness, strength and toughness.

REFERENCES

1. HMRC website *http://www.hmrc.gov.uk/pbr2006/pbrn26.htm*
2. The Guardian *http://www.guardian.co.uk/business/2008/jul/03/oil.alistairdarling*
3. Foster S. *Domestic Mixed Plastics Packaging Waste Management Options Report* ISBN: 1-84405-369-2 (2008)
4. Holton C. *Environ Health Perspect* 105 (4), 388–390 (1997)

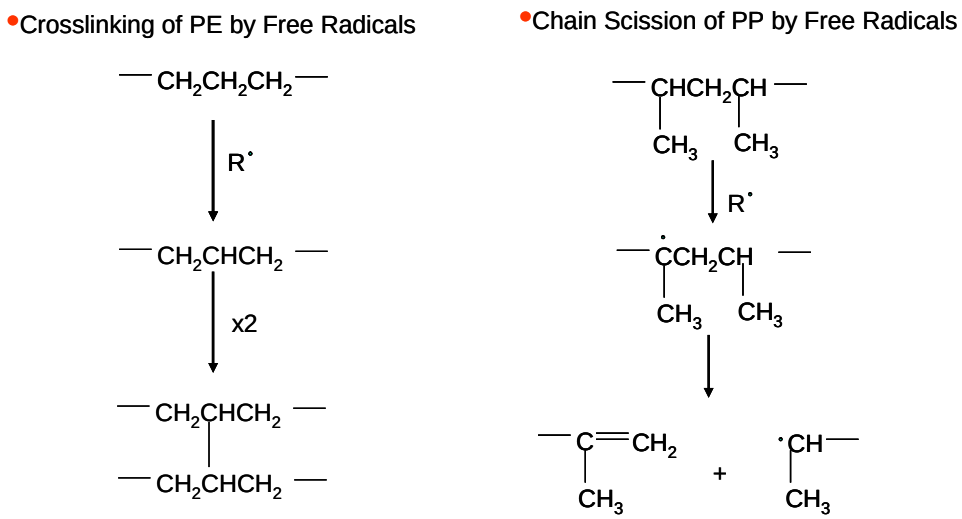

Figure 1 – Schematic representation of crosslinking and chain scission reactions.

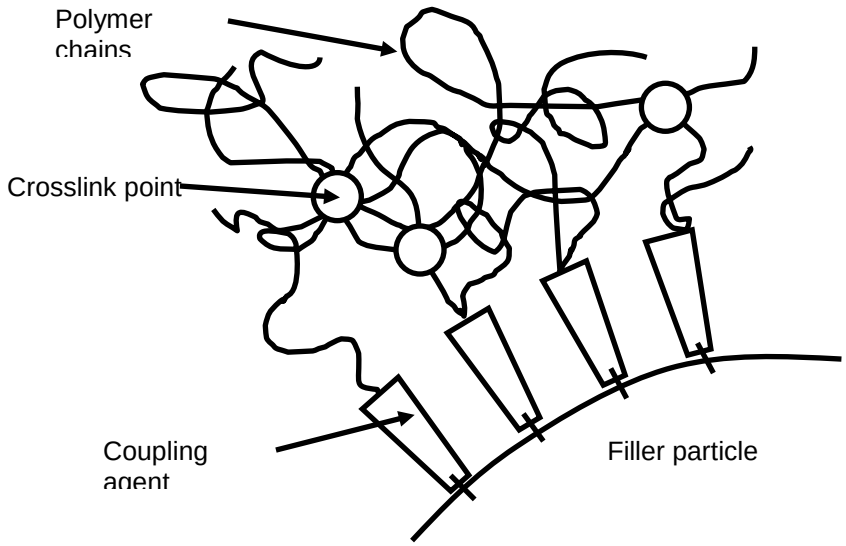

Figure 2 – Schematic representation of crosslinking in the interphase.

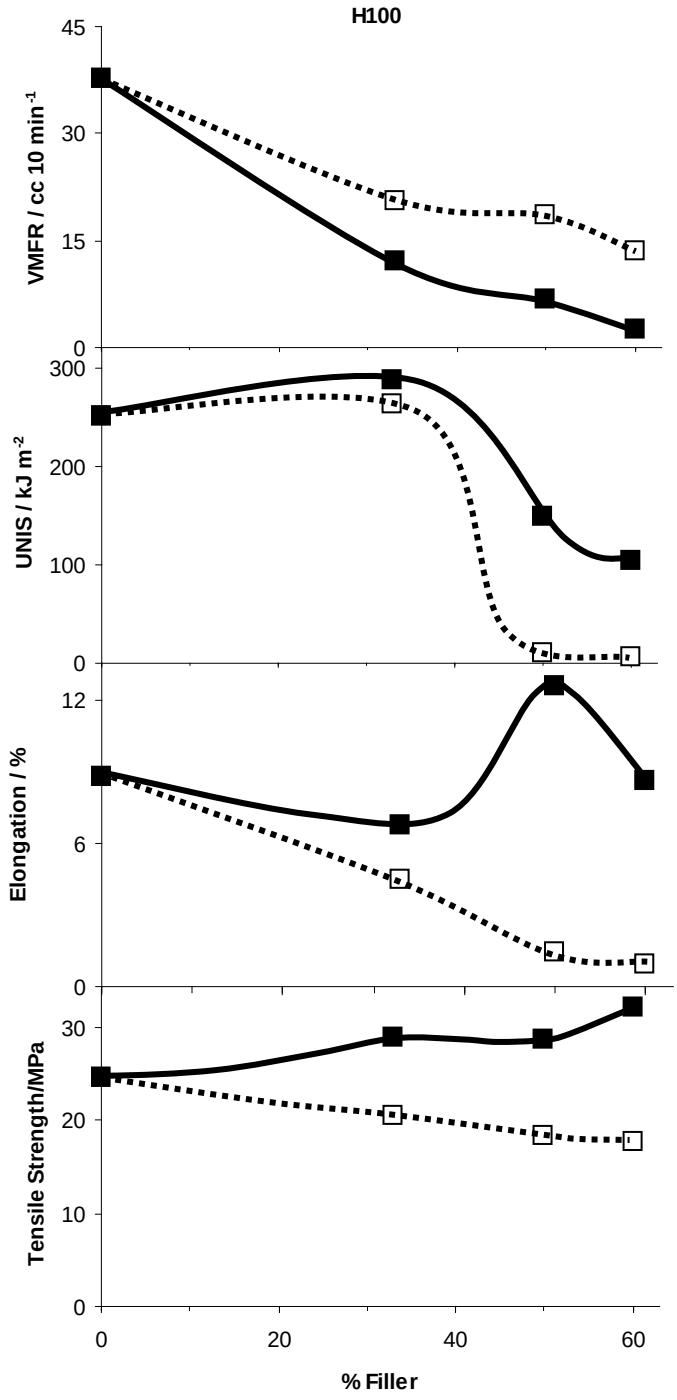

Figure 3 – Plots of properties vs filler level for composites based on high density polyethylene, where □ represents unmodified filler, and ■ represents modified filler.

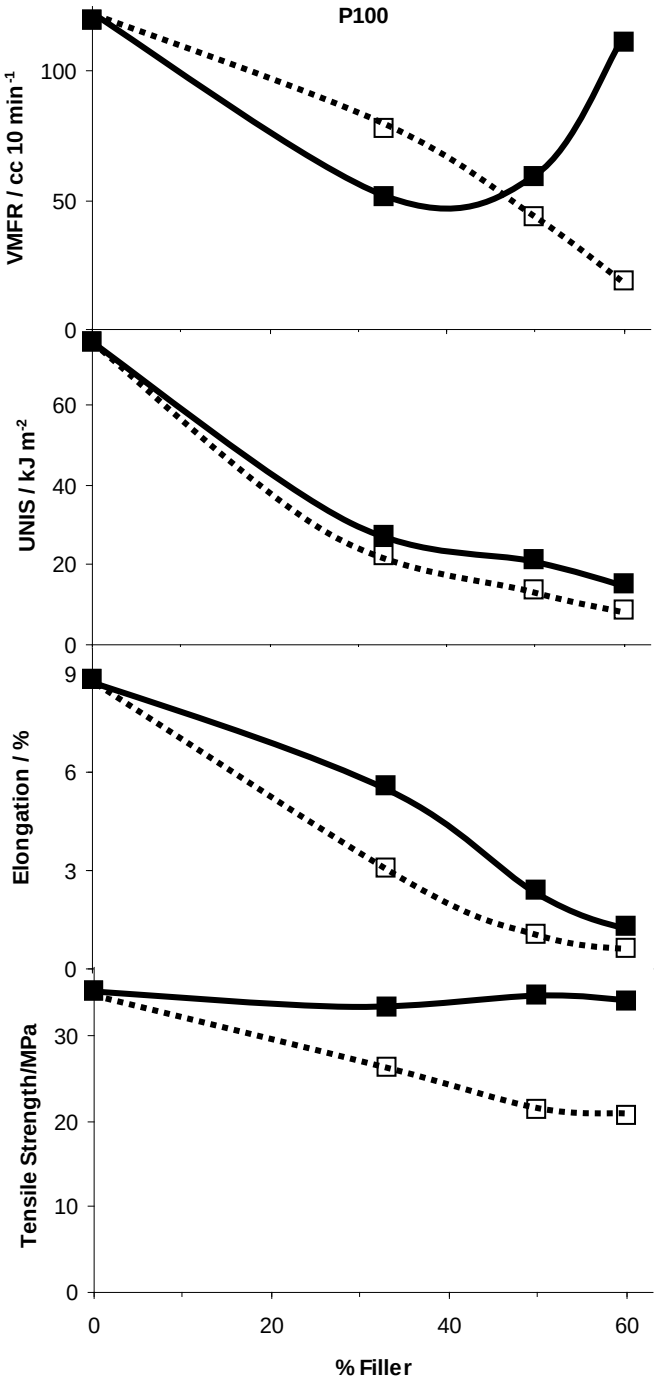

Figure 4 – Plots of properties vs filler level for composites based on polypropylene, where □ represents unmodified filler, and ■ represents modified filler.

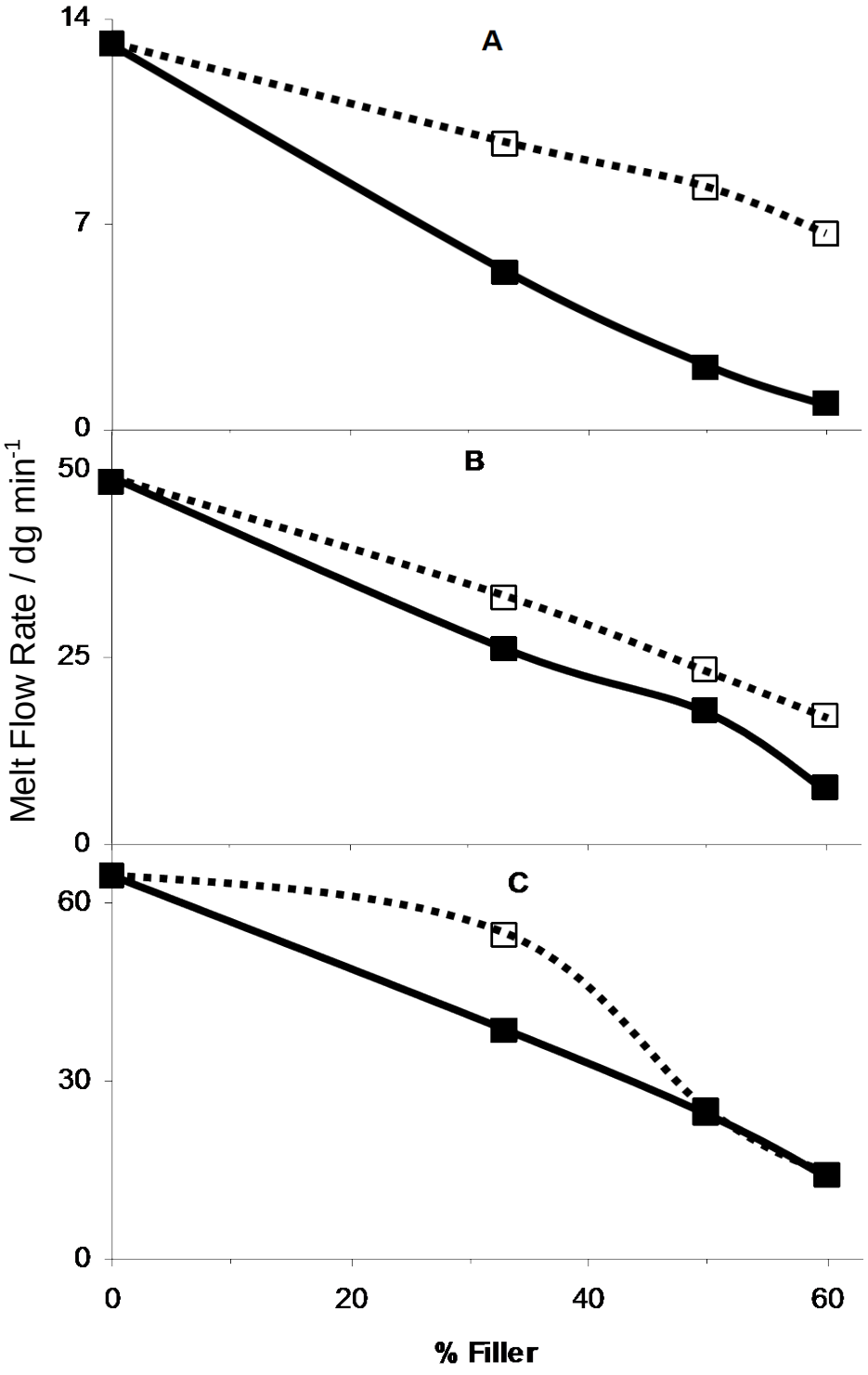

Figure 5 – Plots of melt flow rate vs filler level for PIPW based composites, where □ represents unmodified filler, and ■ represents modified filler.

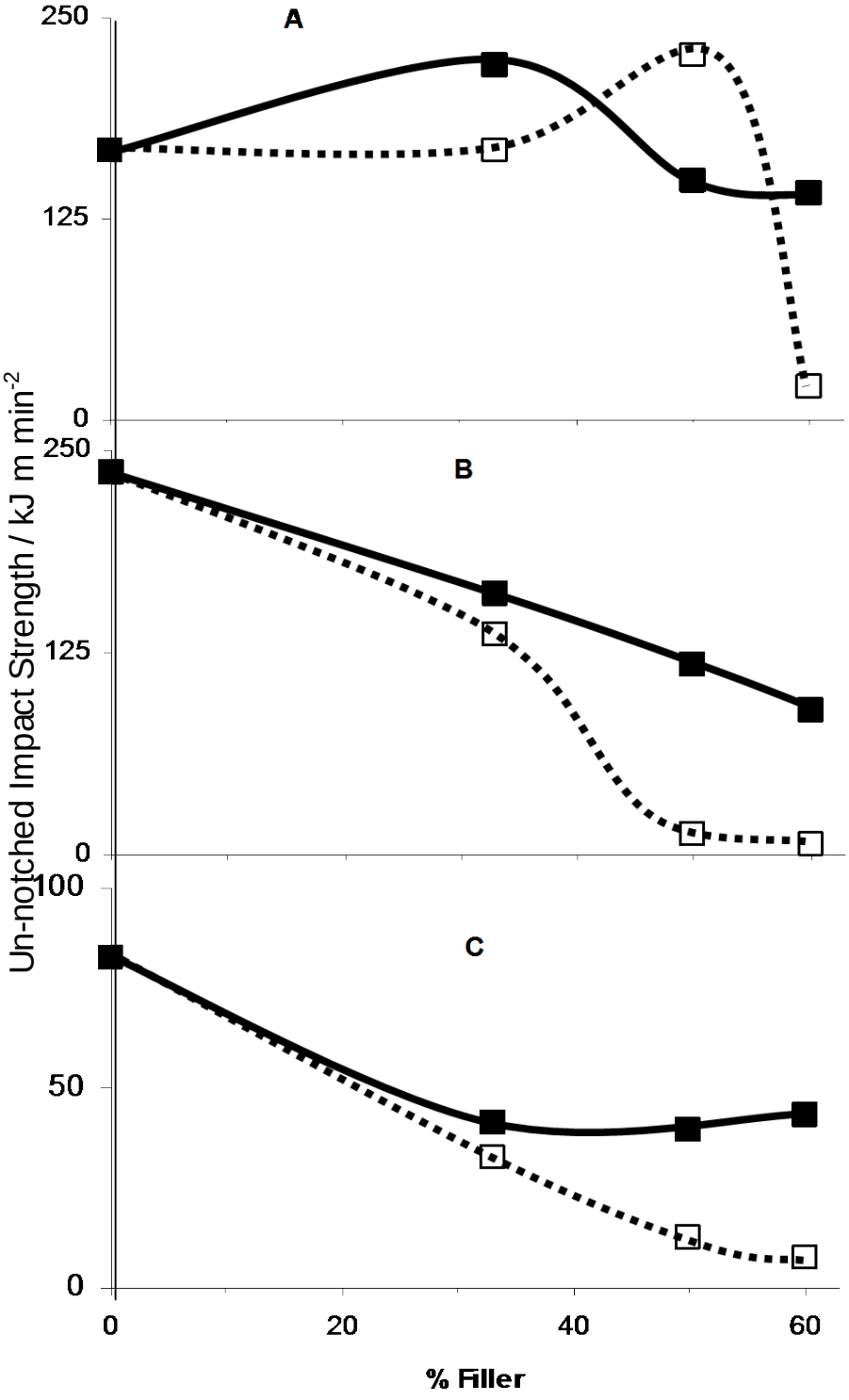

Figure 6 – Plots of UNIS vs filler level for PIPW based composites, where □ represents unmodified filler, and ■ represents modified filler.

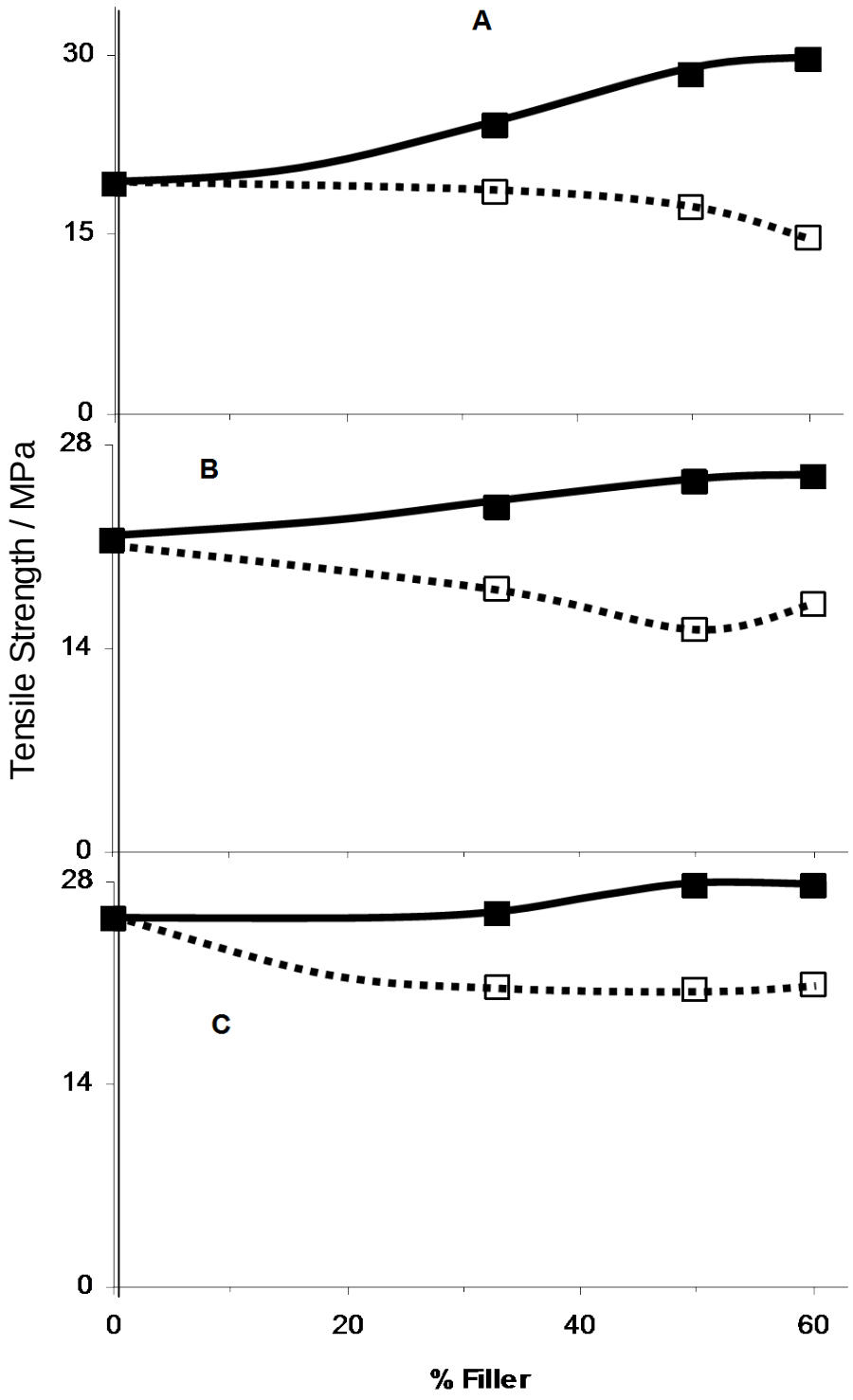

Figure 7 – Plots of tensile strength vs filler level for PIPW based composites, where □ represents unmodified filler, and ■ represents modified filler.

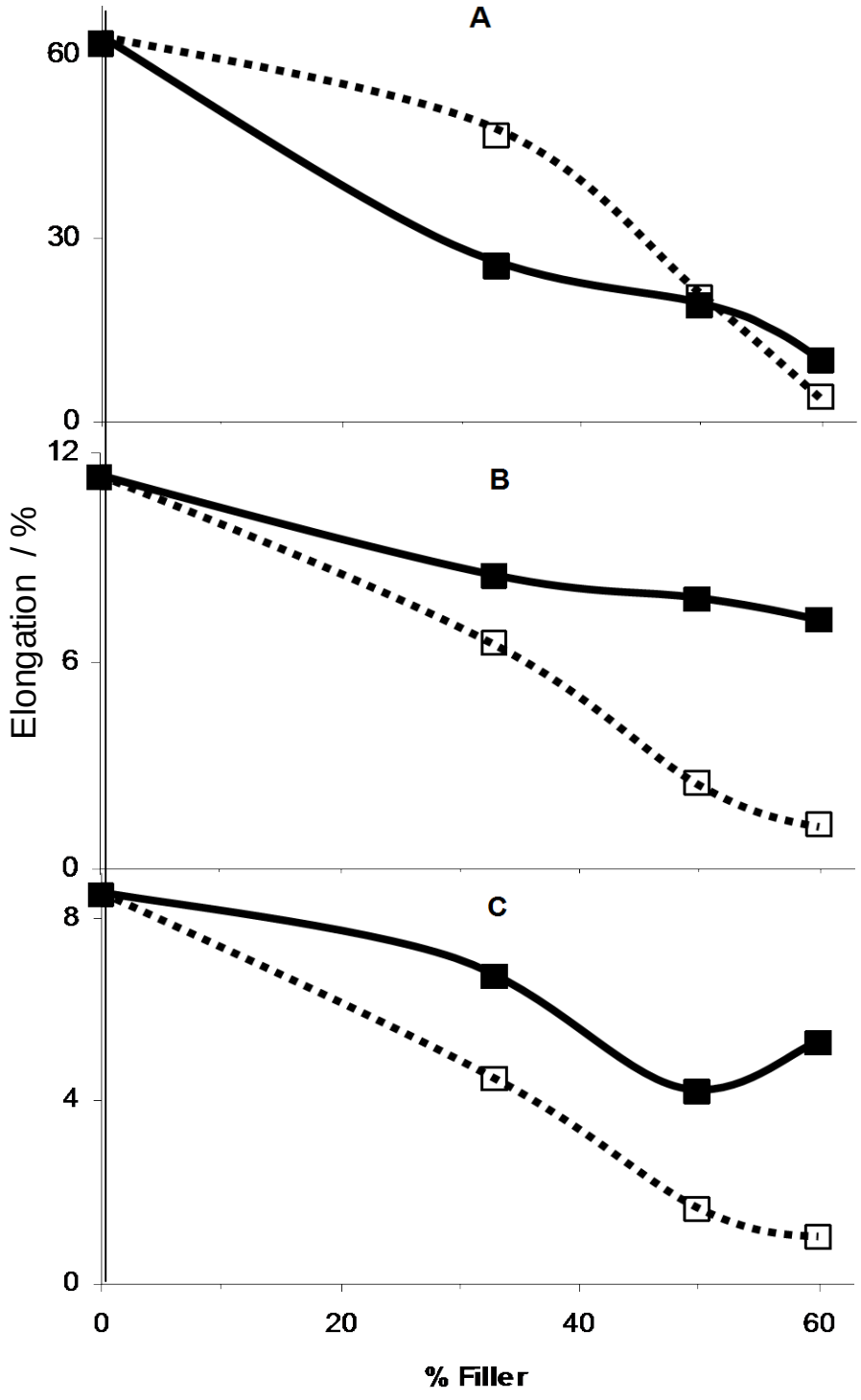

Figure 8 – Plots of elongation vs filler level for PIPW based composites, where □ represents unmodified filler, and ■ represents modified filler.

II – Conference paper presented at the Eurofillers Conference, Alessandria, 2009

THE ROLE OF ACTIVATED FILLER SURFACES IN THE COMPATIBILISATION OF MIXED POLYOLEFIN WASTE – AN ECONOMICALLY VIABLE ALTERNATIVE TO SEPARATION

Christopher Liauw[1], Clint Bainbridge[1], Graham Lees[1], Roger Rothon[1,2], Dean Thetford[3], Patrick Sunderland[3], John Schofield[3]

[1.] Manchester Metropolitan University, Centre for Materials Research, Faculty of Science and Engineering, Chester Street, Manchester, M1 5GD, UK - c.m.liauw@mmu.ac.uk; Bainbridge.clint@hotmail.com; g.c.lees@mmu.ac.uk
[2.] Rothon Consultants, 3 Orchard Croft, Guilden Sutton, Chester, CH3 7SL, UK – rogerrothon@btinternet.com
[3.] Lubrizol Limited, Hexagon Tower, Delauneys Road, Blackley, Manchester, M9 8ES, UK –dean.thetford@lubrizol.com, patrick.sunderland@lubrizol.com, john.schofield@mmu.ac.uk

Abstract
In situ treatment of ground calcium carbonate (GCC) with Lubrizol Solplus® C800 (an unsaturated carboxylic acid type surface modifier) has led to significantly improved mechanical properties of composites based on mixed polyolefin waste blends. The strength of the modified composites matched or exceeded the unfilled matrix materials. Impact toughness and modulus trends, point to formation of filler-matrix interfacial region of reduced crystallinity due to random coupling of PP and PE to the filler surface. This approach eliminates the need for separation.

Introduction
The increasing tax on land-fill [1], along with mounting environmental pressure to recycle has provided significant drive for serious attempts at recycling of post-consumer polymer waste. Furthermore, with political pressure to reduce our dependency on oil [2], and an increasing volume of plastics production, recycling is seen as both an environmentally friendly and a politically attractive option. Current trends in recycling of post-consumer polymer waste involve collection, sorting, shredding, washing, and further sorting to produce reclaimed feed stocks with varying purities. However, with each additional step additional costs are incurred and this may therefore not be the most economically appealing option. These factors place a big question mark on the viability of separation of the polyolefin fraction of polymer waste.

Polyolefines make up about 70 % of the post-consumer polymer waste stream [3]. As polyolefins generally have a density of less than unity, they can easily be float-separated from the denser polystyrene (PS), polyethylene terepthalate (PET) and polyvinylchloride (PVC) fraction. Whilst polyolefins are of similar polarity, they will not form a miscible blend due to the different chain conformations in the crystal lattice which prevents co-crystallisation and drives phase separation. Furthermore, branching in low density polyethylene adds further complexity which needs to be considered in relation to miscibility of other polyethylenes.

Our approach to this problem is to use the interfacial area within a particulate filled composite as a compatibilising interface. Lubrizol Solplus C800 is now an established unsaturated acid type coupling agent that is effective in PE and PP that is highly filled with basic fillers [4][5]. It is anticipated that both PE and PP chains in a blend would be coupled to a filler surface modified with C800. Such an effect together with peroxide induced crosslinking in the filler-matrix interfacial region is likely to reduce the ability to crystallise, thereby giving the interfacial region an elastomeric character. The latter will afford the composites a unique balance of strength and stiffness.

Experimental

Three samples of post-industrial polymer waste (PIPW) were examined. All three were polyolefin blends. Sample A was mainly polyethylene with less than 10% polypropylene present. The polyethylene component was predominantly low density polyethylene. Sample B was richer in polypropylene (c.a. 25%), whilst sample C was even richer in polypropylene (60% wt). These ratios were determined experimentally using differential scanning calorimetry, and relating fusion peak areas in the PIPW to those of HDPE/PP blends of known composition. These samples will be referred to as PIPW A, PIPW B and PIPW C, respectively. The ground calcium carbonate (GCC – Imerys Carbital 110) was dry blended with 1.2 % wt. (on the filler) Solplus C825. The latter is the 50 % w/w active silica bound form of C800. In order to initiate formation of macro-radicals, 5 % wt. (on C800) dicumyl peroxide (DCP – Akzo Perkadox® BC-40B) was also added. It should be noted that our previous work has shown that in-situ treatment of filler via pre-mixing with C825 is just as effective at pre-treating the filler with the 100% active C800 liquid. The PIPW was initially supplied in a washed, flaked form which was then extruded on a 40mm Betol twin screw extruder to form granules. The composites were compounded on a Thermo-Electron HC24 twin screw extruder (L:D ratio 28:1) at filler levels of 0% wt, 33% wt, 50% wt and 60% wt, both with and without C800 and peroxide. The set barrel temperature was 200 °C. After compounding, the composites were injection moulded at 200 °C into tensile and impact test pieces. The moulded tensile test pieces (BS2782) were tested at 50 mm min^{-1}. Charpy impact testing was performed on unnotched test pieces. The melt-flow rate was obtained at 200 °C using a 10 kg mass.

Results, Discussion and Conclusion

The results shown in Figure 1 are expressed as the change in the recorded property on C800 modification relative to the respective unmodified composite, for the purposes of this paper we have denoted this ratio (Equation 1) the interfacial activity (Int. Act.) in this way the effect of the surface modification is emphasised.

$$\text{Interfacial activity} = \frac{\text{Property when C800 modified}}{\text{Respective unmodified property}} \qquad (1)$$

At 60 % wt GCC, the Int. Act. flexural modulus for the PIPW samples show that increasing levels of PP led to reduced stiffness on C800 modification, an observation when taken together with the Int. Act. un-notched impact strength (UNIS) data, indicates some form of toughening mechanism that could arise due to reduced crystallinity (i.e. more elastomeric character – considering the T_g's of the polymers) within the interphase region. The latter could be due to random coupling of PP and PE macro-radicals to the filler surface and crosslinking of the PE component within the interphase region. The Int. Act flexural modulus data for

the virgin polyolefins is probably confounded by crystallinity related factors; the HDPE loses stiffness at higher filler levels due to crosslinking (leading to reduced crystallinity) in the interphase region. The latter is corroborated by the increased Int. Act. UNIS. However, PPH probably increases slightly in relative stiffness due to faster crystallisation of shorter chains and a possible increase in crystalline content. These aspects will be examined using DSC and will form part of the presentation. The effect of C800 modification on MFR shows the potential limitations of the approach; excess PE in the blend can lead to excessive melt viscosity due to localised crosslinking. Thanks to the predominance of chain scission on peroxide attack, the PP component in the PIPW serves to mediate the effect of the crosslinking within the PE phase. The significant chain scission in the virgin PPH based composites is particularly apparent at 60 % w/w GCC. The tensile strength data (not shown) for the PIPW samples demonstrates achievement of composite tensile strength at least equivalent to the respective unfilled matrix.

Use of in-situ C800 modified GCC filler surfaces has been shown to effectively compatibilise post-industrial mixed polyolefin waste to a level where the properties can be considered more useful than those of currently available recycled polyolefins.

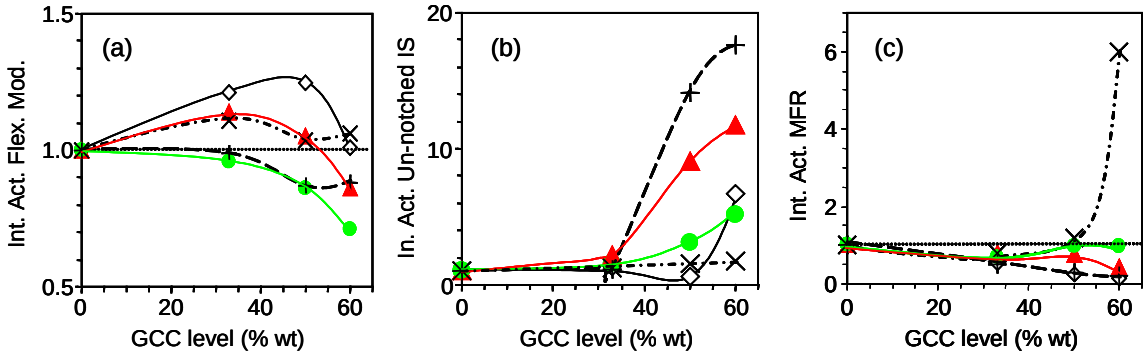

Figure 1 – (a) Int. Act. Flexural modulus, (b) In. Act. un-notched impact strength and (c) Int. Act. melt flow rate versus GCC level. Long dashed line denotes composites based on 100 % virgin HDPE and the dot – dashed line denotes composites based on 100 % virgin PP homopolymer. ◊ PIPW A (ca. 10% PP), ▲ PIPW B (ca. 25 % PP), ● PIPW C (ca. 60 % PP).

References

1. HMRC website *http://www.hmrc.gov.uk/pbr2006/pbrn26.htm*
2. The Guardian *http://www.guardian.co.uk/business/2008/jul/03/oil.alistairdarling*
3. Foster S. *Domestic Mixed Plastics Packaging Waste Management Options Report* ISBN: 1-84405-369-2 (2008)
4. C.M. Liauw, G.C. lees, R.N. Rothon, V. Voliotis, F. Wild, P. Sunderland, J.D. Schofield, D. Thetford, *Composite Interfaces*, 2006, *13*, 717.
5. Lubrizol Solplus® C800 information literature

III – Conference paper presented at the International Conference on Interfaces & Interphases in Multicomponent Materials (IIMM), Sheffield, 2010

A Novel Approach to Polyolefin Recycling (IIMM 2010 Sheffield, UK)

C. Bainbridge[1]*, C. M. Liauw[1], G. C. Lees[1], R. Rothon[1], J. Schofield[2], P. Sunderland[2], D. Thetford[2]

1. Centre for Materials Science Research, Dalton Research Institute, The Manchester Metropolitan University, Chester Street, Manchester, M1 5GD.
2. Lubrizol Limited, Hexagon Tower, Delauneys Road, Blackley, Manchester, M9 8ES, UK

The aim of this project is to find a more economically viable alternative to separation of post-consumer polyolefin waste into the individual PP and PE type components. The approach taken in this study involves blending the mixed polyolefin waste with a filler and a skilfully developed additive package. The additive package is comprised of the filler and a coupling agent, which provides a mechanism by which an immiscible polyolefin blend can be compatibilised within the interfacial region between polymer and filler[1].

Thus far, the action of the unsaturated acid coupling agent Lubrizol Solplus® C800 together with a dicumyl peroxide (DCP) initiator[2] has been evaluated in polyethylene and polypropylene and in blends of these two polymers both with and without calcium carbonate filler[3]. C800 has the ability to couple both polyethylene and polypropylene components of the blend to the filler surface (and potentially join polyethylene and polypropylene sequences away from the filler surface). The former effect appears to promote formation of an elastomeric interfacial region which leads to very good strength-toughness balance.

The objective of this presentation is to delve deeper into what is actually happening in these composites, both in the bulk matrix and within the interfacial region between the filler surface and the bulk matrix. This has been investigated initially via examination of how the mechanical response of the composites (Fig. 1), and crystalline content of blend components (Fig. 2), varies relative to the respective unfilled blends as a function of PE to PP ratio and the presence of the C800 and DCP. The composites and blends will also be Soxhlet extracted with a range of solvents of varying boiling point in order to determine which component prefers to bond to the filler and to establish if any PE to PP coupling occurs. Filler/blend residues from the latter extractions will be analysed using FTIR and DSC.

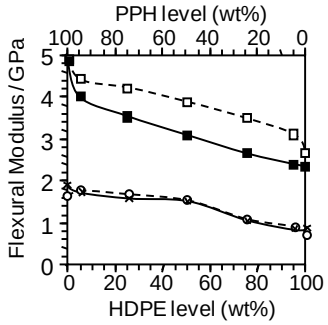

Fig. 1. Effect of HDPE / PPH blend composition on the flexural modulii of: composites containing 60 wt% unmodified (□) and modified $CaCO_3$ (■), o unfilled blend with **no** C800/DCP, X unfilled blend **with** C800/DCP.

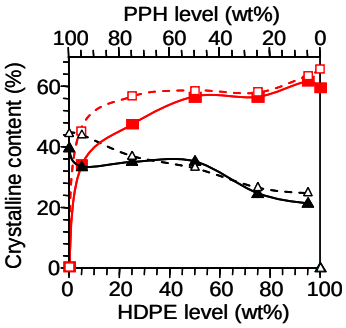

Fig. 2. Plot of crystalline content versus binary blend composition for the HDPE (red ■) and PPH (black ▲) blend components in composites containing 60 wt% $CaCO_3$. Open symbols represent unmodified filler, closed symbols represent modified filler.

Note: The term "modified filler" denotes composites modified with C800/DCP

References

1) **C. Bainbridge, "Filler-Born Reactive Compatibilisation of Mixed Polyolefin Post-Consumer Polymer Waste: A more viable Alternative to Separation?", High Performance Fillers Conference, Barcelona (2009).**

2) **C. M. Liauw, G. C. Lees, R. N. Rothon, A. Voliotis, F. Wild, P. Sunderland, J. Schofield, D. Thetford, "Evolution of Reactive Unsaturated Interfacial Modifiers for Polyolefin Based Composites", Composite. Interfaces. Vol 13 No 8-9 717-736 (2006).**

3) **C. Bainbridge, "Activated Filler Surfaces for Compatibilisation of Mixed Polyolefin Waste", Eurofillers 2009 Conference, Alessandria (2009).**

IV – Conference paper presented at the Eurofillers Conference, Dresden, 2011

Interphase Structure-Development in Modified Filler, Compatibilised Polyolefin Blends

G. C. Lees[1], C. M. Liauw[1], C. Bainbridge[1], R. Rothon[1], J. Schofield[2], P. Sunderland[2], D. Thetford[2]

1. Centre for Materials Science Research, Dalton Research Institute, The Manchester Metropolitan University, Chester Street, Manchester, M1 5GD, UK

2. Lubrizol Limited, Hexagon Tower, Delauneys Road, Blackley, Manchester, M9 8ES, UK

Abstract

Ground calcium carbonate (GCC), in-situ treated with Lubrizol Solplus® C800 (an unsaturated acid based coupling agent) and dicumyl peroxide (DCP), has been shown to significantly influence the mechanical properties of blends of polyethylene and polypropylene relative to the unfilled blends and to respective composites based on untreated GCC. These property changes are considered to occur as a consequence of the C800 causing the formation of a compatibilising interfacial region in which polymer crystallization is inhibited. This paper examines how this interphases affects specific mechanical properties and details the differences between the bulk morphology and the interphase morphology. This latter aspect has been achieved by isolation of the interphase region via selective solvent extraction studies on composites and unfilled matrix blends (both with and without C800 / DCP) followed by DSC and FTIR analysis on the extracts and residues. These studies have confirmed that the interphase region (the residues) have a significantly lower crystalline content than the bulk regions (the extracts) which thus is more elastomeric that the bulk matrix and explains the property changes observed.

Introduction

The increasing tax on land-fill [1], along with mounting environmental pressure to recycle has provided significant drive for serious attempts at recycling of post-consumer polymer waste. Furthermore, with political pressure to reduce dependency on oil, and an increasing volume of plastics production, recycling is seen as both an environmentally friendly and a politically attractive option. Current trends in recycling of post-consumer polymer waste involve collection, sorting, shredding, washing, and further sorting to produce reclaimed feed stocks with varying purities. However, with each additional step additional costs are incurred, therefore the economic viability of separating the polyolefin fraction is questionable.

Polyolefins make up about 70 % of the post-consumer polymer waste stream [2]. As polyolefins generally have a density of less than unity, they can easily be float-separated from the denser polystyrene (PS), polyethylene terepthalate (PET) and polyvinylchloride (PVC) fraction. Whilst polyolefins are of similar polarity, they will not form a miscible blend due to the different chain conformations in the crystal lattice which prevents co-crystallisation. This results in phase separation which adversely affects the mechanical properties of the blends. If such polyolefin blend could be compatibilised then improved properties should result without the need to further separate the blend components.

This paper examines a compatiblisation method which involves the addition of ground calcium carbonate (GCC) to the mixed polyolefins together with a coupling agent

(Lubrizol Solplus® C800) and an activator, dicumyl peroxide. [3], [4]. In this system the PE and PP chains in the blend would be coupled to the filler surface via C800. The "fixing" of the dissimilar polymer chains at the filler surface should then result in a good strength – toughness balance for these composite materials. It is also considered likely that the forced mixing of the dissimilar chain structures in the filler-matrix interfacial region is likely to reduce the ability of either chain to crystallise, thereby giving the interfacial region an elastomeric character. If this is the case then changes to the structure of the coupling agent may allow the characteristics of the interphase region to be modified which in turn could be used to manipulate the properties of the blend.

Experimental

All composites studied were based on Borealis HD120MO PP homopolymer (PPH) (MFR 8 dg min^{-1}) (2.16 kg 230 °C)) and Borealis MG7547s high density polyethylene (HDPE) (MFR 4 dg min^{-1}) (2.16 kg 190 °C)). The GCC (ground marble) used was Imerys Carbital® 110.
The composites were melt blended at 200 °C using a Thermo-Prism HC24 28:1 L:D co-rotating twin screw extruder and the dried, pelletised strands injection moulded to form tensile and impact test pieces using a Battenfeld BA 200 CD machine.
Blends of the following combination (PP to PE (% wt)) were prepared: 100:0, 95:5, 75:25, 50:50, 25:75, 5:95 and 0, both with and without C800 / DCP. The latter were added at 0.90 % wt and 0.05 % wt of blend, respectively. This represents the amount of free coupling agent in the matrix of a composite containing 60 % wt GCC, (assuming zero adsorption of the coupling agent on the filler). Filled blends (60 %wt filler) were also produced both with and without C800 / DCP. The C800 level was 0.6 parts per hundred filler (phf) and the DCP level was 0.03 phf. Note the more easily handled 50 wt% active silica supported version of Solplus® C800 (namely Solplus® C825) was used. The DCP used was Akzo Perkadox® BC40-B (40 wt% active supported on $CaCO_3$).
Tensile and flexural properties were measured at room temperature using British Standard test procedures. Melt flow rates, for the individual polymers and the blends, were measured 200 ^{o}C. with a load of 10 kg.

Results

Initially three samples of post industrial waste, containing different ratios of PE to PP, were examined from unfilled to 60% by weight of calcium carbonate filler, with the filler either untreated or treated with the C800 / peroxide coupling agent system. These results showed that the coupling agent had modified the resultant properties advantageously For example the mechanical properties improved with increasing filler level over the filler range studied, in relation to the unfilled system, when the filler was treated but declined when the filler was untreated. (Figure. 1).

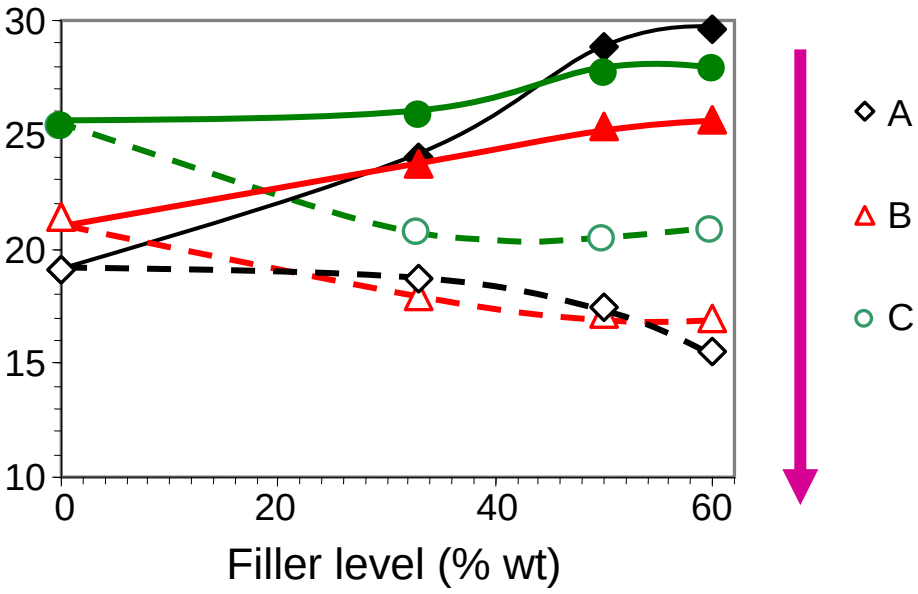

Figure 1 Tensile / Yield Strength (MPa) as a function of Filler Level
A to C increasing PP level in blend, open symbols untreated filler,
closed symbols treated filler.

Of further interest were the observations that flexural modulus was always lower for the treated filler system and that changes in the melt flow rates appeared to be related to the ratio of the PE to PP, with lower melt flow rate at higher PE level in the blend and at higher filler level for the treated system. The reduction in flex modulus was considered to be possibly related to the interphase characteristics whilst the melt flow changes to the differing reaction characteristics of PE and PP to radical reaction. This paper will concentrate on the interphase characteristics and the way in which this region influences the bulk properties of the resultant composites.

In order to study the interphase model blends were prepared using high density polyethylene (HDPE) and polypropylene homopolymer (PPH). The blend ratios covered the range given in the experimental section. Figure 2 shows the trends in flexural modulus as a function of HDPE level for treated and untreated filler added at a filler loading of 60% by weight. It is clearly shown that the treated filler composites have lower flexural modulus over the entire range compared to the untreated filler composites. Also shown are the equivalent results for the unfilled blends both with and without the coupling agent. These have the expected lower modulus but both follow the same line over the entire blend ratios. It is therefore concluded that the lower modulus seen for the treated, filled composites is a consequence of the interphase character and not a consequence of any bulk matrix modification which could have potentially influenced the bulk properties.
Figure 3 shows the percentage crystallinities for both the HDPE and PPH in the blends at the different blend ratios. The results are determined for the bulk matrix of the composites and in relation to the expected values of the HDPE and PPH used are of the order expected. Again this strongly suggests that the bulk matrix has not been changed by the coupling agent system used and that the interphase is likely to be the cause of the flexural modulus results observed.

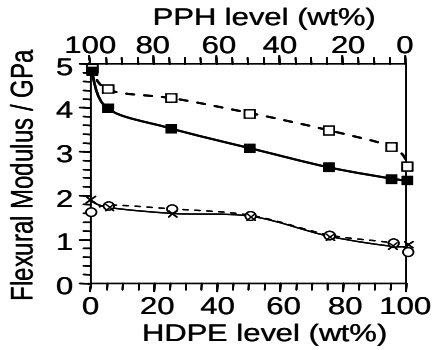

Fig. 2. Effect of HDPE / PPH blend composition on the flexural modulii of: composites containing 60 wt% untreated (□) and treated $CaCO_3$ (■), ○ unfilled blend with no C800/DCP, X unfilled blend with C800/DCP.

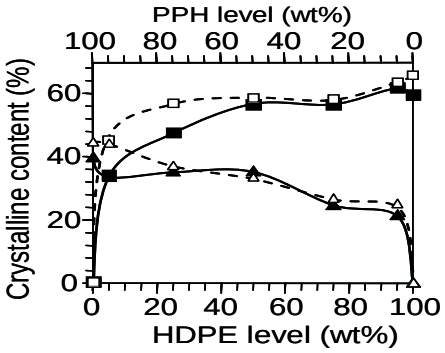

Fig. 3 Effect of HDPE / PPH blend on the crystalline content of composites containing 60 wt% calcium carbonate. HDPE (■) and ▲ PPH. Open symbols untreated filler, closed symbols treated filler

As the coupling agent system should be "fixing" the polyolefin chains to the filler there should be a bound polymer content i.e polymer bound to filler via the coupling agent. This bound polymer will therefore be insoluble and can thus be isolated from the bulk matrix by solvent separation. As the bound polymer effectively is the interphase, characterisation of the insoluble and soluble phases should provide evidence as to whether or not these phases differ and whether or not these difference can account for the observed reduction in the flexural modulus.

Figure 4 shows the percentage bound polymer as a function of the percentage PPH in the initial blends for 60% calcium carbonate filled composites for both treated and untreated filler.

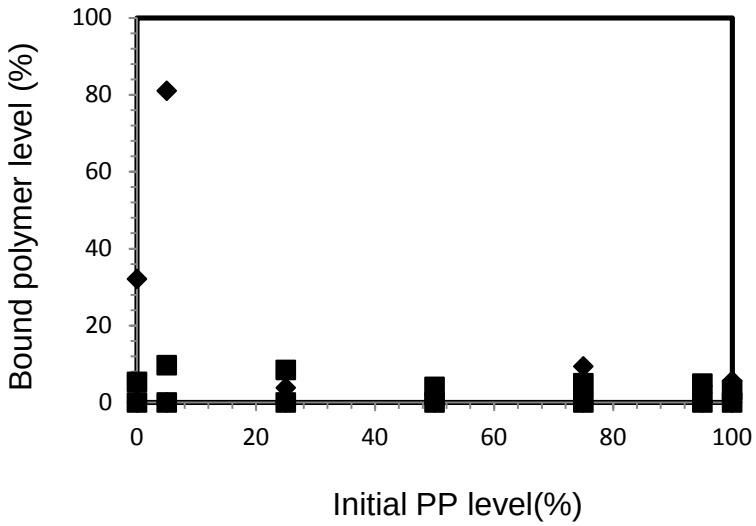

Figure 4 Bound polymer levels as a fuction of initial PP level
□ treated filler composites Δ untreated filler composites

At low PPH levels the untreated filler composites have high insoluble matrix level s starts This may be due to crosslinking of the PE matrix initiated by mechano-oxidative degradation resulting from the melt viscosities associated with use of a high filler content. As PPH content of the matrix increases beyond 25 % wt the bound polymer level falls sharply to a level below that for the equivalent C800-DCP modified composites. This may be due to chain scission related effects in the PP fraction that may also initiate chain

scission at branch points in the PE component. Beyond approximately 75 % wt PP in the matrix, there are hints that the peroxide in the C800-DCP system dominates, leading to chain scission and a hint of a reduction in insoluble matrix content to a level below that in the equivalent unmodified composites. The low insoluble matrix content observed at low PP levels in the C800-DCP modified composites may be related to dominance of chain scission. However at 25 and 50 % wt PPH in the matrix, the insoluble matrix content of the C800-DCP modified composites is higher than the equivalent unmodified composites, an effect that may be related to the PP/PE ratio being conducive to coupling of matrix to the filler via adsorbed C800.

In order to determine the percentage crystallinity levels for both the HDPE and the PPH the ratios of these two polymers were required in both the bound polymer residues and the extracted polymers. As it cannot be assumed that these ratios are the same as the initial blend ratios the values must be determined independently. This was achieved by FTIR analysis and determination of the relative HDPE level from the ratio of the intensities of the methylene CH stretching peak and the methyl ch stretching peak. These values were then plotted against the initial PPH blend values to produce a calibration curve from which the respective PPH values in the extrced samples could be read off.

Figures 5 and 6 show the crystallinity values for both the HDPE and the PPH in the bound polymer residues for the treated and untreated filler composites respectively. The dotted lines on these plots are the crystallinity values of injection moulded samples of unfilled HDPE and PPH for comparison. In both composites the crystallinity levels are generally lower than those of the base polymers. What is particularly noticeable is the extremely low levels of crystallinity for the PPH in the treated filler residue samples. This suggests that the radicals generated to activate the coupling reaction between the matrix and the coupling agent is causing chain scission of the PPH chains which will then undergo additional reactions perhaps producing block or branched copolymer structures with the HDPE.

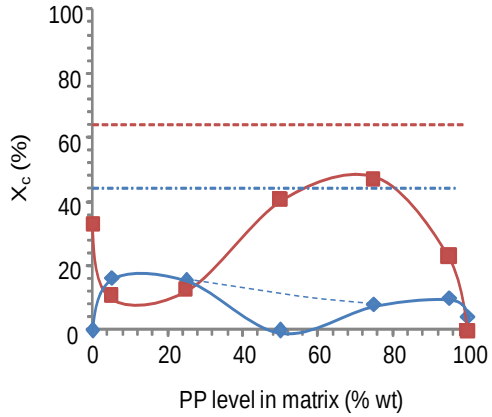

Figure 5 Crystallinity results for extraction residues for treated filler composites
□ HDPE and Δ PPH crystallinity

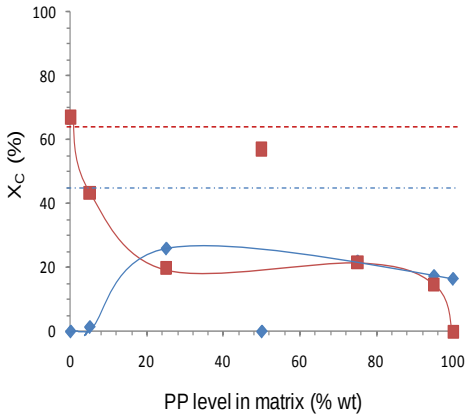

Figure 6 Crystallinity results for extraction residues for untreated filler composites
□ HDPE and Δ PPH crystallinity

Figures 7 and 8 show the crystallinity values for both HDPE and PPH for the soluble fractions of both the treated and untreated fractions respectively. Again the dotted lines are the crystallinity values of injection moulded samples of unfilled HDPE and PPH. In comparison with the results shown in Figures 5 and 6 these crystallinity values are of the order expected for the HDPE and PPH polymers used to form the blends. It is therefore concluded that the formation of the interphase region, particularly in the presence of the peroxide, does change the morphology of this region making it more amorphous and hence more elastomeric.

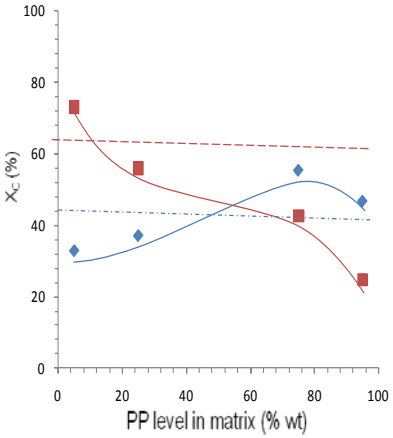

Figure 7 Crystallinity results for soluble soluble extract fraction for treated filler composites
□ HDPE and Δ PPH crystallinity

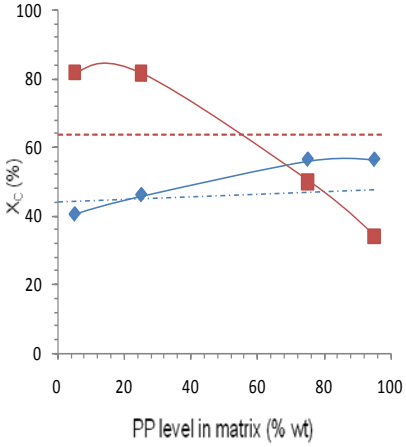

Figure 8 Crystallinity results for soluble solubleextract fraction for untreated filler composites
□ HDPE and Δ PPH crystallinity

It should also be noted that unfilled blend both with and without the coupling system were fully soluble over the entire blend range. This supports the conclusion that it is the interphase which is responsible for the property changes observed and not a bulk matrix effect.

Conclusions

The crystallinity results for both the insoluble and soluble fractions show that the presence of calcium carbonate filler promotes the formation of a less crystalline region around the filler particles. However this interphase region is only able to influence the properties of the composites if it is chemically coupled to the filler surface by an appropriate coupling agent, in this case with Lubrizol Solplus® C800 together with a peroxide activator. Thus the treated filler composites alone promote the mechanical properties of blend of PE and PP.

References

[1] HMRC website http://www.hmrc.gov.uk/pbr2006/pbrn26.htm.
[2] Foster S. Domestic Mixed Plastics Packaging Waste Management Options Report ISBN: 1-84405-369-2 (2008).
[3] Liauw CM, Bainbridge C, Lees GC, Rothon RN, Thetford D, Sunderland, P, Schofield, JD. Proc. *Eurofillers 2009*, Alessandria, Italy, 21-25 June 2009.
[4] Liauw CM, Lees GC, Rothon RN, Voliotis V, Wild F. Sunderland P, Schofield JD, Thetford D. *Composite Interfaces*. 2006;13:717.

APPENDIX 2 – Data sheets for the materials used in Section 2.1

lyondellbasell

Lupolen 3020 K

Polyethylene, Low Density

Product Description

Lupolen 3020 K is a non-additivated, low density polyethylene with high rigidity, good opticals and good chemical resistance. It is delivered in pellet form.

Foodlaw compliance information about this product can be found in separate product documentation.

This product is not intended for use in medical and pharmaceutical applications.

Product Characteristics

Status	Commercial: Active
Test Method used	ISO
Availability	Europe
Processing Method	Cast Film, Blown Film, Injection Molding
Features	Good Heat Seal , Opticals, Good Processability, Good Stiffness
Typical Customer Applications	Film, Shrink Film, Blown Film, Cast Film, Food Packaging Film, Lamination Film, Surface Protection Film

Typical Properties	Method	Value	Unit
Physical			
Density	ISO 1183	0.928	g/cm³
Melt flow rate (MFR) (190°C/2.16kg)	ISO 1133	4.0	g/10 min
Mechanical			
Dart drop impact (50µm, Blown Film)	ASTM D 1709	90	g
Tensile Modulus	ISO 527-1, -2	300	MPa
Tensile Stress at Yield	ISO 527-1, -2	13.0	MPa
Tensile Strength	ISO 527-1, -3		
		20.0	MPa
Note: MD			
		17.0	MPa
Note: TD			
Tensile Strain at Break	ISO 527-1, -3		
		350	%
Note: MD			
		600	%
Note: TD			
Thermal			
Vicat softening temperature (A50 (50°C/h 10N))	ISO 306	97.0	°C
Melting Temperature	ISO 3146	114	°C
Optical			
Haze (50µm)	ASTM D 1003	<7	%
Gloss	ASTM D 2457		
(20°, 50µm)		>80	
(60°, 50µm)		>115	
Film			
Melt Temperature		150 to 190	°C

Additional Properties

Film properties tested using 50 µm thickness blown film extruded at a melt temperature of 170°C and a blow-up ratio of 1:2.5.
Failure Energy, DIN 53373, 50 µm: 3.5 J/mm
Coefficient of Friction, ISO 8295: >80%
Recommended Film Thickness: 15 to 40 µm

Polyethylene
MG7547S

Description

MG7547S is a high-density polyethylene produced by a low pressure process. This grade has an excellent impact strength and low distortion even at low temperatures. It also contains UV-stabilizer, which makes this grade especially suited for outdoor applications.

Applications

Waste bins
Fish crates
Storing cases

Special features

Very good impact strength
Very good toughness

Physical Properties

Property	Typical Value Data should not be used for specification work	Test Method
Density	954 kg/m3	ISO 1183
Melt Flow Rate (190 °C/2,16 kg)	4 g/10min	ISO 1133
Tensile Modulus (1 mm/min) [1]	950 MPa	ISO 527-2
Tensile Strain at Yield (50 mm/min) [1]	10 %	ISO 527-2
Tensile Stress at Yield (50 mm/min) [1]	24 MPa	ISO 527-2
Heat Deflection Temperature (0,45 MPa) [2]	71 °C	ISO 75-2
Charpy Impact Strength, notched (23 °C)	11 kJ/m²	ISO 179/1eA
Charpy Impact Strength, notched (-20 °C)	7 kJ/m²	ISO 179/1eA
Hardness, Shore D	61	ISO 868

[1] Measured on injection moulded specimens acc. to ISO 1872-2
[2] Measured on injection moulded specimens acc. to ISO 1873-2

Processing Techniques

Following parameters should be used as guidelines:

Injection Moulding

Melt temperature	210 - 275 °C	
Holding pressure	As low as possible	Minimum to avoid sink marks.
Mould temperature	10 - 40 °C	
Injection speed	As high as possible.	

Shrinkage 1 - 2 %, depending on wall thickness and moulding parameters

Borealis AG | Wagramerstrasse 17-19 | 1220 Vienna | Austria
Telephone +43 1 224 00 0 | Fax +43 1 22 400 333
FN 269858a | CCC Commercial Court of Vienna | Website www.borealisgroup.com

BOREALIS

Eltex® P HV001PF

Product Technical Information

Polypropylene - Homopolymer

HV001PF is a polypropylene supplied in the form of unstabilized free flowing powder. The spherical morphology and narrow particle size distribution of Eltex® P HV001PF leads to excellent mixing behaviour with additives, fillers and colour concentrates. It is specially designed for film applications (low fish eyes content).

Applications

- Master batches and compounds for films
- Master batches and compounds for sheets
- Master batches and compounds for fibres

Benefits and Features

- Excellent mixing behaviour with additives, fillers and colour concentrates
- Specially designed for film applications

Properties		Test Methods	Values	Units
Physical				
Melt Flow Rate	230°C/2.16kg	ISO 1133	10	g/10min
Density	@ 23°C	ISO 1183	905	kg/m³
Mechanical				
Flexural Modulus	@ 23°C	ISO 178	1600	MPa
Thermal				
Melting Point		ASTM D 3417	161	°C

July, 2008

Published by

INEOS Polyolefins

Polypropylene
HD120MO

Description
HD120MO is a polypropylene homopolymer with a good combination of mechanical properties intended for injection moulding.

Applications

Sanitary equipment	General packaging
Caps and closures	

Physical Properties

Property	Typical Value Data should not be used for specification work	Test Method
Density	908 kg/m3	ISO 1183
Melt Flow Rate (230 °C/2,16 kg)	8 g/10min	ISO 1133
Tensile Modulus (1 mm/min)	1.500 MPa	ISO 527-2
Tensile Strain at Yield (50 mm/min)	9 %	ISO 527-2
Tensile Stress at Yield (50 mm/min)	33,5 MPa	ISO 527-2
Heat Deflection Temperature (0,45 N/mm²) [1]	88 °C	ISO 75-2
Charpy Impact Strength, notched (23 °C)	4 kJ/m²	ISO 179/1eA
Hardness, Rockwell (R-scale)	98	ISO 2039-2

[1] Measured on injection moulded specimens acc. to ISO 1873-2

Processing Techniques
This product is easy to process with standard injection moulding machines.

Following parameters should be used as guidelines:

Melt temperature	230 - 260 °C	
Holding pressure	200 - 500 bar	Minimum to avoid sink marks.
Mould temperature	10 - 30 °C	
Injection speed	As high as possible.	

Shrinkage 1 - 2 %, depending on wall thickness and moulding parameters

Storage
HD120MO should be stored in dry conditions at temperatures below 50°C and protected from UV-light. Improper storage can initiate degradation, which results in odour generation and colour changes and can have negative effects on the physical properties of this product.

Borealis AG | Wagramerstrasse 17-19 | 1220 Vienna | Austria
Telephone +43 1 224 00 0 | Fax +43 1 22 400 333
FN 269858a | CCC Commercial Court of Vienna | Website www.borealisgroup.com

BOREALIS

SOLPLUS® C800

A 100% active coupling agent

Lubrizol

TECHNICAL DATA SHEET

Applications	• Coupling agent for Cabling Applications (basic & amphoteric fillers)
Performance	SOLPLUS C800 is a 100% active coupling agent developed for use with basic and amphoteric fillers including Alumina trihydrate and calcium carbonate. In the above applications, the following benefits are achieved: • Highly cost effective • Low volatility • No alcohol evolution during processing • Effective on both hydroxide and carbonate type fillers
Incorporation	Please refer to the literature (Doc 059)
Addition levels	The level of SOLPLUS C800 required for maximum effect is directly proportional to the surface area of the filler. The dosage level is therefore 6.67mg / m^2 of filler surface area

Typical properties

Appearance	colourless acidic liquid
Melting point (°C)	approx. -30
Flash point (°C)	approx. 100
Boiling point (°C)	approx. 103
Density (g/cm³)	1.194
Gardner Colour	5 max

Packaging and storage	SOLPLUS C800 is packed in 25Kg plastic drums. Shelf life: 2 years. For storage, please refer to the MSDS.
Regulatory status	For detailed information, please refer to the MSDS.

Lubrizol, Ltd.
Hexagon Tower, Blackley
Manchester M9 8ZS, United Kingdom
Tel.: +44-(0)161-721-2004
www.lubrizolcoatings.com

SOLPLUS® C825

A 50% active coupling agent on a precipitated amorphous silica

Lubrizol

TECHNICAL DATA SHEET

Applications	• Coupling agent for Cabling Applications (basic & amphoteric fillers)	
Performance	SOLPLUS C825 is a 50% active coupling agent on a precipitated amorphous silica developed for use with basic and amphoteric fillers including alumina trihydrate and calcium carbonate. In the above applications, the following benefits are achieved: • Highly cost effective • Low volatility • No alcohol evolution during processing • Effective on both hydroxide and carbonate type fillers	
Incorporation	Please refer to the literature	
Addition levels	The level of SOLPLUS C825 required for maximum effect is directly proportional to the surface area of the filler. The dosage level is therefore 6.67mg / m^2 of filler surface area.	
Typical properties	Appearance	colourless acidic powder
	Density (g/cm^3)	1.56
Packaging and storage	SOLPLUS C825 is packed in 20 Kg metal drums. Shelf life: 1 year. For storage, please refer to the MSDS.	
Regulatory status	For detailed information, please refer to the MSDS.	

Lubrizol, Ltd.
Hexagon Tower, Blackley
Manchester M9 8ZS, United Kingdom
Tel.: +44-(0)161-721-2004
www.lubrizolcoatings.com

AkzoNobel
Tomorrow's Answers Today

Perkadox® BC-40B-pd

Product description

Dicumyl peroxide, powder
40% with whiting

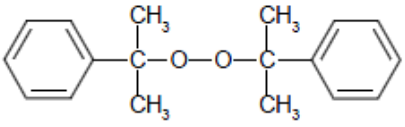

Molecular weight	: 270.4
Active oxygen content peroxide	: 5.92%
actual product	: 2.31-2.43%
CAS No.	: 80-43-3
EINECS/ELINCS No.	: 201-279-3
TSCA status	: listed on inventory

Perkadox BC-40B-pd is a monofunctional peroxide formulation which is used for the crosslinking of natural and synthetic rubbers, as well as thermoplastic polyolefins.

Specifications

Appearance	: Off-white powder
Assay	: 39.0-41.0%

Storage

Due to the relatively unstable nature of organic peroxides a loss of quality can be detected over a period of time. To minimize the loss of quality, AkzoNobel recommends a maximum storage temperature (T_s max.) for each organic peroxide product.

For *Perkadox* BC-40B-pd T_s max. = 30°C

When stored under the recommended storage conditions, *Perkadox* BC-40B-pd will remain within the AkzoNobel specifications for a period of at least six months after delivery.

Thermal stability

Organic peroxides are thermally unstable substances, which may undergo self-accelerating decomposition. The lowest temperature at which self-accelerating decomposition of a substance in the original packaging may occur is the Self-Accelerating Decomposition Temperature (SADT). The SADT is determined on the basis of the Heat Accumulation Storage Test.

For *Perkadox* BC-40B-pd SADT : 80°C

The Heat Accumulation Storage Test is a recognized test method for the determination of the SADT of organic peroxides (see Recommendations on the Transport of Dangerous Goods, Manual of Tests and Criteria - United Nations, New York and Geneva).

Major decomposition products

Methane, Acetophenone, 2-Phenylpropanol-2, α-methylstyrene

Packaging and transport

The standard packaging is a cardboard box for 20 kg peroxide formulation.

Both packaging and transport meet the international regulations. For the availability of other packed quantities consult your AkzoNobel representative.

Perkadox BC-40B-pd is classified as a non-dangerous good according to national and international transport regulations.

Safety and handling

Keep containers tightly closed. Store and handle *Perkadox* BC-40B-pd in a dry well-ventilated place away from sources of heat or ignition and direct sunlight. Never weigh out in the storage room.

Avoid contact with reducing agents (e.g. amines), acids, alkalines and heavy metal compounds (e.g. accelerators, driers and metal soaps).

Please refer to the Material Safety Data Sheet (MSDS) for further information on the safe storage, use and handling of *Perkadox* BC-40B-pd. This information should be thoroughly reviewed prior to acceptance of this product.
The MSDS is available at www.akzonobel.com/polymer.

Applications

Perkadox BC-40B-pd is used for the crosslinking of natural and synthetic rubbers, as well as thermoplastic polyolefins.

- Rubber compounds containing *Perkadox* BC-40B-pd combine good processing safety with a fair speed of cure.
- Safe processing temperature: 130°C (rheometer t_{s2} > 20 minutes).
- Typical crosslinking temperature: 170°C (rheometer t_{90} about 12 minutes).

Akzo Nobel Polymer Chemicals B.V.
Amersfoort, The Netherlands
Tel. +31 33 467 6767
Fax +31 33 467 6151

polymerchemicals.nl@akzonobel.com

Akzo Nobel Polymer Chemicals LLC
Chicago, U.S.A.
Tel. +1 312 544 7000
1 800 828 7929 (Toll free US only)
Fax + 1 312 544 7188
polymerchemicals.na@akzonobel.com

Akzo Nobel (Asia) Co., Ltd.
Shanghai, PR China
Tel. +86 21 6279 3399
Fax +86 21 6247 1129

polymerchemicals.ap@akzonobel.com

www.akzonobel.com/polymer

Carbital™ 110

Carbital 110 is a high whiteness calcium carbonate derived from pure white marble. It is milled and classified to below 10 microns.

IMERYS PERFORMANCE & FILTRATION MINERALS
Par Moor Centre,
Par Moor Road, Par
Cornwall, PL24 2SQ - UK
Tel: +44 1726 818000
Fax: +44 1726 811200

SPECIFICATION

Brightness		95.0 ±1.5
+ 10 microns	(% max)	1.5
Moisture	(% max as produced)	0.2

TYPICAL PROPERTIES

Specific gravity		2.7
Oil absorption	(g/100g)	18
Surface area BET	(m^2g^{-1})	5
Aerated powder density	(kg/m^3)	580
Tapped powder density	(kg/m^3)	1030
pH		9.4

TYPICAL CHEMICAL ANALYSIS

$CaCO_3$	(%)	98.0
$MgCO_3$	(%)	1.8
Fe_2O_3	(%)	0.01
Acid insolubles	(%)	0.2

EINECS No.	207-439-9
CAS No.	47134-1

TYPICAL PARTICLE SIZE DISTRIBUTION

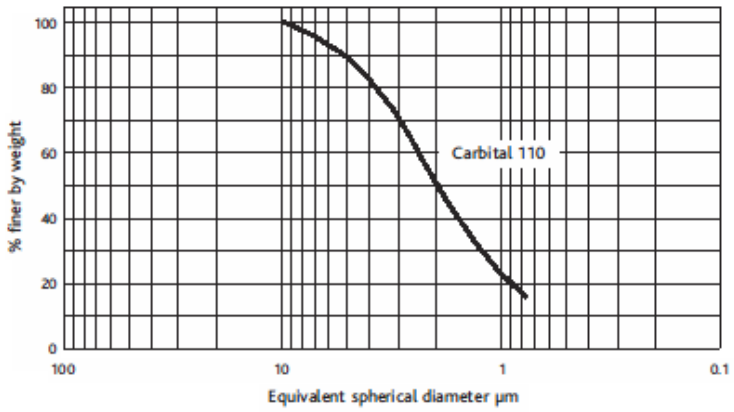

The data quoted are determined by the use of IMERYS Minerals Ltd Standard Test Methods, copies of which will be supplied on request. Every precaution is taken to ensure the products conform to our published data, but since the products are based on naturally occurring raw materials, we reserve the right to change these data should it become necessary. Sales are in accordance with our 'Conditions of Sale', copies of which will be supplied on request.

IMERYS
Performance Minerals

DAT207CC
March 2004 - Third edition.
This data sheet supercedes the data sheet dated October 2001

APPENDIX 3 – Examples of raw data and how they translate into the results discussed in Section 3

I – Melt-flow rate data

Cut Off No	Weight / kg	Time / s	Mass / g	
1	10	10	0.2537	
2	10	10	0.2642	
3	10	10	0.2512	
4	10	10	0.2403	
5	10	10	0.2593	
6	10	10	0.2753	
7	10	10	0.2794	
8	10	10	0.2696	**MFR**
		Average	0.2616	15.696

Where:

$$MFR = \frac{average\ cut\ off\ mass\ (g)}{cut\ off\ time\ (10\ mins)}$$

And:

$$Cut\ off\ time\ (10\ mins) = cut\ off\ time\ (10\ s) \times 60$$

Therefore:

$$0.2616 \times 60 = 15.696$$

For VMFR, volume and density must be taken into account.

So, volume of composite assuming 100g:

$$(60 \div 2.8) + (40 \div 0.91) = 21.43 + 43.96 = 65.39\ cm^3\ (100 g^{-1})$$

Where:

(60 ÷ 2.8) is the percentage (60%) of filler at density 2.8

And:

(40 ÷ 0.91) is the percentage (40%) of polymer at density 0.91

So, density of composite assuming 100g:

$$density = \frac{100}{(60 \div 2.8) + (40 \div 0.91)} = \frac{100}{65.39} = 1.53\ g\ cm^{-3}$$

To calculate VMFR:

$$VMFR = \frac{MFR}{Density}$$

Therefore, using the values from above:

$$VMFR = \frac{15.696}{1.53} = 10.26\ cm^3\ 10\ min^{-1}$$

II – Tensile test data

ISO 527-3 Tensile + Modulii + Break [100S] Test Report

Product Code	: H25P75-60M	**Stress Range**	: 30.00 MPa
Batch Reference	: 155	**Strain Range**	: 100.0 %
Product Description	:	**Primary Speed**	: 5.000 mm/min
Date	: 18/09/2009	**Secondary Speed**	: 50.00 mm/min
Operator	:	**Gauge Length**	: 50.00 mm
Temperature [C]	:	**Change Speed at**	: 0.5000 %
Relative Humidity	:	**Modulus Point 1**	: 0.1 %
		Modulus Point 2	: 0.2 %
		Modulus Point 3	: 0.25 %
		Preload	: 0 N
		Auto Return	: ON

No.	E-Mod. MPa	Yield MPa	Yield %	@ 0.1% MPa	@ 0.2% MPa	@ 0.25% MPa	Break MPa	Break %
1	3983	33.72	2.425	6.65	9.93	11.56	33.58	3.200
2	3284	33.65	2.530	7.66	10.93	12.52	33.35	3.600
3	3570	33.34	2.345	9.04	12.25	13.70	32.71	3.860
4	3415	33.50	2.575	3.668	7.20	8.99	32.91	4.040
5	2869	33.59	2.824	2.926	6.02	7.60	32.81	4.720
6	2363	33.06	2.975	2.891	5.30	6.43	32.88	3.780
Mean	3248	33.48	2.612	5.47	8.60	10.13	33.04	3.867
Median	3350	33.54	2.553	5.16	8.57	10.28	32.90	3.820
Std. Dev.	566	0.2430	0.2413	2.656	2.828	2.899	0.3435	0.506
Minimum	2363	33.06	2.345	2.891	5.30	6.43	32.71	3.200
Maximum	3983	33.72	2.975	9.04	12.25	13.70	33.58	4.720

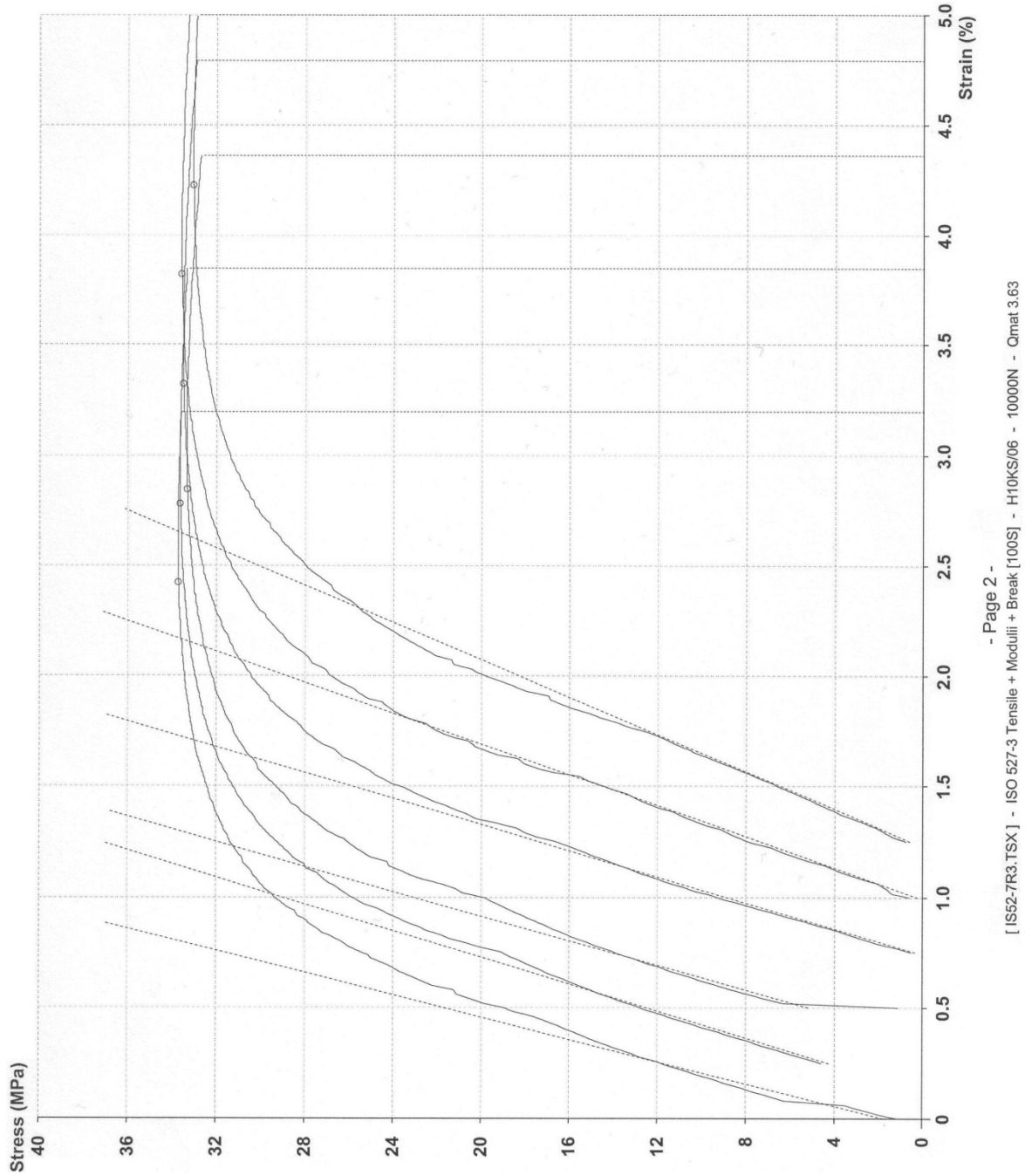

Where:

E-Mod is the value for **Young's Modulus**

Yield (MPa) is the value used for **Tensile Strength**

Break (%) is the value used for **Elongation at Failure**

It is also worth noting that if individual specimen results recorded in the report deviated significantly from the average, they were discarded and both the average and the standard deviation recalculated without the erroneous result. Furthermore, if three or more specimen results were found to be erroneous, the test was repeated with six new test samples from the batch.

III – Flexural test data

ISO 178 Flexural Test Test Report

Product Code	: H100-60U	**Load Range**	: 40.00 N
Batch Reference	: 24	**Extension Range**	: 20.00 mm
Product Description	:	**Speed**	: 5.000 mm/min
Date	: 26/08/2008	**Span**	: 64.0 mm
Operator	:	**End Point**	: 16.00 mm
Temperature	: 20	**Preload**	: 0 N
Relative Humidity	:	**Auto Return**	: ON

No.	Flex.Modulus MPa	Flex.Stress at Max MPa	Deform. at Max mm	Deform. at Break mm
1	2685	27.15	4.460	16.00
2	2653	27.22	4.200	16.00
3	2702	26.99	4.140	16.00
4	2717	27.17	4.080	16.00
5	2679	27.23	4.420	16.00
6	2685	27.33	4.360	16.00
Mean	2687	27.18	4.277	16.00
Median	2685	27.20	4.280	16.00
Std. Dev.	21.78	0.1132	0.1577	-
Minimum	2653	26.99	4.080	16.00
Maximum	2717	27.33	4.460	16.00

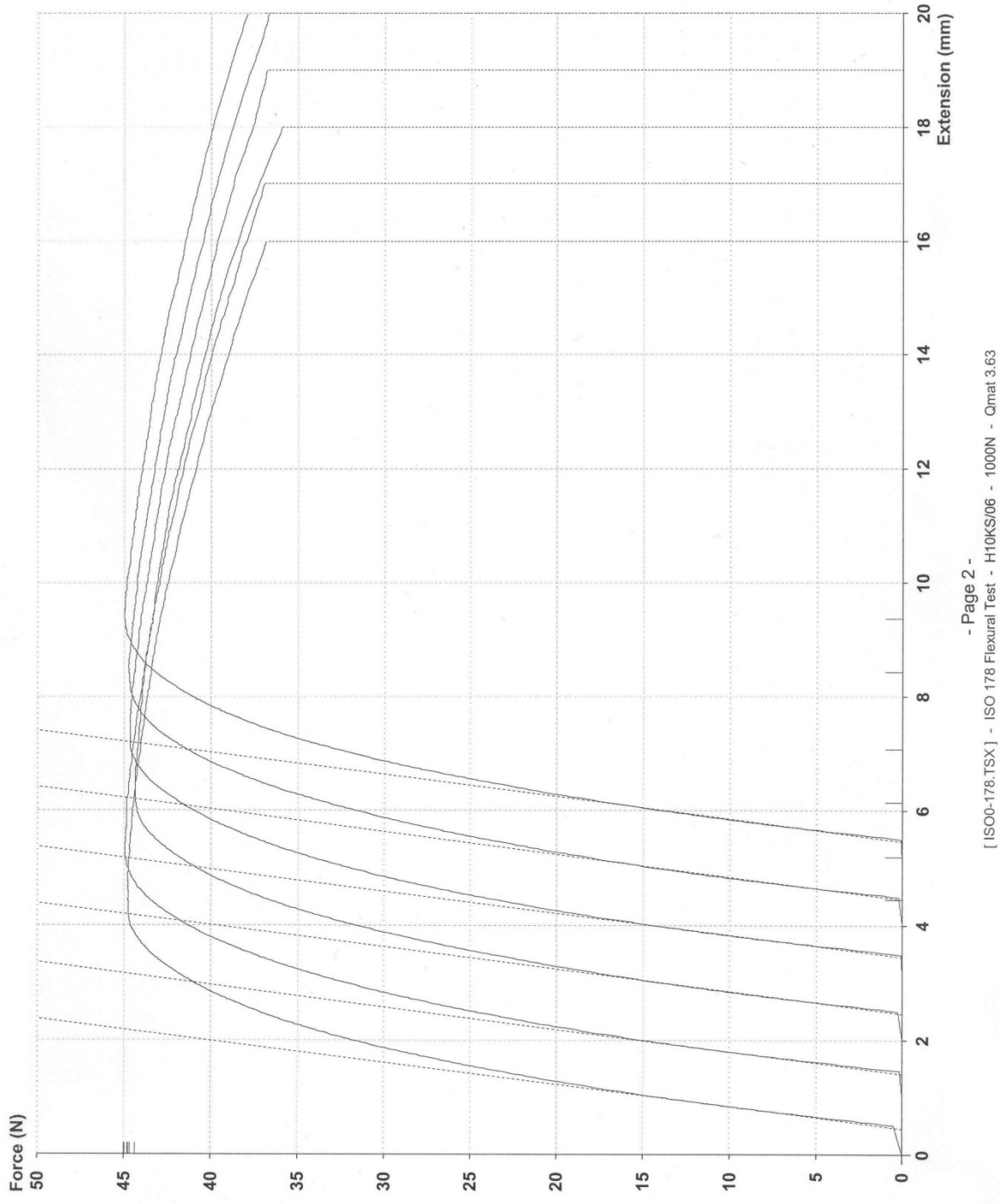

Where:

> *Flexural modulus (MPa)* is used as the value for **Flexural Modulus**, and is converted to GPa by dividing the MPa value by 1000.

It is worth noting that if individual specimen results recorded in the report deviated significantly from the average, they were discarded and both the average and the standard deviation recalculated without the erroneous result. Furthermore, if three

or more specimen results were found to be erroneous, the test was repeated with six new test samples from the batch.

IV – Impact test data

No	T / mm	W / mm	A / mm^2	A / m^2	L / J	E / J	E / kJ	Impact Strength / kJ m^{-2}
1	3.94	7.76	30.57	$3.057x10^{-5}$	0.048	0.288	0.00024	7.85
2	3.95	7.81	30.85	$3.085x10^{-5}$	0.048	0.288	0.00024	7.78
3	3.94	7.82	30.81	$3.081x10^{-5}$	0.048	0.288	0.00024	7.79
4	3.95	7.78	30.73	$3.073x10^{-5}$	0.048	0.264	0.000216	7.03
5	3.95	7.79	30.77	$3.077x10^{-5}$	0.048	0.304	0.000256	8.32
6	3.95	7.80	30.81	$3.081x10^{-5}$	0.048	0.304	0.000256	8.31
7	3.94	7.76	30.57	$3.057x10^{-5}$	0.048	0.288	0.00024	7.85
							Average	7.98

Where:

$$Impact\ Strength\ (kJ\ m^{-2}) = \frac{Energy\ absorbed\ (kJ)}{Area\ (m^2)}$$

Therefore:

$$Energy\ absorbed\ (kJ) = \frac{energy\ absorbed\ by\ specimen\ (J) - energy\ loss\ in\ machine(J)}{1000}$$

And:

$$Area\ (m^2) = \frac{thickness\ (mm) \times width\ (mm)}{1000000}$$

So:

$$Energy\ absorbed\ (kJ) = \frac{0.288 - 0.048}{1000} = 0.00024\ kJ$$

And:

$$Area\ (m^2) = \frac{3.94\ \times\ 7.76}{1000000} =\ 3.057\ \times 10^{-5}\ m^2$$

Therefore:

$$Impact\ Strength\ (kJ\ m^{-2}) =\ \frac{0.00024}{3.057\ \times\ 10^{-5}} = 7.85\ kJ\ m^{-2}$$

V – Differential scanning calorimetry data

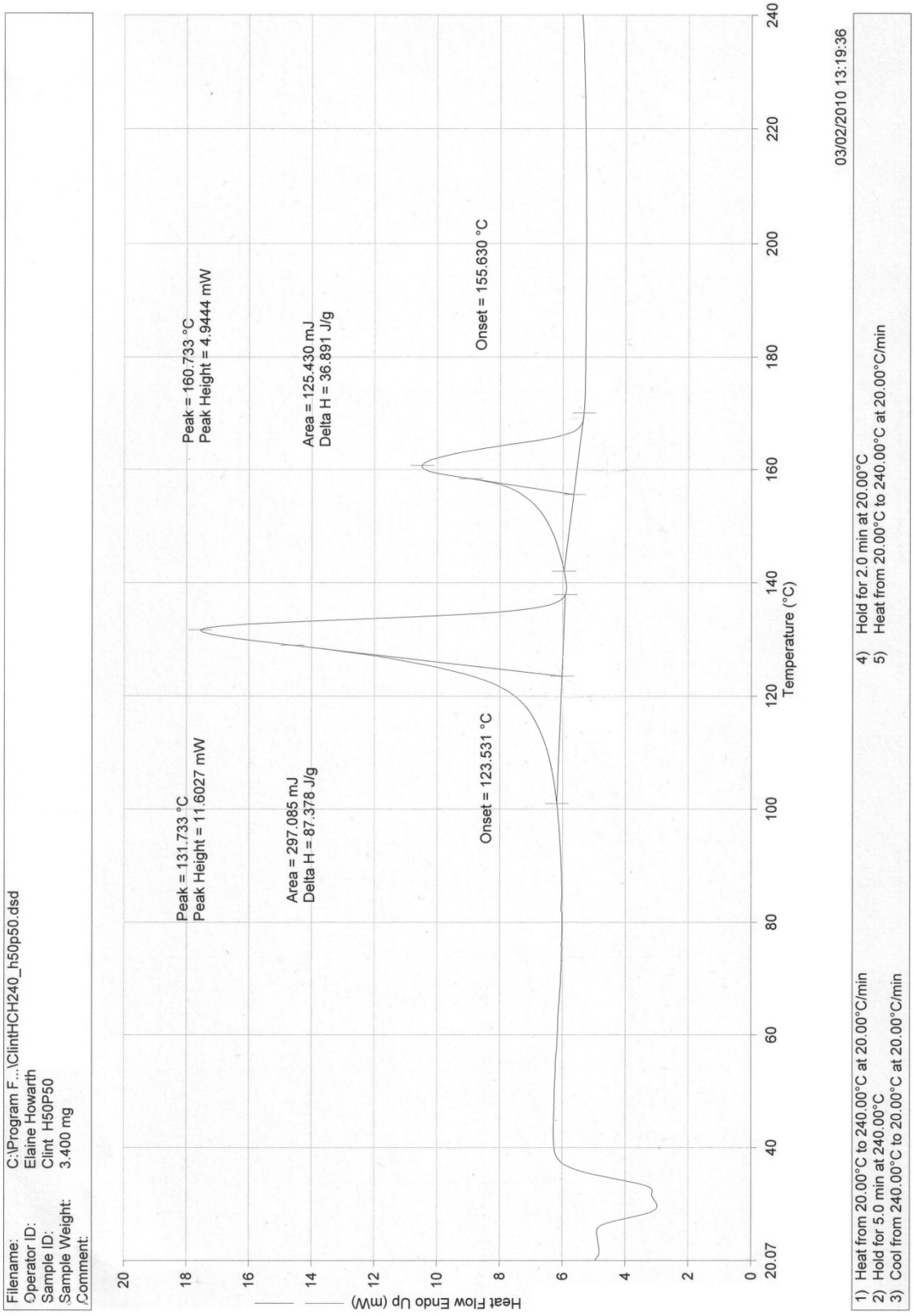

To calculate percent crystallinity of a single polymer sample:

$$Crystallinity\ (\%) = \frac{Heat\ of\ Fusion\ of\ sample\ (J\ g^{-1})}{Heat\ of\ Fusion\ of\ 100\%\ crystalline\ polymer\ (J\ g^{-1})} \times 100$$

Where:

$$Heat\ of\ Fusion\ of\ sample\ (J\ g^{-1}) = \frac{Area\ of\ peak\ (mJ)}{Sample\ mass\ (mg)}$$

However, for a binary polymer blend the ratio of polymers must be taken into account.

Therefore for PE:

$$Heat\ of\ Fusion\ of\ PE\ in\ sample\ (J\ g^{-1}) = \frac{Area\ of\ PE\ peak\ (mJ)}{Sample\ mass\ (mg)\ \times\ ratio\ of\ PE}$$

And:

$$Crystallinity\ of\ PE\ (\%) = \frac{Heat\ of\ Fusion\ of\ PE\ in\ sample\ (J\ g^{-1})}{Heat\ of\ Fusion\ of\ 100\%\ crystalline\ PE\ (J\ g^{-1})} \times 100$$

So for PP:

$$Heat\ of\ Fusion\ of\ PP\ in\ sample\ (J\ g^{-1}) = \frac{Area\ of\ PP\ peak\ (mJ)}{Sample\ mass\ (mg)\ \times\ ratio\ of\ PP}$$

And:

$$Crystallinity\ of\ PP\ (\%) = \frac{Heat\ of\ Fusion\ of\ PP\ in\ sample\ (J\ g^{-1})}{Heat\ of\ Fusion\ of\ 100\%\ crystalline\ PP\ (J\ g^{-1})} \times 100$$

Furthermore, in filled systems the level of filler must be taken into account. So a composite with 60% w/w filler will only contain 40% w/w polymer. This ratio must therefore be included when calculating the heat of fusion.

For a single polymer composite:

$$Heat\ of\ Fusion\ of\ sample\ (J\ g^{-1}) = \frac{Area\ of\ peak\ (mJ)}{Sample\ mass\ (mg)\ \times\ 0.4}$$

However, for a binary polymer composite:

For PE:

$$Heat\ of\ Fusion\ of\ PE\ in\ sample\ (J\ g^{-1}) = \frac{Area\ of\ PE\ peak\ (mJ)}{Sample\ mass\ (mg)\ \times\ 0.4\ \times\ ratio\ of\ PE}$$

For PP:

$$Heat\ of\ Fusion\ of\ PP\ in\ sample\ (J\ g^{-1}) = \frac{Area\ of\ PE\ peak\ (mJ)}{Sample\ mass\ (mg)\ \times\ 0.4\ \times\ ratio\ of\ PP}$$

VI – Fourier-transform infra-red spectroscopy data

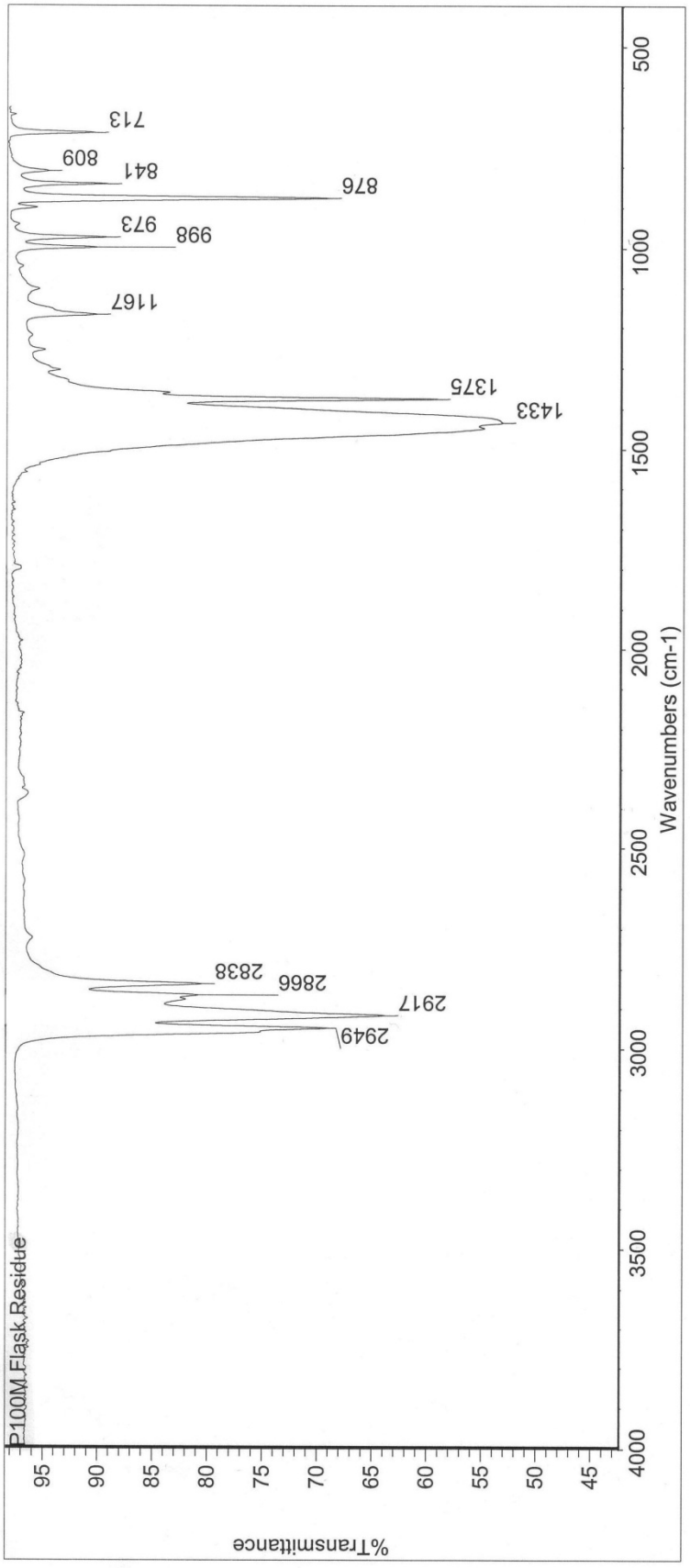

Fri Aug 20 13:11:58 2010 (GMT+01:00)
FIND PEAKS:
Spectrum: P100M Flask Residue
Region: 4000 400
Absolute threshold: 94.883
Sensitivity: 50
Peak list:

Position:	713	Intensity:	90.469	Position:	1167	Intensity:	90.245
Position:	809	Intensity:	94.672	Position:	1375	Intensity:	59.097
Position:	841	Intensity:	89.267	Position:	1433	Intensity:	53.214
Position:	876	Intensity:	69.131	Position:	2838	Intensity:	80.572
Position:	973	Intensity:	89.378	Position:	2866	Intensity:	80.867
Position:	998	Intensity:	90.171	Position:	2917	Intensity:	63.862
				Position:	2949	Intensity:	69.117

VII – Dynamic mechanical thermal analysis data

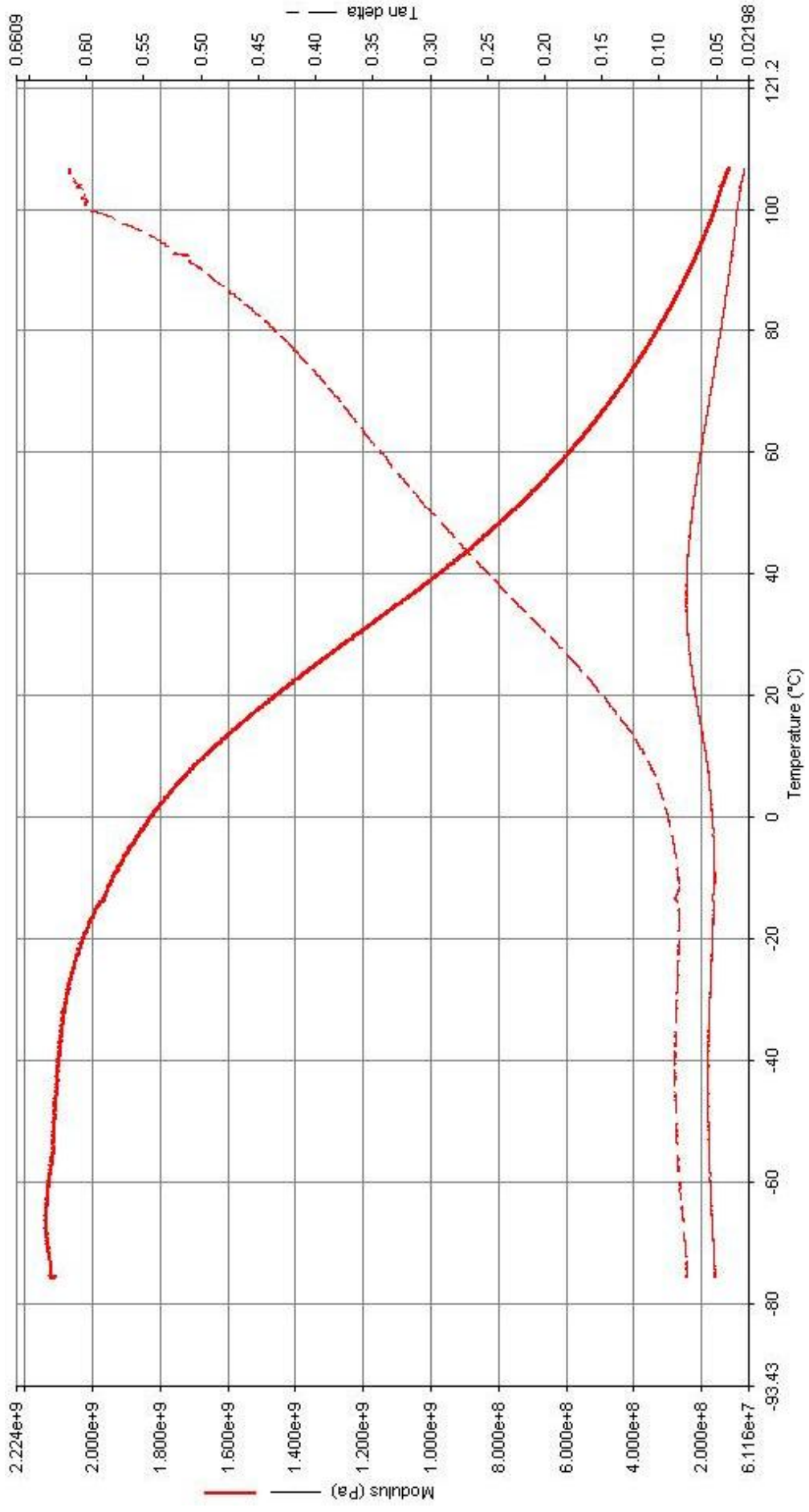

VIII – Thermo-gravimetric analysis data